SCHRIFTENREIHE ZUR WASSERWIRTSCHAFT

TECHNISCHE UNIVERSITÄT GRAZ

Martin Hochedlinger

Assessment of Combined Sewer Overflow Emissions

44

Graz, Juli 2005

Im Eigenverlag des
Instituts für Siedlungswasserwirtschaft und Landschaftswasserbau

Herausgeber:
Univ.-Prof. DDipl.-Ing. Dr.techn. Harald Kainz

Technische Universität Graz, Stremayrgasse 10, A-8010 Graz
Tel. +43(0)316/ 873-8371, Fax +43(0)316/ 873-8376
Email: office@sww.tugraz.at

ISBN 3-85444-044-8

Vorwort des Herausgebers

Die Bewirtschaftung der Niederschlags- und Mischwässer zum Schutz unserer Gewässer wird die Herausforderung der österreichischen Abwasserwirtschaft in den kommenden Jahren. Der Entwurf der Verordnung über die Begrenzung von Emissionen aus Mischwasserentlastungen in Mischkanalisationen (2001) und das 2006 erscheinende neue ÖWAV-Regelblatt 19 „Richtlinie für die Bemessung von Regenentlastungen in Mischwasserkanälen“ fordern einen Mindestwirkungsgrad der Weiterleitung von Schadstofffrachten zur Kläranlage. Der Nachweis für die gespeicherten und weitergeleiteten Mischwasserfrachten erfolgt durch eine Modellrechnung mit geeigneten Programmen für entsprechende Niederschlagsreihen.

Eine messtechnische Erfassung der entlasteten bzw. weitergeleiteten Mischwasservolumenströme ist sehr aufwendig und kann nur an einzelnen Mischwasserentlastungen erfolgen. Über diese Messwerte werden die Modellrechnungen kalibriert und die vielen Unsicherheiten der Eingangsdaten des Modells, wie Niederschlagsverteilung, -intensität und -höhe, Versiegelungsgrad, Oberflächenretention, Abflussbeiwerte, etc. teilweise kompensiert.

Der hydraulische Stress der entlasteten Mischwässer stellt sicherlich für kleine Gewässer im Flachland, wie z.B. Grabenlandbäche, eine relevante Belastung dar. Für die meisten Gewässer ist jedoch die entlastete Schmutzfracht das maßgebliche Kriterium. Die Schmutzfrachten von Kohlenstoff- und Stickstoffverunreinigungen sowie anderer Parameter werden bei der Betrachtung des Weiterleitungsgrades bei Mischwasserabfluss im Entwurf der AEV Mischwasser und dem ÖWAV-Regelblatt 19 nur über eine Abschätzung ermittelt. Dies hat große Vorteile für die praktische Umsetzung dieser Vorgaben und bildet eine wesentliche Randbedingung für eine zukünftige, erfolgreiche Umsetzung.

Dipl.-Ing. Dr. Martin Hochedlinger befasst sich in seiner Arbeit eingehend mit den beachtlichen Unsicherheiten und Fehlern von Niederschlags- und Abflussmesswerten. Der Schwerpunkt der Arbeit bildet die Auswertung, Interpretation und Kalibrierung einer UV/VIS-Sonde, die über mehrere Jahre online Äquivalenzwerte für CSB- und Feststoffkonzentration bei einem Mischwasserüberlauf im grazer Kanalnetz im Rahmen eines universitätsübergreifenden Forschungsprojektes lieferte. Die vorliegende Arbeit belegt, dass mit einer an die lokalen Abwasserverhältnisse angepassten Kalibrierung dieser Sonde quantitativ brauchbare Messungen in einer sehr hohen zeitlichen Auflösung durchgeführt werden können. Diese Arbeit deutet somit die Möglichkeit an, mittelfristig eine schmutzfrachtgesteuerte Bewirtschaftung von Mischwasseranlagen umsetzen zu können.

Graz, im Juli 2005

Harald Kainz

ACKNOWLEDGEMENTS

I would like to express my gratitude to my research supervisor, Professor Dr. Harald Kainz. He gave me the possibility and freedom to express my own ideas. His practical expertise and broad experience influenced this thesis.

I also gratefully acknowledge Professor Dr. Wolfgang Rauch for reviewing my thesis and the fruitful scientific discussions.

Dr. Günter Gruber, my colleague during the works, who has made the work rich in scientific and personal experience to me, which are useful for my future occupational career. Dr. Vilmos Vasvári has been a great support and contributed with many discussions in the field of urban hydrology. I would like to thank Prof. Dr. Boris Kompare and Nataša Atanasova, friends and colleagues from Ljubljana, for the introduction and their support in WEKA. Special thanks to Werner Sprung who supported me by modelling questions. I would also like to express my appreciation to Dr. Franz Gundacker for starting my interest in urban drainage and waste water treatment and for many fruitful discussions as a colleague and a friend, some of them late at night in the pub.

A big “thank you” to all the people who contributed to this work: the diploma students Christian Dorfer, Gregor Haas, Philipp Haring, Martina Kettner, Michaela Thaler and Michael Wedenig without many of the measurement campaigns and the modelling work would not have been possible. Arthur Fischer-Colbrie, Tanja Eibler, Roland Fuchs, Heinz Felver, Harald Gerhold, Silvia Higgersberger-Mixner, Brigitte Kainz, Hans Martin, Roswitha Pauritsch, Thomas Riedrich, Bernd Stojanovic and Bettina Vogl for their technical aid, organisation work and lab analysis. The success of the 24-hours measurement campaigns is a result of teamwork by these colleagues and friends. I am grateful to my friends and colleagues, Prof. Dr. Peter Kauch, Dr. Daniela Fuchs-Hanusch, Dr. Evelyn Krall, Mikloś Patziger, Gerald Gangl, Jörg Kölbl and Heimo Theuretzbacher-Fritz, at the institute who lent support and encouragement and created a very pleasant atmosphere for work.

I would also like to thank Richard Cheese for his support and proofreading this thesis.

My private thankfulness I would like to dedicate to my parents Christine and Alois Hochedlinger, who always encouraged me in my way.

Last, but not least, I would like to thank Sylvia, Martina and Franz who spared no effort in sharing my rare spare time and encouraged me during the last time.

Graz, June 2005 Martin A. Hochedlinger

What we know is just a drop,

what we do not know is an ocean.

Isaac Newton

ABSTRACT

During heavy storms huge flows have to be carried in the combined sewer system. The flow to the waste water treatment plant is limited due to its capacity. Hence, storage structures or combined sewer overflows have to be constructed to guarantee a limited flow to the waste water treatment plant. Therefore, it is of high importance to quantify these pollution sources from combined sewer overflows which directly spill the untreated wastewater into the receiving water. An accurate assessment of the overflow loads is possible by means of measurement data and simulations. The results of modelling depend strongly on the quality of model calibration and validation. This thesis will consider many kinds of errors which influence measurements like concentration, flow or precipitation measurements. Thus, a very careful and accurate data investigation is necessary. Innovative online-measurement technologies are able to provide the required data quality. The pollution concentration determination is achieved by means of the absorbance surrogate parameter. Five different linear regression methods are used for this absorbance concentration coherence. This small chain link in data determination for model input has a strong influence on the quality modelling results, and therefore, also a major influence on the assessment of combined sewer overflow loads. On the basis of correct absorbance and concentration coherences, corrected flow and precipitation measurements, a quality model was calibrated and validated for a long-term quality simulation. The results of this thesis demonstrate the high scattering range in overflow results based on different regressions. The knowledge gained will provide information for other researchers and engineers in quality modelling and can also be the basis for a possible future sewer real time control with the aim of load minimisation.

KURZFASSUNG

Bei Starkregenfällen treten in einem Mischwasserkanal große hydraulische Frachten auf. Aufgrund der limitierten Zulaufmengen zur Kläranlage, müssen im Entwässerungssystem entweder Speicherbauwerke oder Mischwasserüberläufe vorgesehen werden, damit die Kläranlagenzulauflimitierung eingehalten werden kann. Mischwasserüberläufe werfen das ungeklärte Abwasser direkt in den Vorfluter ab. Es ist daher von großer Wichtigkeit, diese punktuellen Verschmutzungsquellen quantifizieren zu können. Eine genaue Abschätzung dieser Mischwasserentlastungsfrachten kann nur mit Hilfe von Messdaten und Simulationsrechnungen erfolgen. Da die Aussagekraft von Modellrechnungsergebnissen stark von der Kalibrierung und Validierung abhängig ist, ist es wichtig, möglichst exakte Messdaten zu erheben. Innovative Online-Messtechnik kann diese geforderte Güte von Daten liefern. In dieser Dissertation wird versucht, alle Arten von Konzentrations-, Mengen- und Niederschlags Messfehlern zu berücksichtigen. Die Ermittlung von Verschmutzungskonzentrationen wird mit Hilfe des Surrogatparameters Absorption erzielt. Für den Absorptions-Konzentrationszusammenhang wurden verschiedene lineare Regressionsmethoden gewählt. Dieses kleine Kettenglied in der Ermittlung von Eingabedaten für die Modellrechnung hat einen großen Einfluss auf die Ergebnisse der Schmutzfrachtsimulation und daher auch einen großen Einfluss auf die Abschätzung der abgeworfenen Schmutzfrachten in den Vorfluter. Die Ergebnisse unterstreichen die große Ergebnisbandbreite an Hand verschiedener Regressionsgleichungen für die ermittelten Schmutzfrachten trotz sorgfältiger Kalibrierung und Validierung. Das gewonnene Wissen kann in der Anwendung von Schmutzfrachtmodellierung verwendet werden. Auf Basis der Mess- und Modellierungsergebnisse soll es zukünftig möglich sein eine Kanalechtzeitsteuerung durchzuführen mit dem Ziel der Frachtminimierung bei Entlastungen in den Vorfluter.

CONTENT

1. INTRODUCTION

The increasing number of pavements in urban areas has lead to an increase in waste water flow as well as rain volume in the sewer system. The effluent of a waste water treatment plant is not the only impact to the watercourse; the effects on receiving water only can be described by considering all kind of pollution sources (see Figure 1-1). Hence, the pollution point source of combined sewer overflows is important to integrate in analysis. Therefore, the exact assessment of emissions from combined sewer system helps in providing data for an integrated view of the whole urban drainage system.

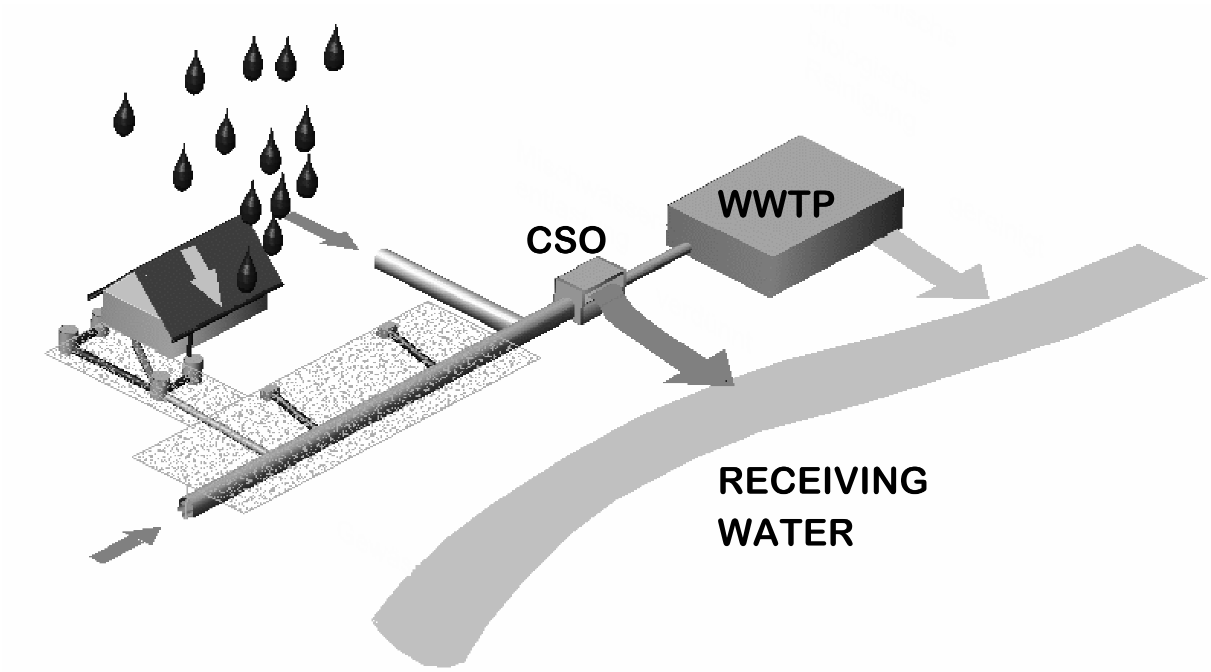

Figure 1-1 Point Pollution Sources of the Urban Drainage System from CSOs and WWTPs (Sprung, 2004)

1.1. CHALLENGE

Quality models can determine the pollution load spilled into the receiving water, but generally used values like rain weather concentration as recommended in the ATV A 128 German Standard do not entirely give the real concentration in the sewer system which is modelled. The real behaviour of pollution during heavy storms, which often causes a remobilisation of sewer deposits, is too complex to reproduce in quality models. However, the real sewer behaviour of pollution concentration as well as of the flow should be archived during a storm; this can be done by measuring. The measurement results should be used for model calibration instead of using empiric concentration values taken from literature. An insufficient model calibration inevitably leads to “wrong” model results. Therefore, it is of high importance to measure reliable data. The challenge of reliable combined sewer measuring data can be reasoned with the high variability of pollution concentrations as well as for flow. Sampling by automatic sampler is often limited by the sampler bottles and only can give the concentration behaviour during a storm to a certain degree. However, nowadays by means of online measurements it is possible to measure “concentrations” with a high temporal solution, and therefore, to exactly describe the concentration – discharge behaviour in a sewer system. Concentrations can not be directly measured and surrogate parameters have to be used to determine final concentrations. The coherence of surrogate parameter like absorbance and of pollution concentrations depends, as also in most parameters, on the specific waste water properties, meaning the right correlation of the absorbance and resulting concentration have to be detected. However, sometimes it seems a cumbersome undertaking to measure reliable and accurate values which are necessary for model calibration and validation.

1.2. AIM OF THE THESIS

The aim of the thesis is the analysis of combined sewer overflow emissions. Therefore, measurements are needed to assess theses overflow loads. For the concentration measurements a UV/VIS spectrometer is used which measures the surrogate parameter absorbance. For this purpose different regression methods are used and the applicability analysed. The main aim is to detect the influence and scattering range on calculated or simulated overflow loads by means of the different regression methods. On the basis of these regressions mean value concentration should be calculated and compared with values from literature. Are the values given from literature applicable for the use of modelling and calculation of overflow loads, is a main question which should be researched. The main input parameter, their influence on the results and the scattering range should be elaborated to give recommendations which data have to be collected very carefully to obtain accurate and reliable modelling and calculation results. These parameters regard the flow measurements, concentrations measurements as well as precipitation data.

1.3. METHODOLOGY

The whole methodology and overview of the thesis is displayed in Figure 1-2 by means of a flowchart.

Chapter 2 gives a brief introduction to stormwater management and its structures. The existing regulations and guidelines for combined sewer structures are explained as well as the different effects of combined sewer overflows on the receiving water to give an overview of the main challenges or “problems” in urban drainage at storm events.

Chapter 4 considers all kind of flow and concentration sewer measurements. Therefore, the sewer monitoring station and its measurement devices which was installed is explained in detail.

It gives an overview of the basic principles of the measurement systems used in the Graz sewer monitoring station and its application in sewer measurement practice. For flow measurement two radar systems were used and for concentration measurements an UV/VIS spectrometer was applied. Experiences and drawbacks made during the measurements complement the chapter.

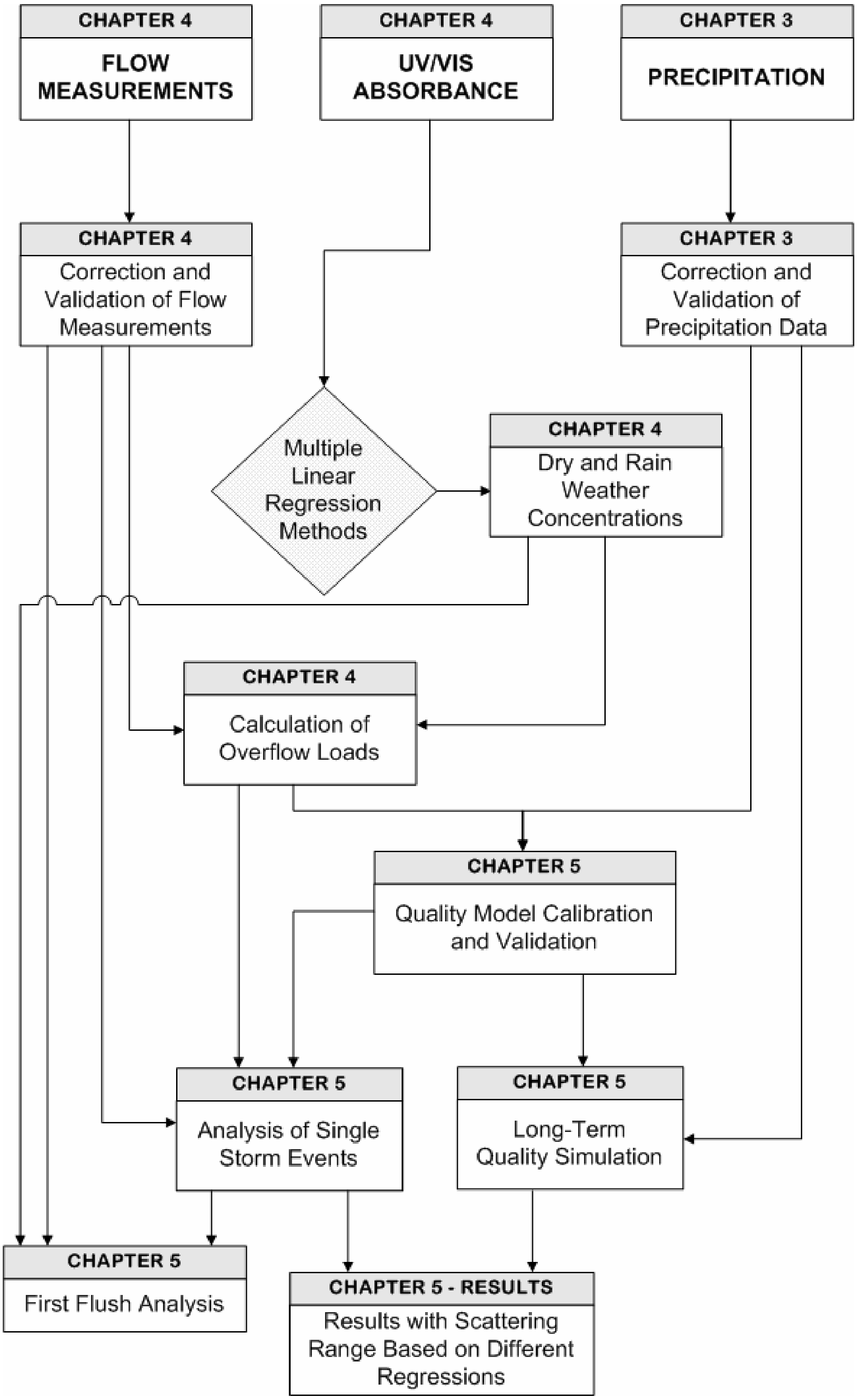

Figure 1-2 Methodology and Overview of the Thesis

Following research methods are used in this thesis for different analysis and describe own research work:

- In chapter, 3 the consideration is given to precipitation correction of the tipping bucket gauge by means of different kind of regressions (linear equation, power function and polynomial equation) which are based on a dynamic gauge calibration. A comparison of tipping bucket and weighing gauges demonstrates the needs of such corrections for short-term modelling. The influence on quality modelling results of corrected and uncorrected data is emphasised. However, a tipping bucket gauge correction is not necessary for long-term simulation. For a short-term modelling a correction is recommended to consider the tipping gauge errors.

- The inflow measurements are determined by means of a radar system. For a validation of these flow data a 24 hours flow measurement campaign was carried out. On the basis of three methods (radar system, Q-logger by means of Doppler principle, tracer measurements) the radar system was validated. Hence, after a sewer cross-section area correction and flow correction the reliability of the radar system could be proofed.

- The determination of how to get from absorbance measurement to equivalence concentration parameters by means of different regression methods is the main focus in this thesis. The company gives a default coherence equation between absorbance and concentrations which has to be adapted to the existing waste water properties. This can be done with an improvement of the default calibration by means of measurements. Therefore, three measurements campaigns were carried out to assess all kind of measurement errors and to achieve data for the default calibration improvement. By means of these three measurement campaigns data for training and calibration were measured to develop own absorbance concentrations coherence equations.

- On the basis of five different regression methods (simple linear regression, least median squares regression, M5 model tree regression, support vector machine using sequential optimisation algorithm, partial least squares regression) own absorbance concentration equations for the Graz-West combined sewer overflow were developed for the parameter total Chemical Oxygen Demand, soluble Chemical Oxygen Demand and Total Suspended Solids. For the validation of these regression results a multi-stage validation process was carried out. On the basis of this validation process possible model overfitting was detected as well as accurate and poor regression results. In most cases complex regressions like partial least squares regression deliver accurate equations but complex models are also susceptible for possible model overfitting. For the parameter Total Suspended Solids a very simple model is sufficient for accurate values.

- On the basis of correct flow data and concentrations values mean concentration values were calculated by means of the two component method. Hence, for the total Chemical Oxygen Demand parameter for the Graz-West sewer catchment mean rain weather concentrations of 223 to 444 mg/l result. This concentration is a mean input parameter for quality modelling.

- Quality modelling is the focus in chapter 5 with its model calibration and validation. The results of the simulation are shown for the whole scattering range to demonstrate the influence on the results by different kind of input data on the basis of different statistical linear regression methods.

- A first flush analysis shows the drawback of quality modelling which can not exactly reproduce single storm events due to the not possible consideration of the remobilisation of sewer solids. The used regression method for concentration calculation has a major influence also on first flush analysis.

The thesis is finally concluded in chapter 6 and points out the main research results of the thesis. Recommendations for future research needs and also improvements of the already existing monitoring station are given.

2. STORMWATER MANAGEMENT

The expeditious conveyance of stormwater from urbanised areas was motivated primarily by reasons of convenience and the reduction of flood damage potential. The removal of domestic wastes from households using waterborne conveyances was also found to be convenient. Such practices to improve the quality of urban life, however, have resulted in other problems, such as artificially induced flooding, increased erosion, and environmental degradation stemming from the pollution of receiving waters. As a result, attention has focused on the comprehensive management of urban drainage systems, which includes, in addition to the ancient use of conveyances such as channels and pipes, the implementation of storage and treatment facilities as well as real-time control of entire systems. The objective of this practice, commonly referred to as stormwater management, is to intelligently utilise components of drainage systems in a manner that will improve the quality of urban life while protecting the environment in a cost-effective manner (Adams & Papa, 2000).

History has given cities a mixture of infrastructure for urban drainage and water pollution control. The various systems were conceived at different times, planned with different philosophies, designed according to different criteria, and built to operate differently. It is therefore not surprising that as a metasystem, this collection of infrastructure has many residual problems, problems that require not one solution but a set of solutions.

The two problems residual to the operation of combined sewer systems are the occurrence of combined sewer overflows and the occurrence of combined sewer surcharge conditions resulting in sewer backup and flooding. Although the sewer backup problem is not directly related to receiving water quality problems, it is indirectly related inasmuch as the remediation of sewer backup problems may compete with the remediation of water quality problems for funding.

2.1. COMBINED SEWER SYSTEMS AND COMBINED SEWER OVERFLOWS

Piped systems consist of drains carrying flow from individual properties, and sewers carrying flow from groups or properties or larger areas. Sewerage considers the whole infrastructure system: pipes, manholes, structures, pumping stations, etc. There are basically two types of conventional sewerage system: a combined sewer system in which wastewater and stormwater flow together in the same pipe are carried, and a separate system in which wastewater and stormwater are kept in separate pipes. A combined sewer pipe has a significantly larger diameter than the foul sewer in a separate system draining the same catchment. Hence, the combined sewer compared with the foul sewer will have lower flow depths and greater contact between the liquid and the pipe wall in dry weather, when the wastewater flow-rate is relatively low. This leads to a greater sewer deposition risk. In dry weather, the system carries the wastewater flow, but during rainfall, the flow in the sewer increases as a result of the addition of stormwater. Even in quite light rainfall, the stormwater flows will predominate, and in heavy falls the stormwater could be fifty or even hundred times the average wastewater flow (Butler & Davies, 2000). It is simply not economically feasible to provide capacity for this flow along the full length of the sewers – which would, by implication, carry only a tiny proportion of the capacity most of the time. The inflow to a waste water treatment plant (WWTP) is limited due to the WWTP's capacity. It would be unfeasible to provide the whole capacity of wastewater and stormwater in the treatment process. Therefore, the solution to solve this challenge is to provide structures in the sewer system which, during medium or heavy rainfall, spill flows above a certain level out of the sewer system and into the receiving water. Such buildings are combined sewer overflows (CSOs).

The basic function of a CSO is displayed in Figure 2-1. During rainfall the inflow consists of stormwater mixed with wastewater. Part of the flow is retained in the sewer system and is carried to the WWTP. The amount of this flow is an important characteristic of a CSO, and is referred to as the 'setting'. The rest is overflowed to the receiving water – the overflow or 'spill flow'. These untreated discharges affect the environment of the receiving water. Storm flows can be highly polluted, especially early in the storm when the increased flows carry the remobilised sewer deposits – so called 'first flush'. CSOs cause pollution, and this a significant drawback of the combined sewer system.

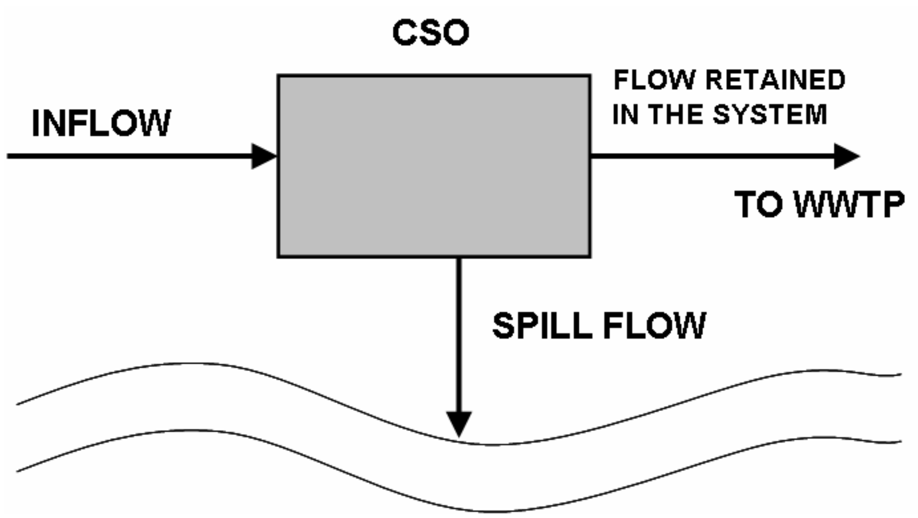

Figure 2-1 CSO Inflow and Outflow (Butler & Davies, 2000)

One CSO's main function is the hydraulic task: to divide the inflow into an outflow which is a continuation flow to the WWTP and the overflow which will be spilled into the receiving water. This task can be achieved by means of a weir. If the flow surface in a CSO is below the weir crest, flow continuous to the WWTP. If the flow-rate increases, the water level surfaces also increases. When the water surface is above the weir crest, part of the flow passes over the weir while the rest will be carried to the WWTP. There is a correlation between the spilled flow-rate and the water level above the crest. A higher water surface level in the CSO results in higher spill flows. The continuation flow also increases slightly by increasing water levels due to an increasing velocity and a resulting higher discharge rate through the throttle.

Another CSO main function is related to pollution. The ideal, of course, would be that all pollution is carried to the WWTP, but this does not hold in reality. However, the splitting between continuation flow and spilled flow is in the same ratio as for pollution loads, especially for fine suspended and dissolved material. These impacts are most serious when CSOs are poorly designed or operated ineffectively. Sewers which create backwater as a possible result of sewer deposits problems may also cause CSOs to operate poorly. In extreme cases, the CSO will spill even in dry weather conditions. Hence, this causes serious pollution to the receiving water (Butler & Davies, 2000).

2.2. Legal Regulations and Standards

The following sub-chapters give a brief description of some regulations, standards and guidelines of combined sewer overflows and their effects on the watercourse. A very detailed description of different requirements for CSOs in the EU is given by Fenz (1999).

2.2.1. Draft of Austrian Stormwater Regulation – "AEV Mischwasser"

The draft of this regulation (BMLFUW, 2001) defines emission limits for overflow loads from CSOs. In detail, this is limited by minimum stormwater pollution loads for the whole catchment of a WWTP which have to be carried to the WWTP for six different parameters depending on the WWTP population equivalence (PE) and the mean annual precipitation depth.

Table 2-1 Minimum Annual Load to WWTP in % of the Whole Catchment Area of Combined Sewer Systems on the Basis of Different Population Equivalences

	≤ 5 000 PE	> 5 000 - ≤ 50 000 PE	> 50 000 PE
TSS	70	75	80
NH_4-N	55	60	65
Total Nitrogen-N	55	60	65
Total Phosphorus-P	55	60	65
COD	55	60	65
BOD_5	55	60	65

Allowed reduction of the load to WWTP in % in dependence of the annual precipitation height:

- > 600 – ≤ 800 mm, allowed reduction of 5%
- > 800 – ≤ 1200 mm, allowed reduction of 10%
- > 1200 mm, allowed reduction of 15%

An overview of the requirements is given in Table 2-1. The dry weather load has to be subtracted for the continuation load which has to be carried to the WWTP. The percentage of the continuation load can be reduced, depending on the precipitation height. The consideration is for the load which is carried to the WWTP for the whole catchment area. In the case of non-compliance with the requirements, solutions are also given in the regulation. In this case, for example an unpaved surface, infiltration of rain water, sewer maintenance to reduce sewer depositing and the “right” situation of CSOs are recommended.

2.2.2. DRAFT OF AUSTRIAN GUIDELINE 19 FOR CSO DESIGN

The draft of this guideline (ÖWAV, 2003) does not give recommendations for CSO structure designs. The aim of this guideline is to provide the same definition as the Austrian Stormwater Regulation with regard to continuation load rates. Furthermore, the receiving water is also considered. Some simplifications are made for load which is carried to the WWTP, calculation like a fully mixed dry weather load and rain weather load as well as a constant temporal concentration in the storm load. The efficiency factor can be calculated with following equation (Fenz & Rauch, 2004):

$$\eta = \frac{\left(VL_{SW} - VL_{DW}\right) \cdot C_{SW} - VL_{SFL} \cdot C_{SF}}{\left(VL_{SW} - VL_{DW}\right) \cdot C_{SW}} \cdot 100 = \frac{VL_{RW} \cdot C_{SW} - VL_{SFL} \cdot C_{SF}}{VL_{RW} \cdot C_{SW}} \cdot 100$$

where:

- η .... load efficiency factor [%] which is carried to the WWTP
- VL_{SW} .... annual storm load sum [m³/a]
- VL_{DW} .... annual dry weather load [m³/a]
- VL_{RW} .... annual rain weather load [m³/a]
- VL_{SFL} .... annual spilled load [m³/a]
- C_{SW} .... concentration during a storm [mg/l]
- C_{SF} .... concentration in the spilled load during a storm [mg/l]

The guideline also gives a simplified design. If the flow (to the WWTP) efficiency factor is kept this also holds for the NH_4-N, total nitrogen parameter, the total phosphorus parameter, COD and BOD_5. This is really a wily approach. A parameter such as ammonium is totally soluble in the waste water and therefore this parameter has the same continuation efficiency factor as for the flow. Parameters which have a soluble and a particular part like, for example, COD, also satisfy the requirements because the regulation is already kept with the soluble part efficiency factor (is equal to the flow efficiency factor) and the particular part increases the efficiency factor. Of course, in this case the exact efficiency factor is not known. Hence, under this assumption the efficiency factor can be written with the next equation:

$$\eta_{RF} = \frac{V_{RF} - V_{SF}}{V_{RF}}$$

where:

- η_{RF}............. flow efficiency factor [%] which is carried to the WWTP
- V_{RF} .... annual rain volume [m³/a]
- V_{SF} .... annual spilled flow [m³/a].

For the TSS parameter sedimentation has to be considered. This guideline not only considers emission calculation, it also gives guidance on the assessment of the effects in the receiving water. Hence, it is an integrated approach regarding urban drainage systems.

2.2.3. ATV-A 128E German Standard

ATV A 128 is a design standard for stormwater structures on the basis of an emission calculation. It gives no recommendations for the effects of CSO impacts on the receiving water. The annual COD pollution load is used as the indicator for spilled pollution load. The basis is a calculated fictitious annual spilled COD load from CSOs and WWTP. These loads are necessary for the design of storage structures. Hence, the fictitious spilled load will not give in most cases the real load. This should not led to the assumption of changing the storage volume. Even the loads are probably in most cases underestimate the approach delivers useable design volumes. But the proposed COD values are mostly not useable for an exactly assessment of overflow loads which is explained in the following sentences. Only COD surface potential is considered which is reasoned through the very complex interaction between sewer deposits accumulation and remobilisation. Hence, by means of a annual effective precipitation depth of 560 mm and a annual COD surface potential of 600 kg/(ha.a), a mean COD rain weather concentration of 107 mg/l results. The mean COD dry weather concentration is assumed with a value of 600 mg/l, the COD effluent concentration from the WWTP with a value of 70 mg/l. Higher dry weather concentrations can be considered as well as the annual precipitation depth and the influence of sewer deposits. Unfortunately, the sewer deposits and its remobilisation only a minor influence in the ATV-A 128E standard (and only influences the dry weather concentrations), and therefore, can not assess the real first flush behaviour in sewers. On the basis of these concentrations, the annual spill rate can be calculated which has to be below the allowed spill rate. To keep this required spill rate, a certain storage volume in the sewer system is necessary. Hence, the COD dry weather concentration as well as the rain weather concentrations directly influences the design capacity.

2.2.4. URBAN POLLUTION MANAGEMENT - FOUNDATION FOR WATER RESEARCH (UK)

The Urban Pollution Management Manual (FWR, 1998) is a planning guide for wet weather wastewater discharge into a watercourse regarding the whole system in an integrated analysis.

For example, it also gives recommendations for toxic discharges which are very difficult to define for single parameter. Therefore, a toxicity-based consents (TBCs) was developed. These are derived from laboratory and field ecotoxcicological studies on fish and invertebrates. Results are expressed as LC50 values that indicate short-term lethal concentrations of a particular pollutant resulting in 50% mortality. This standard consists of a relationship between three variables: pollutant concentration, return period of an event in which that concentrations is exceeded and the duration of the event. Table 2-2 shows this three-way relationship for dissolved oxygen and unionised ammonia based on sustaining cyprinid fisheries.

Table 2-2 Intermitted Standards for Dissolved Oxygen and Ammonia Concentration and Duration Thresholds for Sustaining Cyprinid Fisheries (FWR, 1998).

Return Period [months]	DO Concentration [mg/l]*)		
	1 hour	6 hours	24 hours
1	4.0	5.0	5.5
3	3.5	4.5	5.0
12	3.0	4.0	4.5
	NH_3-N Concentration [mg/l]**)		
1	0.150	0.075	0.030
3	0.225	0.125	0.050
12	0.250	0.150	0.065

*) applicable when NH_3-N < 0.02 mg/l
**) applicable when DO > 5 mg/l, pH > 7 and T > 5°C

2.2.5. EUROPEAN WATER FRAMEWORK DIRECTIVE

The EU-WFD (EU, 2000) requires the establishment of quality and quantity measurements. The directive is to contribute to the progressive reduction of hazardous substances emissions to the water course. The directive recommends the use of an integrated approach, meaning the renunciation of just an emission approach and the consideration of river basin management. These requirements can only be fulfilled by means of measurements and monitoring of the whole system (watercourse, groundwater, sewer system, WWTP).

2.3. CSO EMISSIONS AND ITS EFFECTS ON RECEIVING WATER

The impacts on receiving water result from diffuse natural and anthropogenic sources as well as from point sources like CSO spill flows, WWTP and industry. The effects on receiving water depend on the impact duration and intensity and also from the self-treatment of the receiving water itself. The different kinds of effects (physical, chemical and toxic) are displayed in Table 2-3.

Table 2-3 Effects on Receiving Water (Seggelke, 2002)

	Kind of Impacts	Kind of Effects	Kind on Affected Receiving Water
Physical	Change of Hydraulic Flow	Discharge Behaviour, Hydraulic Stress	Steep and Slack Brooks, Small Rivers
	Temperature	Complex	Steep Brooks
	Solids	Deposits Change, Sedimentation of Coarse Material	All
Chemical	Nutrients (P, NH_4, NO_3)	Supports the Trophic Growth	Small and Large Estuaries
	Organic Matter (Protein, Sugar, Fat)	Supports the Saprobic Growth	Estuaries
Toxic	NH_3, NO_2	Acute or Chronically Toxic, Change of Biocide	All

Receiving water effects can be classified in acute or short-term (hours), delayed or medium-term (days) and cumulative and chronic, respectively, or long-term effects. Sewerage spills result in acute or delayed effects whereas effluents from WWTP generally affect the receiving water accumulatively. In case of a storm it is also possible to have acute effects on the receiving water (Rauch & Harremoës, 1996) from the WWTP. The extent and importance of individual processes will depend on the temporal and spatial scales displayed in Figure 2-2.

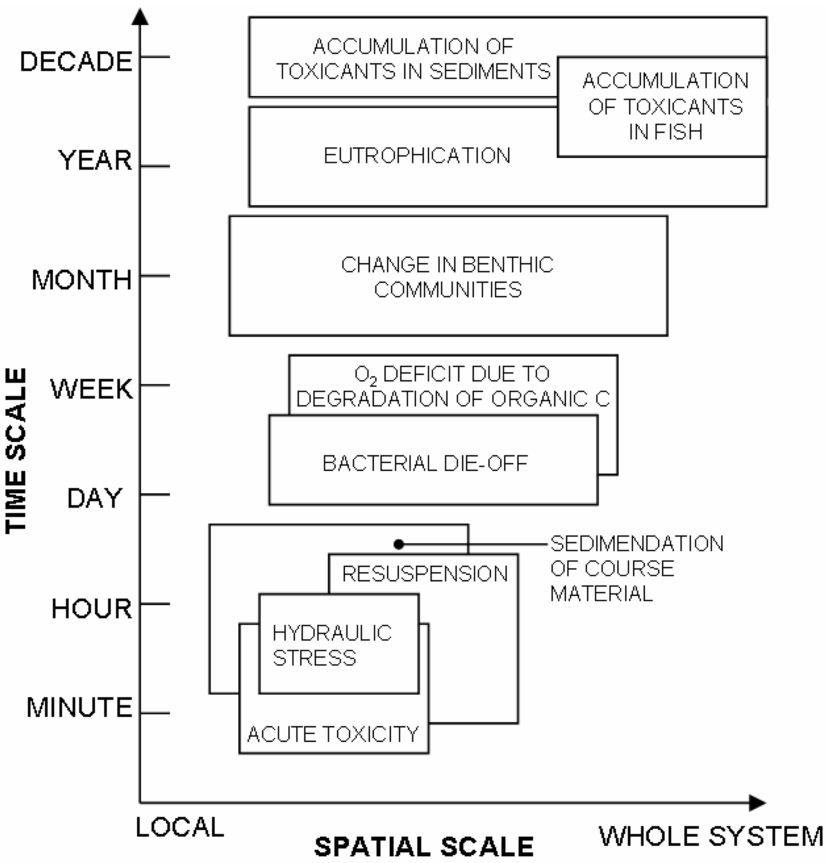

Figure 2-2 Time and Spatial Scales for Receiving Water Impacts (after Aalderink & Lijklema, 1985; quoted in House et al., 1993)

2.3.1. HEAVY METALS AND OTHER TOXIC CONSTITUENTS

Marsalek et al. (1997) reports, that heavy metals are the most prevalent toxic contaminant found in urban runoff. In urban runoff, commonly found heavy metals are lead, zinc, and copper. Other toxic pollutants found in stormwater include phthalate esters, phenols, oil, greases and polycyclic aromatic hydrocarbons (PAHs).

2.3.2. SUSPENDED SOLIDS

The most prevalent form of stormwater pollution is suspended matter that is either eroded by stormwater or washed off paved surfaces by stormwater. Suspended solids increase the turbidity of the receiving water, thereby reducing the penetration of light, resulting in decreased activity and growth of photosynthetic organisms. The increased turbidity also detracts from the aesthetics of natural waters. In addition, the clogging of fish gills has been attributed to the presence of suspended solids. Combined sewer overflows typically contain high suspended solids concentrations. The solids that settle in the receiving water pose long-term threats resulting from their oxygen demand and gradual accumulation of toxic substances. Sedimentation and other forms of physical separation are often an effective means of removing suspended solids from stormwater.

2.3.3. OXYGEN DEMANDING MATTER

Sufficient levels of dissolved oxygen (DO) in the water column are necessary to maintain aquatic life, growth, and reproductive activity as well as to maintain aerobic conditions. The introduction of stormwater containing oxygen-demanding organic matter can impair the receiving water quality by reducing the DO levels such that it is unable to sustain certain forms of aquatic life and can further cause the water to become foul. Rauch & Harremoës (1996) showed that the minimum DO level occurs mostly some kilometres downstream from the CSO discharges. Fenz & Nowak (1998) described the few clear defined criteria given in literature for effects of short-term oxygen deficit on biocenosis and on specific organisms.

2.3.4. EUTROPHICATION

Excessive growth of aquatic weeds and algae occur where there is a discharge of large quantities of nutrients such as nitrogen or phosphorus. This can lead to oxygen depletion, anaerobic conditions in bottom muds, fish kills and in aesthetic problems. These are long-term problems especially in shallow, stagnant waters such as lakes and estuaries, but rivers may also be affected. Intermitted discharges are usually a relatively small constituent of the total nutrient load. In most cases for the growth of weed and algae the limited nutrient is phosphorus.

2.3.5. AMMONIUM / AMMONIA

Higher ammonium concentration in the receiving water results from highly short-term spill loads when the microbiota and its nitrification potential can not be adapted to the new river conditions. Ammonia can be toxic to fish at high temperatures and ph-values (> 8) in watercourses due to the dissociation equilibrium of ammonium and ammonia. Hence, at high storms and higher temperatures (e.g. in the summer) a higher danger for toxic ammonia due to more photosynthesis processes result.

The ammonia concentration coherence can be expressed with following equation (after Emerson, 1975; quoted in Fenz & Nowak, 1998):

$$\frac{NH_3 - N}{NH_4 - N} = \frac{1}{\left(1 + 10^{(pK_S - pH)}\right)} \text{ with } pK_S = \frac{2729.92}{T} + 0.09018 \left(T \text{ in K}, 0°K = -273.2°C\right)$$

2.3.6. Hydraulic Stress

The hydraulic stress effect depends on the correlation of the spilled flow and the receiving water discharge and river bed material as well as on duration and frequency of overflows. These flows can result in a destruction of the river bed due to erosion of reaching the critical shear stress. The high discharge leads to a loss of the benthic division in the river bed sediments. Hence, at large spill flows it is also possible of river bed mobilisation and re-agglomeration of river bed sediments. Therefore, the re-population potential of a river is of high importance (Gammeter & Krejci, 1998).

2.3.7. Aesthetics

In addition to chemical and biological impacts, public perception of water quality is also important. Research has shown that the public has a good idea of what might be considered a polluted river, but is less certain as to what might be considered a clean river. The public tends to misperceive as polluted rivers, even rivers of high chemical and biological quality. However, solids of obvious sanitary origin near to receiving waters are considered to be offensive (Butler & Davies, 2000).

3. PRECIPITATION MEASUREMENTS

Precipitation gauges are commonly seen as robust and reliable. There are a lot of possible precipitation failures (e.g. wind, evaporation, etc.) and gauge specific failures, especially for the tipping bucket gauge. In this research, two kinds of gauges are used – the tipping bucket gauge and the weighing gauge. The tipping bucket rain gauge has become probably the most popular recording rain gauge, used by most weather service agencies. The reason for such widespread popularity comes from the very simple mechanics exploited for direct measurement of rainfall and the reliability of the instrument (La Barbera et al., 2002). It can easily be updated in its data acquisition and storage components as long as new electronic devices become operationally available. Finally, maintenance work is reasonable and the cost is affordable even in the case of rather extended networks. A weighing gauge is used for comparisons in this thesis to avoid systematic errors of tipping bucket gauges in the measurements. Preferences for weighing system have already been shown by Seibert & Morén (1999).

A lot of uncertainties are involved in sewer system overflow emissions modelling. These uncertainties about the model input are (for example rainfall data as well as spatial rainfall input) model simplifications of the physical reality and uncertainties about the model parameters. Willems & Berlamont (1999) show the importance of the consideration of uncertainties and the resulting risk for designs. For an uncertainty analysis on the basis of detailed statistical analysis more than hundred rain events and its simulation in the sewer system model are recommended. In order to limit the simulation time, a simple reservoir model can be implemented.

This chapter will also present the effects of corrected and non-corrected precipitation data used for single events and long-term pollution quality modelling. The use of single design storms is maybe too simplistic for long-term simulation. Detrimental effects may occur on many different time scales. The variation in the rain input must reflect what has been observed historically, from peak intensities lasting only a few minutes right down to variations in annual precipitation. Thus, historical rain series have become necessary in the analysis of urban hydrology (Arnbjerg-Nielsen et al., 1998).

Generally, there are different kinds of precipitation errors from different sources. The apparent differences between gauges and measurement stations may originate from the following sources, respectively (Mikkelsen et al., 1997):

- sampling errors
- differences in physiography and micro-climate
- measurement errors

Sampling errors originate from the use of a limited sample for estimation. It is not trivial to find out whether the variation is due to sampling errors or to systematic differences between stations and gauges. It is expected that differences in physiography (altitude, landscape topography, etc.) will be reflected in spatial variations of rainfall properties relevant to the design of sewer system, and that models can be formulated for prediction at ungauged locations. However, part of the variation may be caused by variation on a relatively small spatial scale compared with the physical extent of sewer catchments. Although differences in micro-climate (temperature, shelter conditions, etc.) contribute a considerable part of the observed variation. The same goes with measurement errors no matter whether they are systematic (bias due to imperfect calibrations at the rain gauges) or non-systematic (measurement noise).

3.1. LOCATION OF PRECIPITATION GAUGES

Two precipitation gauges and two brook flow measurement stations were installed in the year 1989 in a small urban research area in the east of Graz (Waltendorf District). The first two tipping bucket gauges were “Hohensinner” and “Lang”. In the year 2003, four additional tipping bucket gauges were installed in Graz (Figure 3-1). Two of these gauges (one tipping bucket gauge and one weighing gauge) are in Klusemanngasse, which provide the precipitation data for modelling.

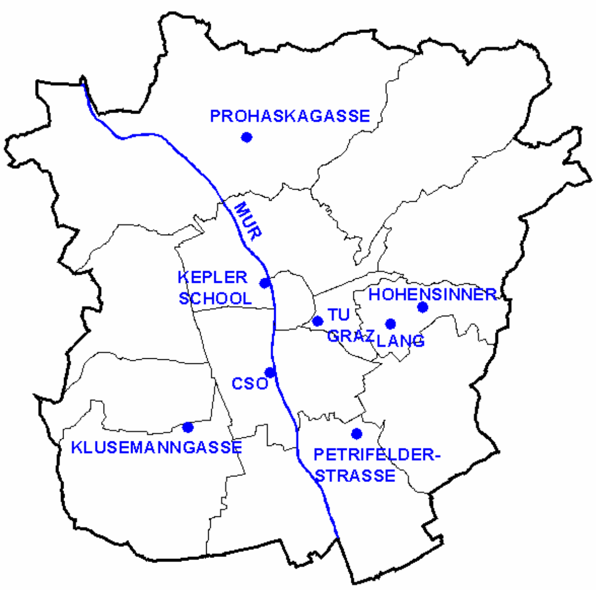

Figure 3-1 Overview of the Precipitation Gauge Stations and the Graz-West CSO Monitoring Station (Vasvári et al., 2005)

The position of the two gauges (Klusemanngasse), placed directly side by side, is in the south of the catchment area. Unfortunately, only these two gauges have so far been installed, although big efforts have been made to increase the number of gauges in the catchment area. The tipping bucket gauge is MODEL 52202 from the

YOUNG Company and the weighing gauge is the PLUVIO type from OTT. The two devices have been positioned at the same height and with a distance of approximately 5 m to each other. With this kind of installation it is not possible to eliminate the influence of wind or temperature, but the impact to the two devices is the same. Due to this positioning with the same external influences a comparison seems feasible to identify tipping bucket gauge errors.

3.2. SYSTEMATIC ERRORS IN PRECIPITATION MEASUREMENTS

Random errors are caused by mechanical and electrical disturbances of the gauge, data transmitting errors and clogging the tipping bucket gauge. The existence of such random influences is easily seen when comparing the amount of recorded precipitation of two gauges at the same site. Despite the environmental and observational conditions being the same, there is usually a difference in the measured data from both gauges (Rauch et al., 1998). The precipitation measurement error sum can reach an error up to 30% (Rauch et al, 1998; Thaler, 2004). Fankhauser (1998) has already pointed out the effect of systematic errors for precipitation data of tipping bucket rain gauges.

The main components of the systematic error in precipitation measurement have already been described in detail by Rauch et al. (1998) and are:

3.2.1.1. WIND AND BLOWING SNOW

Every rain gauge influences the wind and results in turbulences which swirl especially small drops. Hence, only major drops can reach the collecting funnel of the gauge. In Central Europe the wind error is in the summer smaller than in the winter. The precipitation in summer has, on average, bigger drops due to storms. This error is inevitable on high mountains also with a wind protection device due to the main precipitation is in form of snow which can be easily scattered. The error from the wind is dependent on the shape of the measurement device and the height where the gauge is positioned.

3.2.1.2. WETTING OF INTERNAL WALLS

Water adheres to the walls of the tipping buckets which can not be measured. The amount of adhesion water depends on the profile, design, size, material and age of the measurement device.

3.2.1.3. EVAPORATION

It is also possible that part of the rain water can evaporate. Depending on the emptying interval the error can be minimised by a high interval. Also the profile, the colour, the material, the isolation and the positioning height influence the evaporation error.

3.2.1.4. Splashing

Splashing are drops which are bounded by the surrounding area and fall into the measurement device or splash from the measurement device onto the surrounding area also causing errors. Theses errors result from the rain intensity, the wind velocity, the measurement height position and kind of installation of the device. Devices installed in-plane result in higher splashing errors than devices which are installed in, for example, a height of 1.50 m.

3.3. Weighing Gauge

The weighing gauge is the PLUVIO type from OTT with a collecting area of 200 cm² where the liquid as well as the solid precipitation falls. The collecting pot is directly installed on the platform of a load cell which measures the amount of precipitation weight. A strain gauge is used for the weighing process. The strain gauges warps in the case of a force effect. The coherence of this change from Ohm's resistance can be written as:

$$\frac{\Delta R}{R} = k \cdot \varepsilon \text{ with } \varepsilon = \frac{\Delta \ell}{\ell}$$

where R is the resistance measured in Ohms, ΔR is resistance changing, k is the k-factor of sensitivity, ε is the relative strain, ℓ is the length of the strain gauge's wire and $\Delta \ell$ is the changing of the length.

Strain gauges are electrical resistances which are changed by mechanical stress. If a strain gauge gets stretched, the resistance increases; otherwise if a strain gauge is compressed, the resistance decreases. The resistance change through tensile and pressure strength is called piezo-resistive resistance effect.

The strain gauges are bonded on the weighing gauge housing. Electrical resistance changing results from a change of the strain gauge length. Expansion and compression and the resistance changing are in a definite ratio, the so-called sensitivity or k-factor. The strain changing ε and the measured weight can be determined knowing the k-factor and the resistance changing ΔR.

The whole weight in the precipitation collecting pot of the can be displayed in 1/10 mm. 1/10 mm is equivalent to 2 g of weight when the collecting area is 200 cm². An increase of 1/10 mm activates an impulse by a relay contact. The advantages of the weighing gauge compared with the tipping bucket gauge are:

- high measurement resolution at extreme storms without losses
- possibility of solid precipitation measurement without melting before
- no evaporation loss by solid precipitation melting

Two simple tests were carried out to quantify the measurement reliability of the weighing gauge. The results of theses tests can be seen in Table 3-1. The highest relative deviations of actual and recorded precipitation height are 6.5% for test 1 and 6% for test 2. On the basis of these result the measurement data of the weighing gauge can be seen as accurate and reliable. Therefore, the results of the weighing gauge are useable for a comparison with the data of the tipping bucket gauge.

Table 3-1 Check of the Measurement Accuracy of the Weighing Gauge

		Test 1		Test 2	
Weight	Actual Precipitation Height	Recorded Precipitation Height	Relative Deviations	Recorded Precipitation Height	Relative Deviations
[g]	[mm]	[mm]	[%]	[mm]	[%]
5	0.250	0.250	0.000	0.260	4.000
5	0.250	0.240	-4.000	0.245	-2.000
5	0.250	0.250	0.000	0.260	4.000
5	0.250	0.255	2.000	0.240	-4.000
5	0.250	0.250	0.000	0.255	2.000
10	0.500	0.500	0.000	0.505	1.000
10	0.500	0.525	5.000	0.515	3.000
10	0.500	0.495	-1.000	0.510	2.000
10	0.500	0.510	2.000	0.515	3.000
10	0.500	0.510	2.000	0.500	0.000
15	0.750	0.780	4.000	0.780	4.000
20	1.000	1.065	6.500	1.060	6.000
35.8	1.790	1.790	0.000	1.805	0.838
35.8	1.790	1.785	-0.279	1.775	-0.838
50	2.500	2.500	0.000	2.520	0.800
100	5.000	5.015	0.300	4.995	-0.100
159	7.950	7.925	-0.314	7.965	0.189
159.3	7.965	7.990	0.314	7.965	0.251
250.15	12.508	12.495	-0.100	12.500	-0.060

3.4. TIPPING BUCKET GAUGE

Tipping bucket rain gauges are the most popular recording rain gauges. The provide high accuracy when recording low-to-intermediate intensity rainfalls, a superior mechanism for actuating circuits, suitability for remote recording and reliability distinguish tipping bucket rain gauges. This type of gauge produces rainfall data in digital form which can be easily processed by computers. On the other hand, tipping bucket rain gauges are known to underestimate the rainfall at higher intensities due to the loss of rainwater during the movement of the bucket. At low intensities the recorded intensity may exceed the actual intensity (Marsalek, 1981). Marsalek (1981) discussed the non-linearity of tipping bucket rain gauges, the reasons of these phenomena, and the need of dynamic calibration. Marsalek (1981) analysed the influence of surface tension of tipping bucket material at volumetric calibration. A function of actual intensity with regard to the movement of tipping buckets was presented.

Niemczynowicz (1986) investigated three different types of tipping bucket rain gauges and assumed a simple power equation to fit the measured data, where the correlation coefficients amount to over 0.999. Comparing the errors in calculated rainfall intensity when using a constant bucket volume for linear and non-linear calibration Niemczynowicz (1986) found out that the error varies in the intensity range between 0 and 5 mm/min from about 19% to about -10%.

To reduce the independence of the measurement of the actual rain intensity a siphon can be installed between the bucket and the funnel, below the funnel outflow. However, as both siphon and bucket are discrete samples, the relative size of the volumes is important. Overgaard et al. (1998) investigated the optimal ratio of the effective volume of the siphon to the volume of the bucket. The optimum size of the siphon has to be less than the half size of the bucket. Considering the dynamic volume of the siphon, the effect on the volumetric accuracy should be assessed based on a volume of the siphon of 35 to 45% of the bucket volume.

La Barbera et al. (2002) analysed the statistical influence of systematic mechanical errors on for example the disaggregated rain data, the Gumbel distribution of extreme rainfalls, and the depth-duration-frequency curves. Their conclusion was that these errors substantially affect the derived statistics. Furthermore, the equivalent sample size was derived, which quantifies the equivalent number of calibrated data that would be needed to achieve the same caused by the influence of systematic mechanical errors in uncalibrated data sets.

3.4.1. CALIBRATION PROCESS

The tipping bucket rain gauge (MODEL 52202 from the YOUNG Company) used in the catchment area of the Graz-West CSO (Klusemanngasse) essentially consist of four components:

- collector funnel
- tipping bucket
- data recorder
- collecting receptacle

The collector funnel has an area of 200 cm². Accordingly, the volume of the tipping buckets amounts to 2 cm³, which corresponds to a precipitation depth of 0.1 mm. The data recording interval is time-variable, the time of each individual tip is registered as a binary signal in the permanent memory. The measured rainwater ends up in the collecting receptacle (Figure 3-2).

A simple calibration device developed especially for field calibration consists of a peristaltic pump with a transparent hose. The calibration equipment serves for adjustment and continuous supply of a constant flow rate. The central part is a MCP-360 peristaltic pump. The pump with tubing of different diameters has to be calibrated first either in the laboratory or in the field in spite of the available rating curves given by the pump manufacturer.

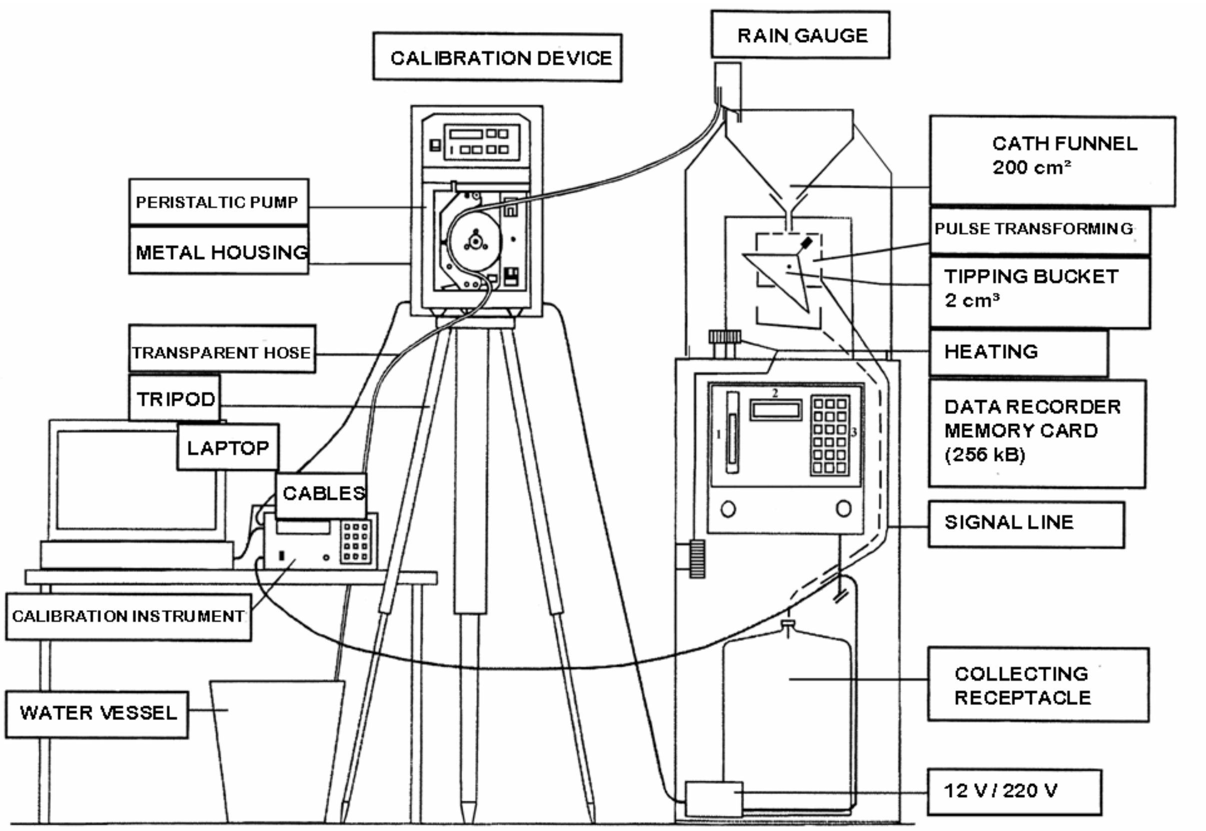

Figure 3-2 Sketch of the Calibration Device (Vasvári, 2005)

The tubing of smaller diameter is suitable for intensities up to 1 mm/min and the larger one allows intensities up to 7 mm/min. The flow is fed via transparent tubing to the funnel of the rain gauge. The water flows into the tipping buckets and is collected in a receptacle below (Figure 3-2). Tap water is used for the calibration. During the measuring process, the electronic system records the signals produced by the tipping buckets. The flow rate of the pump and the measured intensity of the simulated precipitation in two independent measuring processes are recorded. The flow rate can be converted into a certain intensity in relation to the funnel area of 200 cm².

As only the resolutions per minute can be adjusted directly, not the pumping rate of the pump, the resolutions per minute in steps of ten were chosen. This was done due to measurable whole number tips. The duration of measurement is determined by the number of tips. The number of tips varies according to the setting between 5 and 15.

3.4.2. CORRECTION OF TIPPING BUCKET GAUGE DATA

The reference value of the intensity is known on the basis of the number of rotations of the peristaltic pump. So, a variance comparison between recorded and actual intensity can be determined which is a base for the tipping bucket gauge data correction.

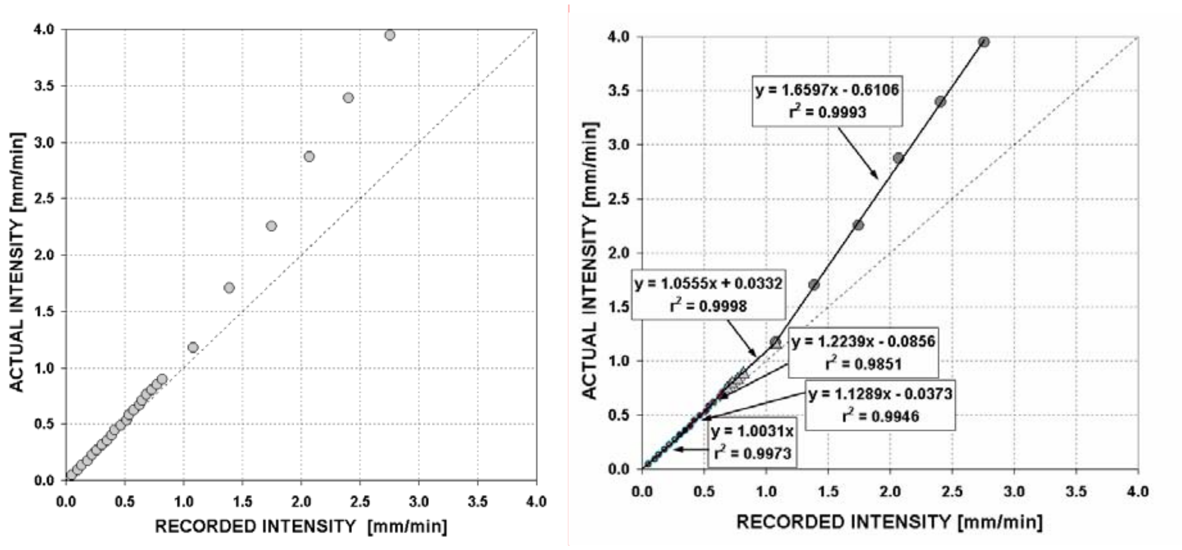

Figure 3-3 Actual vs. Recorded Intensity (Left Figure) and the Calibration Curves for Linear Regression (Right Figure)

The calibration curves were adjusted by five linear regression lines (Figure 3-3). The general formula of linear regression is given in following equation:

$$i_0 = a_1 \cdot i + b_1$$

The coefficients of the linear function are a_1 and b_1. The actual intensity i_0 from the flow rate of the peristaltic pump and the recorded intensity i from the frequency of tipping bucket movements are determined. The results are shown in Table 3-2 and Figure 3-3.

Table 3-2 Calibration Parameters for Linear Regression of the Klusemanngasse Tipping Bucket Rain Gauge an the Resulting Stability Index

Recorded Intensity i [mm/min]		a_1	b_1	r^2
From	To			
0.0000	0.2965	1.0031	0.0000	0.9973
0.2965	0.5084	1.1289	-0.0373	0.9946
0.5084	0.7055	1.2239	-0.0856	0.9851
0.7055	1.0655	1.0555	0.0332	0.9998
1.0655	2.8000	1.1660	-0.6106	0.9993

The ranges of linear regression have to be defined subjectively considering the stability index r². The difficulty in this subjective trial-and-error-method is finding a satisfying result. The most exact method is, of course, the interpolation between each actual and recorded intensity value pair. This leads to a high number of regression lines with a stability index r² and a correlation coefficient of 1, respectively.

It is also possible to describe the calibration curves with other functions with only one equation. Therefore a power and a squared polynomial function were analysed in detail.

The power function can be written in the form of:

$$i_0 = a_2 \cdot i^{b_2}$$

The value of the power function coefficient a_2 is 1.1735 and the value of the exponent b_2 equals to 1.1142 (Figure 3-4). The resulting power function for the calibration for the Klusemanngasse tipping bucket gauge can be displayed as:

$$i_0 = 1.1735 \cdot i^{1.1142}$$

A stability index of r²=0.9981 and a correlation coefficient of r=0.999 results, respectively. The value of 0.9981 seems to be satisfying, but further analysis showed poor results during storm events with high intensities with this kind of correction equation.

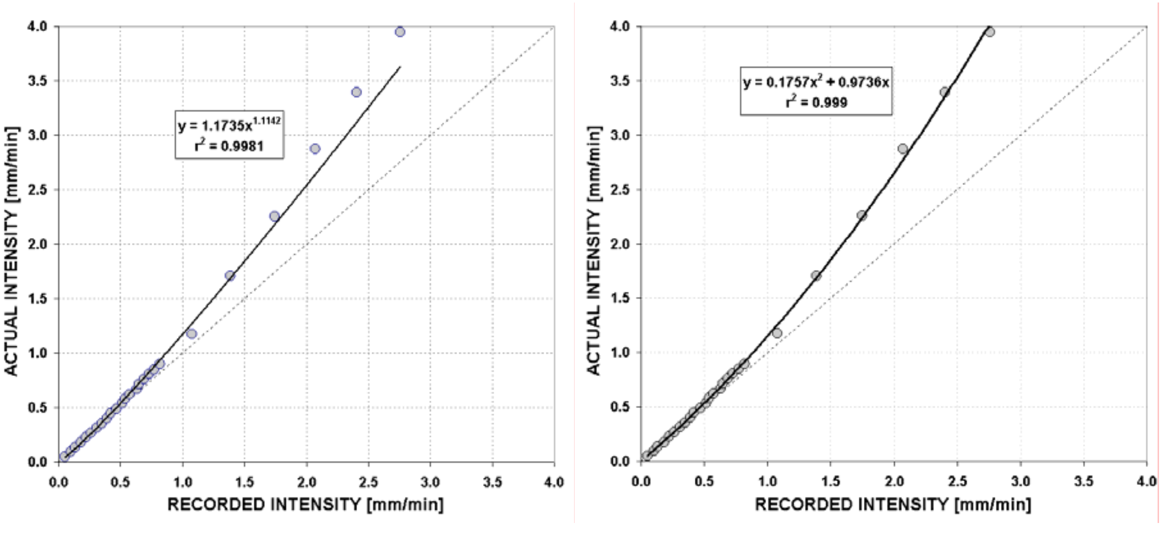

Figure 3-4 Calibration Curves by Power (Left Figure) and Polynomial Function (Right Figure)

The second function was a polynomial one in the form of:

$$i_0 = a_3 \cdot i^2 + b_3 \cdot i$$

With the factor a_3 of 0.1757 and the factor b_3 of 0.9736 the polynomial function can be expressed as:

$$i_0 = 0.1757 \cdot i^2 + 0.9736 \cdot i$$

A stability index of 0.999 and a correlation factor of 0.9995 can be reached with this polynomial function for the correction of the Klusemanngasse tipping bucket gauge. Reliable results can be calculated for Klusemanngasse with this second order polynomial function. In addition to these calibration function results, the ranges of rain intensities also have to be considered. Rain intensities with values of 2 mm/min occur extremely rarely in this CSO Graz-West catchment area.

The correction factor c [-] is calculated by the following equation and is a ratio between actual and recorded intensity:

$$c = \frac{i_0}{i}$$

By means of the correction factor c the actual intensity i_0 can be directly determined from the recorded intensity i as displayed in the following formula:

$$i_0 = c \cdot i$$

where the correction factor c is given as a function of recorded intensity (Vasvári, 1995).

3.5. COMPARISON OF TIPPING BUCKET AND WEIGHING GAUGE DATA

The recorded data of tipping bucket gauge were corrected, due to gauge's errors. The correction values depend on the value of the intensities.

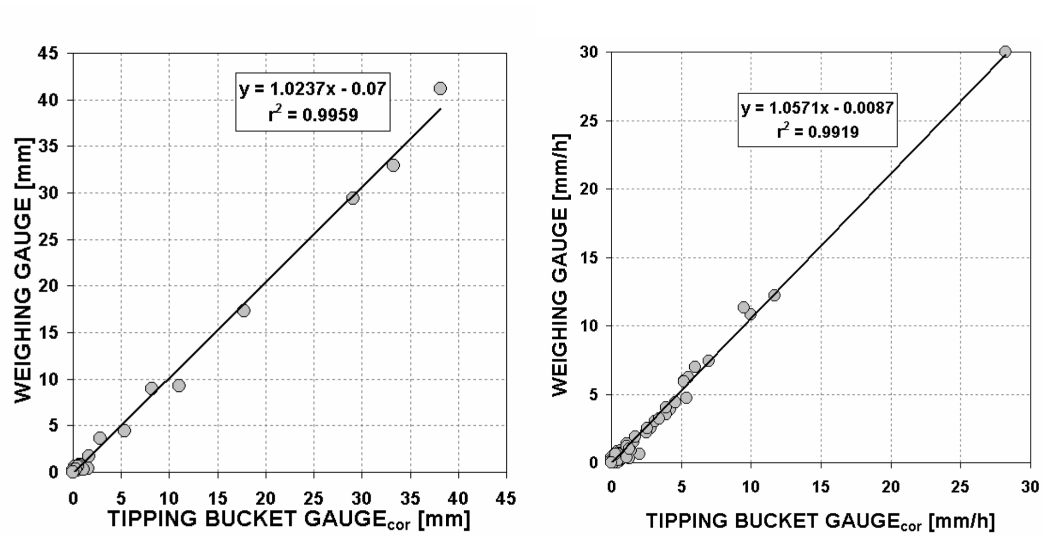

Figure 3-5 Weighing Gauge vs. Tipping Bucket Gauge (Left-Daily Precipitation, Right-Intensity)

To demonstrate the reliability, for example via comparison of precipitation data, it is important to have accurate data as these data will be further used for sewer quality modelling. The correlation between daily precipitation from the weighing gauge and the tipping bucket gauge resulted in a stability index of r^2=0.9959 and a correlation factor of r=0.998 (Figure 3-5), respectively. This result shows good correspondence of these two measuring systems to daily precipitation. The result of the intensity analysis showed similar results to daily analysis. In analysis a stability index of r^2=0.992 had been calculated.

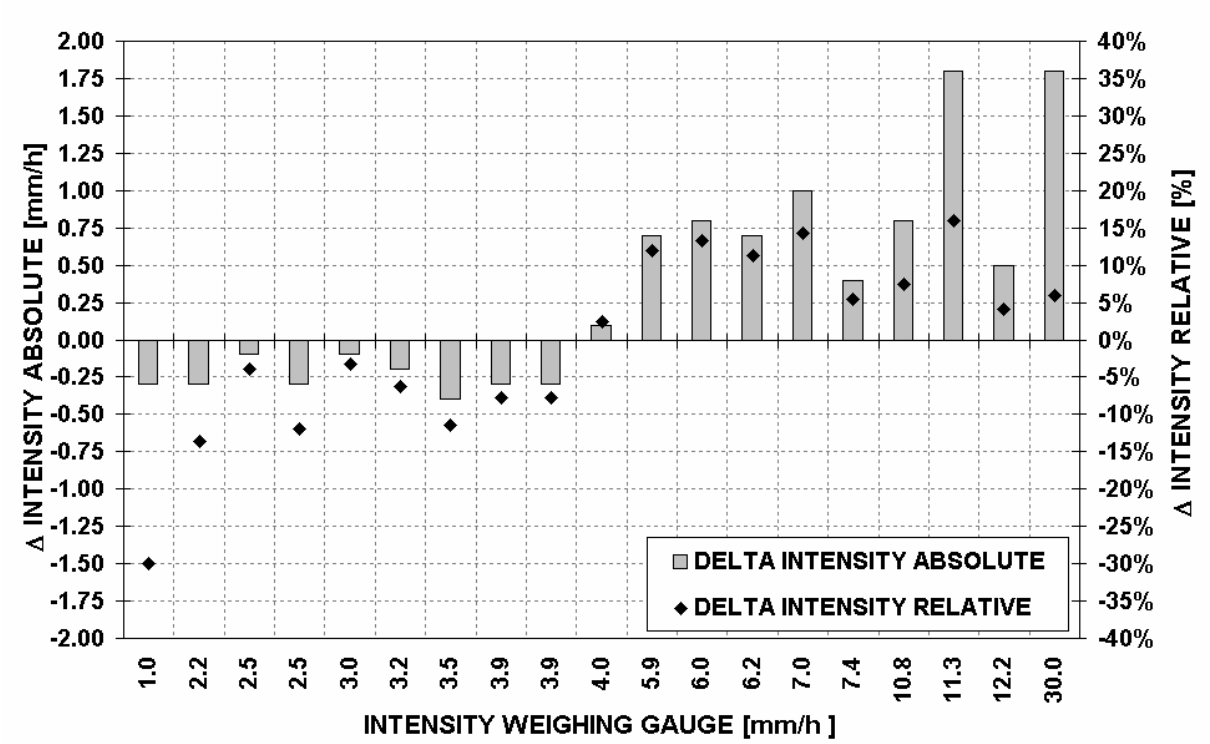

Figure 3-6 Absolute and Relative Intensity Differences between Weighing and Tipping Bucket Gauge

Figure 3-6 shows the absolute and relative differences of measured data between the tipping bucket and weighing gauge with reference to the intensity of the weighing gauge values. Clearly can be seen the influence of adhesion for low intensities. The smaller sums of tipping bucket precipitation data for heavy rains and resulting higher intensities can be explained with the loss of rain during the bucket movement which is also approved by Tekusová et al. (2003).

Table 3-3 Comparison of Rain Depth over a 6-Month Period with Raw and Corrected Data

	Uncorrected Precipitation Data	Linear Function	Power Function*⁾	Polynomial Function
Rain Depth of a 6-Month Period	384.5 mm	399.1 mm	344.7 mm	395.4 mm
Relative Difference	-	+4.7%	-11.2%	+4.3%
Absolute Difference	-	+10.6 mm	-39.8 mm	+10.9 mm

*⁾ power function does not apply for the tipping bucket gauge Klusemanngasse

Table 3-3 shows the precipitation height over a 6-month period of measured raw data and its correction with different kinds of functions. The power function does not fit for the tipping bucket gauge, although the stability index has a value of 0.9981. The large deviations support this assumption. A comparison of the other two correction functions (linear and polynomial) display low differences which would lead to the assumption that a correction of precipitation is not necessary.

3.6. RAIN DATA CORRECTION AND ITS EFFECTS ON QUALITY MODELLING

The highest recorded storm event demonstrates the necessity for precipitation correction. On the 17th of July a storm took place with a rain depth of 38.1 mm (raw data). The maximum intensity reached was 3 mm/min; the intensity of the whole event was 0.49 mm/min for uncorrected data. The corrected data with polynomial function achieved a value of 45.2 mm precipitation height for the whole event and an average intensity of 0.58 mm/min. The difference of corrected and uncorrected data results in 7 mm or 18.6% relating to the raw data.

Table 3-4 Comparison of Load Quality Modelling for COD_{tot}, COD_{sol} and TSS over a 6-Month Period on the Basis of Corrected and Uncorrected Tipping Bucket Gauge Data (modified after Hochedlinger et al., 2005b)

	Differences	Uncorrected Precipitation Data	Linear Function	Power Function*)	Polynomial Function
Rain Depth	absolute [m³]	384.5	399.1	344.7	395.4
	relative [%]	-	4.7	11.2	4.3
Overflow Volume	absolute [m³]	47 266	49 331	42 680	49 254
	relative [%]	-	4.4	-9.7	4.2
Overflow Load	absolute [m³]	21 700	22 621	19 559	22 587
COD_{tot} [1)]	relative [%]	-	4.2	-9.9	4.1
Overflow Load	absolute [m³]	5 670	5 842	5 051	5 833
COD_{sol} [2)]	relative [%]	-	3.0	-10.9	2.9
Overflow Load	absolute [m³]	9 870	10 297	8 908	10 281
TSS [3)]	relative [%]	-	4.3	-10.9	2.9

*) power function does not fit for the tipping gauge Klusemanngasse

1) based on SVM using SMO (240-250) with a mean dry weather concentration of $COD_{tot,eq}$ of 930 mg/l and a mean rain weather concentration of $COD_{tot,eq}$ of 444 mg/l and a mean dry weather flow of $Q_{DW,24}$ of 29.2 l/s

2) based on SVM using SMO (250-260) with a mean dry weather concentration of $COD_{sol,eq}$ of 305 mg/l and a mean rain weather concentration of $COD_{sol,eq}$ of 113 mg/l and a mean dry weather flow of $Q_{DW,24}$ of 29.2 l/s

2) based on SLR (600-647.5) with a mean dry weather concentration of TSS_{eq} of 314 mg/l and a mean rain weather concentration of TSS_{eq} of 206 mg/l and a mean dry weather flow of $Q_{DW,24}$ of 29.2 l/s

A quality model was calibrated and verified based on corrected precipitation data and measured pollution concentration data. It is possible to display the inflow and overflow behaviour with reliable input data.

The effects of corrected and uncorrected precipitation data are displayed in Table 3-4. The table demonstrates the of 6-month period load quality modelling of Graz-West CSO for precipitation volume, overflow volume and overflow load for

$COD_{tot,eq}$, $COD_{sol,eq}$ and TSS. The results of Table 3-4 are similar to those of Table 3-3. These results could lead to the assumption of non-necessity for precipitation correction. This assumption can not be made for heavy storm events. An in-depth analysis of storm events with very high rain intensities evidences the necessity for precipitation correction.

As an example, Table 3-5 shows the result of modelling of the storm event of 17th of July 2003. For every correction method a difference of 17.1% to 18.6% results compared with the raw (uncorrected) data. This makes a difference of overflow volume of 8.4% to 10.4%. The overflow loads of COD_{tot}, COD_{sol} and TSS are in a similar range.

Table 3-5 Comparison of Load Quality Modelling for COD_{tot} for the 17th July, 2003 on the Basis of Corrected and Uncorrected Tipping Bucket Gauge Data (modified after Hochedlinger et al., 2005b)

	Differences	Uncorrected Precipitation Data	Linear Function	Power Function	Polynomial Function
Rain Depth	Absolute [m³]	38.1	44.9	44.6	45.2
	Relative [%]	-	17.9	17.1	18.6
Overflow Volume	Absolute [m³]	5 366	5 925	5 825	5 818
	Relative [%]	-	10.4	8.6	8.4
Overflow Load	Absolute [m³]	2 395	2 642	2 598	2 595
COD_{tot}	Relative [%]	-	10.3	8.5	8.4
Overflow Load	Absolute [m³]	612	675	664	663
COD_{sol}	Relative [%]	-	10.3	8.5	8.3
Overflow Load	Absolute [m³]	1 108	1 223	1 203	1 202
TSS	Relative [%]	-	10.4	8.6	8.5

1) based on SVM using SMO (240-250) with a mean dry weather concentration of $COD_{tot,eq}$ of 930 mg/l and a mean rain weather concentration of $COD_{tot,eq}$ of 444 mg/l and a mean dry weather flow of $Q_{DW,24}$ of 29.2 l/s

2) based on SVM using SMO (250-260) with a mean dry weather concentration of $COD_{sol,eq}$ of 305 mg/l and a mean rain weather concentration of $COD_{sol,eq}$ of 113 mg/l and a mean dry weather flow of $Q_{DW,24}$ of 29.2 l/s

2) based on SLR (600-647.5) with a mean dry weather concentration of TSS_{eq} of 314 mg/l and a mean rain weather concentration of TSS_{eq} of 206 mg/l and a mean dry weather flow of $Q_{DW,24}$ of 29.2 l/s

The influence of corrected and uncorrected precipitation data from the tipping bucket gauge is shown for a storm event with high rain intensities. Over a longer period, the effects of corrected and uncorrected data cancel each other out and result in small differences. The effects for quality modelling of precipitation are often underestimated. Therefore, the accuracy of precipitation data is of high importance.

4. SEWER MEASUREMENTS

Sewer monitoring data contain important information about sewer processes and are further used for design, maintenance and research. The emitted pollution loads result not only from dry weather flow and surface runoff, but also from the remobilisation of sewer deposits and sewer slime during storm water events. Resuspended deposits are often the main cause of the total pollution, but the processes which lead to remobilisation (Bertrand-Krajewski et al., 1998) and those prior to formation of sewer sediments are highly complex and can only be described with limited accuracy by deterministic models. One reason for the remaining problems with regard to a dynamic description of these processes is the lack of dynamic data with sufficient quality for model calibration and validation. Although the application of online techniques has found its way to sewer monitoring it is cumbersome for the maintainer to achieve reliable values. Gruber et al. (2004a) published the wastewater concentrations in sewer systems by means of online techniques.

The amount of inflow (Figure 4-1) to a waste water treatment plant (WWTP) is limited by its capacity. At the treatment plant it would be unfeasible to provide this capacity including stormwater in the treatment process. For example the German A 131E standard specifies approximately two times of the dry weather flow for the inflow flow to WWTP. Hence, the variability of inflow is limited and the collected values are well known.

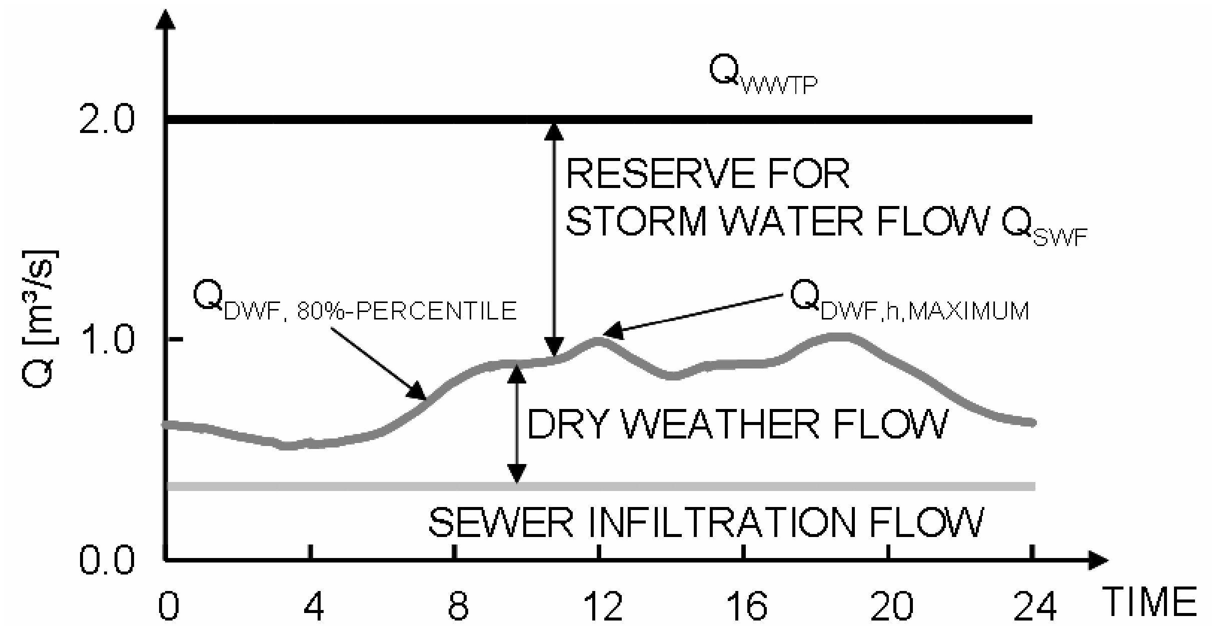

Figure 4-1 Design Flow for Waste Water Treatment Plants (Gujer 2002)

A combined sewer carries both wastewater and stormwater. During rainfall, the flow in the sewers increases as a result of additional stormwater. Even in quite light rainfall, the stormwater flows will predominate, and in heavy rainfalls the stormwater could be fifty or even one hundred times the average wastewater flow (Butler & Davies, 2000). It is a fact that this huge variability of flow can not be measured as accurately as inflow measurements of the WWTP.

Table 4-1 Aims of Monitoring in Urban Drainage and its Requirements

	In the Field (local tasks)	Operating Requirements	Stormwater Management	Research Requirements
Purpose	Adjustment of definite values (e.g. discharge) or activation of a definite process (e.g. storage tank flushing)	Information about operation of plants, failure detection, optimisation of human-resources for maintenance and inspection	Optimised utilisation of existing capacity	Maximum of collecting data to improve existing knowledge or generate new knowledge
Data Transmission	Not implicitly necessary	To deploy labour for immediately elimination of disturbance	Necessary for stormwater management on the basis of input values; transmission depends on the storm event via gained data (short time intervals)	For statistical analysis not necessary; for control analysis absolutely important with high resolution of data and short time intervals
Measurement Accuracy	Rather accurate; the values are basis for engagement decisions	Not exactly; data information is used for a roughly quantification of sewer system status	Precise due to decision making based on gained data	Highest accuracy; data are further analysed; wrong values lead automatically to wrong analysis and resulting false conclusion
Visualisation	For monitoring stations convenient to prove values; otherwise unessential	Overview of e.g. water level in a storage tank; illustration of time series	Overview of e.g. water level in a storage tank; illustration of time series	Directly for analysis dispensable; for failure detection useful
Data Storage	Unnecessary	Long time storage practical to compare previous with current events	Conditional required; verification of storm water management procedure and of effectiveness	Absolutely essential for a possible re-calculating and analysing of data with new approaches

The concentration behaviour of pollution in combined sewers is similar. The concentrations also show a wide range in both dry weather flow and storm water flow due to the remobilisation process of sewer sediments (flush effect). During dry weather, the concentration behaviour is like the flow behaviour. During the night the values of pollution parameters decrease influenced by possible ground water infiltration. In addition, the load of sanitary waste water also decreases. At noon or in the evenings the inflow increases just like the concentration values of the pollution parameters. Thus, the ratio between the minimum and maximum value for concentration can be a factor of four to five. In the case of a storm event, the minimum concentration is considerably lower due to dilution. The maximum concentrations reach nearly the same value as in dry weather.

In terms of maintenance and human-resources optimisation, it is reasonable to gain an overview of the actual situation of flow behaviour by means of adequate measurements and transmission technology. Possible adaptations can be performed on the basis of these measurements with regards to the analysis of collected data in achieving better water protection. Hence, the data collection is subjected to different defaults regarding chosen objectives (Weyand 2001). In one case it can be the information pool for control tasks, in another case it can be the basis for statistical analysis. Table 4-1 shows the aim and the resulting requirements for urban drainage monitoring.

In 1998 a research cooperation was founded in Austria in order to investigate innovative forms of measurement and processing of water quality data. In a first project phase the impact of agricultural land use and a municipal wastewater treatment plant on the river Pöllau were used to exemplify the possibilities of various innovative measurement techniques. Later the project was extended to include a detailed investigation of the processes within a treatment plant. The above-mentioned directives were one reason to continue these cooperative studies and lead to a successive project with the title “Innovative Technology for Integrated Water Quality Measurement” (IMW) (Gruber et al., 2003). The main focus of the project was the design and operation of a water quality network which is suitable to support decision making on a catchment scale. Therefore a modular monitoring station was designed, which is suitable for application in sewers, wastewater treatment plants and surface water bodies. Each of the participating universities (University of Technology Vienna, University for Natural Resources and Applied Life Science, University of Technology Graz) focuses on one of these main fields of water quality monitoring. The focus of Graz was sewer monitoring. Therefore, a sewer monitoring station was installed in combined sewer overflow chamber. Hence, the aims of the project fulfil almost all requirements of Table 4-1. The practical aspects are considered as well as the scientific requirements. Only in one point the attention has not been so deep. There was no consideration given to the economic and optimisation of labour input.

The variability of concentrations and flows has been already described, but there are boundary conditions which should be considered by use of probes and online sensors in combined sewers. Scheer & Schilling (2003) described the different conditions in detail. Waste water ingredients consist of a huge amount of different substances like soluble compounds, particles, solids, grease etc. Almost every imaginable material is found in waste water. Hence, the use of probes has to consider these facts, which are not so significant at a WWTP due to the use of screens.

The use of a sampler or probes for concentration measurements involves the direct contact of waste water with the sampler tube or the probes and often can result in possible clogging. Clogging is a build-up of solids which creates a partial or total blockage of a sewer. Commercial activity, particularly where fats and greases are discharged into drainage systems, can lead to clogging of even the larger sewers. Thus, cables should be installed close to the wall and all parts in contact with waste water should be clog-free. For pressure and velocity probes it is especially advisable to use this kind of construction. At the CSO measurement station in Graz problems occurred in the beginning due to clogging of solids at the bow of the pontoon due to low flow during the night hours. This problem was solved by means of fitting a slightly inclined baffle downstream from the pontoon, which causes a retaining of the sewer flow of some centimetres. The pontoon is installed so high that the deposition of solids is avoided (Gruber et al., 2005).

The compounds of the waste water are not dispersed constantly over the whole sewer section. Normally, waste water is not a homogenous mixture (Wöhrle & Brombach, 1991). It is very difficult to locate a representative sampling position in a combined sewer. Additionally, the infrastructure has to be considered for a monitoring station. A local power supply, as well as a possibility of water supply, has to exist. The equipment must be protected against demolition and vandalism. Sewer safety requirements with regards to explosion-proof probes have to be kept. Either the sensors are explosion-proof or an automatic switch-off is guaranteed. As at a WWTP, the accuracy of measurements depends on the effluent to the inflow of a WWTP due to increasing pollution concentration of the waste water. In combined sewers this inaccuracy is considerably higher. Wöhrle & Brombach (1991) quantified an error of approximately ± 20% for every researched compound, assuming that the sampling position is representative. The position of the sampler tube in the bottom of the sewer can easily gain concentrations up to six-times those of the mean value.

4.1. Other CSO and Sewer Monitoring Stations

The following subchapters will give an overview of interesting combined sewer or CSO monitoring research projects. The catchment area, the probes used and the main conclusions are given.

4.1.1. THE "CHASSIEU-LYON" CATCHMENT AREA

Bertrand-Krajewski et al. (2000a) describes the OTHU "Field Observatory for Urban Hydrology" project, which was launched in Lyon (France). A specific public research institution, the "OTHU Research Federation", was created to lead the project. This federation includes 11 Research Laboratories from 6 Universities and Engineering Schools in Lyon, with 4 additional Research Teams. The Rhône-Mediterannée-Corse Water Agency is also associated to the OTHU Research Federation. One of the key actions of the OTHU concerns the evaluation of the impact of an infiltration basin on soil and groundwater. Barraud et al. (2001) reported that a long-term (10 year) experiment will be carried out on an infiltration basin specifically rehabilitated for measurements and operational drainage issues. In the framework of the OTHU project, ten measurement sites located at five experimental catchments have been equipped with sensors (limnimeter, flow velocity sensor, pH, conductivity, temperature and dissolved oxygen sensors).

The catchment is the Chassieu industrial area, located in the eastern suburbs of Lyon. The total surface is 185 ha, with a rather flat topography (mean slope of 4 ‰) and an imperviousness of about 75 %. The groundwater level is deep (13 m from the bottom of the infiltration basin) so that the unsaturated zone is significant and should be of major interest in the pollutants "clearing up" process (Barraud et al, 2001).

The time step for data sampling ranges from 1 up to 5 minutes. The duration of the project is at least 10 years. A significant effort will be devoted to ensure the requested high quality of data. Pollutant concentrations and loads are measured through continuous monitoring of pH, conductivity, turbidity and temperature. Turbidity, because of its rather good correlation with suspended solids and/or COD concentrations, is considered as critical to get continuous information about pollutant concentrations. Sensors working with infra-red wavelength are used: one based on transmission, one based on nephelometry.

Pollutant loads are also evaluated from samples taken with a refrigerated automatic sampler. Two modes of sampling are used: instantaneous sampling to draw pollutographs and mean samples to evaluate the event mean concentrations.
The following pollutants are analysed: suspended solids, organic descriptors (COD, TOC, BOD_5, DOC), nutrients (NO_3-N, TKN, TN, PO_4-P, PT), heavy metals (Zn, Pb, Cr, Cu, Cd), hydrocarbons, pesticides. However, the same pollutants will be measured at all steps from surface runoff to groundwater to quantify ex- and infiltrating pollution, respectively (Bertrand Krajewski et al., 2000b).

All the sensors (except flow meters) are located in a bungalow where a transit tank is continuously supplied with effluent by a peristaltic pump (Figure 4-2). They are connected to a central data logger.

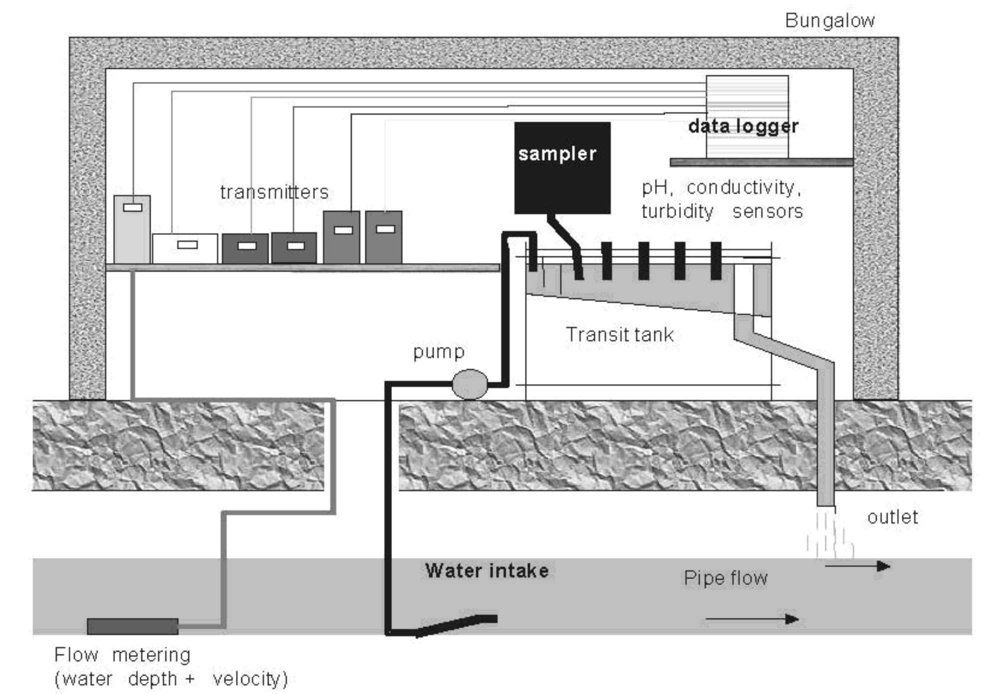

Figure 4-2 Overview of the Sewer Monitoring Station in Chassieu-Lyon (Barraud et al., 2001)

Each sensor has been initially, and will be regularly, calibrated to ensure data quality and reliability. A specific methodology for data validation has also been implemented (Mourad & Bertrand-Krajewski, 2002).

Mourrad & Bertrand-Krajewski (2002) describes that this project comprises of three major aspects:

- The fine calibration of sensors before their installation on sites. This action allows the correction of recorded values and quantification of their uncertainties according to each sensor used and to its specific functioning conditions

- The check-up of instruments and devices data installed on sites. This action is very important to avoid any degradation of measuring conditions, e.g. clogging and/or progressive fouling of sensors by grease, solids and other various wastes. The risk of measuring non representative data (for example, a pH sensor may measure the pH of the fouling layer around the electrode and not the pH of the effluent, a Doppler velocity sensor may be blinded by cans, plastic bags or small branches transported by the flow, etc.) will then be reduced as much as possible. Specific procedures and maintenance frequencies have been established for each sensor.

- The validation of the recorded data. Some sources of errors are unpredictable and data recorded with all the previous precautions can still be affected by faults. The detection of doubtful data and their possible replacement (if necessary, depending on further data treatment and use) are the last tasks to be carried out to ensure data quality control.

4.1.2. THE "LE MARAIS" EXPERIMENTAL URBAN CATCHMENT IN PARIS

From 1994 to 1999, a research program entitled "Production and transport of wet weather pollution in combined sewers" was carried out in Paris, on the Marais experimental catchment. This research had two main objectives:

- A better characterisation of the pollution transported during rain events in combined sewers;

- The assessment, on a single site, of the relative contribution of different sources (runoff, sewage and exchanges with in-sewer deposits) to this pollution.

This type of research should enable targeting of the treatment solutions for urban wet weather pollution – curative as well as preventive – and provide new data which can be used to develop more accurate water quality models (Chebbo et al., 2001).

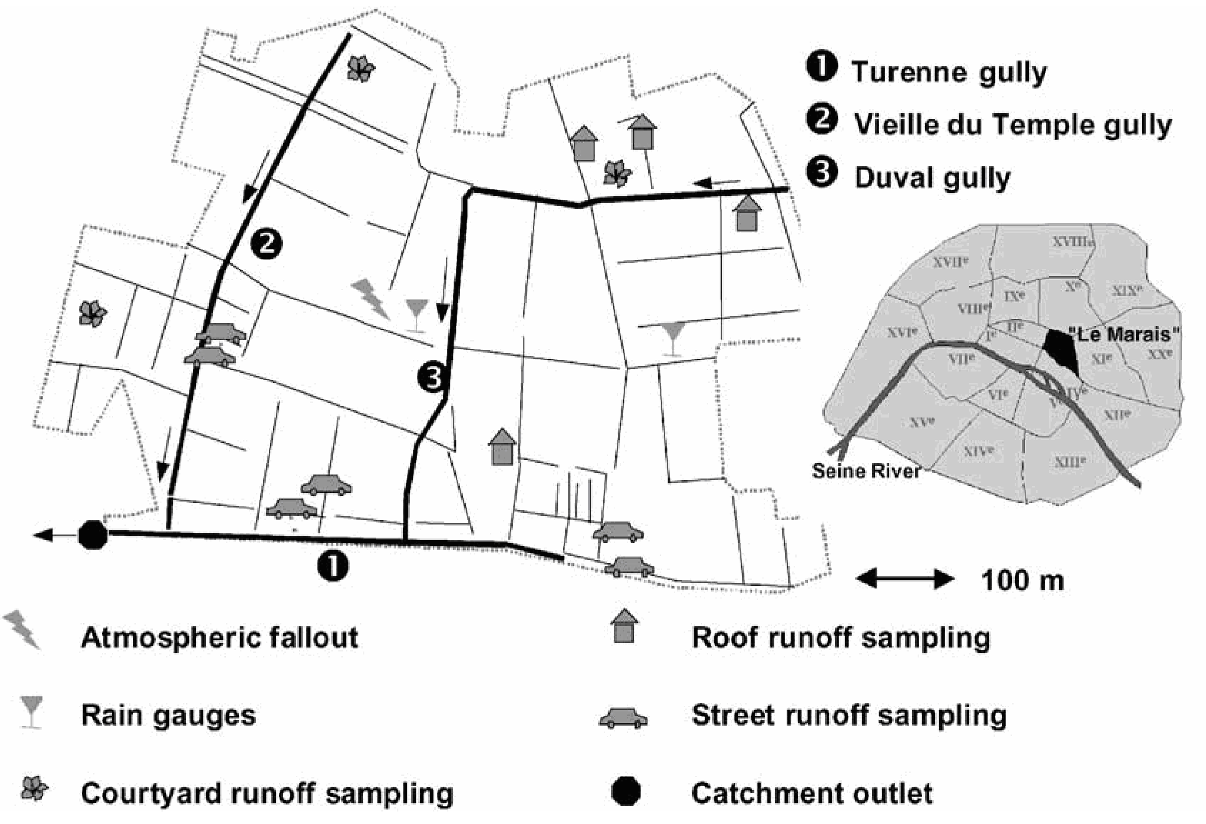

Figure 4-3 Sampling Equipment at the "Le Marais" Urban Catchment (Moilleron et al., 2002)

The Le Marais catchment area (Figure 4-3) is situated in an old residential district of central Paris, with numerous small businesses and almost no industrial activity. It has an area of 42 ha, is densely populated (295 inhabitants/ha) and is 90% impervious.

The catchment area can be divided into roof surfaces (54.4%), streets (22.4%), courtyards (mainly impervious), public squares and gardens (23.2%). The mean slope of the catchment area is 0.84% (Gromaire et al., 2000).

Table 4-2 shows the different measuring points and the equipment deployed at the catchment and the type of measurements carried out. Many precautions were taken to ensure the collection of reliable measurements. The 1st year of research was devoted to acquiring a comprehensive description, of both the surface catchment and the sewer network. This information was used to inform the location of the measurement sites, the choice of the equipment and its installation, as well as the development of analysis protocols. Particular attention was then given to assessing the quality of the measurements carried out and estimating the uncertainty associated with them. This preliminary phase, too often neglected during data collection campaigns, was an indispensable step in ensuring the accuracy and reliability of rainfall, flow and quality measurements. The measurement campaign was carried out over 67 rainfall events for which the concentrations in SS, VSS, COD and BOD_5 were determined over all, or part of, the catchment. Twenty events were studied for heavy metals and 12 events for hydrocarbons. Chebbot et al. (2001) describes that the concentrations were measured for the total sample, for the dissolved phase and for the particle phase. The distribution of pollutants during rainfall and the distribution of particles according to settling velocity were studied for 30 rainfall events at the outlet and for some of these events for road surface runoff.

Table 4-2 Measurement equipment at “Le Marais” (Chebbo & Gromaire, 2004)

		No. Points	Equipment	Type of Measurements
Pluviometry		2	Tipping Bucket Gauge	Rain Hyetograph
Runoff	Roofs	11	Collection Tub	
	Courtyards	3	Automatic Samplers	
	Streets	6	Flow Meter + Automatic Samplers	Hydrograph-Pollutograph and Average Concentrations
Combined Flow at Sewer Outlet		1	Flow Meters + Automatic Samplers	
Sewer Sediments	Type A	70	Sediment Shovel	Volume and Mass of Deposits Pollution Loads
	Biofilms	25	Scraper	
	Water-bed Interface	30	Aspiration Sampler	
			Sampling Box	

The results confirm that a sewer network is not only a transport system, it is also a physical, chemical and biological reactor which affects the quality of urban water by its characteristics. An evolution of the characteristics of wet weather flows has been noticed from the runoff to the catchment outlet. In particular, an increase was observed in the concentrations of SS, VSS, COD, BOD_5 and Cu, in the proportion of particle bound pollutants and in the settling velocities of particles. The assessment of the contribution of different sources to the pollution showed that the exchanges with the organic layer at water–sediments interface make up the main source of wet weather flow pollution for suspended solids, volatile solids, particle bound COD and BOD_5 and copper. Chebbo & Gromaire (2004) reported that this result is of prime importance for the management of wet weather flow pollution. An important reduction of CSOs pollution could be reached through the reduction of this in-sewer pollution stock. For cadmium, lead and zinc, it was demonstrated, on the contrary, that roof runoff provides the main source of wet weather flow pollution on “Le Marais” catchment, due to the corrosion of roof covering materials. In order to significantly reduce the load of these heavy metals in the CSO it appears necessary to reduce their sources in town; in particular via a more judicious choice of the materials used for buildings.

4.1.3. The “Munich-Harlaching” Research Area

From 1975 to 1981 a TU Munich research project for combined sewer measurements was realised. These data have been basis for the further investigations of Geiger (1984). The following considerations give an overview of this research project.
The research area is situated in the south of Munich in the Harlaching district and has an area of approximately 540 ha. The population frequency varies from 50 inhabitants/ha to 250 inhabitants/ha, similar is the situation of impermeable areas with about 25 to 85%. The sewer system is a combined one with an inflow of a sanitary sewer system of 17.4 l/s average flow.

Three precipitation gauges are used in the research area to collect rain data; the rain gauges are also equipped for winter operation. In addition to precipitation and flow measurements, waste water parameters were also quantified. The following parameters were observed: temperature, conductivity, turbidity, total suspended solids (TSS), BOD_5, COD, TOC, Kjedahl-nitrogen and phosphorus.

To quantify stormwater loads it is necessary to determine mean and maximum value of the parameter, a continuous measurement of flow and a high sampling frequency. An exactly chronological synchronisation of the different sampling methods is an absolute requirement. Sufficient calculation and analysis is only possible with an electronic data collection (Geiger, 1984).

A monitoring station was installed at the collection point of the sewer catchment area. The concept of this monitoring station is to automatic waste water sampling for a long period to gain detailed information of the parameters. This monitoring station was controlled by a processing unit which triggered data storage, sampling and a monitoring system. This monitoring station was a quasi-continuous one with five-minute-sampling intervals. Compared with current monitoring stations it was a “half-automatically online” monitoring system.

Sampling was from a continuous waste water flow by means of suction equipment and a sampler with 160 sampling bottles. During dry weather flow sampling had a 90-minutes cycle, during stormwater flow the sampling was based on a determined fictive turbidity load. Figure 4-4 shows the plan of data collection at the Munich-Harlaching monitoring station.

One main problem in this research project was the electrical power supply for rain gauges as well as for the process unit. This problem only could be solved with an external power supply. The complex installation of the power system was essential for long-term monitoring.

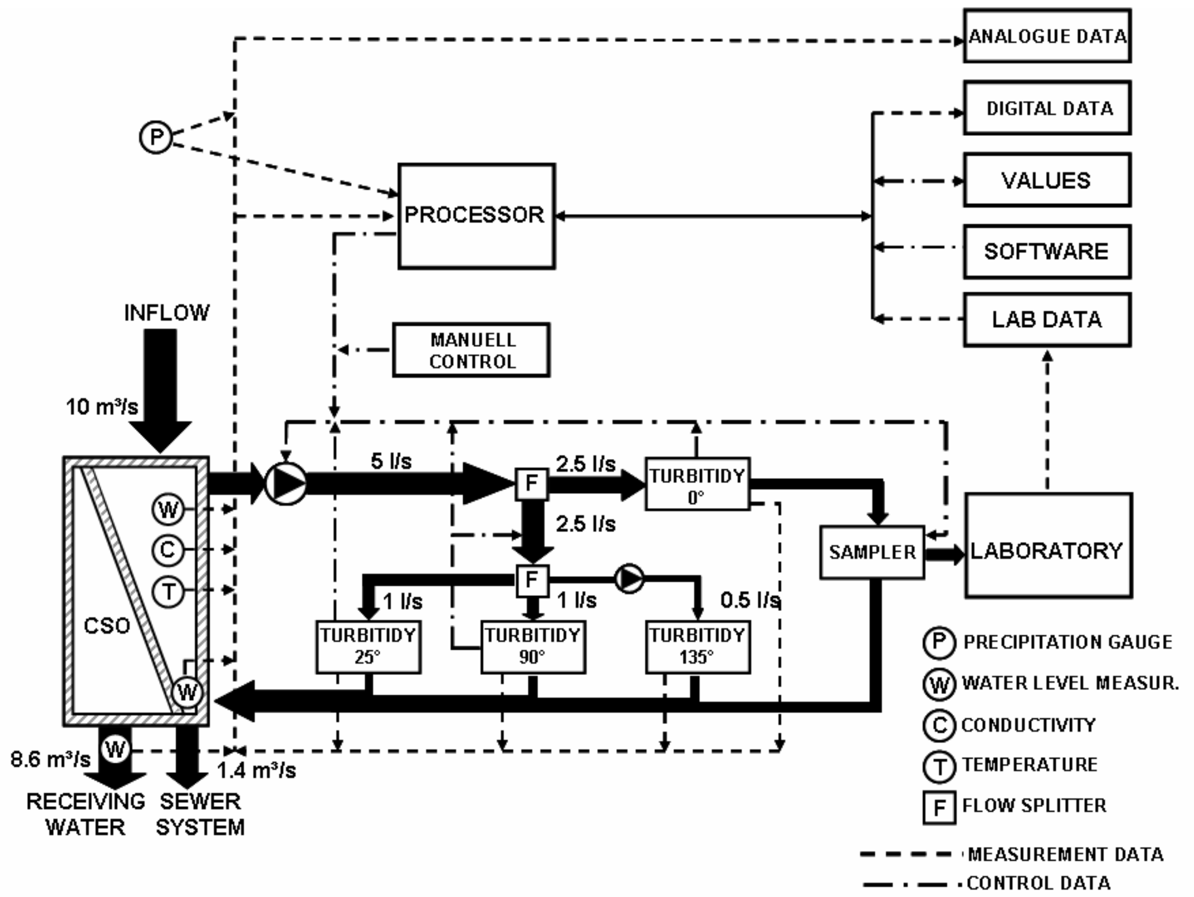

Figure 4-4 Plan of Data Collection of Munich-Harlaching CSO (Geiger, 1984)

An optimal construction of all pumps, pipes and probes was necessary due to difficult conditions in the combined sewer. Each probe was installed in such position that clogging was not possible. The experiences of the research project led Geiger (1984) to the assumption that sensors should not situated directly in the waste water media. A direct incident flow should be avoided. Gruber et al. (2004b) disproved this assumption through experiences in the “Innovative Technology for Integrated Water Quality Measurements“ project.

The implementation of a malfunction alarm system was not realised in the Munich-Harlaching project. The loss of data and operational disturbance was justifiable for the monitoring station. Based on these experiences, even with automatic data collection during storm events a daily allocation of the monitoring station would have been necessary. The immediate analysis in the lab of taken waste water sample due to physical, chemical and biological changing would have been worthwhile. The ideal situation would be an immediate local analysis of the parameters to avoid the influences of temperature or transport. Therefore, the samples were frozen until to analysis in the lab due to the huge amount of samples. Because of the different storing of the samples, the influence of storing time and lab values for the parameters was also determined. Geiger (1984) pointed out the following results from these determinations. COD with a longer conservation time resulted in recognisable lower values and recommended a longer conservation time than four weeks as not practicable. The influence of freezing for the TOC parameter was not noticeable. The BOD_5 parameter could not produce constant values because of the activity of microorganisms also at low temperatures. Hence, not only the value also the freezing time is needed for BOD_5.

The following conclusions of the measurement from the Munich-Harlaching research area can be summarised as follows:

- The frequency of flow characteristic parameters, of pollution concentrations and of pollution loads is event dependant and differs from storm water event to storm water event.

- At the beginning of a storm event, 25% of TSS and 15% of other pollution parameters of all events resulted in a first flush.

- A correlation between the dry period before a storm event and the value of the first flush could not be determined.

- The amount of overflow does not accord with the amount of spilled pollution load.

- The necessity of developing criteria to control CSO emissions with regards to the kind and use of receiving water.

The final conclusion of Geiger (1984) was the effect of receiving water on the one hand, of initial level of water pollution and, on the other hand, of the frequency and duration of CSO emissions. On the basis of the research project and of sewer design experiences, a proposal of limiting values for frequency and duration of overflow loads to receiving water was given (Table 4-3).

Table 4-3 Proposal of Frequency and Duration Limitation of Overflow Events (Geiger, 1984)

Utilisation of Watercourses	Frequency of Overflow Events		Average Overflow Duration (per overflow event)
	Annual	Summer	
	[number]	[number]	[min]
Recreational Use - general	< 20	< 15	< 60
Bathing Water	< 10	< 5	< 30
Fishing Water	< 30	< 20	< 30

4.1.4. THE "STUTTGART-BRÜSNAU" RESEARCH AREA

From October 1966 to October 1968 an extensive sampling project in Stuttgart-Brüsnau took place together with additional pre-investigations from May to September 1966 to quantify boundary conditions of sample preparation before lab analysis.

Table 4-4 Overview of the Stuttgart-Brüsnau Catchment Area (Krauth, 1970)

	Area	Percentage of Area
	[ha]	[%]
Buildings, Parking Areas and Access Paths	7.1	22
Pavements, Streets and Squares	4.9	16
Green and Garden Areas	19.8	62
Impervious Areas	11.9	37
Total Area	31.7	100

The catchment is a combined sewer systems, has a size of 31.7 ha and receives an addition inflow of a sanitary sewer system with 200 to 500 population equivalence depending to the pollution load. The surface has a maximum slope of 6%. Table 4-4 shows an overview of the Stuttgart-Brüsnau catchment area.

The average population density is about 126 inhabitants/ha and increases to an average population density of 336 inhabitants/ha relating to the impervious area. Due to the steep slope of the surface, the slope of the sewer is also quite steep. The minimum slope of the sewer system is 0.5% which is still quite high compared with other sewer systems.

For pollution load calculation in a system, the maximum time of travel is not determinative, but the mean time of travel. The decisive time of travel was defined at 6.6 min with a considering rainfall-runoff intensity of approximately 30 l/(s.ha). The average time was about twice time more with approximately 13 min.

To quantify the pollution load it is necessary to measure the flow as well as the concentration of the pollution. The sampling position was not at the CSO as the overflow channel lead directly to the research WWTP and a loss of solids did not occur. A suction basket was directly positioned in the research WWTP inflow channel which was not dipped in dry weather flow. If the inflow reached more than 20 l/s than an eccentric worm pump started pumping continuously. To avoid freezing of the suction tube a regular cleaning with air pressure was conducted, especially in the winter season. In summer, the cleaning intervals were shorter to prevent a possible influence on the samples of algae growth. For representative sampling a changing of the sample from taking to analysing had to be avoided. An analysis or sample preparation took place not later than 15 hours after sampling. With this research project results regarding, pollution loads as well as mean concentrations resulted. For example a mean concentration in the dry weather flow of 443 mg/l was determined for COD. However, this value has to be considered with the knowledge that the sample was influenced by particle settling.

4.1.5. THE BRAUNSCHWEIG RESEARCH AREA

The research took place in Braunschweig and consisted of three different areas:

- BS I: “Eastern Area”
- BS II: “Downtown”
- BS III: “Braunschweig Total Combined Sewer Catchment”

Table 3-5 displays the typical data and a comparison of the specific sewer catchment areas of Braunschweig. Figure 4-5 shows an overview of the Braunschweig sewer catchment with BS III and the part catchments BS I and BS II. The sewer system is flat for all three highly populated areas.

Table 4-5 Characteristic Data of the Three Catchments (Macke et al., 1987)

	BS I	BS II	BS II
Total Area [ha]	109	144	549
Impervious Area [ha]	63	107	320
Runoff Coefficient	0.58	0.74	0.59
Inclination [%]	0.1	0.1	0.1
Sewer Slope [%]	0.05 – 0.2	0 – 0.2	0 – 1
Time of Transfer [min]	18	35	45 – 60

Only one CSO is situated in the sewer catchment BS I at P1 with the sampling station. Hence, this CSO was the only possibility of spilling. The main overflow to receiving water of the highly meshed sewer system in the area BS II is at point P2. The remaining 80 downtown CSOs are designed for an annual overflow of n < 2. The total BS III catchment with the P3 sampling point has an annual overflow rate of n <8 – 10. Due to the large numbers of throttles and special urban drainage buildings at storm events backwater effects take place. Thus, the depositing of sediments results in permanent sewer deposits.

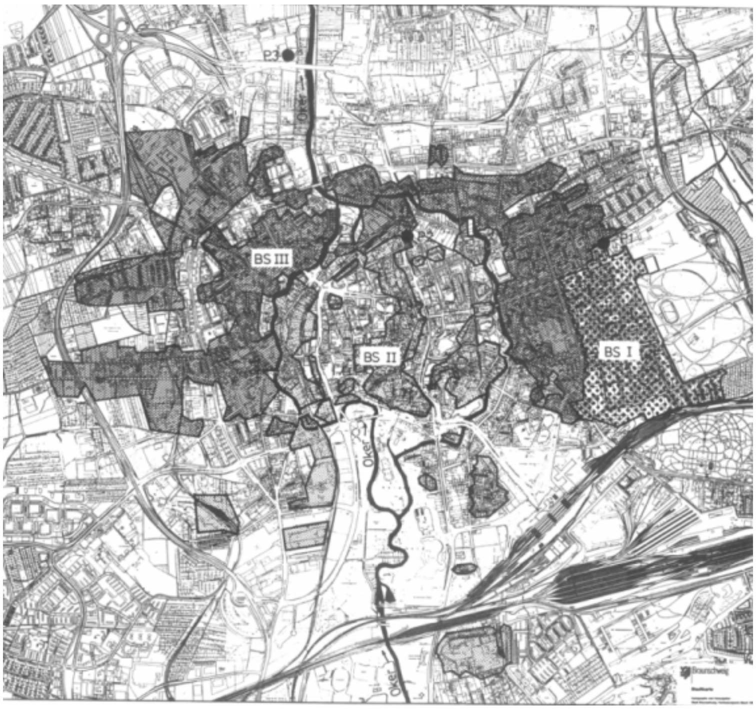

Figure 4-5 Research Area of the Braunschweig Combined Sewer System (Macke et el., 1987)

Since 1998, the measurement program has included precipitation measurement, water level and flow measurements in the sewer as well as dry weather and storm weather sampling. To quantify different precipitation behaviours of the catchment area, six tipping bucket gauges with a 0.1 mm resolution collect rain data. The gauges are uniformly distributed over the city. The continuously registration of sewer flows and CSO overflows is guaranteed with permanent measurement stations of water level and velocity. The related data storage units with rechargeable batteries are explosion-proof and have a measuring interval of two minutes. The data are readout every six weeks.

At the main CSO, an automatic sampler for 16 single samples per storm event is installed in the subsurface including power and water supply. The sampler is triggered flow dependently to guarantee an optimal determination of a possible 1st flush. At the beginning, the sampling time is short and increases with longer sampling time over the storm event. From 1988 till 2000 at the sampling stations in total approximately 500 storm events were completely sampled. In addition, 32 daily dry weather cycles were investigated and from 12 000 single samples 40 000 pollution parameters were analysed. The main parameters were COD, TSS and nutrient parameters.

De Vries (1993) describes the pollution load in the storm event. The total pollution load is divided by part loads depending of the appearance and derivation and its distribution. Basically, the dry weather load part of the storm load depends on the time of day and a certain amount from temporary storage in the sewer system itself. The time distribution of the surface load is affected by hydraulic behaviour on the surface, the amount, kind and properties of pollution potential. The remobilisation of the sewer pollution potential is characterised by hydraulic boundary conditions in the sewer as well as the amount, disposition and characteristics of sewer sediments and biofilm. Table 4-6 gives an overview of pollution loads and storm water concentrations for COD and TSS. De Vries (1993) demonstrates the highly polluted rain weather part of the BS I eastern catchment area.

Table 4-6 Sum of Pollution Loads and Mean Load-Weighted Concentrations of Storm Water Considering Pollution Load Parts (Dry Weather, Surface and Sewer) for the BS I Catchment Area in Braunschweig on the Vasis of 77 Storm Events (de Vries, 1993)

	Load Sum	Concentration	Load Sum	Concentration	Annual Loads	
	COD		TSS		COD	TSS
	[kg/ha]	[mg/l]	[kg/ha]	[mg/l]	[kg/(ha.a)]	
Storm Water	1 749	397	1 933	439		
Dry Weather	450	663	233	343		
Rain Weather (Surface+Sewer)	1 299	349	1 700	457	1 204	1 577

The area of the storm water load curve (Figure 4-6) shows the importance of sewer potential for storm water pollution which totals the main part of load. The steep rise at the beginning compared with the surface potential indicates a fast potential growth after a storm event starting due to remobilisation of sewer potential.

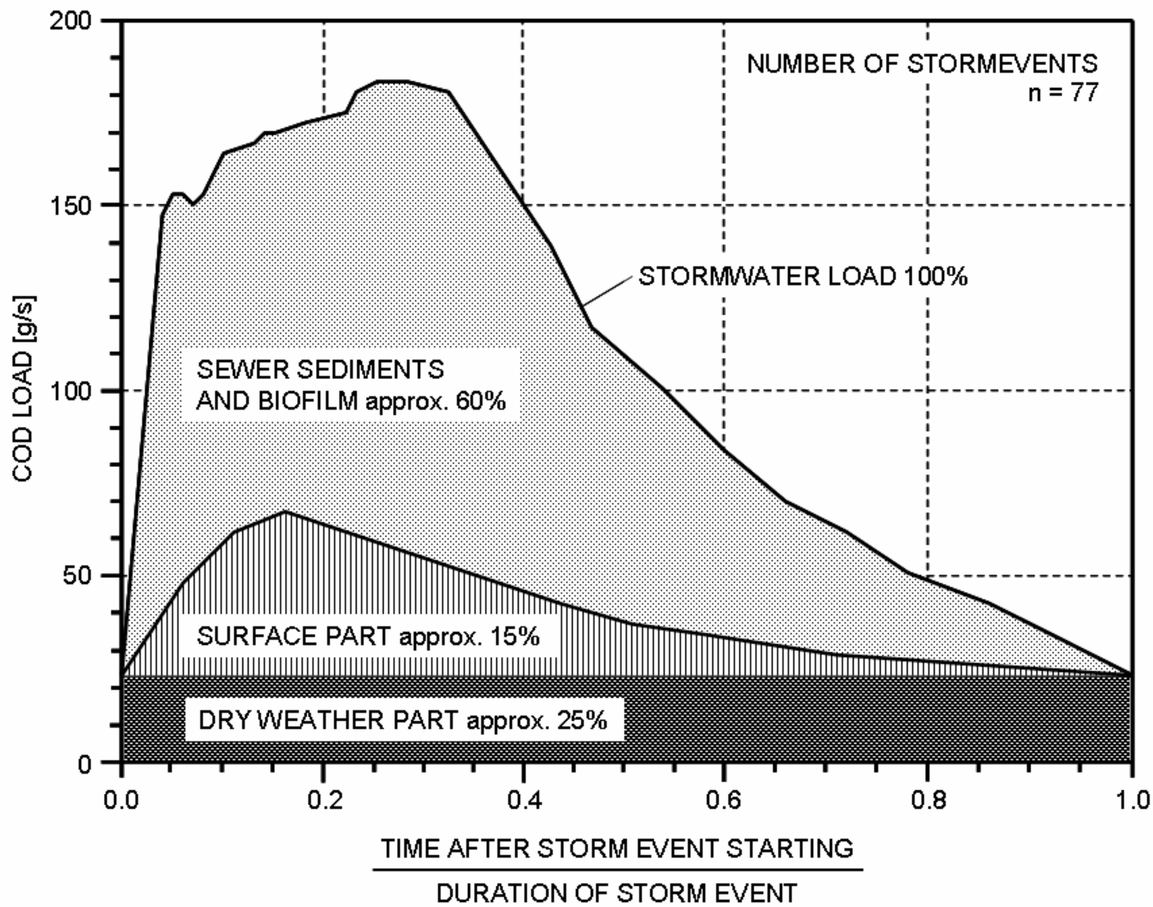

Figure 4-6 Parts of Stormwater Load Considering the Source of Different Parts (de Vries et al., 1993)

The potential results in COD of approximately 60% (without dry weather part) at the BS I catchment. This description can be confirmed by the research results of Reiff (1992). About 65% to 90% of the biofilm flushed away in the 1st minutes of a storm event. Only 15% of the whole storm water pollution comes from the surface potential. The sewer potential exceeds the surface potential by a factor of four. Hence, the assumption of the A 128E German standard (1992) does not fit for flat sewer systems (Macke et al., 2002). In A 128E, the mean pollution of rain weather is only based on the surface potential. The influence of sediments is only minor considered with an allowance at dry weather run-off concentrations. This consideration of the sewer potential can not consider the real behaviour. The investigations of Braunschweig demonstrated that not all sewer deposits are washed out by consecutive storm events. The thesis of a fast wash out of sewer sediments at a storm event does not hold for flat sewer systems (Macke et al., 2002).

Based on the two-components-method, the mean storm water concentrations of COD (Table 4-6) are determined. The A 128E (1992) German standard recommends a COD concentration of 107 mg/l for a sediment-free sewer. This value is a result of following assumptions:

- Annual COD surface potential of 600 kg COD/ha
- Annual precipitation height is 800 mm
- The effective precipitation is 70% of the total precipitation due to loss of precipitation

The following equation shows the achievement of 107 mg/l for COD in the storm water in detail.

$$\mathrm{COD_{SWF}} = \frac{\text{yearly COD surface potential}}{\text{effective yearly precipitation height}} = \frac{600\ [\mathrm{kg\ COD}/(\mathrm{ha}\cdot\mathrm{a})]}{800\ [\mathrm{mm/a}]\cdot 0.70}\cdot 100 = 107\ [\mathrm{mg/l}]$$

The determined thrice higher concentrations by means of measurement data analysis confirms the unconsidered realistic load potential of storm water for flat sewer system of the German standard A 128E (Macke et al., 2002).

The results draw the conclusion of the accumulated pollution potential dependence in the sewer system. The main component of sewer pollution is the wall shear stress τ of considered dry weather pollution. Macke et al. (2002) calculated the critical slope I_{crit} and corresponding wall shear stress τ on the basis of the A 110E German standard. The results of this approach produce quite higher sediments values of sewer potential.

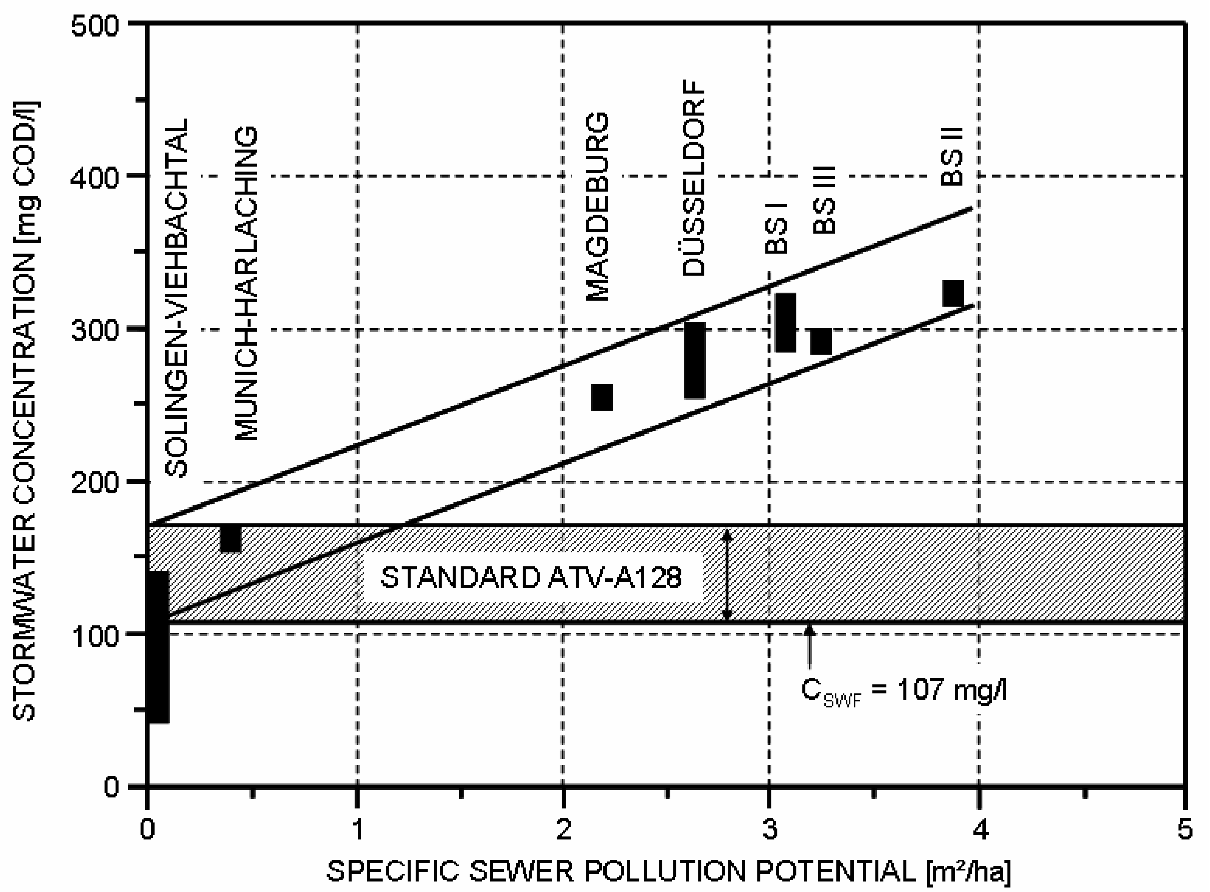

Figure 4-7 Stormwater Concentration vs. Specific Sewer Pollution Potential (Macke et al., 2002)

Figure 4-7 displays the results of sewer potential calculation compared with other research areas. Flat sewer systems predominating in big cities have significant sewer potentials. The COD storm water pollution concentration of 107 mg/l suggested in A 128E is only obtained in steep sewer systems (Macke et al., 2002) where the minimum slope for a deposit-free waste water transport is ensured. The sewer potential is not available as the pollution comes from the surface wash off. With the decreasing slope of the sewer system, the sewer potential increases due to accumulation and remobilisation of sewer sediments. The consideration of the design of sewer sediments of A 128E (hatched area in the figure) does not demonstrably include the real rain water part. In flat sewer systems, which are branched, present a two to three times higher rain weather pollution of approximately 200 till 300 mg/l for COD.

4.2. Flow Measurements Basics and Devices in the Graz-West CSO

The easiest way to describe the stream flow is by using a rating curve which gives the water level and discharge correlation. Due to the typical characteristic hysteresis curve, the application of the rating curve can only be used conditionally. The energy curve and the sewer slope are not parallel at the same water level by an increasing or decreasing flow and, therefore, a different velocity and flow results, respectively.

Hence, the determination of the mean velocity by measurement is reliable for flow calculation.

4.2.1. “FLO DAR^{TM}” CONTACTLESS RADAR FLOW METER

A contactless radar flow meter from MARSH McBIRNEY (Flo Dar^{TM}) is used for the inflow measurement of the sewer. The “**Ra**dio **D**etecting **a**nd **R**anging” method sensors able to locate objects as well as determine velocity. In urban drainage environments, the devices are used to determine flows based on measured water levels and velocities. Figure 4-8 gives an overview of this method.

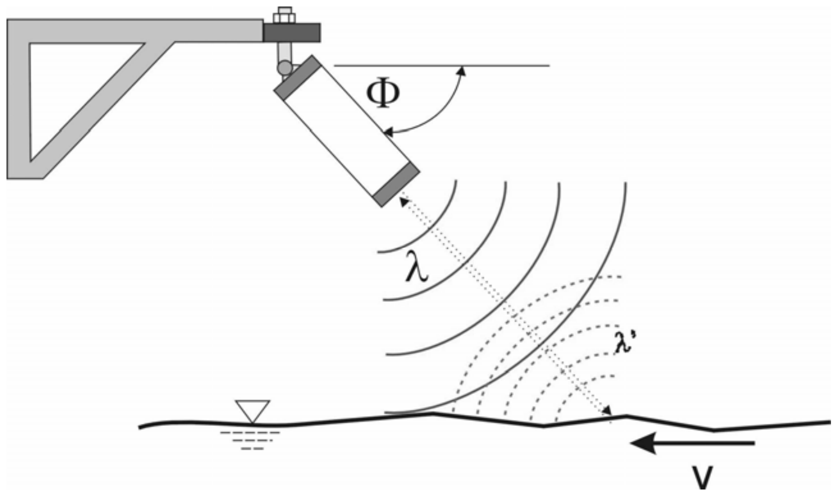

Figure 4-8 Principle of Radar-Doppler Method for Velocity Measurement (Felder & Siedschlag, 2004)

The operational mode of radar is based on echoic-principle of electromagnetic waves. The FloDar measures with microwave radar at a frequency of 24.125 GHz (Sévar et al., 2004). These microwaves are beamed with a duration and an interval of a millionth of second. If these waves are impinged at a balk then the waves are reflected and the reflected beam can be received at the transmitter position. Electromagnetic waves transmit at the speed of light (approximately 300 000 km/s). The distance to a definite point can be determined by means of the measured wave running time. The following equation describes the functional coherence:

$$s = \frac{t \cdot c}{2} \left[m \right]$$

where s is the distance which has to be determined, t is the wave running time and c is the speed of light. A comparison of transmitter frequency by means of the changed echo frequency by the Doppler principle allows a specification of the movement behaviour (velocity and direction).

The Doppler shift describes the wavelength change of sonic or electromagnetic waves if the source of the wave and the scanner moves relatively. Hence, a wavelength shift happens if the wave is bounced off a reflector which moves in relation to the transmitter and receiver (Figure 4-8). The velocity of the water surface can be calculated with this equation:

$$v = \frac{\left(f(\lambda) - f(\lambda')\right) \cdot k}{2 \cdot \cos\varphi} = \frac{\Delta f \cdot k}{2 \cdot \cos\varphi} \left[m/s\right]$$

with:

- v – velocity of the water surface
- k – system constant
- Δf – difference frequency
- λ - transmitted wavelength
- λ' - reflected wavelength

By means of the radar Doppler shift it is possible to also measure velocities of moving objects on the water surface. Assuming that the particles are moving as fast as the water, the velocity of the water surface can be calculated. Thus, the area, the distance and the inclination of the transmitter to the reflecting water surface are measured.

Figure 4-9 shows the velocity distribution in the cross sectional areas from a free flowing open channel which is reflected at the surface. The Flo Dar™ radar device beam senses the velocity spectrum near the surface; it is capable of measuring the velocity distribution in the cross sectional area of the pipe. The velocity spectrum varies depending on the velocity distribution in the pipe. Because of the large spectrum the correction required to calculate the average velocity is reduced to a minimum. In most standard applications this correction is close to one which means sensed velocity is equal to average velocity.

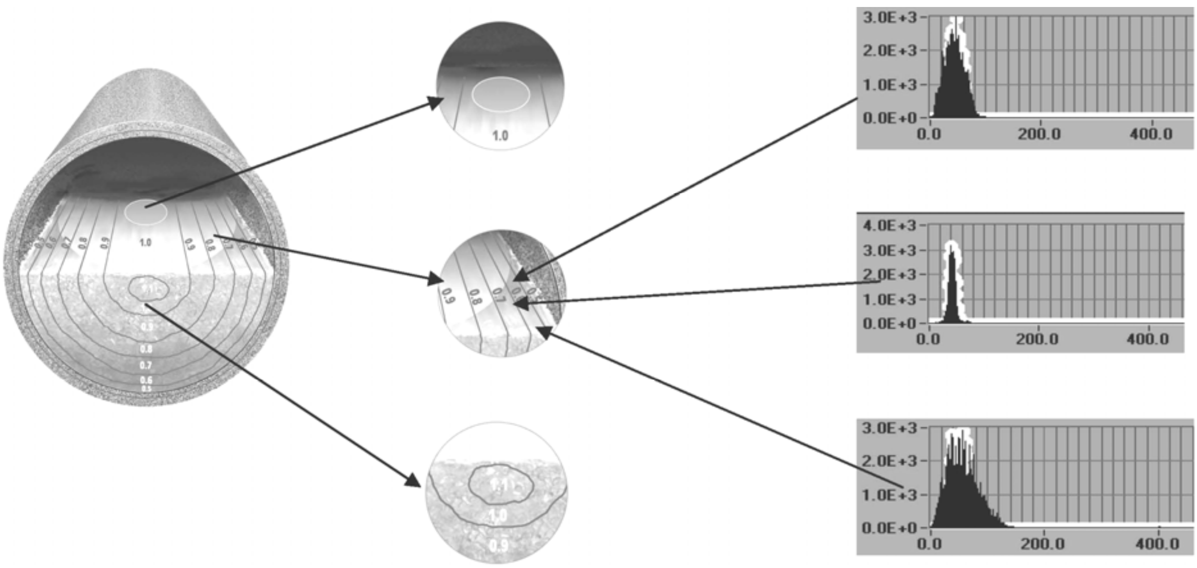

Figure 4-9 Example of Radar Velocity Measurement and its Spectra (Sévar et al., 2004)

4.2.2. Calculation of the Flow in the Sewer

The Calculation of the flow is based on the basis of a continuity equation with the product of mean velocity and flowed area. The mean velocity is estimated with the scale factor k from the measured surface velocity. The scale factor k describes the ratio of average and local velocity. Thus, the following equation can be written:

$$Q = A(h) \cdot k \cdot v_{loc}$$

with:

- Q – flow in the sewer [m³/s]
- A(h) – streamed area as a function of the water level h [m²]
- k – correction or scale factor
- v_{loc} – local measured surface velocity [m/s]

The dimensionless scale factor k can be determined by section and water level depending on the calibrating position. The functional correlation of the k-factor and of average and local velocity can be given by the following equation:

$$k(x, y) = \frac{v_{av}}{v_{loc}(x, y)}$$

Because of the coherence of k(x,y) from the local velocity measurement the k(x,y) is a two-dimensional function of the cross section coordinates x and y. From the previous equation it can be seen the dependency of k(x,y) is defined as the reciprocal value of the dimensionless turbulent velocity distribution. The accuracy of the flow Q is strongest depending on this k factor which is known in most cases very inaccurate. Modern probes gain water level and surface velocity values of high quality. The k factor is strongly dependent on the section geometry of the sewer pipe and especially of the water level. Hence, for accurate flow measurements, recalibrations for every section at different water levels are necessary (Kölling, 2000).

The k factor is dependent on:

- water level
- position of local velocity measurement
- shape of the measurement cross section
- roughness of the channel
- Reynolds' number

The accuracy of traditional in the field calibration like whole section detection or dilution tests is limited due to limited and dangerous conditions in the sewer pipe. Extremely inexact flow measurements are if in the field calibrations are not possible as with overflow channels and the calibration is substituted by estimations. The strongly water level dependent calibration function k(h) can not be compensated for easily with extrapolation of dry weather calibrations. Hence, the accuracy of many flow measurements in sewer systems is not low due to wrong velocity or water level measurements. The calibration in the field is, to put it mildly, insufficient or not available. The simulation of this k factor is a solution to this problem and can be solved as Kölling (2004) presented with SIMK®.

4.2.3. "OCM PRO" ULTRASONIC FLOW METER

The ultrasonic flow measurement principle for velocity is based on the direct run-time of an acoustic signal between two ultrasonic sensors, so-called hydro acoustic oscillators. A sound wave which runs against the flow direction has a longer run-time than a sound wave which moves in the same direction. The difference in running time is directly proportional to the velocity and with a known cross section area it is also proportional to the flow. In free flowing sewers the streamed area is normally variable; therefore the determination of the cross section geometry as well as the water level is needed. Figure 4-10 displays one ultrasonic measurement device with integrated and one with an external water level measurement.

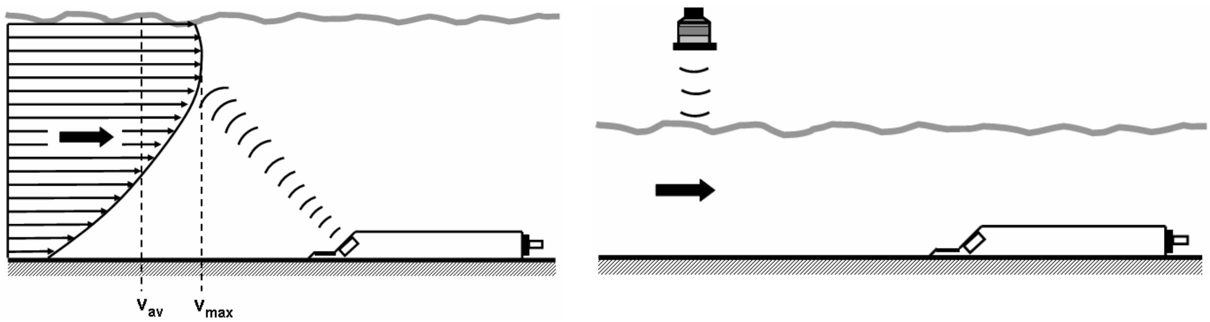

Figure 4-10 Ultrasonic Device with Integrated (Left Figure) and External (Right Figure) Water Level Measurement (Teufel, 2004)

In the CSO Graz-West overflow channel, the ultrasonic device is adapted with an external water level measurement also measuring on the basis of the ultrasonic run-time method. The decision for an external flow measurement is due to its measurement accuracy which is more precise at low flow than the integrated one.

For ultrasonic run-time measurement the transmitter receives a voltage pulse and transforms this pulse in acoustical waves; the run-time in water of these waves is measured. The run-time can be calculated in flow direction:

$$t_1 = \frac{L}{c + v}$$

and against flow direction:

$$t_1 = \frac{L}{c - v}$$

with:

- c – acoustic velocity
- L – length of acoustic distance
- v – flow velocity

If the voltage pulse is not transmitted back-to-back, but transmitting and receiving is simultaneous, then the sonic velocity can be eliminated:

$$v = \frac{L}{2} \cdot \left(\frac{1}{t_1} - \frac{1}{t_2} \right)$$

In practise, the voltage pulse is transmitted diagonally through the water, whereas the transmitter is sending as well as receiving. Therefore the flow velocity is:

$$v = \frac{L}{2 \cdot \cos\Phi} \cdot \left(\frac{1}{t_1} - \frac{1}{t_2} \right)$$

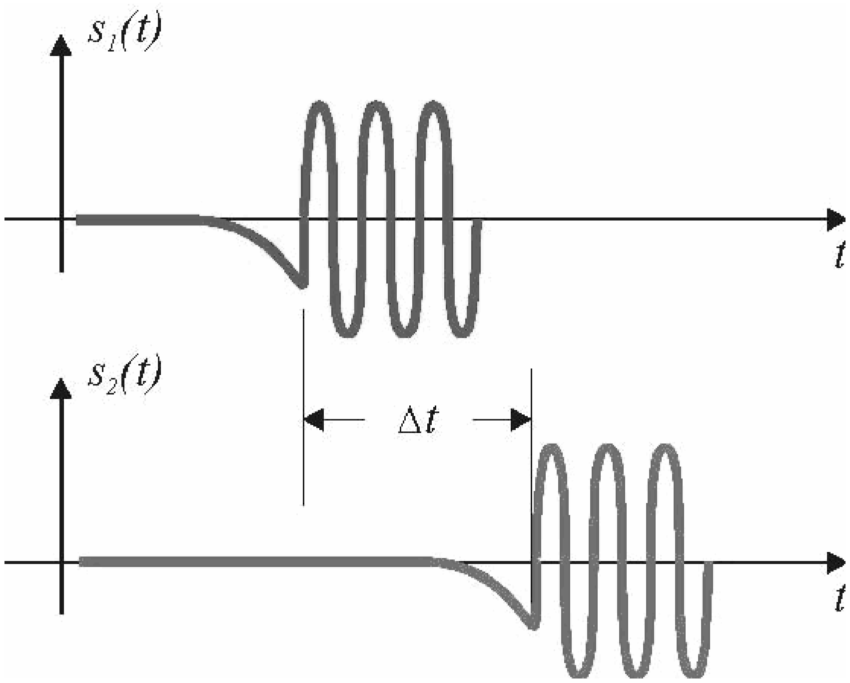

Figure 4-11 Time Series of Transmitting Signal of Sender 1 and 2 (Skripalle, 2004)

Most of the analysis electronics used in the past had the disadvantage that an amplitude device for signal detection with adjacent zero detector was used (Skripalle, 2004). This construction is based on the assumption of the difference between the amplitude of transmitting signal and noise. This assumption looses its validity due to a low transmitting-noise-ratio. Finally, this ratio is a limiting factor for difficult measurements. This limiting factor is the main problem especially for measurement with extreme fluctuations of the quality. Hence, a wrong measurement value results due to unfavourable amplitudes.

Modern methods of signal processing are not based on the amplitude of the signal and determine the next zero point. The correlation in the signal is used instead. This method uses the comparison of time series' transmitting signal (Figure 4-11) to calculate the cross correlation function. This function is a rate of the correlation of time series $s_1(t)$ and $s_2(t)$ which are shifted by the period τ. Knowing the position of the correlation maximum of this function ($\tau = \Delta t$) and other characteristics of the signal the run-time difference and, therefore, the velocity, can be determined with the following equation:

$$\Phi_{s1,s2}(\tau) = \lim_{T\to\infty} \frac{1}{2 \cdot T} \cdot \int_{-T}^{+T} s_1(t) \cdot s_2(t+\tau)\, dt$$

The ultrasonic pulse Doppler principle is a further development of Doppler technology. The ultrasonic pulse Doppler method is based on a short ultrasonic frequency batch with a definite length. With the knowledge of acoustic velocity (temperature compensated), the measurement position is determined by choice of the sending and receiving frequency. For the transmitting signal a definite measurement window and range is accessed, respectively. The frequency shift of the transmitted ultrasonic signal is a value for the velocity in the measurement window. Echoes of particles in other measurement areas have no influence on the velocity measurement.

The correlation method with the "comparison" of two time shifted ultrasonic scans identifies the particles (solids, particulate matter, bubbles) in the water. The 1st scan is realised by means of Doppler pulse principle already described. A millionth of a second after the 1st scan the 2nd scan takes place by saving the echoic sample. The identical measurement area is assured with the help of run-time method.

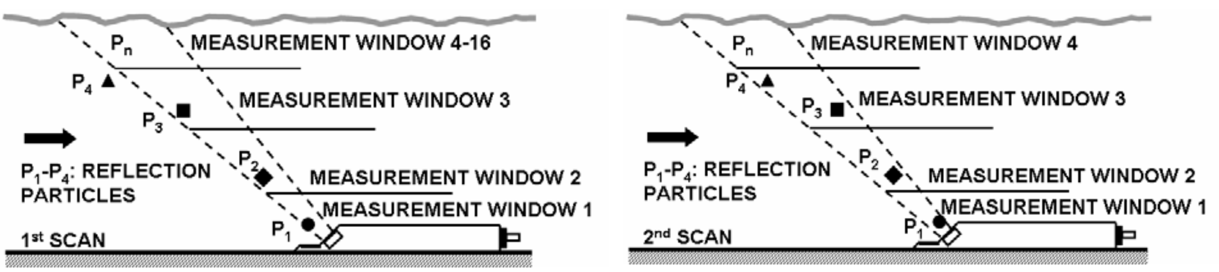

Figure 4-12 Cross Correlation Method of 1st and 2nd Scan of Particles (Teufel, 2004)

The correlation of these two signals produces the time shift determination in consideration of the beam angle and the pulse replication rate. Thus, the velocity of the water can be calculated by these data. Figure 4-12 shows the principle how the ultrasonic signal works on the basis of cross correlation. It can be seen that a maximum of 16 measurement windows can be used for velocity determination. Thus, the measurement of velocity profiles and of half filled pipes is possible.

The influence of the different failures and its summation of measurement devices, especially for flow measurements, will not be explained as many papers have already described the coherences and its effects. Uhl (2000) gives a good overview of this correlation.

4.3. CONCENTRATION MEASUREMENTS BASICS AND DEVICES

4.3.1. ION-SELECTIVE ELECTRODES – NADLER SENSORS

4.3.1.1. MEASUREMENT PRINCIPLE

Ion-selective (ISE) probes are based on the potentiometric measurement principle (Figure 4-13). The probe includes at least two electrodes, a reference and a measurement electrode. The measurement electrode is equipped with a special membrane, capable of binding specific reversible ions. Depending on the activity of the measured ions in the liquid, a varying number of ions will bind to the measurement electrode – resulting in a varying potential difference between the measurement electrode and the reference electrode, which shows a constant potential in reference to the medium. The measured potential is put in relation to the activity of the measured ion by means of a calibration function (Winkler et al., 2004).

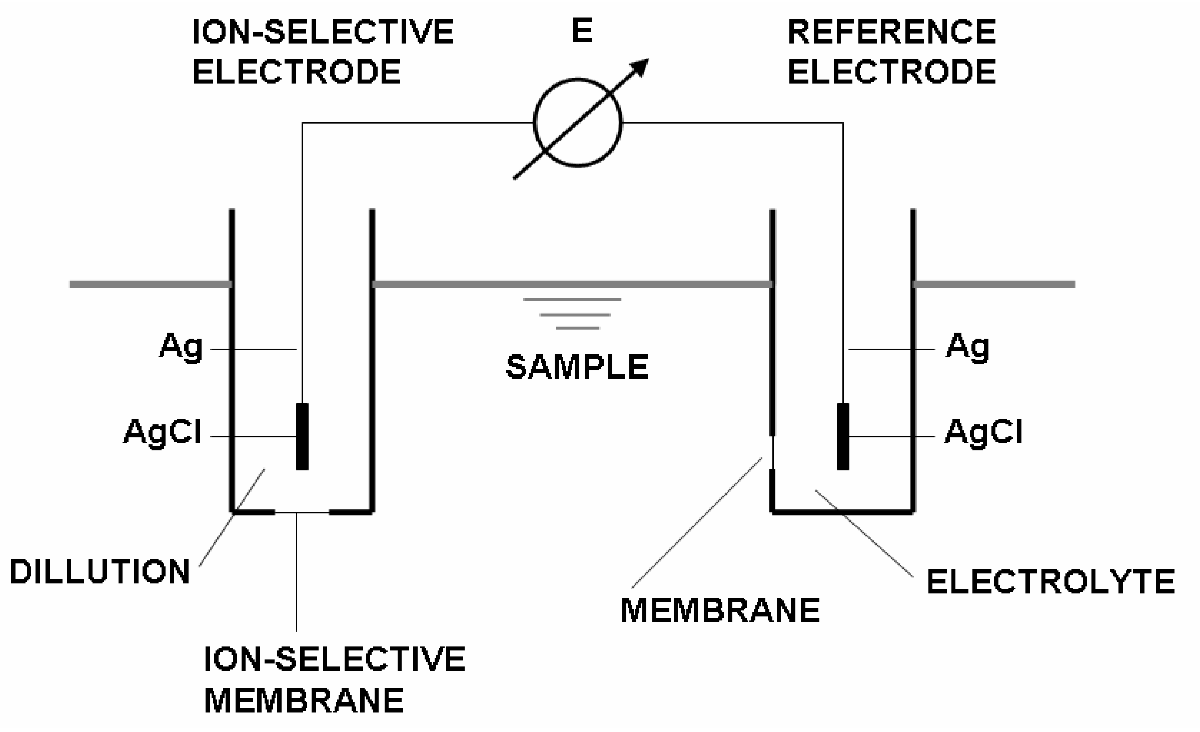

Figure 4-13 Scheme of Measurement Configuration of ISE and Reference Electrodes (VSA, 2003)

The potential difference measurement between a reference electrode and ISE detects the potential ΔE of the measurement electrode with a logarithmic behaviour by a standard background electrolyte can be expressed with following equation:

$$\Delta E = E_2 - E_1 = 2.303 \cdot \frac{R \cdot T}{z_i \cdot F} \cdot \log\left[a_i + \sum_{j \neq i}\left(k_{ij} \cdot a_j^{\frac{zi}{zj}}\right)\right]$$

where ΔE is the potential difference [mV] of two measurements (E_1, E_2), E_1 and E_2 are the measurement potential with an ion activity of a_1 and a_2, F is the Faraday constant of $9.6485 \cdot 10^4$ [A·sec/mol], R is the ideal gas constant of 8.314 [W·sec/(mol·K)], T is the absolute temperature [K], a is the ion activity [mol/l], i and j are the main and interfering ion indices and z describes the ion electrovalence.

It can be seen in the previous equation that the membrane potential varies not only with the activity of the main ion $a_{i,}$ but also depends on the concentration of some other a_j ions, called interfering ions. The interfering ion activity is multiplied in the formula by the relative selectivity coefficient k (Daniel et al., 2004).

4.3.1.2. MEASUREMENT DISTURBANCE

The measurement principle results in a cross-sensitivity to ions with binding properties towards the measurement electrode which are similar to the measurement-ion. The so-called disturbance-ions influence the measured potential difference, which is subsequently interpreted as a change in the activity of the measurement-ion. Two of the most important parameters are ammonium and nitrate for water and wastewater monitoring. Table 4-7 gives an overview on the cross-sensitivities of ISE sensors based on disturbance-ions.

Table 4-7 Properties of ISE-Probes for Water Quality Monitoring (Winkler &Fleischmann, 2004)

Sensor Type	Ammonium	Nitrate	Potassium*	Chloride*
Measurem. Rrange	0.1 – 1 000 $mg_{NH4\text{-}N}$/l	0.2 – 7 000 $mg_{NO3\text{-}N}$/l	0.1 – 10 000 mg_K/l	0.2 – 10 000 mg_{Cl}/l
Resolution	0.1 $mg_{NH4\text{-}N}$/l	0.1 $mg_{NO3\text{-}N}$/l	0.1 mg_K/l	0.1 mg_{Cl}/l
Non-Linear Range	0.1 – 1.0 $mg_{NH4\text{-}N}$/l	–	0.1 – 1.0 mg_K/l	0.1 – 5 mg_{Cl}/l
Cross Sensitivity on Main Disturbance-Ions				
	Potassium 1 : (15 – 30) Sodium 1:1300	Chloride 1 : 300 Bromide 1 : 28 Iodide 10 :1	Ammonium 1 : 120 Sodium 1 : 2000	Bromide 1 : 1 Iodide 20 : 1
*Disturbance-Ion Compensation				

For example, a cross-sensitivity of 1 : 15 of the ammonium electrode on potassium means, that a potassium concentration of 15 mg/l results in the same potential difference between the measurement and the reference electrode as an ammonium concentration of 1 mg/l. A typical potassium content of municipal waste water is

5 g_K/(PE·d) (Winkler et al., 2004), which is almost 50% of the total nitrogen content of 11 g_N/(PE·d). The main source of potassium is food products. Typical concentrations of iodide and bromide in municipal waste water were found to be in the µg/l-range. Therefore, the influences of these ions are usually negligible.

Since the influence of the disturbance-ions at the time of the sensor calibration is compensated automatically, only the concentration variations of the disturbance-ions relative to the concentrations at time of the calibration have a negative impact on the measurement.

4.3.1.3. SENSOR CALIBRATION

The membrane of the measurement electrode "ages" during its application period due to irreversible bindings with measurement- or disturbance-ions, sectional build up of coatings and mechanical stress. For raw wastewater, a lifespan of 3 – 4 months can be expected. All the above influence factors result in a drift of the measurement signal which has to be compensated via periodic calibration; several methods are available (Winkler et al., 2004):

- single-point (offset) calibration, in-line
- two-point calibration (single standard addition)
- multiple-point calibration (multiple standard addition)

It is recommended to carry out a visual check of the probe before any calibration is started – if necessary the probe should be cleaned manually. Supplementary sensors like temperature or pH should be calibrated before the ISE-sensor is calibrated, so that any errors of the automatic temperature or pH-compensation are corrected before the ISE calibration is started.

For the *single-point calibration*, the probe remains in the liquid, and a single reference measurement is carried out. The sampling period should be kept relatively short (approximately 20 – 30 s). The concentration of the measurement-ion at time of the calibration should be in the upper half of the concentration range at the measurement location. In the case that the maximum concentration of the measurement-ion is below 5 mg/l, a *two-point calibration* should be undertaken considering non-linearity in the lower measurement range.

For *two-* and *multiple-point calibration*, the probe has to be removed from the liquid and put into a pot with a grab sample or with a standard of known concentration. Using a grab sample of the actual measurement location has the advantage of automatically sampling compensation of the disturbance-ions. By using standard samples, reference measurements can be omitted – but a *single-point calibration* in-situ has to follow any calibration of standards in consideration of influences from disturbance-ions. The calibration standards need to have sufficient ion activity. Using distilled water for the standard preparation or standards provided by manufacturers solves this problem.

For the *two-point calibration*, the calibration measurements should be carried out with an approximately 20% and 80% concentration range of measurement-ion at the measurement location and an approximately concentration ratio of the standards of 1 : 10. If a grab sample is used, the concentration of the measurement-ion has to be determined by means of a reference measurement before the calibration is started. The 2nd calibration point (approximately 80% of the maximum concentration) can be determined by choosing the volume of added stock solution. The stock solution should be highly concentrated, so that the change of the measurement volume can be ignored during the calibration procedure.

A *multiple-point calibration* can be applied where the concentration range at the measurement location has a wide span. In the lower concentration range of ammonium (< 5 mg_{NH4-N}/l) non-linearity has to be especially considered by means of a sectional linear calibration function.

4.3.2. UV-VIS SPECTROMETER (SPECTRO::LYSER)

The spectrometer used for the monitoring station in Graz is a device from the s::can company, the so-called spectro::lyser. The submersible UV-VIS spectrometer (Figure 4-14) is a spectrometric probe of about 0.6 m in length and 44 mm in diameter. It records light attenuation in the wavelength region between 200 nm and 750 nm and displays and/or communicates the results in real time. The instrument is a 2-beam 256 pixel UV-VIS spectrometer, with a xenon lamp as a light source (Langergraber et al., 2004). The default calibration is an equation which is based on the partial least square regression. Every wastewater has its specific properties, the composition of the different compounds varies, and therefore, every calibration especially for organic compounds has to be adapted to waster water matrix (properties) due to the change of the waste water properties for every catchment.

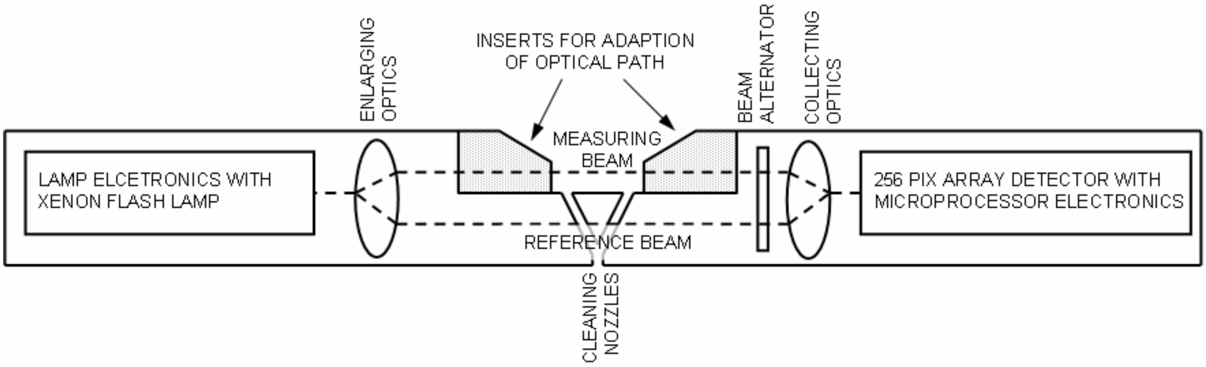

Figure 4-14 UV-VIS Submersible Spectrometer (Langergraber et al., 2003)

The measurement takes place directly in-situ without sampling or sample treatment. Thus, measurement errors due to sampling, transport, storage, dilution etc. are not relevant. A single measurement typically takes about 15 seconds. The instrument is equipped with an auto-cleaning system using pressurised air. In the CSO chamber an explosion-proof version is installed. A path length of 5 mm (length of measurement window) is used for wastewater applications.

4.3.2.1. INTRODUCTION TO UV-VIS SPECTROSCOPY

The basis for optical spectroscopy is the complementarity principle of Bohr and Einstein which describes the frequency correlation calculated by following equation:

$$\Delta E = E_2 - E_1 = h \cdot \nu$$

This formula describes the discrete atomic and molecular energy levels E_i with the frequency ν of electromagnetic radiation. The proportionality constant h is Planck's constant with a value of $6.626 \cdot 10^{-34}$ Js. Instead of the frequency ν, the wave number $\tilde{\nu}$ will be used and, therefore, the equation can be written as:

$$\Delta E = E_2 - E_1 = h \cdot c \cdot \tilde{\nu}$$

with $\nu = c/\lambda = c \cdot \tilde{\nu}$

Absorption spectroscopy in the ultraviolet (UV) and visible (VIS) range can be classified according to Figure 4-15.

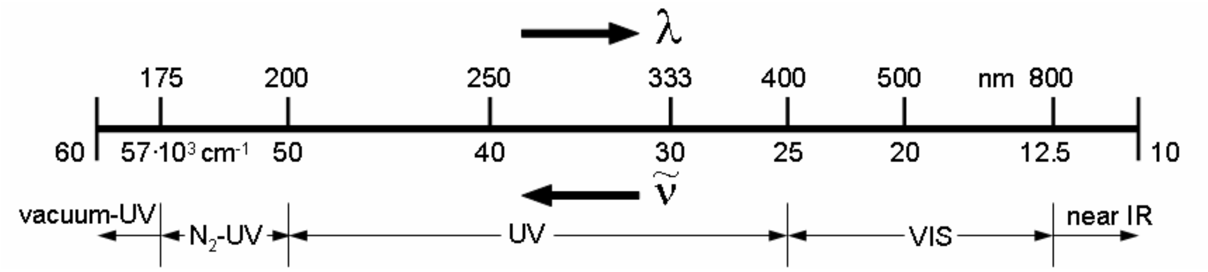

Figure 4-15 Spectra Ranges (Perkampus, 1986)

In the visible spectral range, the interactions of matter and electromagnetic radiation occur, resulting in dye. The ranges described (Figure 4-15) are not definite boundaries due to possible absorption of the molecules beneath 200 nm and above 50 000 cm^{-1}, respectively. The shortwave boundary is device and experiment dependent. The long wave boundary (800 nm) is not really limited due to the device.

The Beer-Lambert law is the mathematical and physical basis for absorption of light in the UV-VIS and IR range for gases and solution (Eichler et al., 1974):

$$\log\left(\frac{I_0}{I}\right)_{\tilde{\nu}} = \log\left(\frac{100}{T\,[\%]}\right)_{\tilde{\nu}} \equiv A_{\tilde{\nu}} = \varepsilon_{\tilde{\nu}} \cdot c \cdot b$$

whereas

$A_{\tilde{\nu}} = \log\left(\frac{I_0}{I}\right)_{\tilde{\nu}}$	extinction and absorbance, respectively
$T_{\tilde{\nu}} = \frac{I}{I_0} \cdot 100 \text{ in } \%$	transmittance
$\varepsilon_{\tilde{\nu}}$	molecular decade extinction coefficient

I_0 is the intensity directed at a sample solution, I is the intensity of monochromatic radiation leaving the sample. c is the concentration of the compound in solution, expressed in [mg/l] and b is the path length of the sample.

$$\varepsilon_{\tilde{\nu}} = \frac{A_{\tilde{\nu}}}{c \cdot b}$$

The molecular decade extinction coefficient $\varepsilon_{\tilde{\nu}}$ is a substance specific term which is dependent on the wave number $\tilde{\nu}$ [1/m] and wave length λ [nm]. The functional coherence of $\varepsilon_{\tilde{\nu}}$ and wave number $\tilde{\nu}$ of a compound is called the absorbance spectra. The ratio of the light intensity beamed to the sample and leaving the sample as a percent age is already explained in the previous equations transmittance. The negative logarithm of this ratio is absorbance. This absorbance value is proportional to the concentration of the dyed solution.

$E(\lambda)_b = b \cdot E(\lambda)_{b=1}$ Lambert's absorbance law

The correlation of the extinction with a specific path length of b is linear to the extinction with b equal to one multiplied with the considering path length b. In practice, the path length is equivalent to the length of the measurement window.

$E(\lambda)_c = c \cdot E(\lambda)_{c=1}$ Beer's law

The extinction of a sample is proportional to the concentration c and is expressed by the equation of Beer's law. The law is only valid until there is no molecular changing (e.g. dissociation). The combination of both laws is expressed in "Lambert-Beer's law" with the following equation:

$$E(\lambda) = c \cdot b \cdot E(\lambda)_1$$

The absorbance is wavelength dependent; if the absorbance for different wavelengths is known, the spectral characteristics of the matter can be displayed. Every substance and dye has its characteristic spectra and therefore can be identified with this spectrum, respectively (Figure 4-18). If more substances are in the compound the spectra are additional superposed (Figure 4-17).

Hence, the concentration of a special compound can be calculated with a constant path length. Scattering can be neglected due to its small amount (Matsché & Ruider, 1982).

4.3.2.2. UV-VIS SPECTROSCOPY AND ITS APPLICATION IN WASTE WATER

Light can be absorbed by molecules due to the interaction between radiation and the electrons of the molecule as already explained. The absorbance depends on the chemical characteristics of the molecule, i.e. the occurrence of C-C double bounds, C-O bonds or C-N bonds and aromatic structures. Other substances, for example nitrate or nitrite also exhibit a specific absorption within the UV-range (Matsché et al., 2002). Hence, only those water substances which have a characteristic bounding can be measured. Therefore, the bound proportions and the used wave length are important for the amount of the absorption for absorbance.

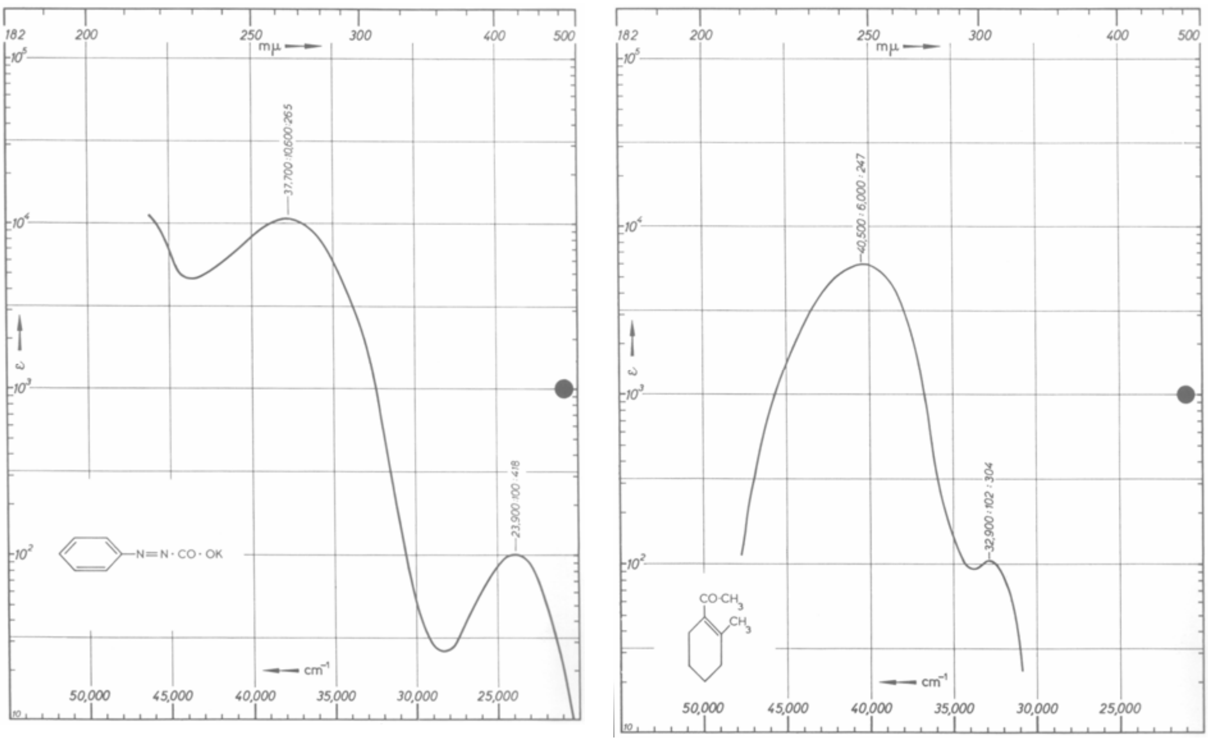

Figure 4-16 Absorbance Spectra of Potassium Phenylazoformate (Left Figure) and Acetyl-Methylcyclohex (Right Figure) (Perkampus, 1992)

Figure 4-16 gives an example of absorbance spectra of potassium phenylazoformate which is an antifreezing compound and of acetyl-methylcylohex (oxidised alcohol compound).

A fundamental problem for the application of absorption measurement in water analysis is that the substances found in the sample show absorbance spectra which interfere. The measured absorption at a specific wavelength is, therefore, the sum of single absorbances of different substances at the applied wavelength (Figure 4-17).

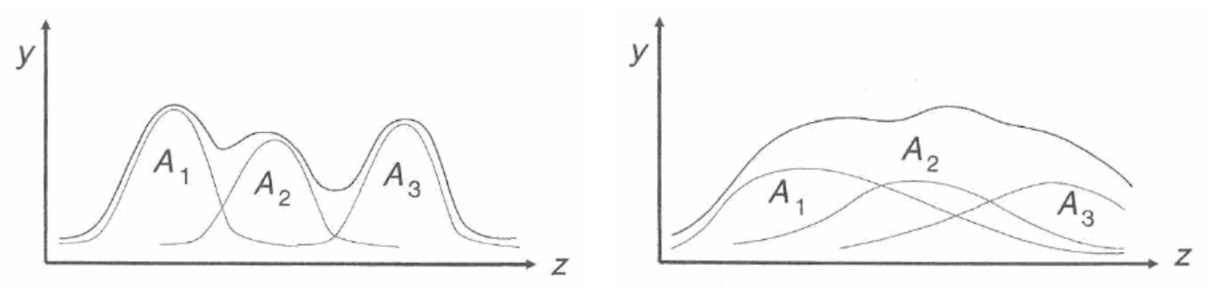

Figure 4-17 Examples of the sum of Single Absorbances (Langergraber, 2004)

In the lower UV-range up to 250 nm, the influence of nitrate and nitrite is the dominating factor. Perkampus (1992) shows the influence of single substances for specific wavelengths. Organic substances occur in the waste water normally as a heterogeneous mixture of different organic compounds. Indeed, there are also organic compounds which have no absorbance in the UV range. Colouring of a water sample also influences the absorption measurement. In this respect, it has to be mentioned that dye is often of organic nature. On the other hand, dye is not always biodegradable and, therefore, not relevant for the oxygen consumption required for the degradation of the organic compounds (Matsché et al., 2002).

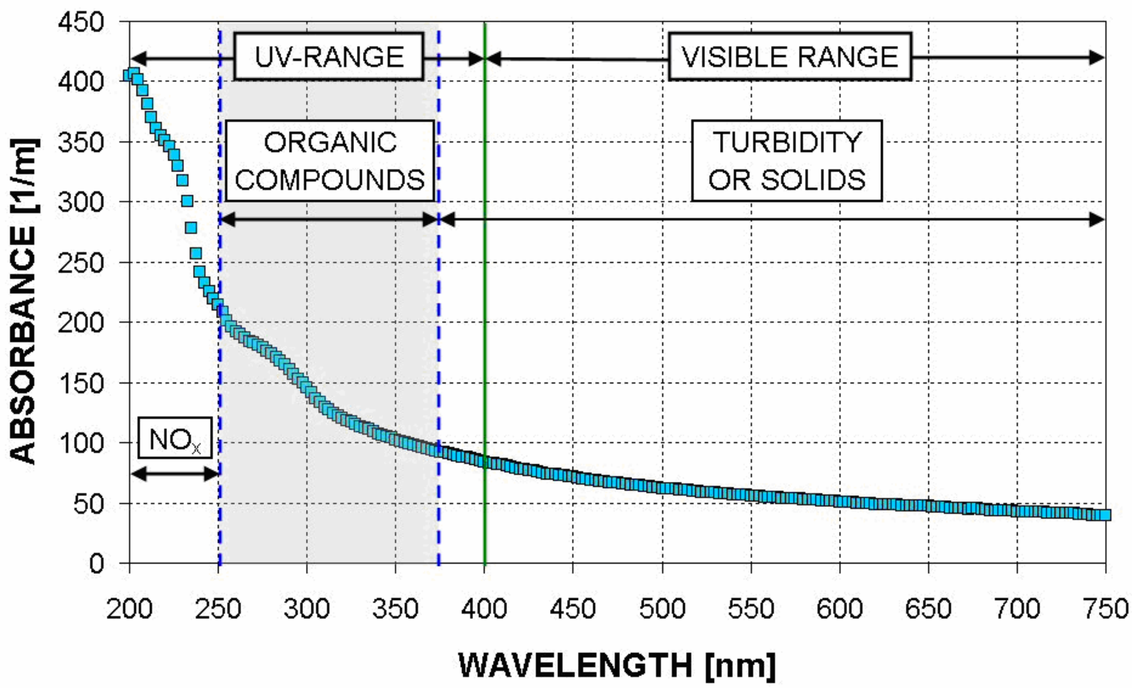

Figure 4-18 Typical Absorbance Spectrum at the Graz-West CSO and the Wavelength Classification Ranges (Hochedlinger et al., 2005a)

Figure 4-18 shows the exemplary absorbance spectra of typical wastewater from the Graz monitoring station. Additionally, typical absorbance ranges (Pons et al., 2004) of the specific substance groups are illustrated. The measured absorbance spectra is a sum of many part absorbance spectra, which is caused by single substances or the effects of scattering and turbidity.

Every calibration model is a compromise between generality and robustness. Normally with the increasing number of wavelengths used, particularities in the calibration data can be better reproduced and, therefore, minor deviations between calculated equivalence values and lab values can be determined. On the other hand, with a large number of wavelengths the probability of a major changing of the weighing factor for a different wastewater matrix increases. If, at the Graz monitoring station, the original calibration model is retained, significant differences between equivalence and lab values result.

Measured absorbencies are calculated in equivalence values (C_{eq}) using statistical calibrations models. The following equation is used for the calculation.

$$C_{eq} = \sum_{i=1}^{n} \left(a_i \cdot \lambda_i\right) + K$$

The number n of used wavelength λ_i is dependent on the measuring system and the specific situation (waste water matrix). The weighing factor a_i of the wavelength is determined in comparison with the analysed lab values. The constant offset K can be used for the specific wastewater matrix adjustment over all single wavelengths. Either a specific wavelength (e.g. 254 nm for organic substances) or defined wavelength ranges are analysed. As the spectrometer measurement is based on the company's default calibration (global calibration), every calibration has to be adapted to the wastewater matrix.

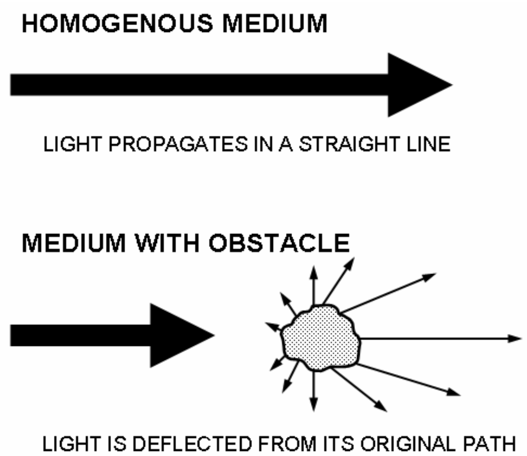

Figure 4-19 Propagation of Light in a Vacuum and in the Presence of an Obstacle (Huber & Frost, 1998)

Additionally it has to be considered that a lot of interference effects influence the measurement results. In an optically homogenous medium of constant refractive index, light keeps moving straight ahead. Any change in the optical properties caused by an obstacle will deflect the light beam from its path (Figure 4-19).

This process is called scattering. It depends on the colour of the light and the nature of the particle, and of the surrounding medium. In the case of a suspension with many particles, the collective effect of the scattering processes creates the overall visual impression of turbidity. Turbidity units, such as FNU (Formazine Nephleometric Units), are applied in an effort to express this qualitative phenomenon quantitatively.

The intensity I_{sc} of the scattered light may be expressed as the following function of five variables:

$$I_{sc} = I_{sc}(c, d, \theta, \lambda, n)$$

where c is the concentration, d the particle diameter, θ the measuring angle, λ the wavelength of the light and n the refractive index of the particles relative to the surrounding medium (for non-spherical particles, shape parameters have to be added). The equation has a complex mathematical structure and can only be solved numerically, with satisfactory results coming from computer simulation (Huber & Frost, 1998).

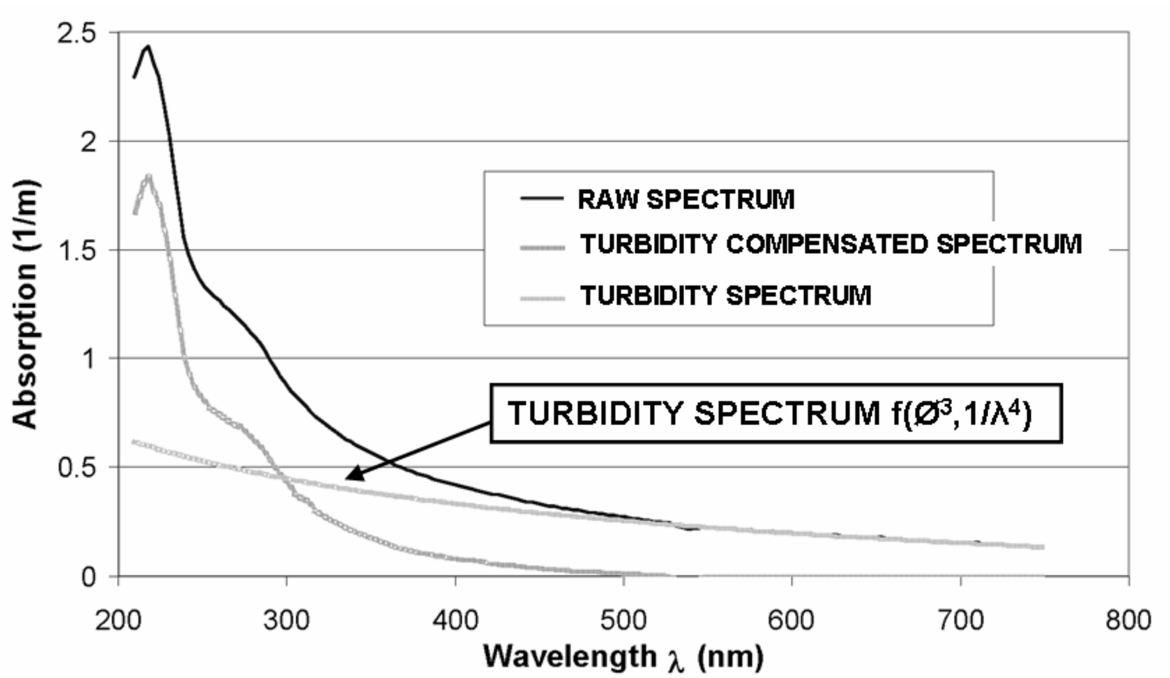

Figure 4-20 Raw, Turbidity and Turbidity Compensated Spectra (Langergraber, 2004)

One of these variables exhibits a very simple correlation: the scattering intensity is a linear function of the particle concentration In turbidimeters, this correlation can be used to determine the concentration. This is possible under the conditions that all other parameters remain unchanged during the measurement. However, under process conditions this might not always be the case and the variable must be studied separately. The coherence between scattering intensity and wavelength (Figure 4-20) as a function of the particle diameter and the well known spectral shape caused by suspended solids depends on the particle diameter d^3 and the wavelength $1/\lambda^4$ (Matsché et al., 2002).

4.4. THE "GRAZ-WEST" SEWER CATCHMENT AREA

The "Graz-West" catchment has a total area of 351 ha and an impervious area of 118.4 ha. Figure 4-21 displays the catchment area with 963 part catchments of the input file for flow quantity modelling. Approximately 13 000 inhabitants live in this catchment; this results in an average population density of 37 inhabitants/ha for the whole catchment and an average density of 110 inhabitants/ha based on the impervious area. In the western part the catchment is similar to a rural area due to its peripheral characteristics. The west is an almost completely residential zone without large industries. The eastern part is highly built-up with some industry. The middle part is a mixture of residential zones and in the north derelict land of a former brewery with nearly no impervious area.

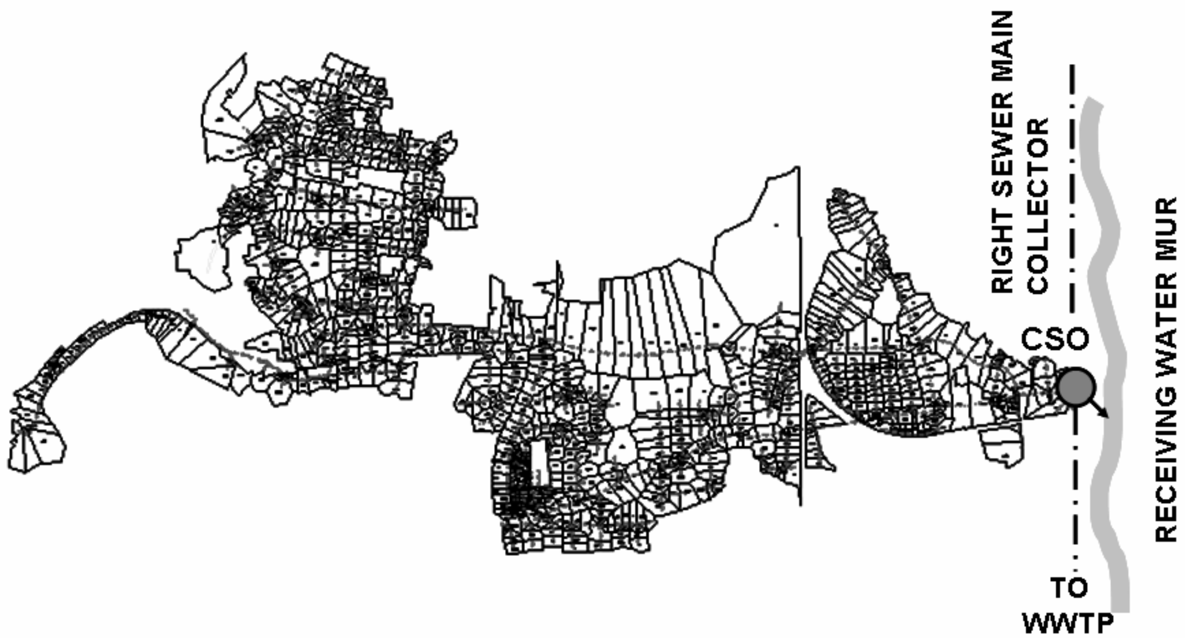

Figure 4-21 "Graz-West" Sewer Catchment Area with 963 Part Catchments (Haring, 2004)

By means of the sewer system data the whole catchment can be divided in three main parts. Figure 4-22 shows the different sewer slopes for Graz-West which have a similar inclination as the survey. The steep part in the western zone of 16.1 ha has a slope from 4 – 10 % and this is rather steep compared with other combined sewer systems. No accumulation of sewer sediments takes place at this sewer pipes due to the high shear stress of the steep slopes. One reach of the sewer system, the most westerly, is a sanitary sewer and has a slope of approximately 20% because the Plabutsch mountain begins. Only some one-family houses are drained by this sewer branch and its influence for further modelling was not considered in detail.

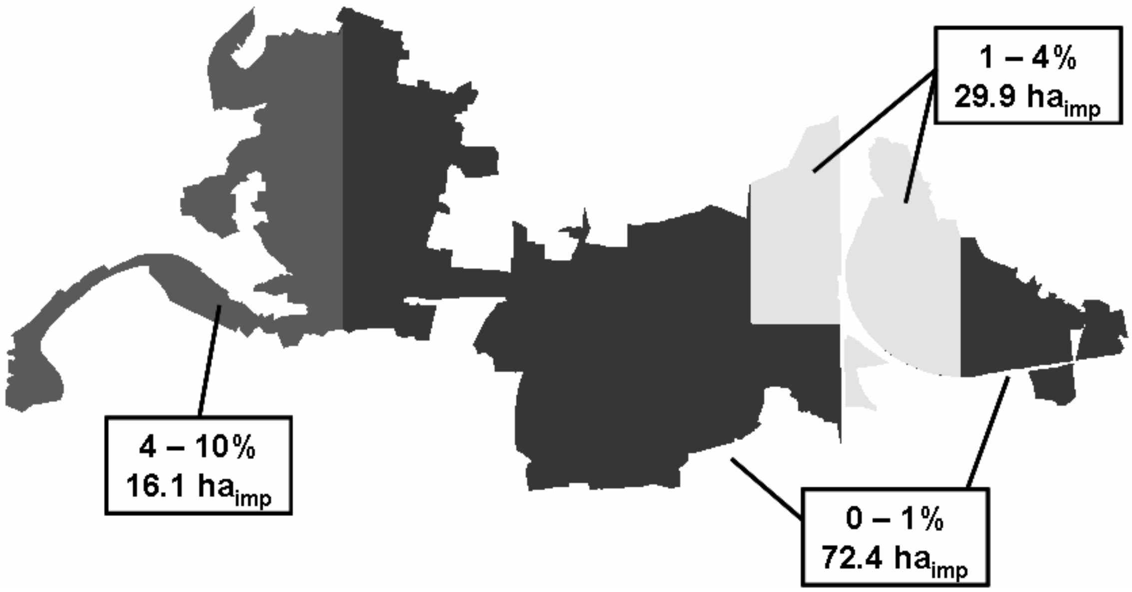

Figure 4-22 Sewer Slope Characteristics of the “Graz-West” Catchment Area

The middle part, which is terraced-shaped, has only a slope of approximately 0.5 % which is the same inclination as the inflow sewer to the combined sewer overflow. This value of slope complies in its city behaviour with a flat sewer system. Afterwards a quite steep area follows with an inclination of maximum 4%. Generally, the sewer system in “Graz-West” can be described as a steep system with a partly rural character and the “Graz-West” CSO is the only possibility for an overflow into the river Mur. There is no urban drainage structure in the catchment area for pre-spilling.

4.5. THE “GRAZ-WEST” SEWER ONLINE MONITORING STATION

The location of the Graz-West sewer monitoring station is situated at the right bank of the river Mur near the so called Bertha-von-Suttner Freedom-bridge (Figure 4-23). Gruber et al. (2004b) gives a detail description of it. The overflow channel of the CSO discharges in the river Mur, which at Graz has an average flow of approximately 120 m³/s and an annual minimum mean daily discharge of 36 m³/s (Hochedlinger et al., 2004b).

The entire sewer system in Graz has about 50 CSOs spilling either directly in the receiving water Mur or in small city brooks which later discharge into the Mur. Except for two sewer pipes with storage capacity (2 km long, Ø 2 000 mm) straight before the WWTP and a stormwater holding tank (12 000 m³ capacity) no other storage capacity is available.

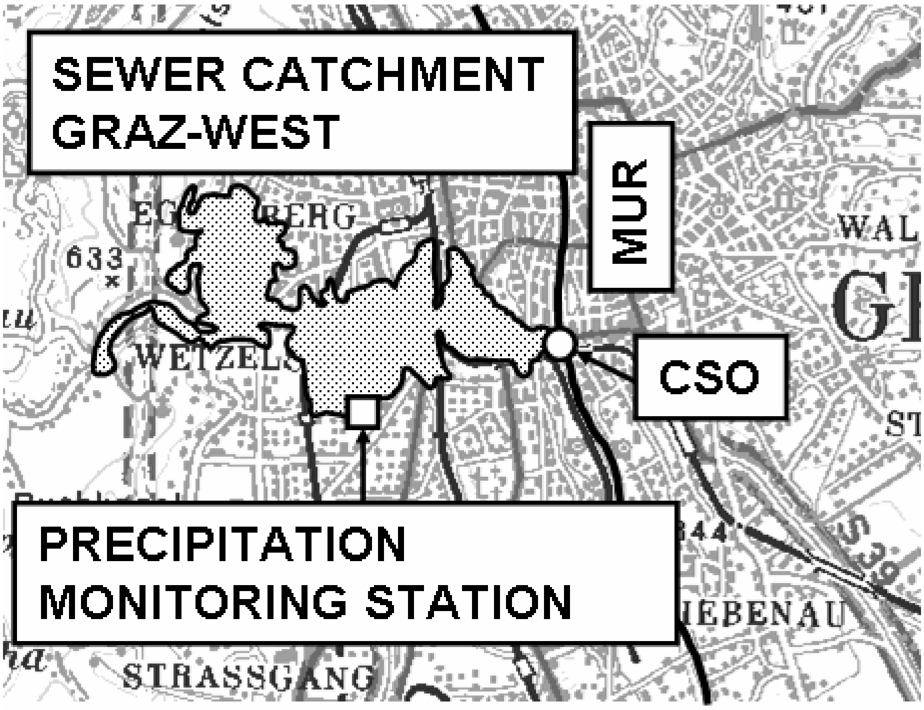

Figure 4-23 Overview of the Graz-West Catchment on the City Map

The principal reasons for this monitoring location decision have been:

- Storm event overflow without pre-spilling
- Accessibility to the CSO
- Accessibility and amount of space for the positioning of the measurement container
- Availability of required infrastructure like power and water supply
- Satisfactory protection against vandalism
- Short travel distance to the institute

The chosen CSO position almost optimally fulfils the requirements except for the accessibility into the CSO. The measurement container could be positioned beside a parking place of a furniture store directly in a green area. This container is necessary for the installation of telemetry, the process unit and the non-explosion proved probes. Right beside the container is the central heating room of the furniture store with an available water and power supply. Additionally, the access to the container is given from the parking place.

The “Graz-West” CSO consists of a curved overflow weir and a rather short throttle (Ø 600 mm). The throttle discharges already after approximately 3 m into the right sewer main collector which crosses the CSO chamber. This crossing of the main collector greatly complicates the access to this CSO chamber. Additionally, the available entrance is not given through the sole manhole due its access over a main street in Graz. Hence, regular and safe entrance to this manhole into the CSO is not feasible.

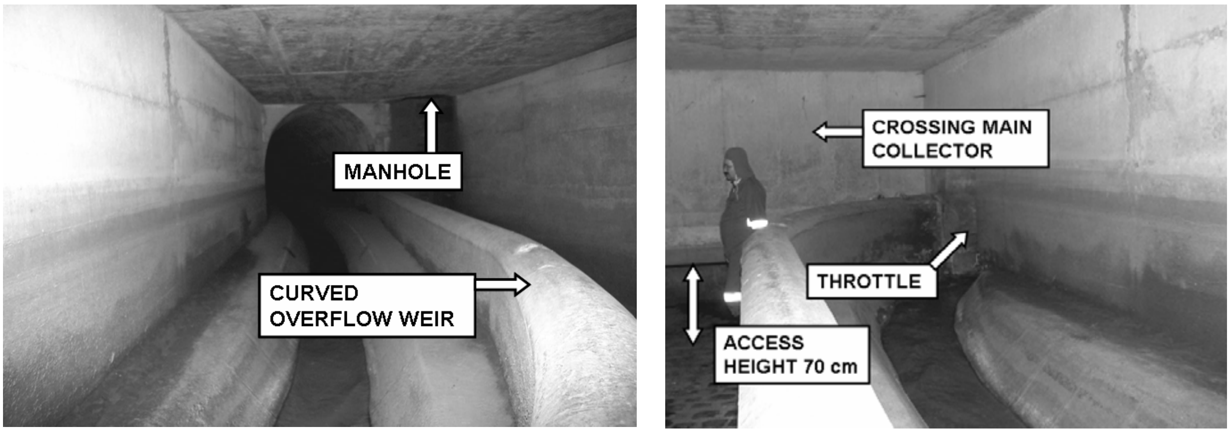

Figure 4-24 CSO Chamber with Inflow Channel, Curved Overflow Weir and Unaccessible Manhole from the Main Street (Left Figure View against Flow Direction); CSO Chamber with Throttle and Crossing Main Collector in the Back (Right Figure View in Flow Direction)

Primarily, the access to the CSO chamber only was give through the 90 m long overflow channel from the river Mur. This kind of entrance is not allowed due to safety requirements. To guarantee a continuous access to the CSO chamber an additional manhole on the top of the overflow channel was built (Figure 4-25).

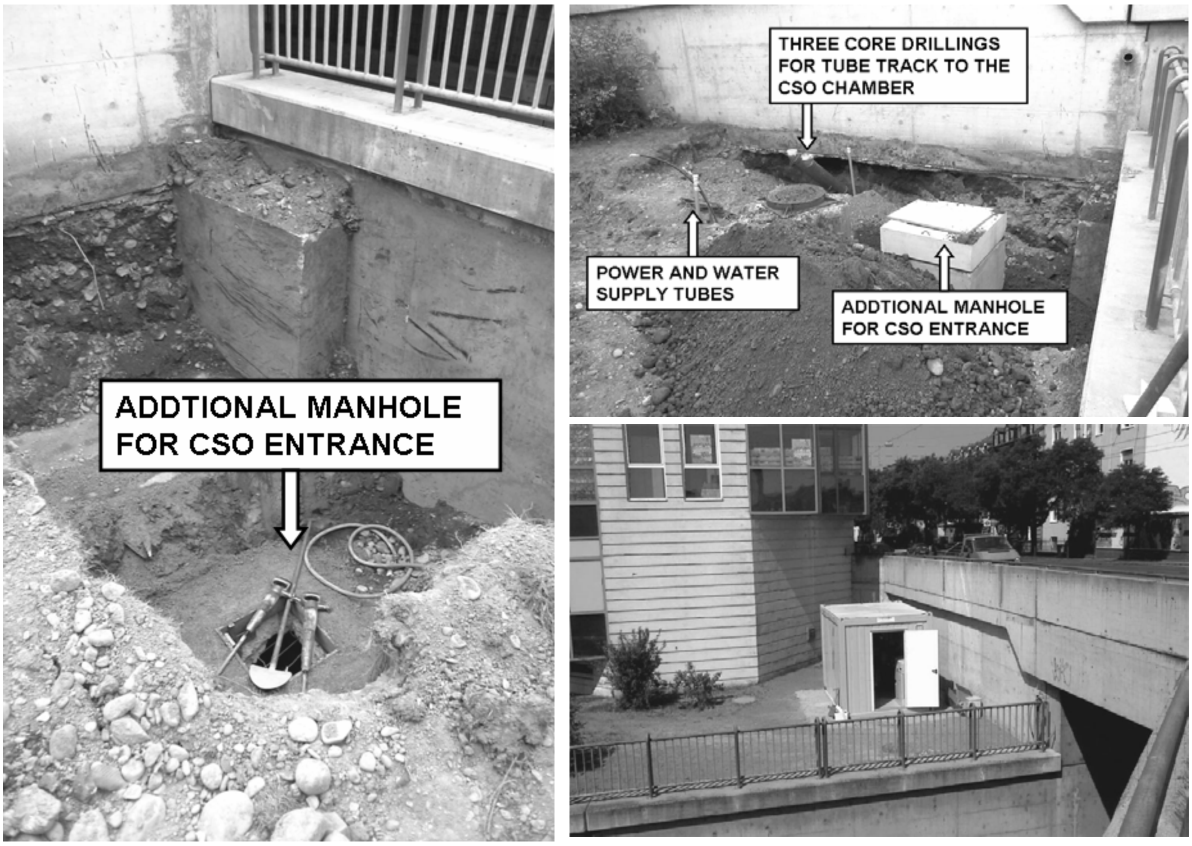

Figure 4-25 Finished Construction Work - Additional Manhole (Left Figure), Infrastructure Adjustment (Right Top Figure) and Measurement Container (Right Bottom Figure)

Additionally, three core drillings through the ceiling of the chamber were bored. These recesses allow the laying of the pipes to the chamber for the data cables and tubes from the measurement container. Figure 4-26 gives an overview of the installed equipment and monitoring system in the CSO chamber.

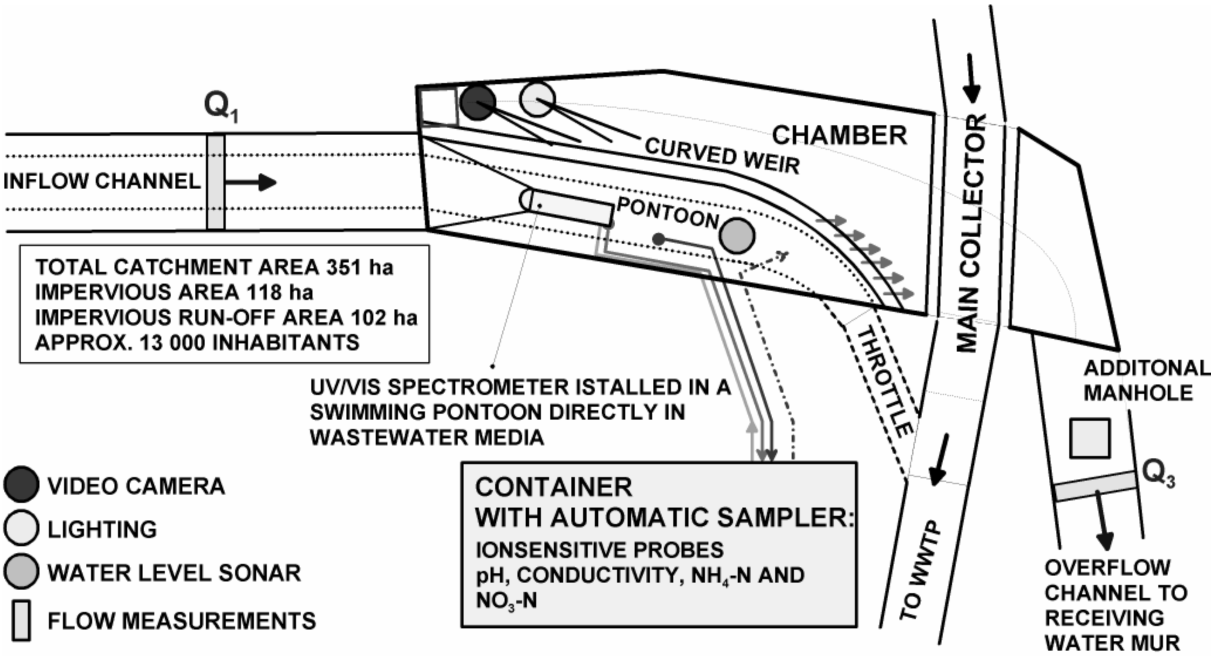

Figure 4-26 Layout & Instrumentation of Sewer Monitoring Station (Hochedlinger et al., 2005a)

The probes used in the sewer have to be explosion-proof. Therefore, non-explosion proof probes were installed in the measurement container. For these purposes, the installation and operation of a bypass was necessary. The pumping height for suction is about 6 m without pump losses; this is nearly the physical boundary of possible suction. For the suction an explosion-proof peristaltic pump was chosen to guarantee the bypass flow (Figure 4-27).

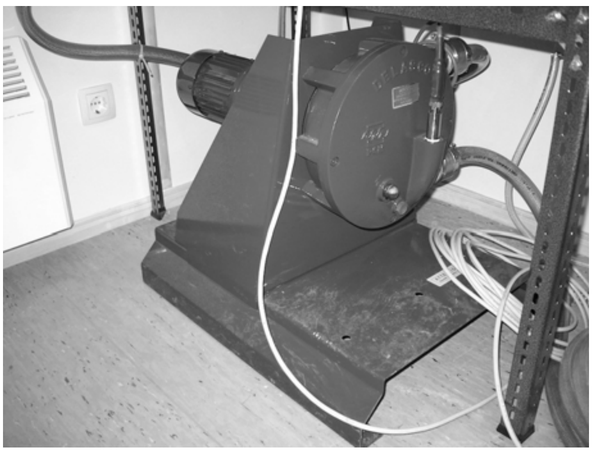

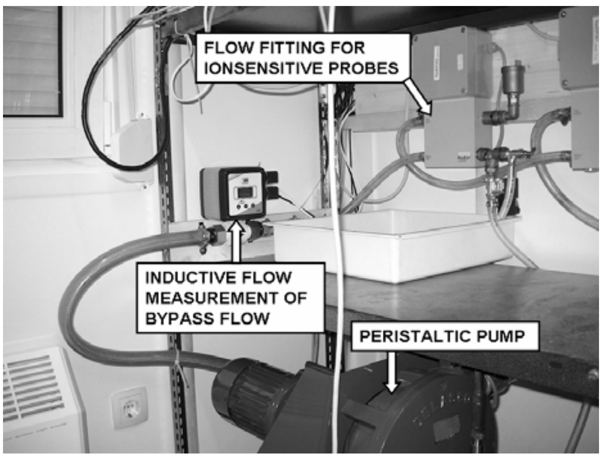

Figure 4-27 Peristaltic Pump (Left Figure) and Inductive Flow Measurement for Bypass (Right Figure)

The advantage of the explosion-proof peristaltic pump is the feasibility of an installation fixed to the ceiling directly in the CSO chamber which would avoid possible suction problems due to the physical suction height. The flow capacity of this peristaltic pump is 3 l/min. The flow through the bypass is measured by an inductive flow measurement device. Additionally, the bypass is equipped with a fitting with automatic water cleaning. In this fitting the ion-selective probes and the regarding reference electrode are installed as well as the probe for temperature measurement (Figure 4-28). Hence, the parameter ammonium-nitrogen, nitrate-nitrogen, potassium, pH-value, conductivity and temperature are measured with these sensors.

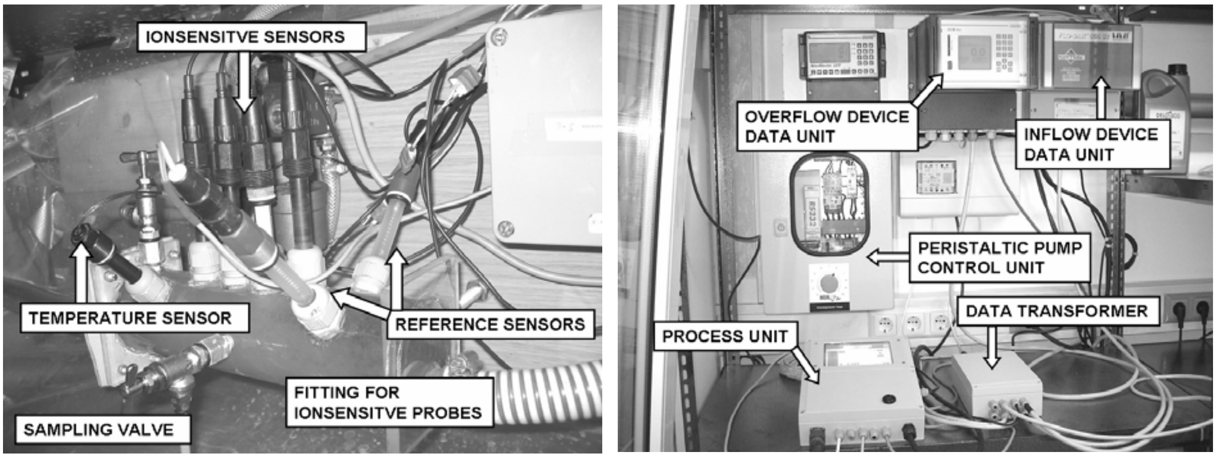

Figure 4-28 Bypass Fittings for Probes (Left Figure); Control and Data Transmission Devices (Right Figure)

Furthermore, an automatic sampler with a cooling is positioned in the measurement container in case of a storm event to gain reference samples. The tube of the sampler is fixed on the back of the pontoon for representative sampling as is near the measurement window of the spectrometer. The telemetry devices like the process unit for data collection and transmission to the database server in Vienna, the power supply of the monitoring station as well as data transformer of flow and water level measurement devices are also installed in the container.

The swimming pontoon is directly situated in the waste water media with an integrated submersible UV/VIS-spectrometer to collect absorption data and resulting concentrations of COD, TSS and nitrate (Figure 4-29). Additionally, a sensor for the temperature measurement of the waste water is installed in the spectrometer.

The positioning of the spectrometer in the overflow channel to quantify the concentrations of the spilled overflow loads would also fulfil this requirement. The situation in the waste water sewer gives the possibility of gathering additional information in the dry weather period. Thus, the pontoon was fixed with iron cables from the ceiling and the wall of the CSO chamber (Figure 4-29). Thus, a submersible position of the spectrometer is possible to measure also the concentrations in the night hours. During a storm event the swimming pontoon guarantees a representative sampling at the measurement window to obtain overflow concentrations. The pontoon can also return to its original position due to the iron rope fixings after the ending of a storm event. The measurement window of the spectrometer is cleaned by air pressure at regular intervals depending on the measurement intervals. Normally, the measurement interval is three minutes, but it decreases to one minute at storm events due to its triggering by the water level measurement. Therefore, the cleaning with air pressure is adjusted after every fifth measurement which means a 15 minute cleaning interval at dry weather and a 5 minute cleaning interval during storm weather.

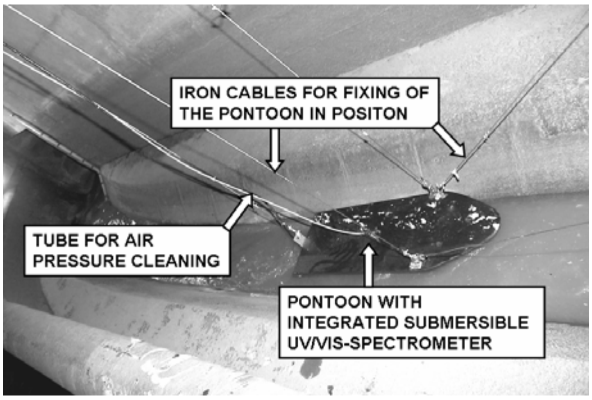

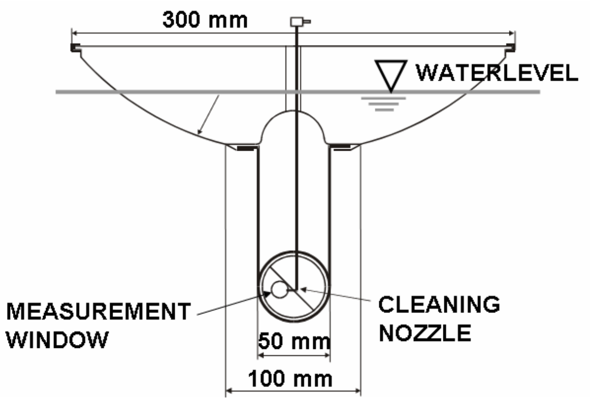

Figure 4-29 Installed Pontoon with Iron Cables Suspension (Left Figure); Cross Section of the Pontoon in the Right Figure (s::can, 2005)

The contactless radar flow meter from MARSH McBIRNEY (Flo-Dar™ type) is installed with an integrated ultrasonic water level measurement. Incoming flows can be determined based on the measured velocity of the radar velocity sensor and of the height of the ultra sonic level sensor. For the measurement in the overflow channel, an ultrasonic device from NIVUS (Type OCM Pro) is used, based on a cross correlation method with external water level measurements.

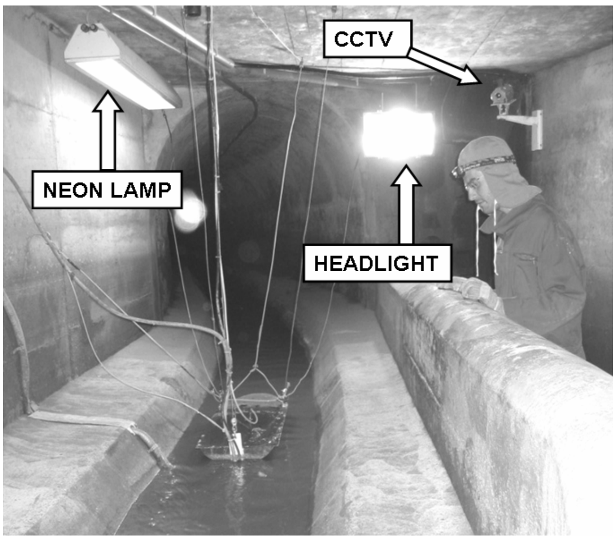

Figure 4-30 CCTV (Left Figure) and Light Equipment Arrangement (Right Figure)

Not even a temporary measurement of the flow through the throttle was possible due to not finding a suitable flow device. No kind of inductive flow measurement device could be found for the throttle diameter of 600 mm and because of the low confidence of the device manufacturers, respectively. Thus, there was no possibility of a hydraulic balance of inflow, overflow and flow to the throttle. This kind of verification would be rather simple and therefore tracer tests were used for the verification; these tracer tests will be explained later in chapter 4.7.

In addition, an ultra sonic device installed in the chamber on the ceiling of the chamber triggers the automatic sampler and activates a VTR to record the overflow event on tape. A monitoring camera is installed in the chamber and serves for control and observation of the pontoon. A headlight fixed on the edge of the chamber provides optimal illumination and is switched on during storm events by the water level triggering (Figure 4-30).

4.6. OPERATIONAL EXPERIENCES OF SEWER ONLINE MONITORING

Since October 2002 Graz the sewer-online monitoring station has been running continuously and had recorded 54 overflow events up to the end of September 2004. Due to a failure in the process unit in August 2003 for two weeks and for one week in March 2004 the measurement station could not gain data at these times. Therefore, in August 2003 approximately 11 000 m³ of flow were spilled into the receiving water. The total amount of this flow was measured by an automatic counter fitted in the measurement device.

The standard measuring interval was triggered at three minutes. The switching to a one minute measuring interval, which is the smallest possible measuring interval, is triggered at a water level of 40 cm. The headlight in the CSO, the CCTV and the VTR are switched on at water level of 75 cm which is immediately before the overflow starts.

The automatic cleaning interval of all probes – pressurised air for spectrometer and water cleaning for the ISE fitting – is the same interval for all probes. Due to an impossible changing of the cleaning interval the cleaning is operated after every fifth measurement. In the case of normal intervals, the measuring interval is 15 minutes; in the case of the intensive intervals it takes five minutes. Hence, in the intensive interval a loss of data happens on occasions due to the probe cleaning. Experiences had up to now shown the importance of independent control of cleaning and measuring, which is not implemented in the Graz monitoring station.

4.6.1. EXPERIENCES WITH THE PONTOON

To enable measurement during dry weather during the night in the sewer the pontoon was fixed only few centimetres above the invert with iron cables. This position led to daily clogging on the bottom of the pontoon and, therefore, a lot of maintenance work in the CSO chamber was necessary. Finally, the installation of a steel baffle is inclined 12° degrees in the direction of the flow was the solution to the problem (Figure 4-31).

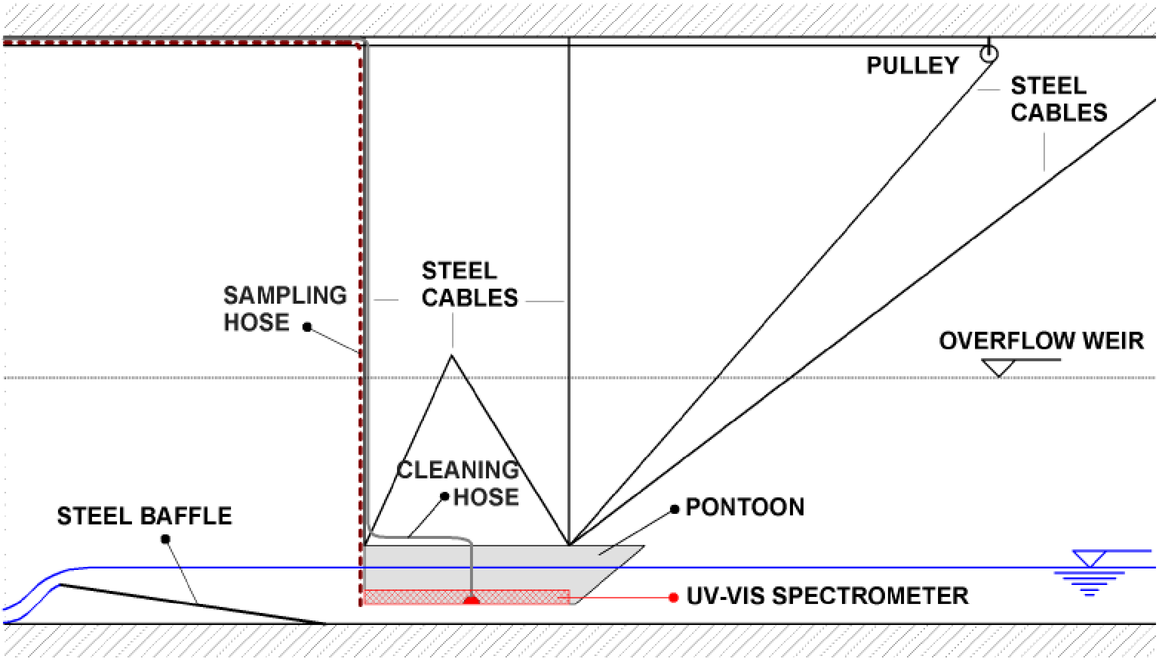

Figure 4-31 Fixed Position of Pontoon with Iron Cables and Steel Baffle

Due to this baffle, a backwater of some centimetres was produced and so the bottom of the pontoon could be fixed a little bit higher. This position decreased the clogging risk. Only in winter when the streets are sanded and a following washing of the sand into the sewer was than an increase depositing in front of the baffle. This situation led to clogging of the pontoon and more maintenance work.

The installation of a pulley with an iron cable leading to the measurement container has facilitated the maintenance work. Hence, a slight clogging often can be compensated for by a simple lift of the pontoon with the pulley.

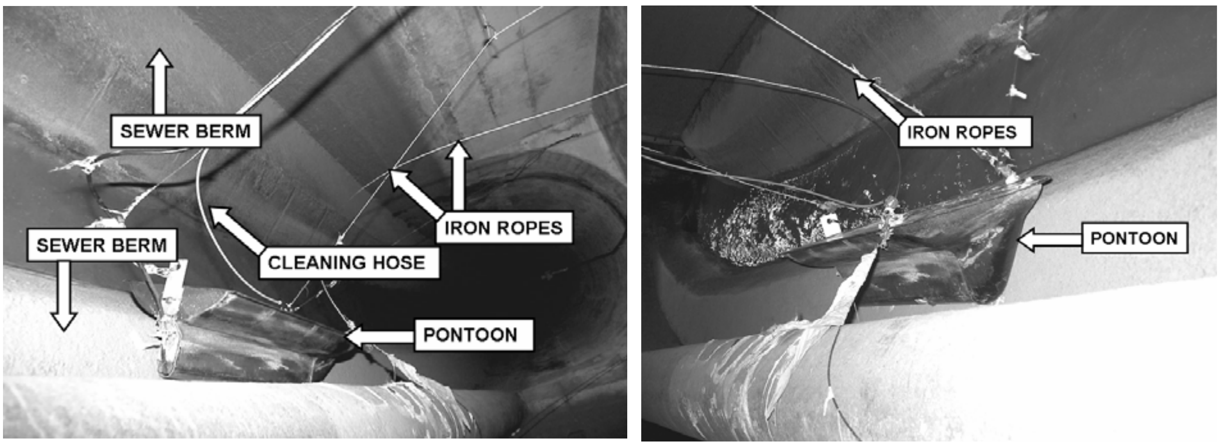

Figure 4-32 The Position of the Pontoon after the 1st Overflow Event

After the first overflow event the pontoon did not return to the sewer pipe. It lay on the sewer berm (Figure 4-32).

By means of videotaping it was possible to detect the problem in detail and so side steel cables were installed to guarantee a return of the pontoon to its starting position after the end of an overflow event.

4.6.2. EXPERIENCES WITH THE SPECTROMETER

Almost no problems were registered with the UV-VIS spectrometer. The maintenance work for this probe have been limited to occasionally cleaning the measurement window was broken. However, in the middle of August the cleaning device of the measurement window was failed. During a storm event the mechanic stress probably broke the screw thread of the cleaning tube. Thus, the measurement window was not cleaned from the time of this mishap. Figure 4-33 shows the influence and the resulting drift of this lack of cleaning of the measurement window due to a growth of biofilm on the measurement window. First, the increasing of absorbance and concentrations were not recognised. The line of the minimum concentrations clearly displays the drift in the figure. An exact value of this influence can not be estimated exactly because of possible influence of storm events. But the concentrations, shown in the figure for COD_{tot}, have a difference b approximately 550 mg/l between unaffected and affected biofilm growing on the measurement window.

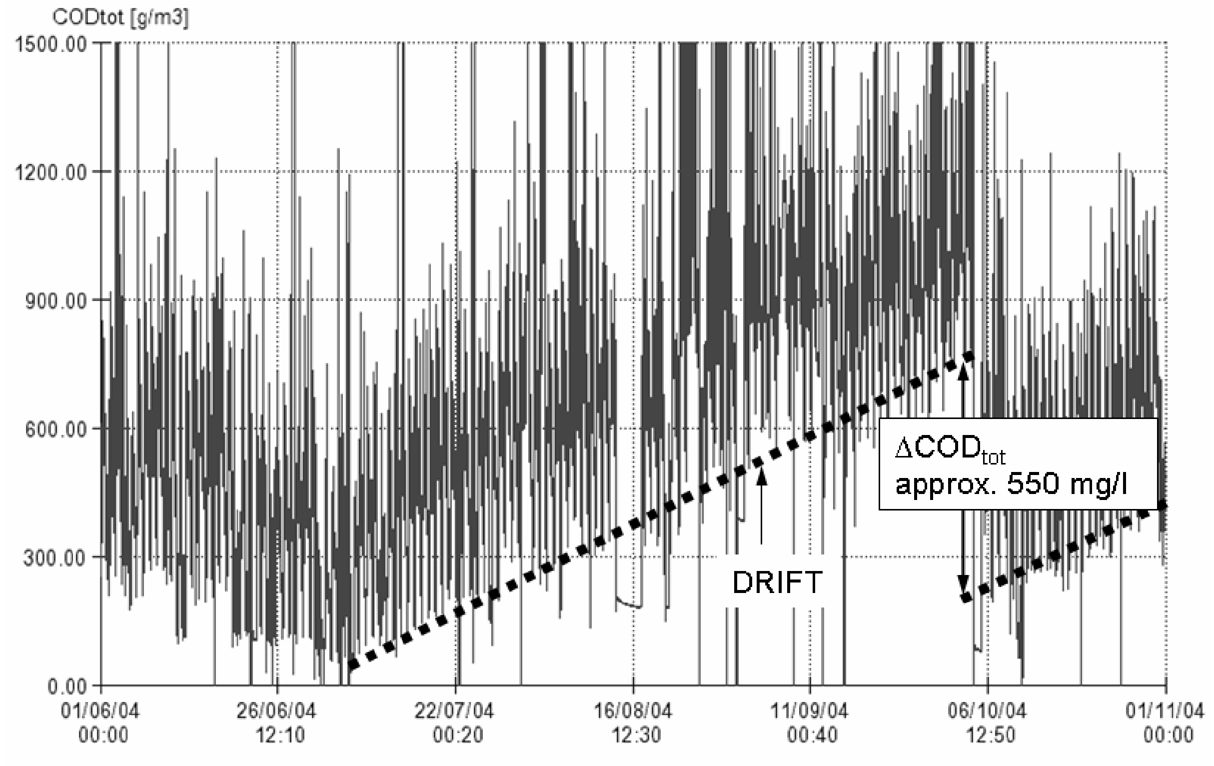

Figure 4-33 Example of a drift in the spectrometer data due to broken pressurised air cleaning

Unfortunately, no automatic data control was implemented to verify this drift. An application tool for error determination would certainly identify such data behaviour.

4.6.3. Experiences with the Bypass Operation

Soon after the starting the monitoring, an intermittent operation of the bypass, especially the bypass fittings, was recognised. The fittings from the manufacturer had been only used until this monitoring project for pure water and never tested in waste water. Thus, the dimension of the tubes, the water cleaning and the installation of the ISE probes in the fittings (Figure 4-34, left figure) were not practicable for waste water measurements.

Figure 4-34 Manufacturer's Fitting – Clogging Susceptible (Left Figure); New Prototype – Waste Water Suitable (Right Figure)

Therefore a new fitting was developed for the waste water measurement to guarantee clog-free monitoring. The primarily sucking point of the tube for the bypass was also replaced due to clogging at the tube start. So, the sucking point was placed before the steel baffle. The tube was fully installed in the sewer beam.

4.6.4. Experiences with the Flow Meters

Both flow meters send the data in analogue form to the process unit from 4 to 20 mA. At the beginning, the dynamic of the flow behaviour and its resulting values were unknown. For the upper 20 mA limit, a definite flow was established. Regrettably, the upper measurement limit for inflow and spill flow was underestimated (Figure 4-35). Hence, the upper limit was raised to cover all the expected flow values. Due to this changing of the upper limit was made; a changing in the lower measurement range could be also recognised.

A systematic validation and calibration of the inflow meters will be presented in chapter 3.6., Validation of Flow Measurement. For the overflow device, and in the case of a storm event, validation seems to be very difficult and almost impossible.

Hence, the continuous measurements of the flow meters now work perfectly. Both measurement devices could be operated without appreciable operational problems. Even the ultrasonic device, which is installed in the invert of overflow channel, experienced no clogging. The water level device based on ultrasonic broke down shortly after the monitoring started, so in December 2002 a new one was installed and was been running without problems since that time.

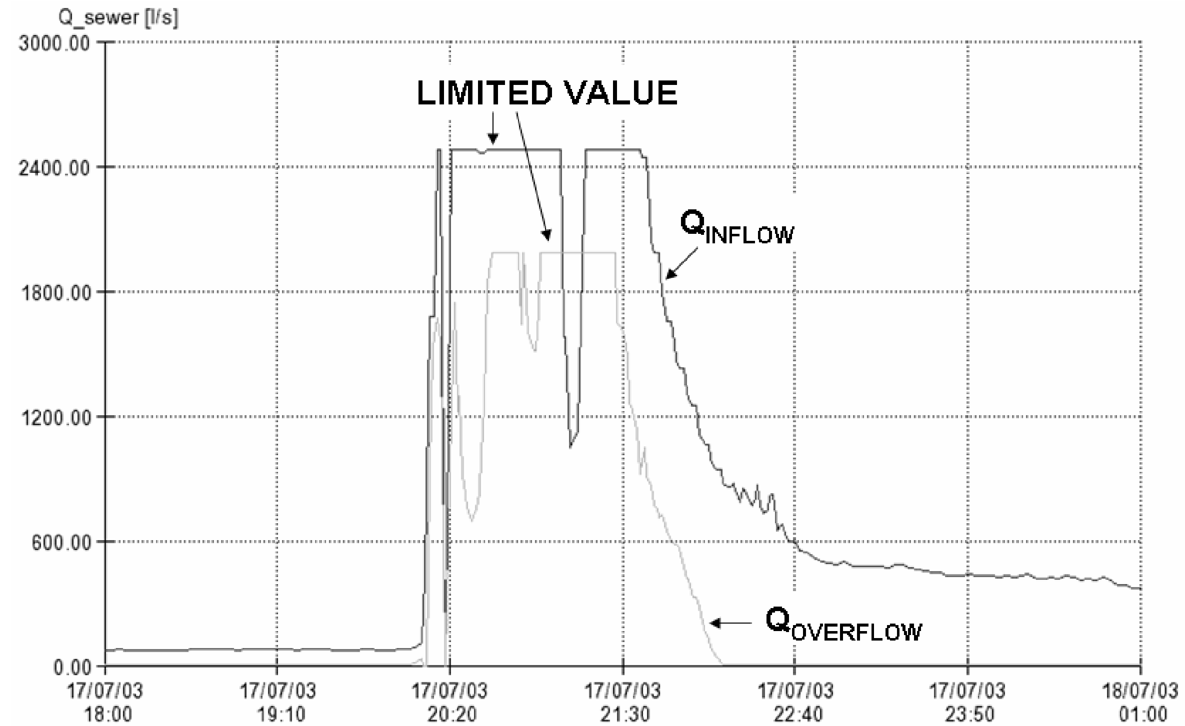

Figure 4-35 Overstepping of the Flow Measurements for Inflow and for the Overflow

During night minimum of the inflow a completely measurement of the inflow is impossible.

4.7. Validation of Inflow Measurements

The cross sectional area A(h) can be determined by means of the water level and the average flow velocity. The water level measurement is measured as already described with the external ultrasonic water level device. The average flow velocity is measured by a radar system described in chapter 4.2. The average velocity can be calculated by following equation by means of measured velocity and the calibration factor k:

$$\overline{v} = k \cdot v_{measured}$$

Therefore, the inflow can be determined by $Q = A(h) \cdot v_{measured} \cdot k$.

This formula shows the importance of accurate water level measurements to get areas calculated as accurately as possible. First, the cross section designed in the year 1914 was taken for the water level – area coherence calculation. Unfortunately, an exact allowance of the cross section resulted in different areas (Figure 4-36). The invert height as well as the profile of the invert and the berm of the sewer are completely different as designed in the plan of the year 1914. Either the invert was already cast in the wrong height position or it is also possible that the width of the invert profile was reduced due to repair work. Hence, the berm was heightened.

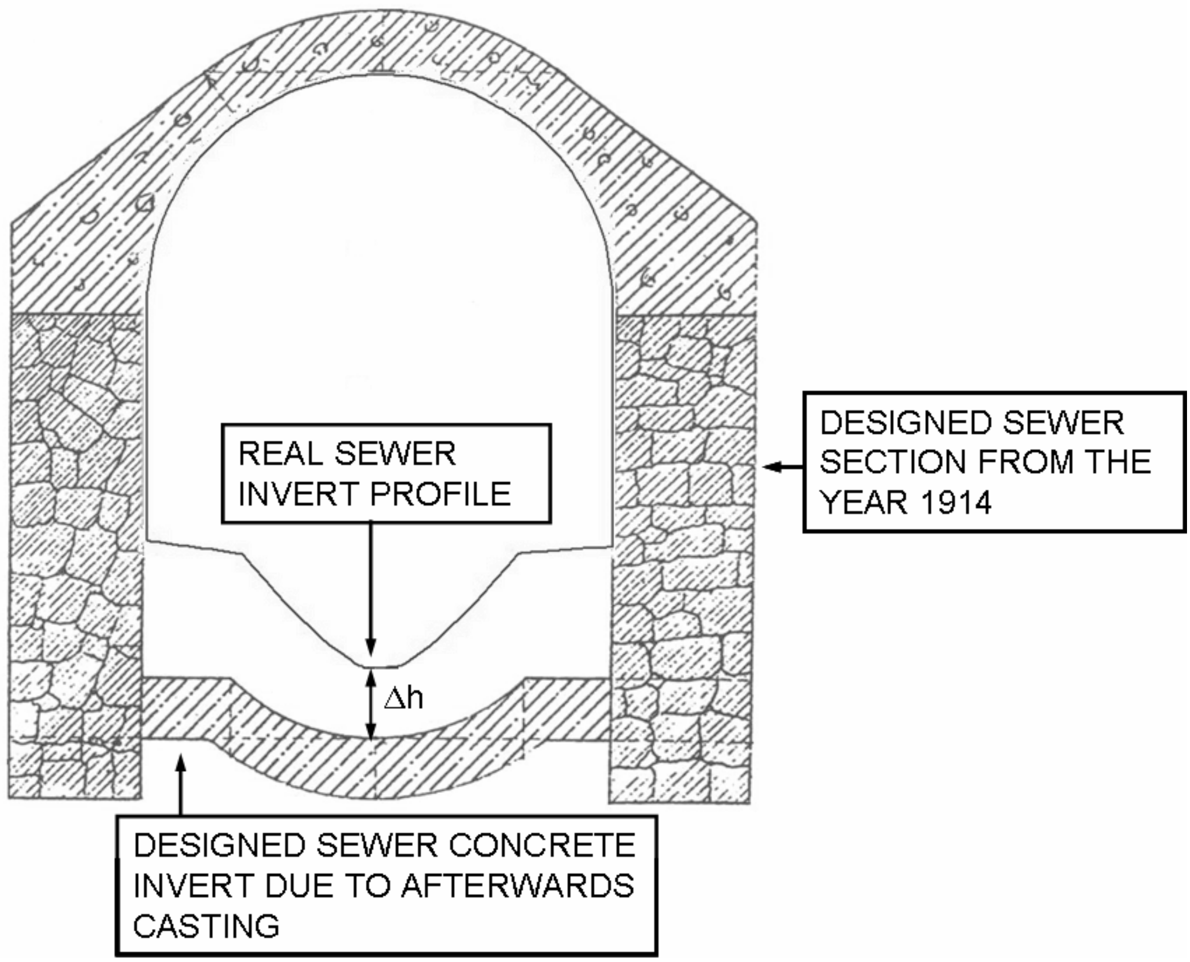

Figure 4-36 Actual Measurement Cross-Section for Inflow Measurement – Graz-West

For the actual cross section the real water level – area behaviour was determined and compared with the old wrong coherence. This comparison is displayed in Figure 4-37. The dark line shows the wrong old correlation on the basis of the design documents and the grey line is the result of the water level – area coherence by means of the allowance. The grey dots show the difference of the area calculated on the basis of the old plan and the area determined by means of the allowance. It seems that the differences are only marginal. But for dry weather flow the difference can reach a value of nearly 100%, meaning the double flow was gained. During heavy storms with extremely large flows this results in a difference of about 10%.

Hence, all collected data and the resulting flows were corrected to guarantee accurate data for a later modelling.

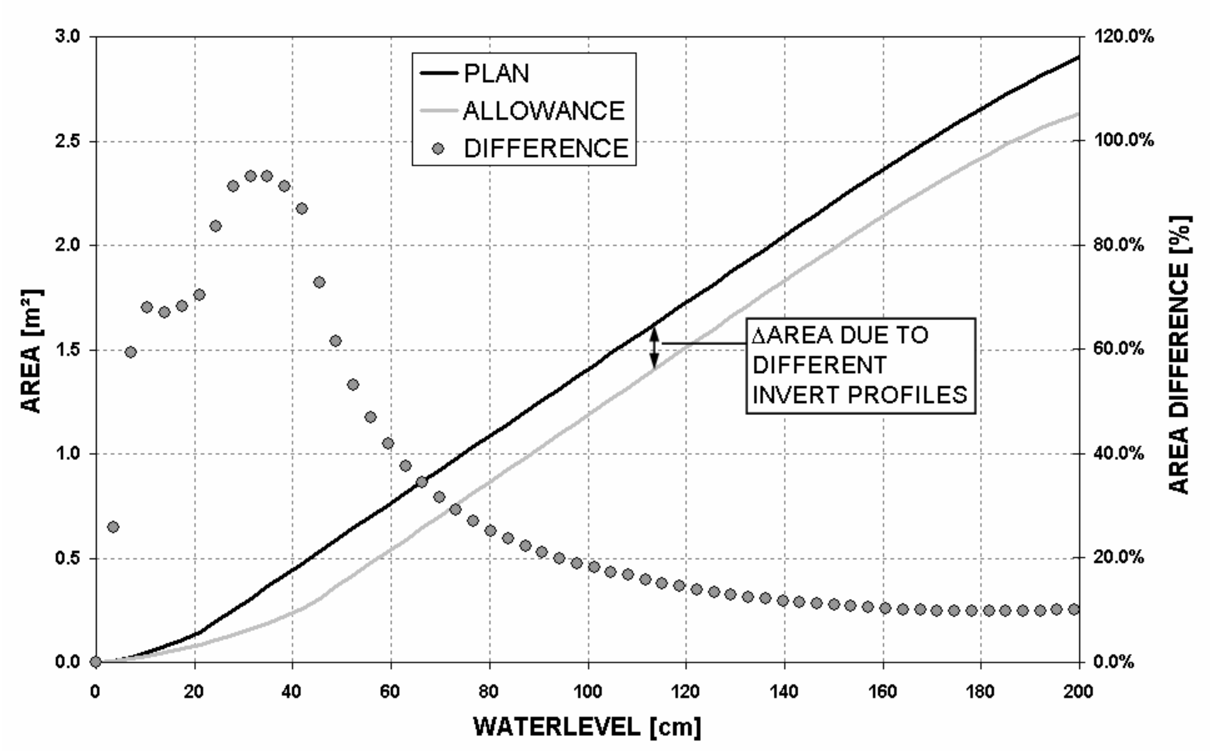

Figure 4-37 Water Level – Area Coherence (Haas, 2005) - Modified

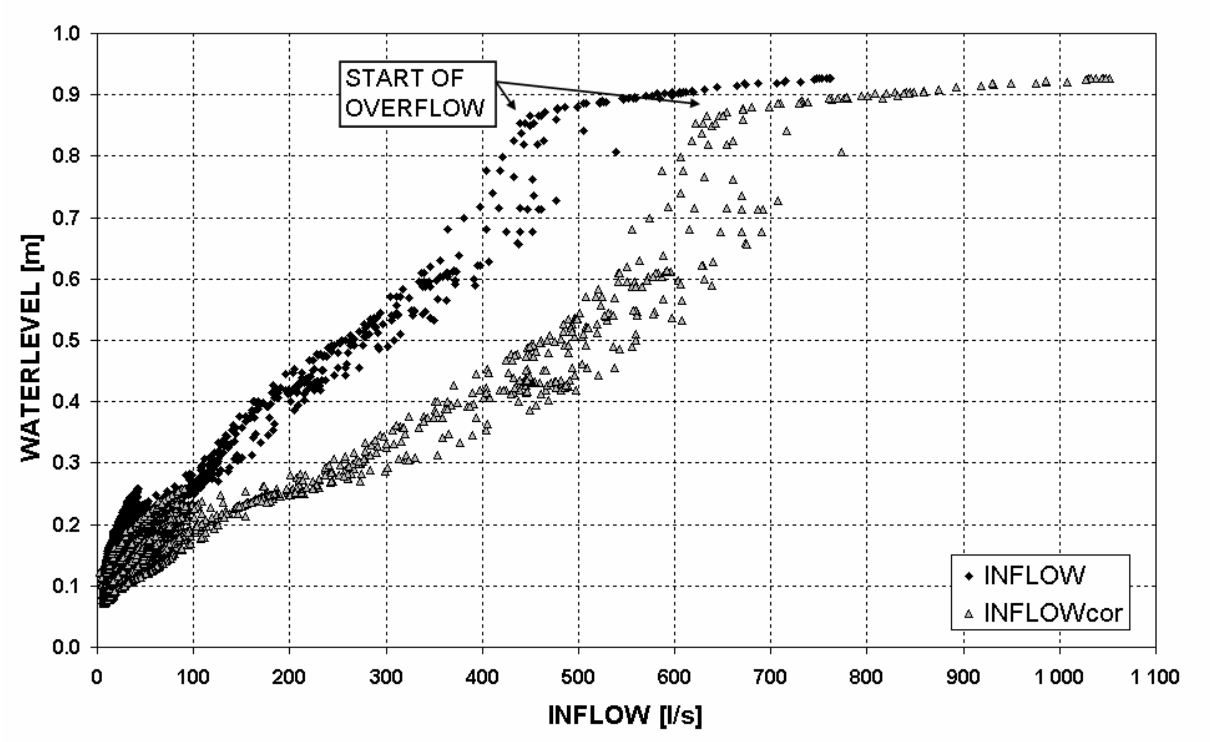

Figure 4-38 Comparison of Corrected and Uncorrected Inflow Rating Curves – Exemplary for November 2002

The effects of corrected and uncorrected inflow data can be seen in Figure 4-38. This figure shows an example for November 2002. Both rating curves show a wide range scattering, this range indicating a typical characteristic hysteresis curve. Therefore, this figure demonstrates that a flow measurement only on the basis of water level measurement can not reproduce the flow exactly. Due to different inclination of the energy line (increasing or decreasing flow) the velocity is not always the same value with identical water levels. At a height of about 0.85 m (Figure 4-38) the influence of backwater is seen, displayed due to the crossing sewer main collector through the chamber.

Figure 4-39 shows a comparison of sewer flow measurement by means of three different methods. A 24-hours flow measurement campaign was carried out from 31st of March to 1st of April. The 1st method is the already described FloDar radar system. The 2nd one is a portable Q-logger which determines the velocity on the basis of the Doppler principle. The velocity is not measured only at one point but in an inclined measurement window (cylinder). The water lever is measured with an integrated pressure sensor which does not have an automatic atmospheric pressure fluctuation compensation. Due to constant weather conditions such an effect could not be recognised. The 3rd principle is the tracer measurement method with common salt. To guarantee a completely intermixture the intake position was about 40 meters from the conductivity measurement position. The variability of the conductivity in the sewer was considered, too. A very exact and detailed description of this measurement campaign is given by Haas (2005).

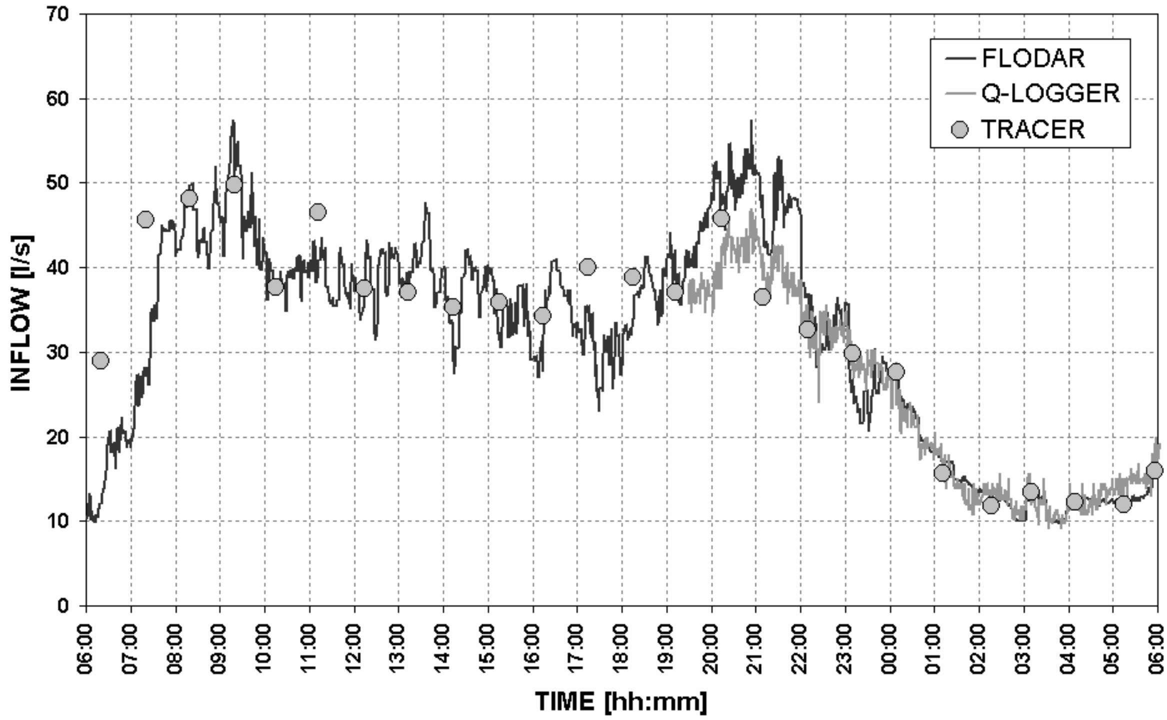

Figure 4-39 Time Series Comparison on the Basis of Different Measurement Methods from 31st to 1st of April 2003 (Haas, 2005)

Figure 4-39 confirms that all three measurement methods result in similar values. The accurate data of the radar system device and its area correction have been validated. This comparison was only made for a dry weather day.

Table 4-8 Result of Inflow, Overflow Discharges and Mean DW Flow on the Basis of Corrected Data

Year	Month	Number of Overflow Events	Sum Overflow Time	Sum Inflow	Sum Overflow	$Q_{DW,24}$
			[min]	[m³]	[m³]	[l/s]
2002	October	3	435	99 514	5 704	25.6
	November	2	112	75 861	1 588	25.3
	December	3	153	79 503	641	26.1
2003	January[1)]	0	No Flow Measurements Available			
	February	0	0	42 472	0	28.2
	March	0	0	48 690	0	28.6
	April	0	0	71 028	0	24.4
	May	1	66	73 427	290	27.3
	June	9	502	124 944	15 550	30.1
	July	6	661	143 367	24 158	29.9
	August[2)]	1	36	57 597	732	29.9
	September	1	84	95 613	1 078	29.5
	October	3	375	129 392	11 731	32.9
	November	3	146	105 365	2 519	30.9
	December	0	0	93 172	0	29.3
2004	January	0	0	83 244	0	28.9
	February	0	0	80 359	0	29.2
	March	1	136	119 385	785	33.6
	April	1	40	72 618	701	24.4
	May	5	649	108 094	13 689	30.0
	June	11	1 149	205 948	41 841	33.4
	July	9	688	171 319	25 944	37.6
	August	5	206	95 908	5 409	28.1
	2002	8	700	254 878	7 934	25.7
	2003	24	1 870	985 067	56 058	29.2
	2004	32	2 868	936 875	88 369	30.7
	total	64	5 438	2 176 820	152 361	29.1

1) no Q measurements due to FloDar device malfunction

2) 14 days malfunction of process unit – data loss

It is important to know the exact flow value due to the spillflow in the overflow channel during a storm. Thus, a validation of the flow meter in the overflow channel during a storm event should be carried out. It was not possible to pump as large flows into the overflow channel as needed for flow verification. A stay in the overflow chamber during a storm is impossible and too dangerous. So, the only method for verification is with tracer measurements. Until now it has not been possible to gain reliable tracer measurement data. Theoretical it is possible to validate the overflow meter but due to the boundary conditions it is extremely difficult to carry out an overflow meter validation. But it is very important for future validation at a storm event to get comparison data of the flow measurements.

Table 4-8 displays the results for every single month of inflow and overflow discharges. Additionally, the monthly mean dry weather flows are presented. The monthly mean dry weather flows of every month based on corrected data have almost the half value than uncorrected ones (Hochedlinger et al., 2004a).

In the considered period, 64 overflow events could be determined. In the period between 21st of August 2003 to 1st September 2003 a data loss due to malfunction of process unit happened. During this time some overflow events took place due to heavy rainfalls. But these overflow events could not be recorded. An additional counter at the flow device measured a flow of about 11 000 m³ which was spilled in this period in the receiving water.

4.8. VALIDATION OF CONCENTRATION-MEASUREMENTS

For the concentration determination, the “global” calibration provided by the manufacturer gives the coherence of absorbance and general communal waste water. This global calibration which is based on the partial least squares regression is to correlate measured absorbance and to determine concentration of a single substance and compounds, respectively. Of course this correlation can not display the “true” behaviour for every sewer system due to different waste water matrices. A waste water matrix can be described as the specific properties at a catchment or monitoring station due to different composition of the wastewater. Hence, the concentration of a parameter based on the global calibration should be seen as a recommended value. By means of reference measurements it is possible to generate a local calibration which better reproduce the coherence of measured absorbance and the determined concentrations.

The reliability of the samples taken by the automatic sampler, especially at storm events, was also verified. Therefore, the sampling started at a water level of 70 cm which was triggered by the ultrasonic device in the CSO chamber. 23 bottles with a volume of approximately 800 ml (there was a slight variation due to changing solids in the waste water) were filled consecutively.

Many trials showed the sampling time to fill the bottle at approximately 80 seconds including the pivoting of the filling nozzle. Information about the exact filling time was important for the chronological attribution of sampling, because the automatic sampler only recorded the starting time. At the same time, the UV-VIS spectrometer measured in intensive intervals of one minute.

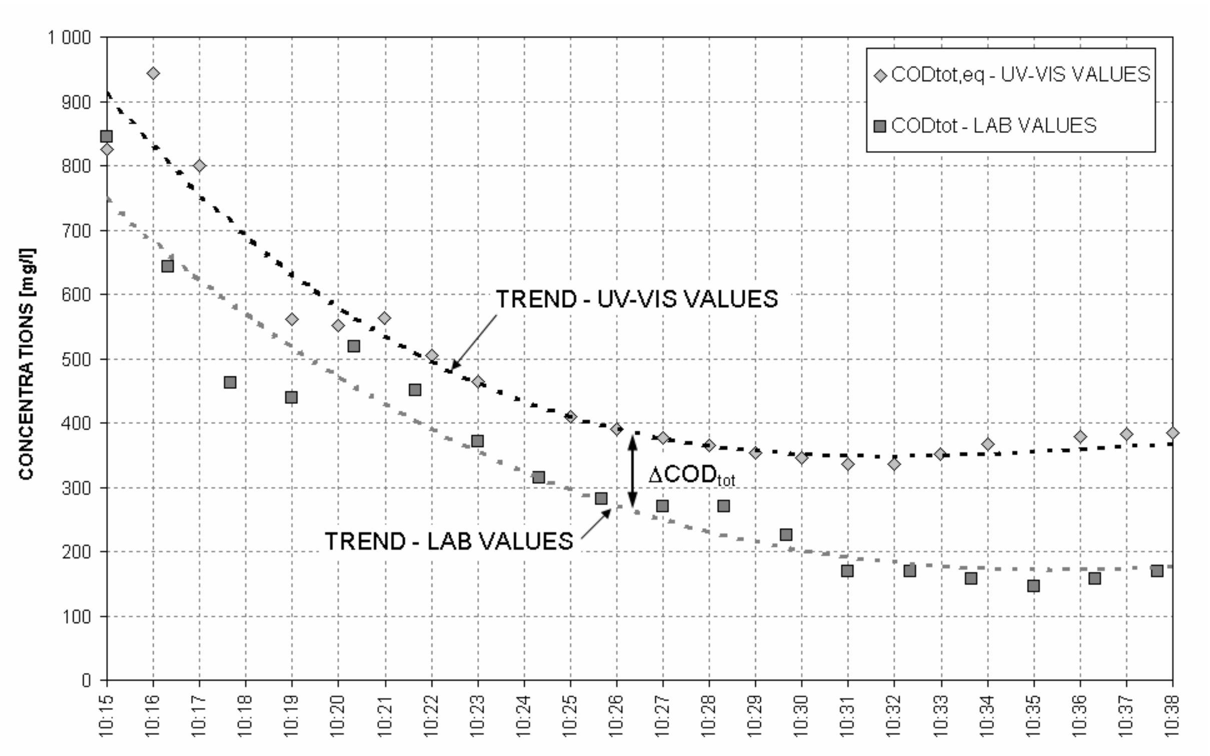

Figure 4-40 Comparison of a Storm Event of UV-VIS and Lab Values of COD_{tot} – 18th June 2003

In the months of June, July and August 2003 single samples were taken and analysed in the lab from 12 overflow events 299 (for all data see appendix). Thus, follow parameters were analysed in detail - NH_4-N, NO_3-N, TSS and COD_{tot} – and compared with the measured online values. Figure 4-40 shows the example of a value comparison for the storm event on the 18th of June 2003. The detailed values of this storm event for COD_{tot} and TSS are presented in Table 4-9.

It can be seen (Figure 4-40) that the difference of COD_{tot} between UV-VIS values and lab values is almost an equal value over the whole storm event. This difference maybe caused by two reasons:

- a loss of solids and, therefore, lower COD_{tot} values resulted due to sucking loss of particles of the automatic sampler. COD_{tot} consists from the soluble part (COD_{sol}) and from the particular part. Thus, a loss of solids results in lower values. This assumption could be rebutted by means of analysis based on the 3rd measurement campaign.

- The 2nd assumption, which was approved with the 3rd measurement campaign, is based on the global calibration. Hence, the comparative measurements lead to several measurement campaigns to adapt the default settings (global calibration) to the waste water matrix in Graz (local calibration).

Table 4-9 UV-VIS and Lab Values of COD_{tot} and TSS – 18th June 2003

Date	Time	$COD_{tot,eq}$ UV-VIS Values	COD_{tot} Lab Values	TSS_{eq} UV-VIS Values	TSS_{eq} Lab Values
[dd.mm.yy]	[hh:mm:ss]		[mg/l]		
18.06.03	10:15:00	825	845	464	600
18.06.03	10:16:00	943	-	572	-
18.06.03	10:16:20	-	642	-	445
18.06.03	10:17:00	800	-	479	-
18.06.03	10:17:40	-	462	-	371
18.06.03	10:19:00	561	439	320	301
18.06.03	10:20:00	551	-	325	-
18.06.03	10:20:20	-	518	-	384
18.06.03	10:21:00	563	-	341	-
18.06.03	10:21:40	-	450	-	347
18.06.03	10:22:00	504	-	290	-
18.06.03	10:23:00	464	371	265	256
18.06.03	10:24:20	-	315	-	247
18.06.03	10:25:00	409	-	236	-
18.06.03	10:25:40	-	281	-	193
18.06.03	10:26:00	390	-	223	-
18.06.03	10:27:00	376	270	212	213
18.06.03	10:28:00	365	-	202	-
18.06.03	10:28:20	-	270	-	176
18.06.03	10:29:00	353	-	193	-
18.06.03	10:29:40	-	225	-	169
18.06.03	10:30:00	346	-	191	-
18.06.03	10:31:00	336	169	179	148
18.06.03	10:32:00	337	-	178	-
18.06.03	10:32:20	-	169	-	145
18.06.03	10:33:00	351	-	185	-
18.06.03	10:33:40	-	157	-	145
18.06.03	10:34:00	368	-	194	-
18.06.03	10:35:00	-	146	-	145
18.06.03	10:36:00	378	-	200	-
18.06.03	10:36:20	-	157	-	115
18.06.03	10:37:00	382	-	203	-
18.06.03	10:37:40	-	169	-	128
18.06.03	10:38:00	384	-	203	-
18.06.03	10:39:00	385	191	204	144
18.06.03	10:40:00	382	-	206	-
18.06.03	10:40:20	-	202	-	174
18.06.03	10:41:40	-	225	-	174
18.06.03	10:42:00	356	-	183	-
18.06.03	10:43:00	345	202	175	197
18.06.03	10:44:00	342	-	173	-
18.06.03	10:44:20	-	225	-	180
18.06.03	10:45:00	340	-	173	-
18.06.03	10:46:00	339	-	170	-
18.06.03	10:48:00	344	-	172	-

4.8.1. 1ST MEASUREMENT CAMPAIGN

The aim of the 1st measurement campaign was, as already explained, to improve the manufacturer's global calibration. Hence, a 24 hour dry weather sampling was carried out with hourly sampling. Every hour a "fingerprint" (absorbance spectra) was taken by the UV-VIS spectrometer and, in addition, the automatic sampler took waste water samples. The samples from the automatic sampler were immediately conserved with 5% diluted hydrochloric acid and additionally cooled by the sampler refrigerator. Thus, a reduction in the COD_{tot} parameter was prevented due to limited biological decomposition. The reliability for the parameter values of this conservation method had already been tested in the lab; the maximum difference between hydrochloric acid conservation and no conservation was below 5%. This is in an acceptable range.

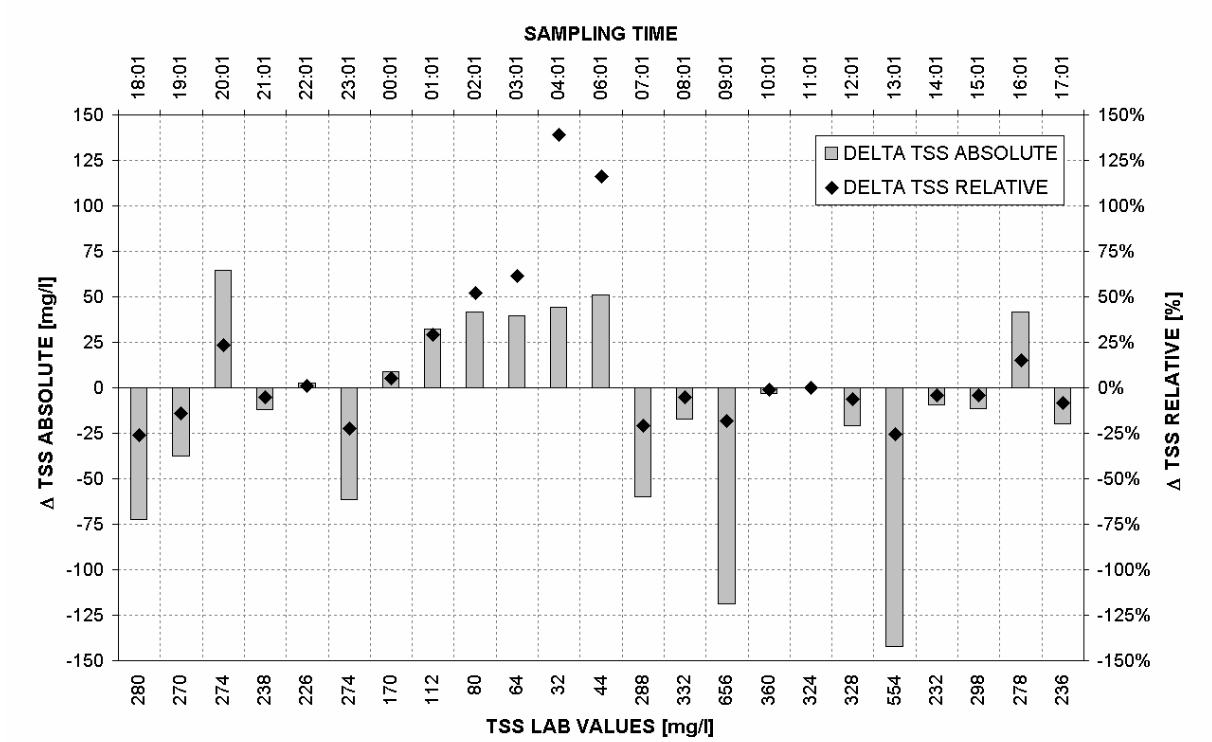

Figure 4-41 Absolute and relative deviations of UV-VIS and lab values of TSS (Gruber et al., 2004a)

Table 4-10 shows all the analysed data from the 1st measurement campaign of the parameter COD_{tot} and TSS. Figure 4-41 displays the comparison and the resulting deviations of lab and UV-VIS values. The lower abscissa presents the analysed values in the lab and the upper abscissa the sampling time. The ordinates show the deviations of the UV-VIS values to the lab values, the right ordinate indicates the absolute differences of concentrations in mg/l; the left one presents the relative differences in percent.

The biggest absolute deviation of -142 mg/l was measured at 13^{00} and a regarding relative difference of -25.6%. The greatest relative deviation of 139% can be recognised with the sample at 4^{00}.

A well defined trend can especially be seen in the samples taken in the night. Low values influenced by possible ground infiltration are reproduced with the global calibration in higher values compared with the lab values. Whereas higher values for example at noon are reproduced in results with lower values compared with the lab values. Hence, the influence of ground water infiltration and its changing waste water matrix can be determined. Additionally, five samples of a storm event are displayed in form of grey triangles. These five samples are a little bit out of the linear trend range of the 1st measurement campaign.

Table 4-10 COD and TSS Values of 1st Measurement Campaign

Date	Sampling Time	$COD_{eq,tot}$ UV-VIS Values	COD_{tot} Lab Values	TSS_{eq} UV-VIS Values	TSS Lab Values
[dd.mm.yy]	[hh:mm]		[mg/l]		
07.07.2003	18:01	547	763	208	280
07.07.2003	19:01	581	763	232	270
07.07.2003	20:01	757	964	338	274
07.07.2003	21:01	570	740	226	238
07.07.2003	22:01	567	673	229	226
07.07.2003	23:01	541	695	212	274
08.07.2003	00:01	516	606	179	170
08.07.2003	01:01	450	493	144	112
08.07.2003	02:01	418	381	122	80
08.07.2003	03:01	399	358	103	64
08.07.2003	04:01	334	224	76	32
08.07.2003	05:01	324	224	-	-
08.07.2003	06:01	389	398	95	44
08.07.2003	07:01	674	774	228	288
08.07.2003	08:01	759	863	315	332
08.07.2003	09:01	1 059	1 261	537	656
08.07.2003	10:01	818	951	357	360
08.07.2003	11:01	751	818	324	324
08.07.2003	12:01	717	973	307	328
08.07.2003	13:01	818	1 128	412	554
08.07.2003	14:01	546	641	222	232
08.07.2003	15:01	667	774	286	298
08.07.2003	16:01	716	796	320	278
08.07.2003	17:01	626	730	216	236

Figure 4-42 displays the lab values (abscissa) and the UV-VIS values (ordinate) of TSS. A linear regression trend of these values results in $y = 0.71 \cdot x + 63.3$. The corresponding stability index R^2 is 0.91 and, therefore, the correlation factor r results in 0.95 of the defined regression and the values. The offset 63.3 mg/l over the whole range is quite high. If the trend line is forced through the zero-point (grey line) the resulting equation can be written as $y = 0.90 \cdot x$, which seems a better reproducibility of the UV-VIS and lab values coherence. The stability index of 0.83 and the correlation factor of 0.91 show that, in this case, the correlation can not be displayed so exactly. Generally, the company's calculation equation can reproduce the real values (lab values) satisfactorily; of course the high offset of about 60 mg/l should be improved by local calibration.

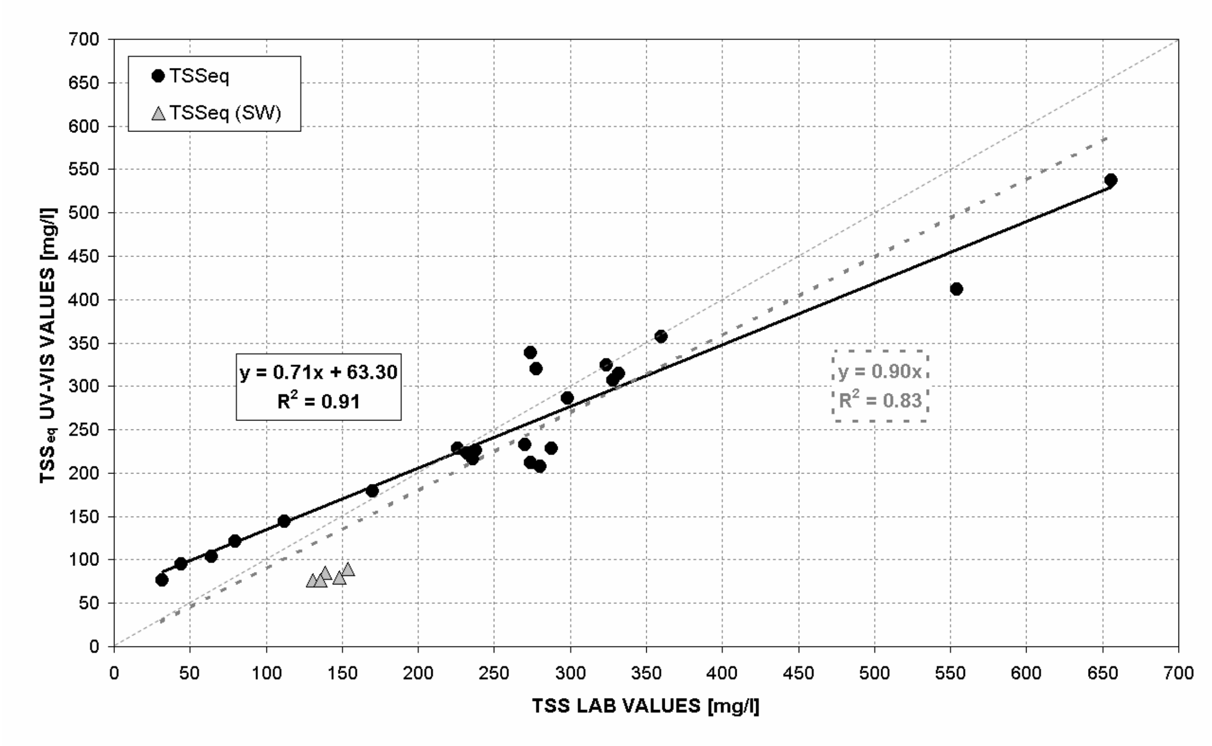

Figure 4-42 UV-VIS vs. Lab Values of TSS of 1st Measurement Campaign

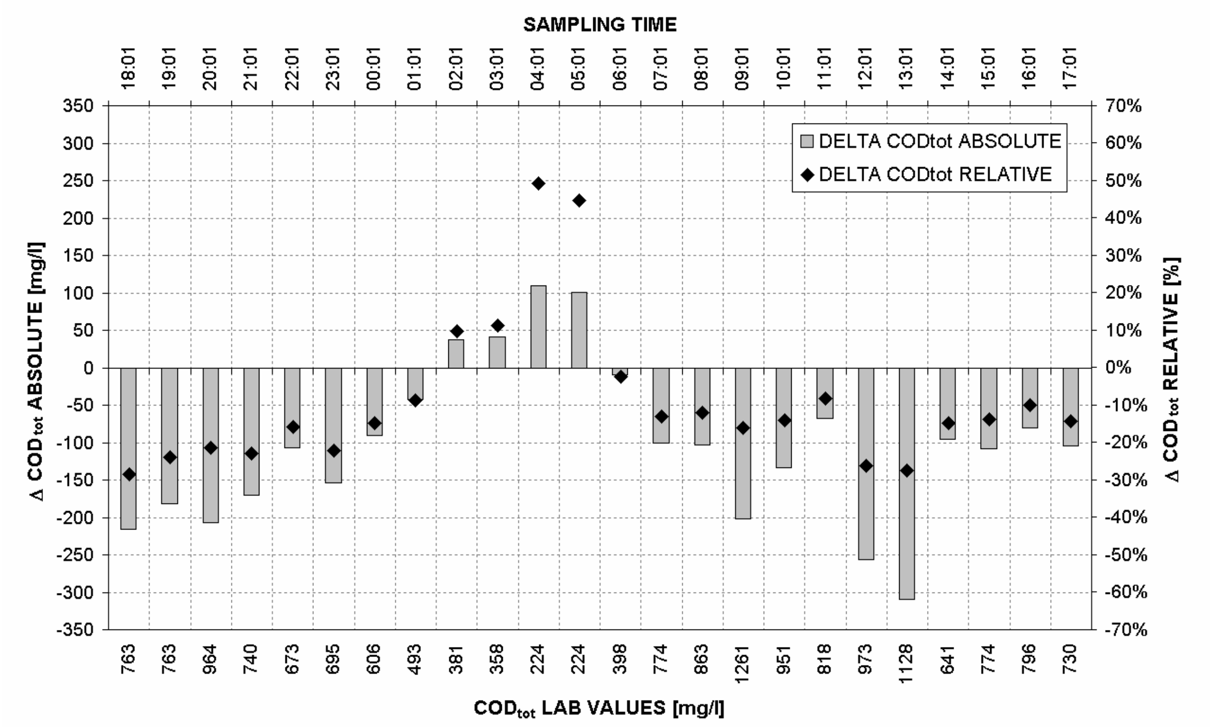

Figure 4-43 Absolute and Relative Deviations of UV-VIS and Lab Values of COD_{tot}

The trend, which can be recognised with the TSS parameter, is rather more clearer for the COD_{tot} parameter. Figure 4-43 displays this well-defined trend. From 2^{00} until

5^{00} the influence of groundwater infiltration and, therefore, the changing of the waster matrix due to dilution can be recognised.

The maximum absolute difference of 310 mg/l is at 13^{00} and a corresponding relative difference of 27%. The maximum relative difference can be seen 4^{00} with 49%.

Figure 4-44 shows the comparison of lab and UV-VIS values for COD_{tot}. A linear trend of these values with a stability index on 0.92 and a correlation factor of 0.96 demonstrates the small scattering of the values and the linear behaviour of UV-VIS and lab values. The offset of approximately 148 mg/l is unacceptably high. Interestingly, the five storm water samples (grey triangles) fit very well in the linear trend of COD_{tot}.

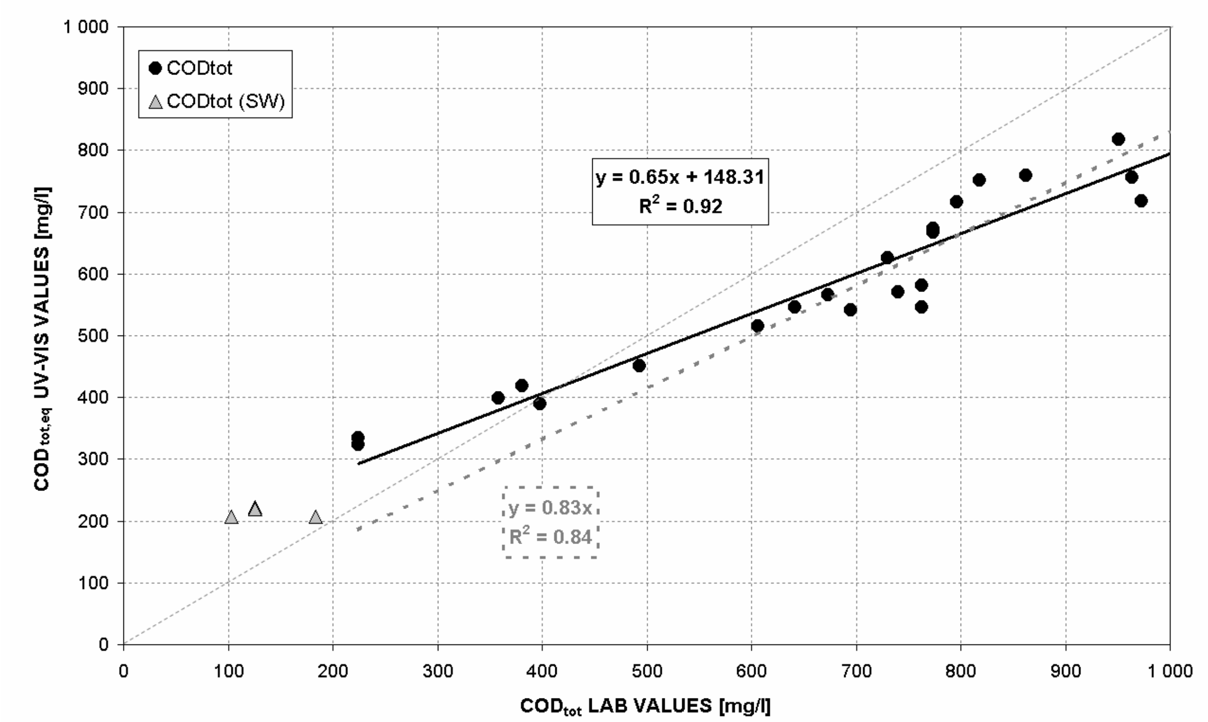

Figure 4-44 UV-VIS vs. Lab Values of COD_{tot} of 1st Measurement Campaign

Finally, the fact of a no zero absorbance measurement has to be pointed out. Actually, before the reference measurement it should be checked whether the probe measures zero absorbance with distilled water. If the measurement has a value higher than zero, the offset has to be set to zero. Therefore, all measurements of the 1st campaign have to be considered carefully due to the unknown value of this offset.

4.8.2. 2ND MEASUREMENT CAMPAIGN

A zero referencing (Figure 4-45) was carried out for the 2nd measurement campaign to quantify the offset value of absorbance measurement. Unfortunately, the offset absorbance was measured but not stored and not set to zero. Hence, the data (offset absorbance spectra) was digitalised by means of a screenshot and the absorbance was corrected manually with this result. The influence of the offset from possible biofilm growth on the measurement window can be seen in Figure 4-45.

To guarantee a reliable zero referencing the measurement window should be cleaned to remove possible biofilm. In this case, a double intensive cleaning by washing up-liquid and further intensive cleaning with distilled water was carried out. Thus, a fully removal of scum is possible which influence the absorbance measurement.

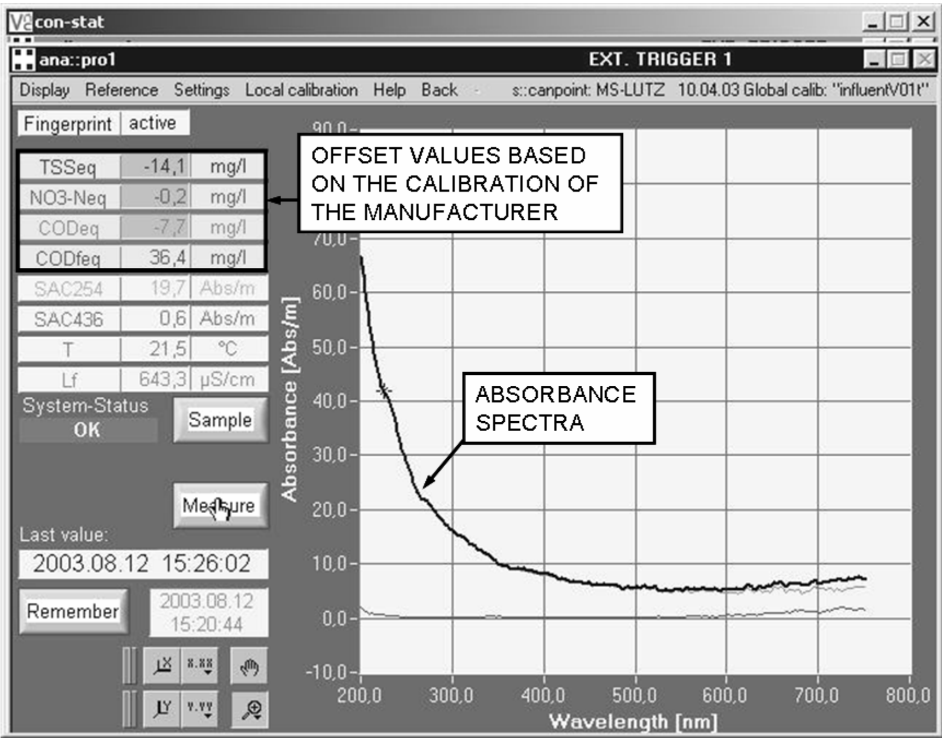

Figure 4-45 Zero Measurement of Absorbance Spectra for 2nd Measurement Campaign

The absolute and relative deviations of TSS from the 2nd measurement campaign are displayed in Figure 4-46. The influence of groundwater infiltration can also be recognised. The absolute difference of 179 mg/l of TSS can be recognised at 21^{00} in the evening. The company's calibration reproduces too low values at high concentrations and at low concentrations values that are too high. The maximum relative deviation of 151% was recorded at 20^{00} and 21^{00}. An overview of the values of this 2nd campaign is given in the table A-12 in the appendix.

Figure 4-47 presents the wide scattering range of approximately 250 mg/l in this campaign. To highlight this scattering the area is displayed in a grey colour to point out this scattering. This scattering can be affirmed with a stability index of 0.59 and a corresponding correlation factor of 0.77. An assumption of linear trend forced through the zero point results in an insufficient stability index of 0.44. The five storm event samples, drawn as grey triangles, are in the lower scattering range.

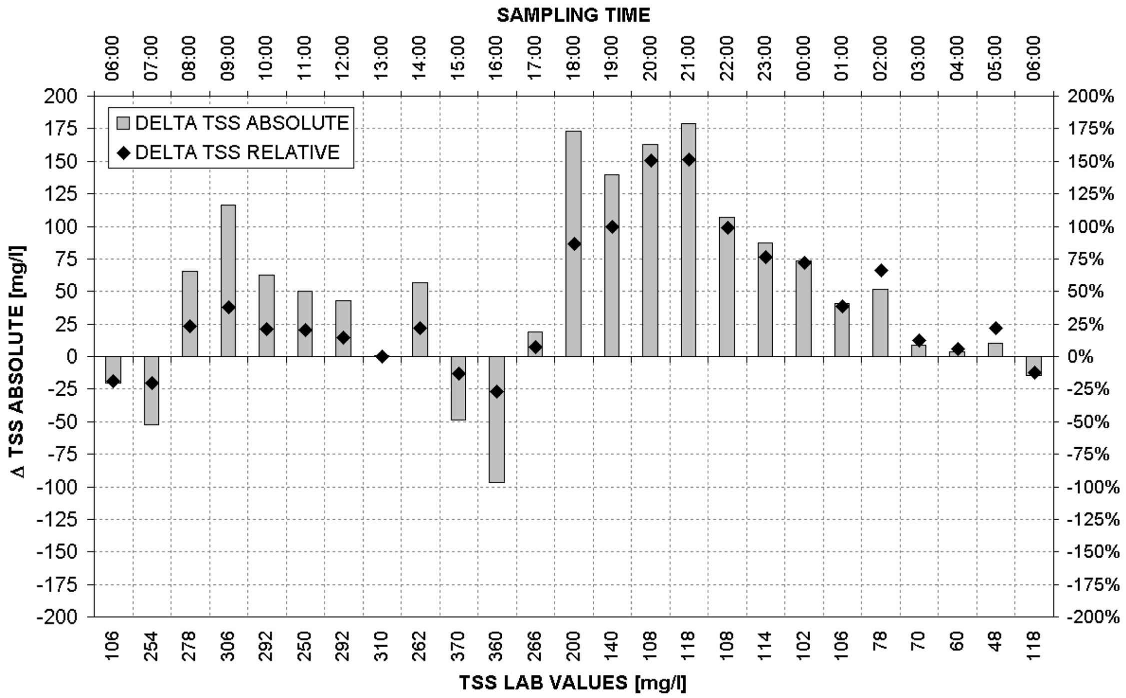

Figure 4-46 Absolute and Relative Deviations of UV-VIS and Lab Values of TSS of 2nd Campaign

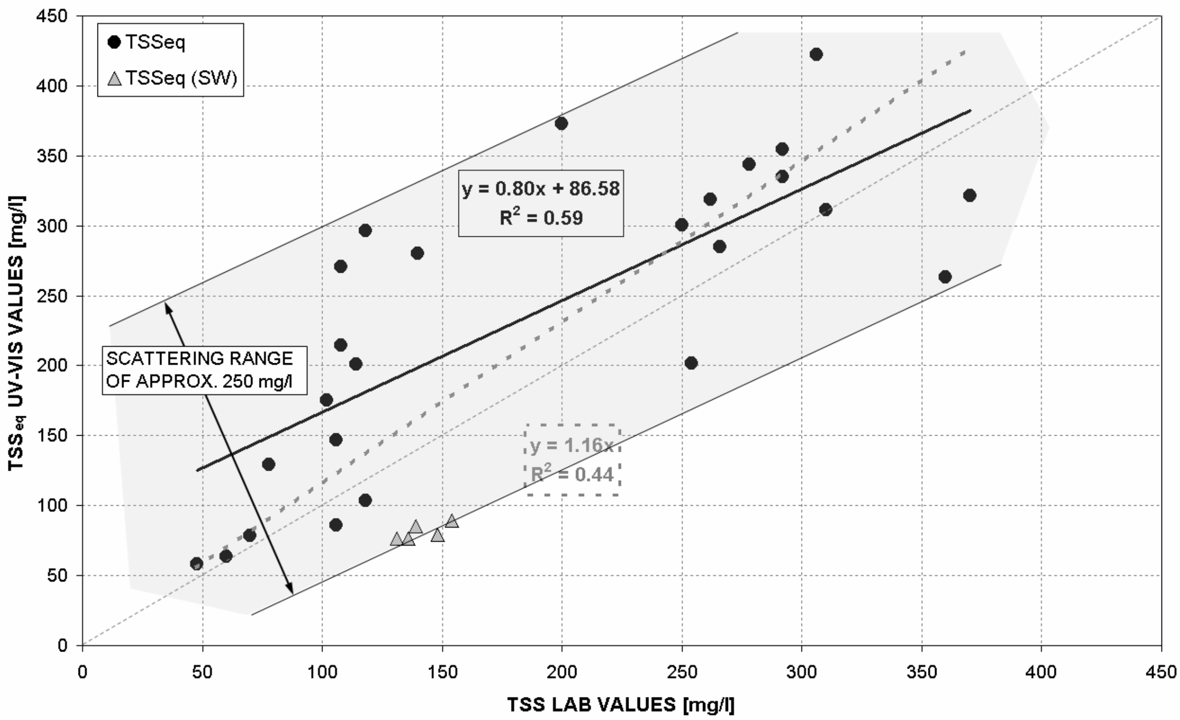

Figure 4-47 UV-VIS vs. Lab Values of TSS of 2nd Measurement Campaign

The behaviour of groundwater infiltration at night hours can be especially recognised for COD_{tot} and the insufficient global calibration of the company shows the necessity of an improving local calibration. The maximum relative difference of 60% was measured at 5^{00}, the absolute deviation is only 99 mg/l (Figure 4-48). In the evening, at high concentrations, the maximum difference is 295 mg/l.

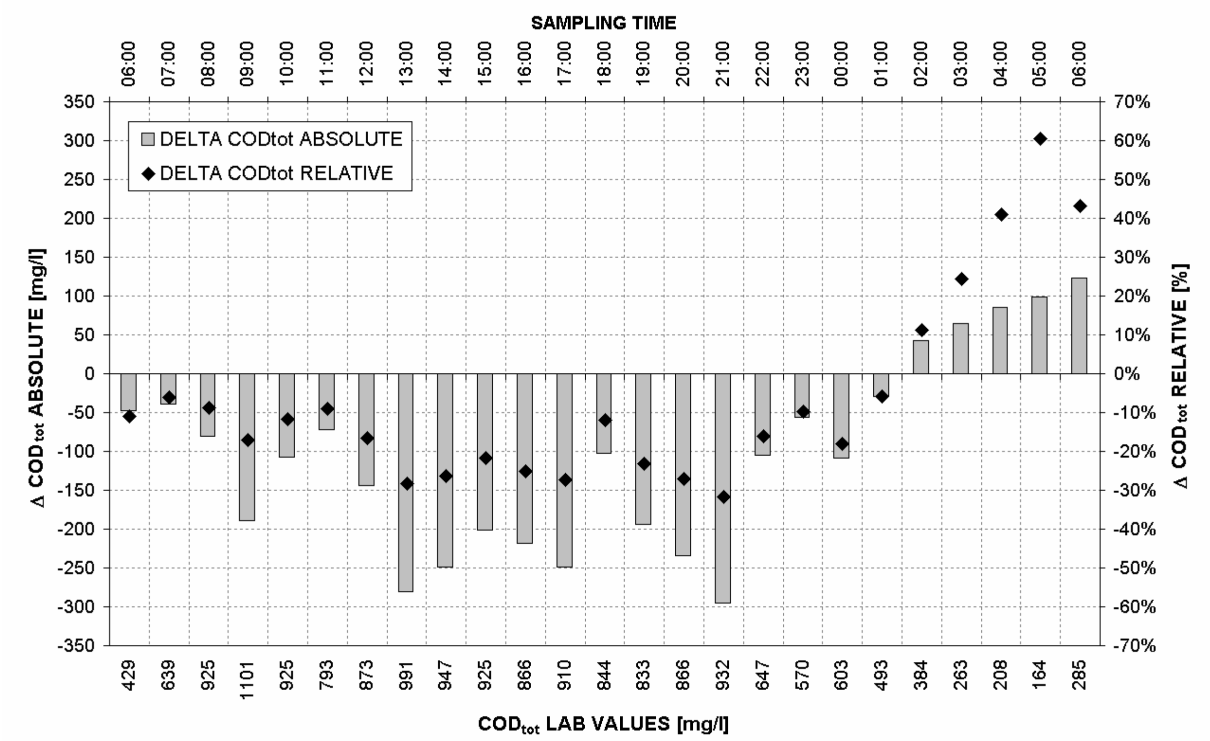

Figure 4-48 Absolute and Relative Deviations of UV-VIS and Lab Values of COD_{tot} of 2nd Campaign

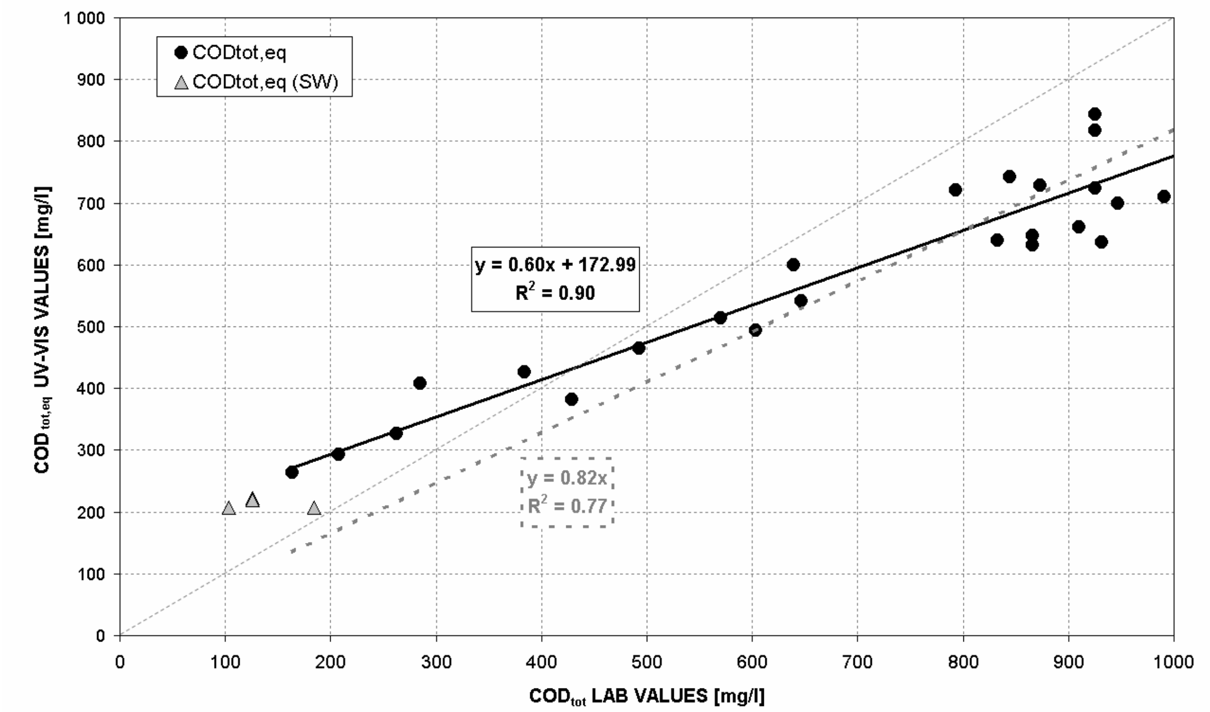

Figure 4-49 UV-VIS vs. Lab Values of COD_{tot} of 2nd Measurement Campaign

Figure 4-49 presents the diagram of UV-VIS and lab values for COD_{tot} from the 2nd measurement campaign. The inclination of the linear trend line is 0.60·x with an offset of 173 mg/l. The five storm samples (grey triangles) fit very well in this linear trend, which shows that the coherence of UV-VIS and lab values have to be adapted. Almost no scattering of the COD_{tot} values could be recognised during the 2nd campaign which is also expressed by the stability index of 0.90 and the correlation factor of 0.95.

4.8.3. Improved Local Calibration

The importance of global calibration improvement to a local calibration has been explained in the previous two chapters. The consequence of an improved calibration is displayed in Figure 4-50. The diagram shows the varied measurement values of the COD_{to} parameter $_t$ for the period of 3rd January to 6th January 2004. It can be clearly seen in the figure that in the analysed period the global calibration (provided by the manufacturer) resulted in too low values at high concentrations compared with the improved local calibration which is based on measured absorbance spectra of the 1st and 2nd measurement campaign. Hence, it can be concluded from the results that for the waste water matrix at the CSO in Graz the global calibration, especially for COD_{tot}, results mostly in values that too low for the dry weather concentration. Therefore, a calculation of the dry weather load based on the global calibration would be wrong.

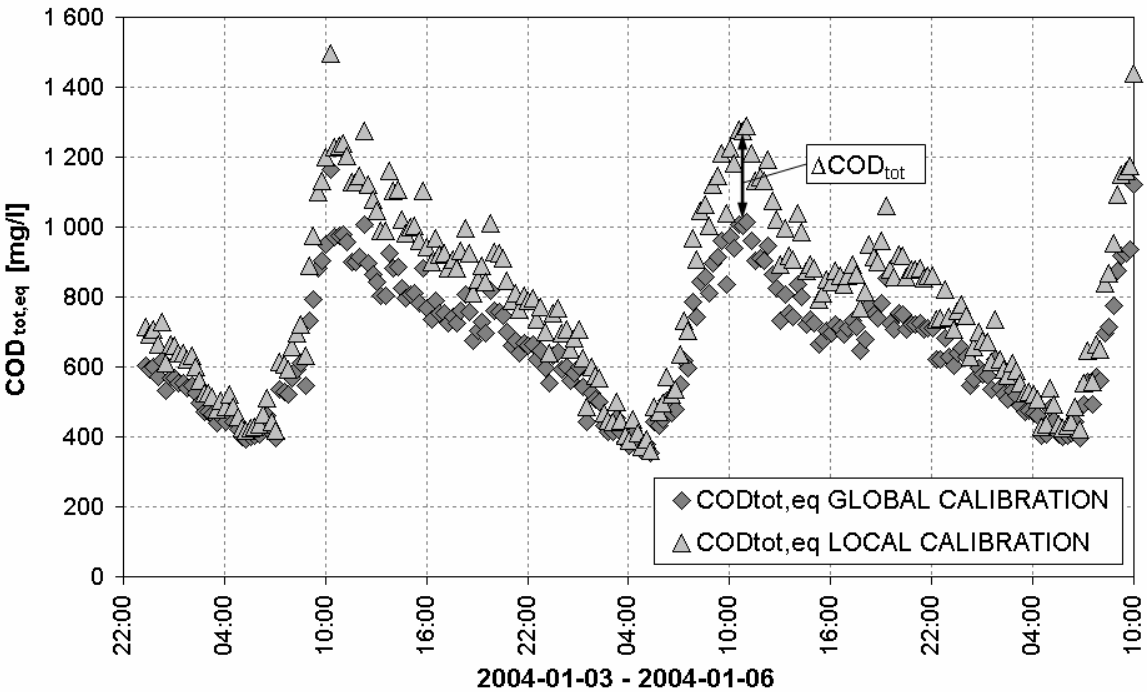

Figure 4-50 Effect of Local Calibration for COD_{tot} (Wedenig, 2004)

All spectrometer measurements also record the complete absorbance spectra (fingerprints). Therefore it is possible to recalculate the values offline for all concentration either with adapted local or a new generated local calibration. Thus, a correction and improvement of the concentrations can be made.

The comparison of the lab and the equivalence values from the UV-VIS measurement show extensive differences for the parameter $NO_3^- - N$. The accomplished local calibration improvement did not deliver satisfactory results. Thus, research work was abandoned regarding a closer analysis of this parameter. One possible explanation for the insufficient results for nitrate is due to the measurement range. At the CSO monitoring station the nitrate values are rather low. For UV-VIS measurement in waste water for nitrate a path length (measurement window) of 1 or 2 mm is recommended to gain reliable nitrate data, which can not fulfilled by the used spectrometer in Graz with a path length of 5 mm.

The improved local calibration for COD_{tot} and for TSS is an excellent solution and provides reliable data confirmed by sensitive analysis and different verifications.

4.8.4. 3RD MEASUREMENT CAMPAIGN

On the basis of the accomplished measurement campaigns and the measurement values gained (IDs), a validation of the online values is not only possible by means of further improving of the local calibration. The existing know-how is used to generate a new calibration which is a local calibration for the Graz monitoring station. This calibration provides a coherence like the global calibration but also with a linear equation. Therefore, from 31st March to 1st April 2004 a 3rd 24 hour measurement campaign was carried out. This campaign differed to the other two measurement campaigns by additional sampling not only with the automatic sampler also a manual sampling by scooping directly in the sewer. Additionally, a 2nd UV-VIS spectrometer was assigned to provide reference measurements to the installed spectrometer in the pontoon.

The aim of this 3rd measurement campaign was to detect possible ascertainable failures and their influences on the measurements, for example:

- Sampling and its sampling position
- Transport of the samples
- Sample conditioning
- Sample conservation

To quantify the influence and the effects on sampling, two different kinds of sampling were carried out. On the one hand, the samples were taken with an automatic sampler by a hose installed in the back of the pontoon. On the other hand, samples were taken manually by scooping. In addition, the two spectrometers also delivered online values. An overview of the different sampling positions is displayed in Figure 4-51.

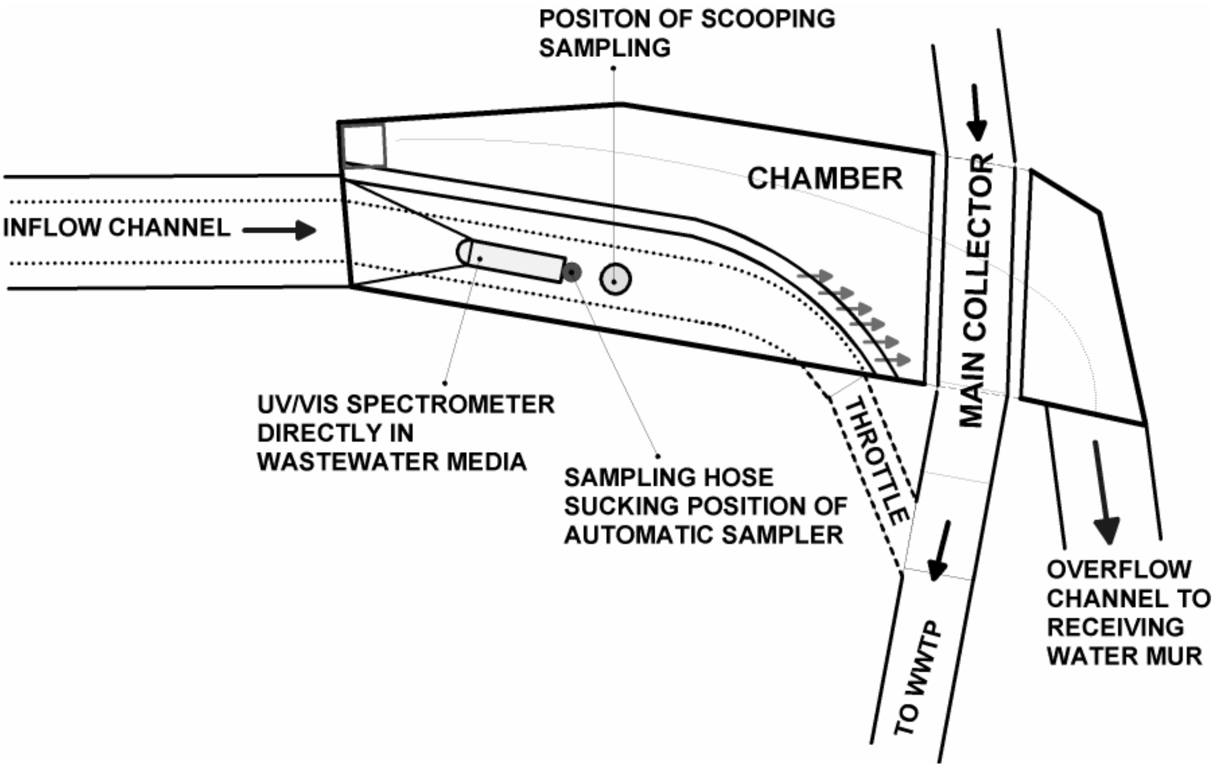

Figure 4-51 Sampling Positions in the CSO Chamber for 3rd Measurement Campaign

4.8.4.1. Referencing of the Two UV-VIS Probes

The 1st step of the measurement campaign was the comparison measurement of the UV-VIS spectrometers. Hence, the probe installed in the pontoon was removed.

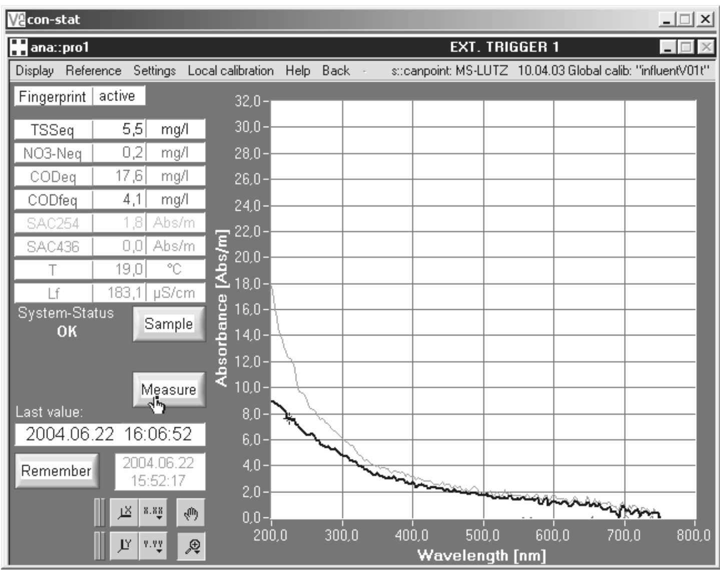

Figure 4-52 Absorbance spectra of distilled water (left figure) and reference measurement of the two UV-VIS spectrometer (right figure)

A zero reference was carried out on both spectrometers where absorbance and the absorption spectra of distilled water were measured. In this case no absorbance (Figure 4-52) should be measured; otherwise the offset absorbance has to be set to zero. Afterwards, a validation of the two spectrometers with communal waste water was carried out (Figure 4-52). Finally, both probes measured the same absorbance spectra. One spectrometer was again installed in the pontoon.

The following recommendations are given for a zero referencing. All substances, e.g. organic compounds or grease should be removed from the measurement window. The best way to have an absolutely clear window is to first clean intensively with diluted hydrochloric acid and afterwards with ethyl alcohol to guarantee reliable measurement values. Cleaning with washing up liquid never guarantees an absolutely clean measurement window.

4.8.4.2. MEASUREMENTS IN THE FIELD

The samples from the 24 hour measurement campaign were taken by two different methods. On the one hand, the samples were taken by sucking by manual triggering with an automatic sampler equipped with a peristaltic pump. On the other hand samples were taken by manually scooping in the CSO chamber at the same time. Hence, with the scoop a 50 l pot was charged continuously as long as the automatic sampler needed for sucking of the waste water samples. After the scooping, a permanent stirring guaranteed a representative part sampling. The sucking of the automatic sampler took about 180 seconds, varying due to the consistence of the waste water.

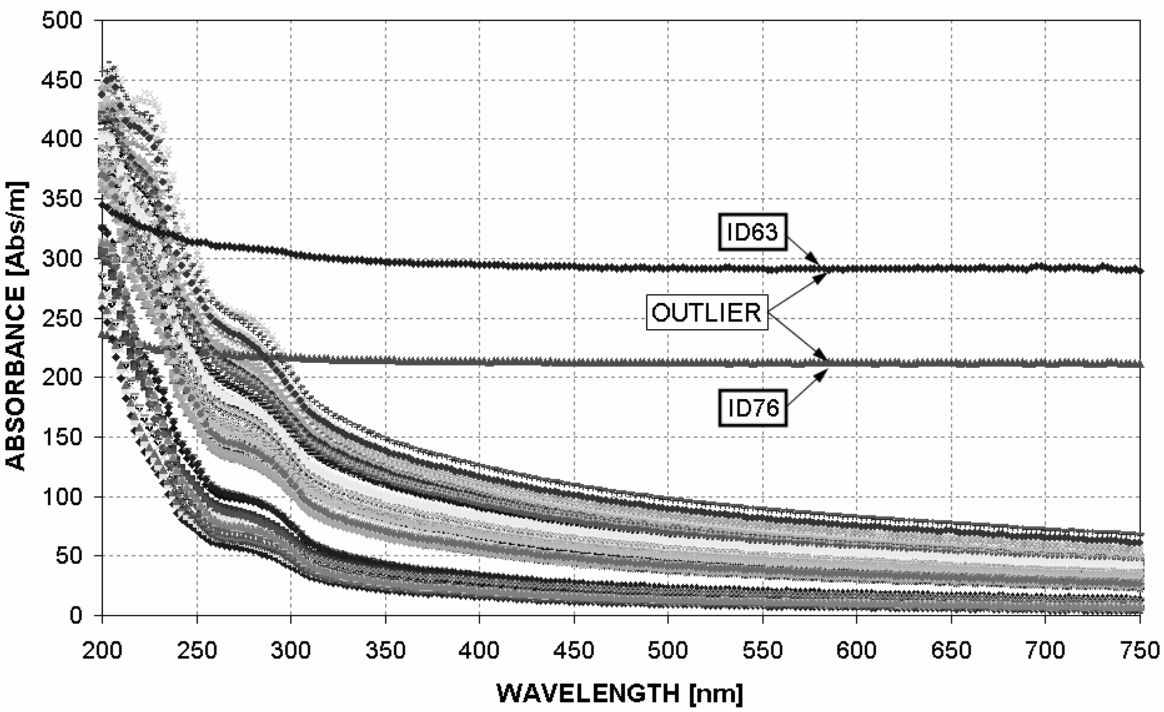

Figure 4-53 All IDs of the UV-VIS Spectrometer Installed in the Pontoon of the 3rd Measurement Campaign – Typical Absorbance Spectra for Communal Waste Water

During the sucking duration all measured fingerprints (IDs) were recorded and stored those from the UV-VIS probe. All IDs during the 24 hour measurement campaign are displayed in Figure 4-53. Interestingly the two outliers indicate a false absorption measurement. If at the measurement e.g. a sheet of paper is situated in front of the measurement window the probes measures the absorbance and turbidity of paper. The nearly horizontal absorbance spectra emphasises this assumption. The two outliers were eliminated and therefore not considered for a later analysis and calculation to prevent wrong results.

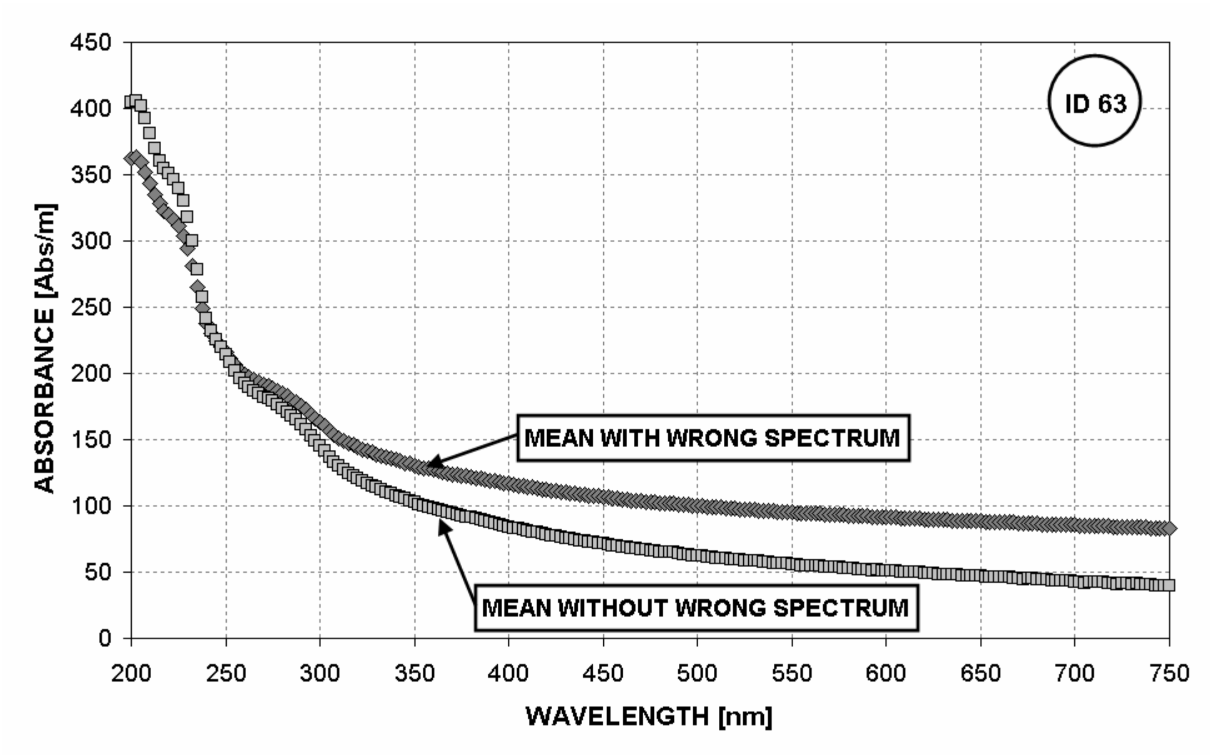

Figure 4-54 ID63 (Absorbance Spectra) of 3rd Measurement Campaign

Every concentration in this 3rd measurement campaign is based on four absorbance spectra. The mean of the absorbance will be used for the concentration calculation. Hence, if the absorbance values are wrong the resulting concentrations are also wrong; therefore a closer analysis shall be made.

Figure 4-54 shows the effect for ID 63 of the mean with wrong spectrum (four absorbance spectra) and without the wrong spectrum (three absorbance spectra) included. Although the difference of two possible mean absorbance spectra is only marginal, the effect can be quite high. All the following concentration values are calculated on the basis of the global calibration. The difference for COD_{tot} is a slight one due to the wavelength taken for concentration calculation in the range of about 250 nm. The resulting COD_{tot} value, including the false spectrum, is 583 mg/l and the value without the wrong spectrum is 562 mg/l. This difference would be in an acceptable range. But for the TSS parameter, this difference is quite high. The value, including the false spectrum, results in 458 mg/l; without the wrong spectrum it equals 249 mg/l. A resulting difference of 46% is the consequence, which is, of course unacceptable.

Figure 4-55 shows the results of ID 76. As already recognised at the ID 63 the effect of a false spectrum is presented. In this case as already recognisable in the figure the deviations are significant. The difference can already be seen at the COD_{tot} parameter with the correct value of 430 mg/l and false one of 269 mg/l. A similar result is noticeable for the TSS parameter with 71 mg/l (without wrong spectrum – three absorbance spectra) and 425 mg/l (wrong spectrum included – four absorbance spectra). Hence, the importance of an absorption verification is demonstrated and its effect when not taken into consideration. The solution of this problem could be an automatically check which could be based on an analysis of the 1st deviation of the absorbance spectra. But data check only of the raw measurement values (absorption) should be undertaken due to a possible false interpretation of concentrations of the absorbance and concentration coherence.

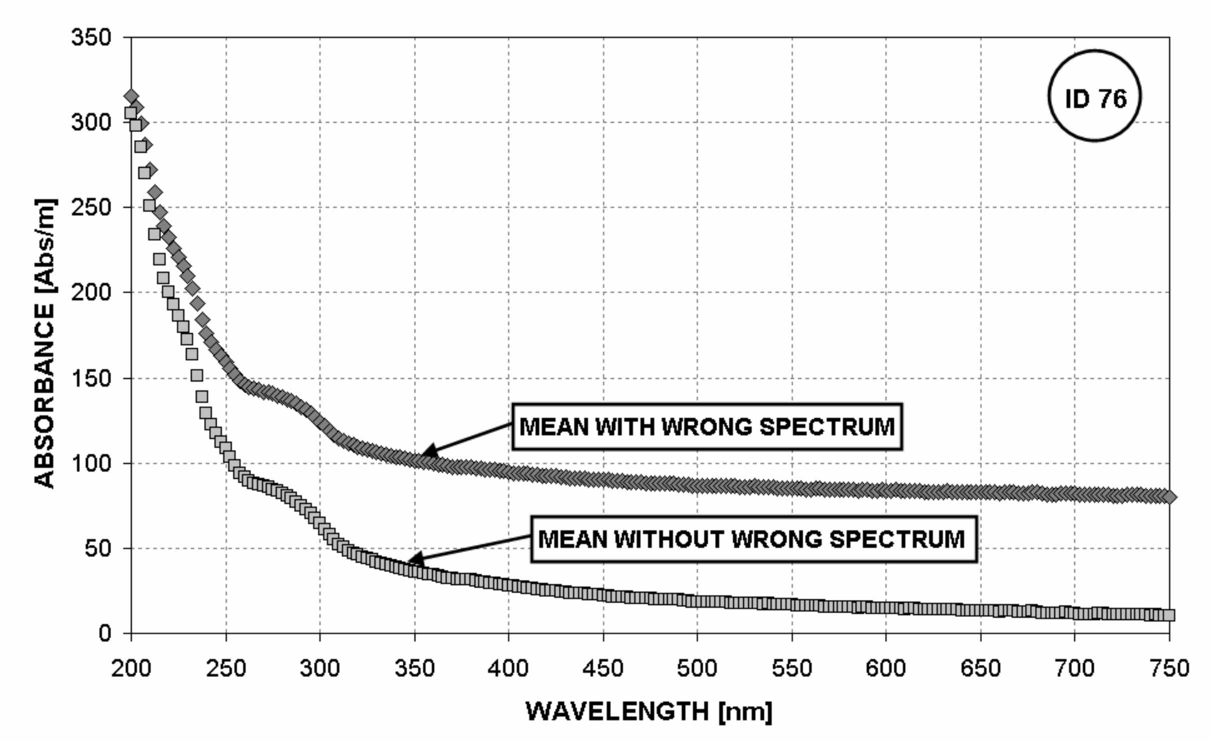

Figure 4-55 ID76 (Absorbance Spectra) of 3rd Measurement Campaign

Finally, the scooping sample and the sample taken by the automatic sampler were also measured with the 2nd UV-VIS probe in the field and its values recorded and stored. Subsequently, the immediate transport to the lab to prevented possible biological degradation.

4.8.4.3. LAB ANALYSIS

After the sample transport, an immediate absorbance measurement by the 2nd spectrometer was made. Afterwards, the samples were homogenised. An absorbance measurement of instantaneous homogenised samples did not provide sufficient results due to the existence of too many bubbles which adulterated the measured absorbance.

All parameters in the lab were analysed twice to prevent a false analysis. Due to limited capacity in the lab, it was only possible to analyse all COD samples every 3rd hour. The remaining samples were frozen at -20° C and analysed a week later.

4.8.4.4. RESULTS OF 3RD MEASUREMENT CAMPAIGN

Both UV-VIS probes measured similar absorbance spectra and therefore similar equivalence concentrations resulted.

Interestingly, the values of the automatic sampler and of scooping resulted in only minor differences. These differences can be recognised for COD_{tot} as well as for the TSS values. As these were almost no differences between the spectrometer values from the pontoon spectrometer installed in the pontoon and from the sampler values measured by the 2nd probe, the assumption of no loss during sucking was confirmed. Additionally, the similar measurement results of scooping and automatic sampler samples can be seen.

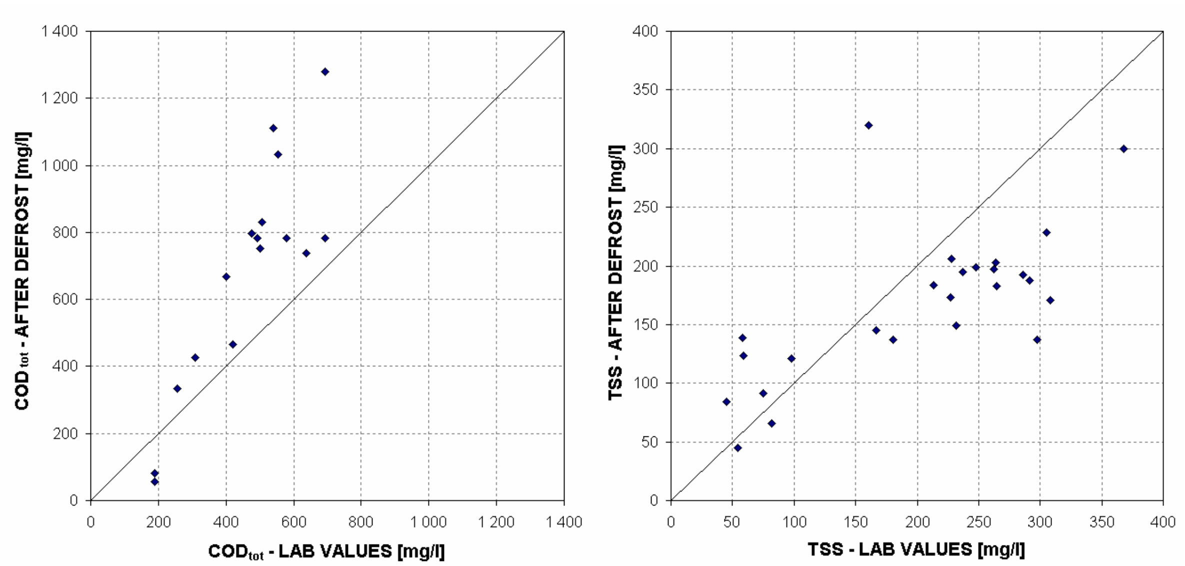

Figure 4-56 Comparison of the Measurement Results of the 3rd Measurement Campaign for COD_{tot} (left figure) and TSS (right figure)

The differences of COD_{tot} values between lab values and values after defrost can be seen in Figure 4-56. The default settings (global calibration) fit quite well for the TSS parameter. Therefore, an improvement of the global calibration for TSS is in this case not absolutely necessary. High differences between frozen and unfrozen samples are recognised (Figure 4-56). But a clear trend could not be detected. Geiger (1984) analysed this influence. The influence of sample aging is also displayed by Baurés et al. (2004).

The assumption of a good fitting global calibration is displayed in Figure 4-57. In this diagram the UV-VIS values are the ordinate values and the lab values are the abscissa values. A linear regression line through these nine value pairs results in an offset of approximately 13 mg/l and stability index of 0.96. The correlation factor of 0.98 demonstrates the small scattering which is in this case only about 75 mg/l.

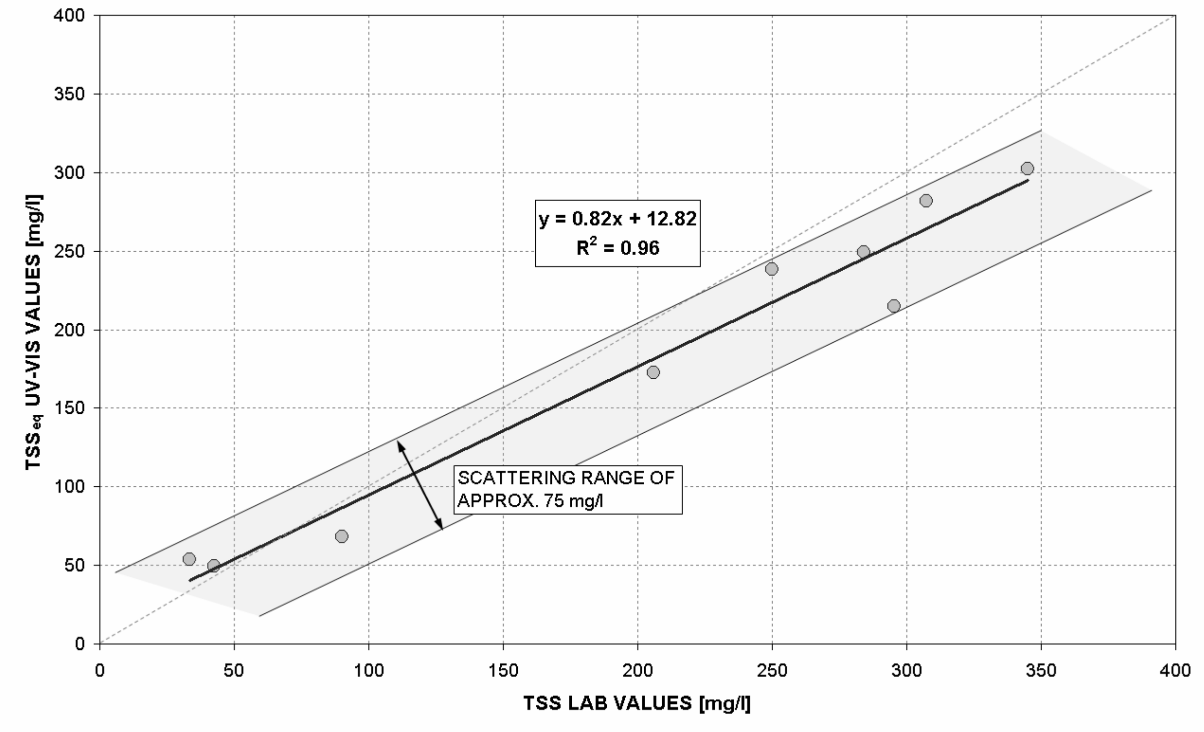

Figure 4-57 UV-VIS vs. Lab Values of TSS of 3rd Measurement Campaign

The information of no loss of solids from the automatic sampling is important for further storm event sampling. This sample can be seen as a representative one which could not be confirmed with 1st and the 2nd measurement campaign.

No influences on the sample transport were recognised due to the low outside temperature of 5° C in the night and 15° C at noon. The transport time took approximately 20 min which depends, of course, on possible heavy traffic. In this period, no distinguishable decomposition could be identified.

The samples were analysed before as well as after homogenisation to determine the effects of sample preparation (homogenisation). Influences on the values by sample preparation could also not be recognised. Due to high energy input it was not possible to measure reliable absorbance spectra immediately after homogenisation. After some time, typical absorption spectra of waste water could be measured again.

Due to limited lab capacity it was not possible to analyse all the samples immediately. The rest were frozen in accordance with the Austrian standard requirements. After about one week these samples were also analysed. A part of the instant analysed samples were also frozen for a possible comparison of frozen and unfrozen analysed samples. The results can be seen in Figure 4-56. Although the samples were frozen according to the standard, significant differences resulted. For the COD_{tot} values could be recognised showing that most of the frozen samples had higher concentrations than the immediately analysed samples. A clear trend and a well-defined coherence of this concentration increase could not be determined. For the TSS values the frozen samples also produced high concentration differences compared with the instantaneous analysed samples. Lower values were recognised for the frozen samples.

4.8.4.5. COMPARISON OF 2ND AND 3RD MEASUREMENT CAMPAIGN

A comparison follows to verify the plausibility of the 2nd and the 3rd measurement campaign. This comparison is displayed in Figure 4-58. Due to the variability in the dry weather flow curve, a comparison of absolute values has only limited significance.

In Figure 4-58, the lower abscissa displays the COD_{tot} lab values, both ordinates show absolute and relative differences of the spectrometer values to the lab values, respectively. The absolute differences between the 2nd and 3rd measurement campaign show similar sizes. The relative deviations from the 3rd measurement campaign are up to 30%. The absolute differences result up to 300 mg/l. The change from negative to positive differences can be recognised at both measurement campaigns.

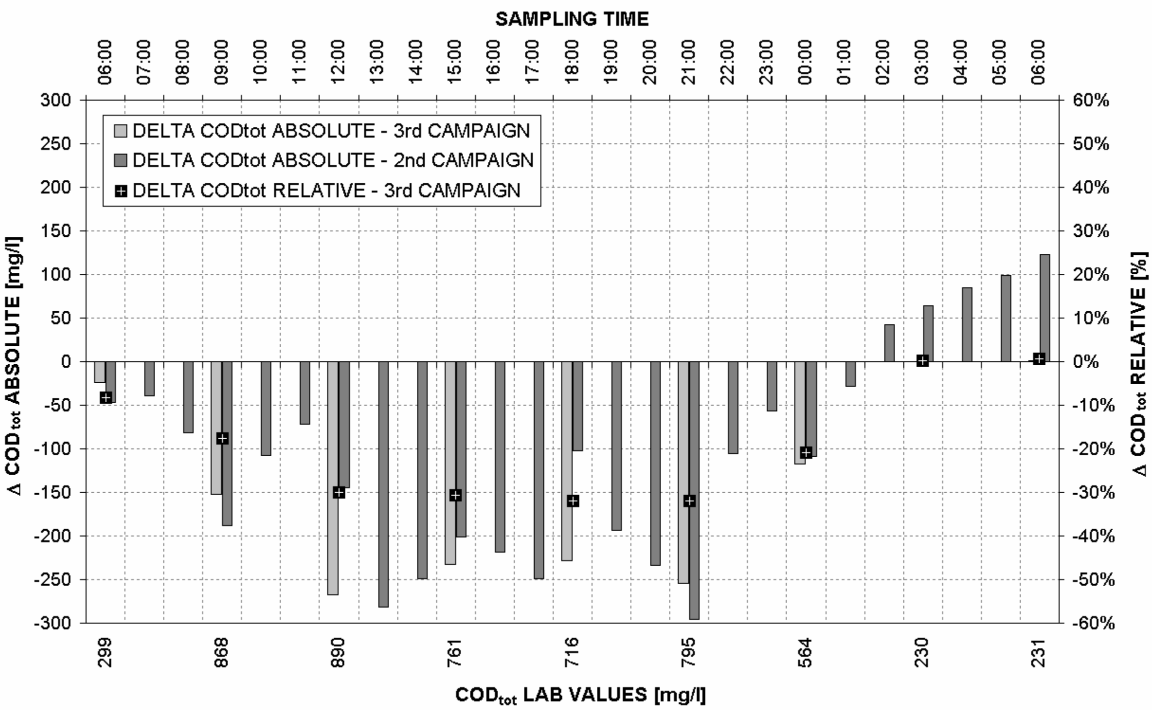

Figure 4-58 Absolute and Relative Deviations of COD_{tot} Values of 2nd and 3rd Measurement Campaign

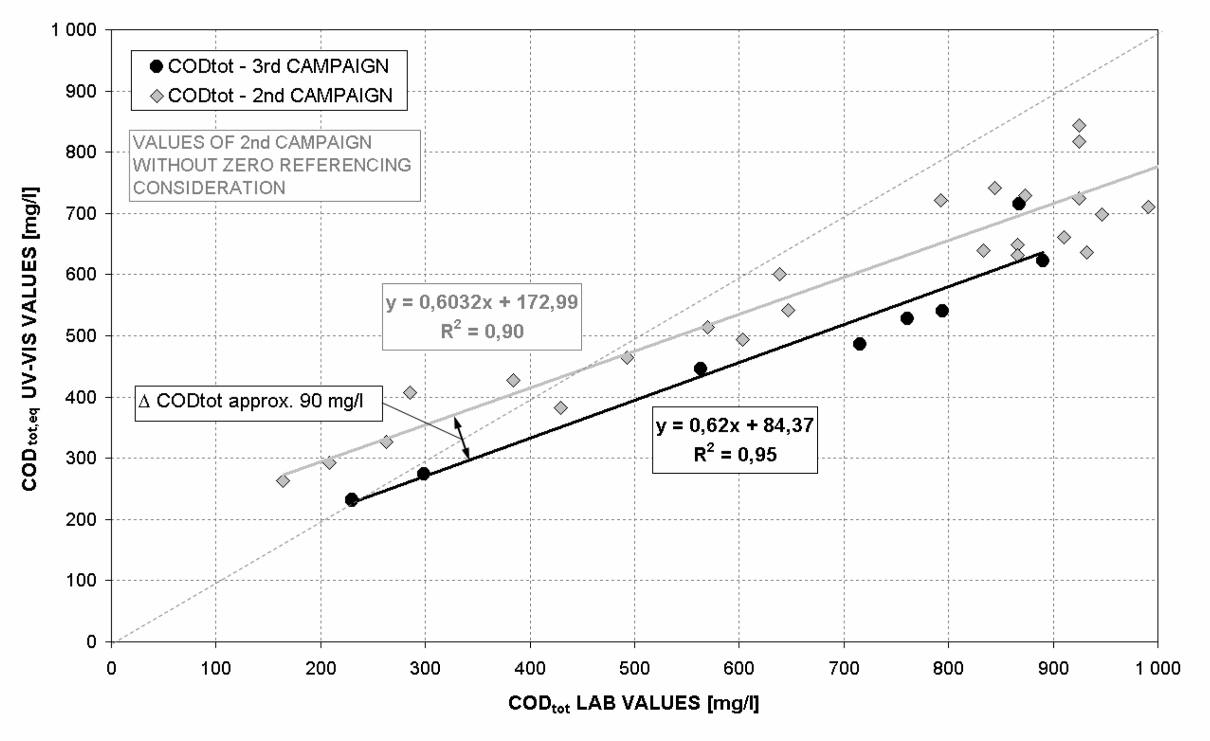

Figure 4-59 Comparison of COD_{tot} UV-VIS and Lab Values from 2^{nd} and 3^{rd} Measurement Campaign

Figure 4-59 shows a comparison of COD_{tot} UV-VIS and lab values from the 2^{nd} and 3^{rd} measurement campaigns. Both linear trend lines have almost the same inclination of 0.60·x for the 2^{nd} campaign and of 0.62·x for the 3^{rd} campaign. The measurement values of the 3^{rd} measurement campaign have a lower scattering than the scattering range of the 2^{nd} measurement campaign. This low scattering is expressed in a stability index of 0.95 for the 3^{rd} measurement campaign and a resulting correlation factor of 0.97. A difference of approximately 90 mg/l results between the two lines. This difference can be explained by an unconsideration of the accomplished zero absorbance referencing.

4.9. NEW LOCAL CALIBRATION DEVELOPMENT FOR THE GRAZ-WEST CSO

Based on the absorbance measurements and the measured lab values of the 2^{nd} and 3^{rd} measurement campaigns a new calibration was generated by means of different multiple linear regression methods which will be explain and verified in detail in the following chapters. Therefore, the absorbance values of the 2^{nd} measurement campaign were recalculated manually to consider the zero reference measurement as previously described. A regularly cleaning of the measurement window at least twice a year and zero referencing is recommended.

Only some selected examples from the in-depth analysis of the different multiple regression methods are given here. The rest are displayed in the appendix.

The 1st step of regression modelling is the analysis of the absorbance of every wavelength and the corresponding pollution value. By means of the correlation factor calculation it is possible to determine the wavelength range which has the most influence (Figure 4-60). This determination only gives preliminary information This pre-analysis should only be seen as an additional decision tool.

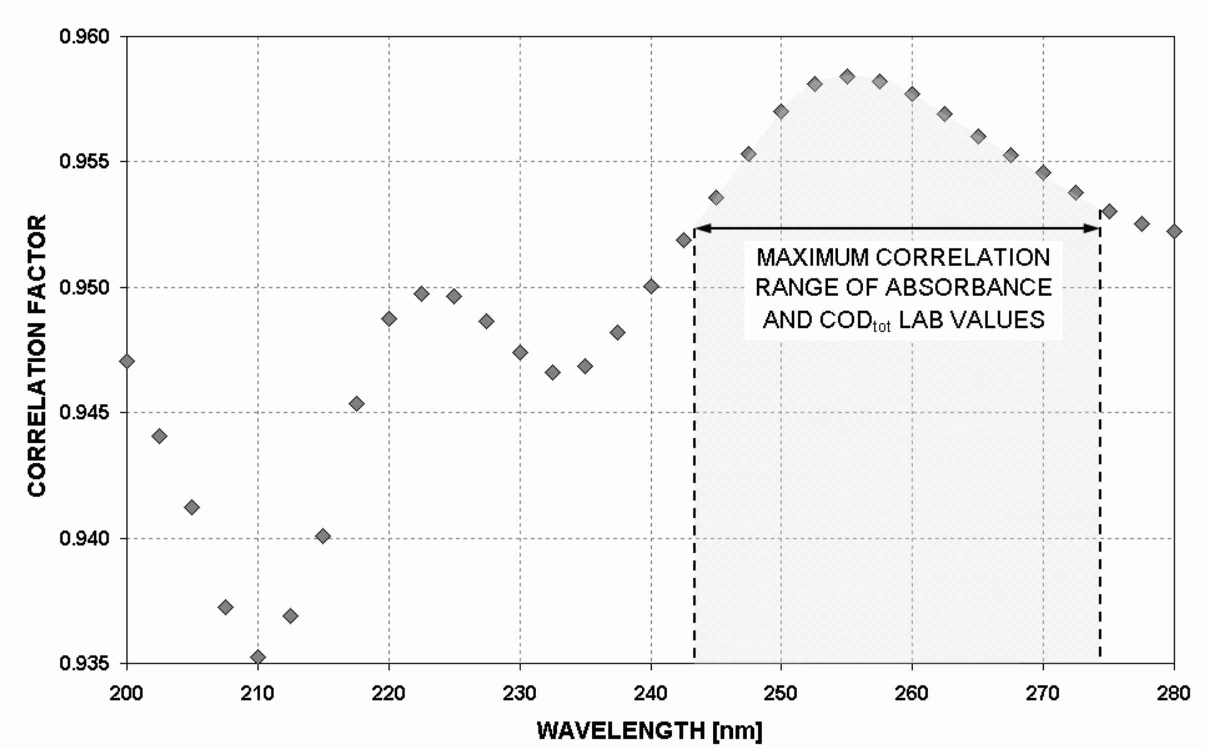

Figure 4-60 Wavelength Values vs. COD$_{tot}$ Values and Resulting Correlation Factor

Figure 4-61 shows the decision process to quantify the quality of determined regression results. This decision process was carried out for all regression methods.

The 1st step of this process is the validation of the determined equations. Based on the two measurement campaigns two different correlation coefficients were calculated for the resulting function depending on the analysed wavelength range. One coefficient was computed with a cross correlation method; the other one on the basis of percentage split. The detailed explanation for both these methods is given later.

The 2nd step is the validation of the estimated and measured dry weather data of the three different parameters from each measurement campaign. The 1st validation can be made on the basis of the calculated Pearson's correlation coefficient. The correlation coefficient is a dimensionless value of linear correlation. The correlation value can yield between -1 and 1. A value of +1 and -1 indicates a completely positive and negative linear correlation, respectively. If the correlation coefficient equals 0, then the two variables are linearly independent. Admittedly, it can be a non-linear coherence.

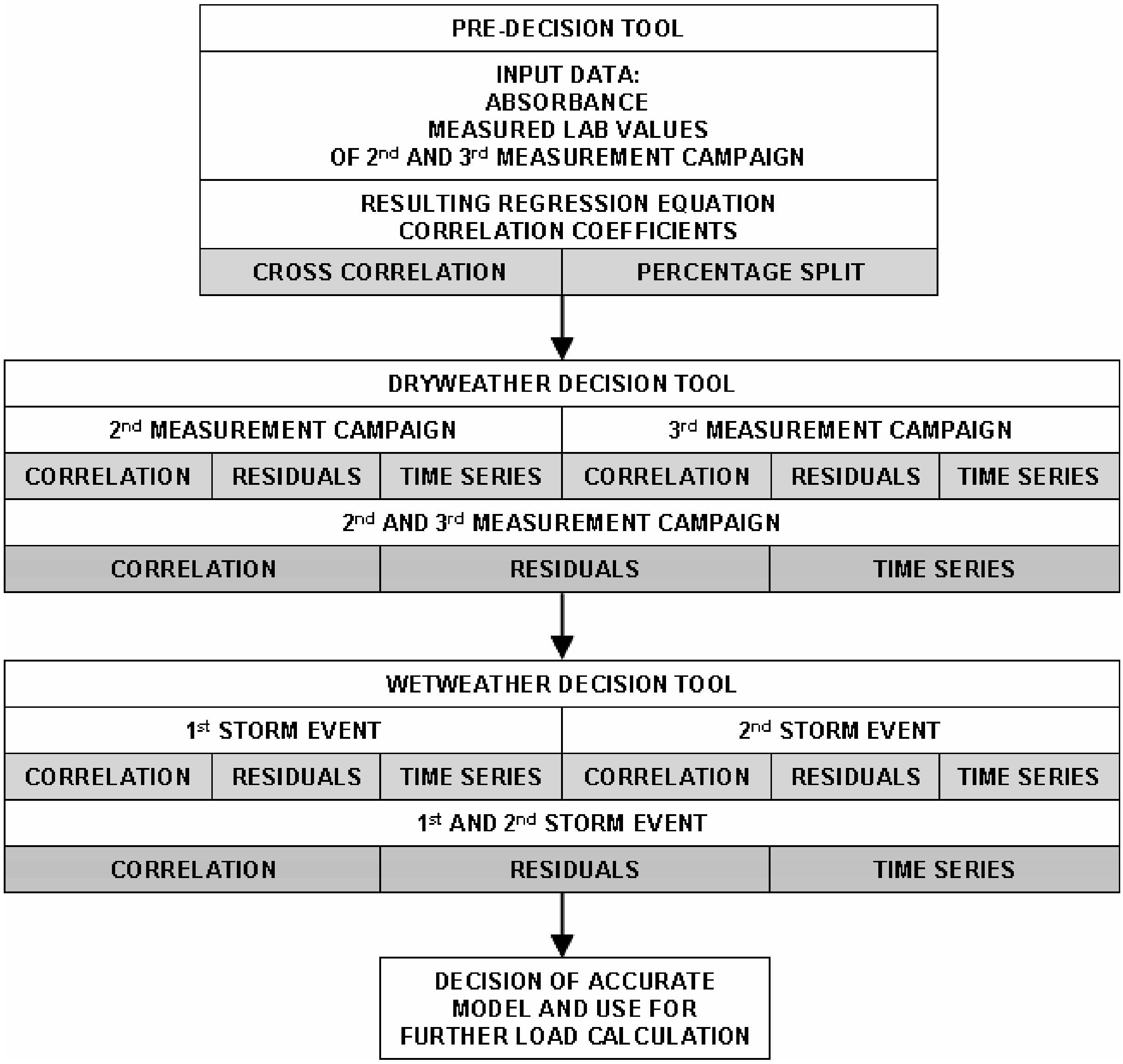

Figure 4-61 Decision Making Process of Different Equations from Regression Calculation

Correlation does not imply causation. The correlation coefficient is not an of the coherence direction. The squared correlation coefficient is the stability index, which is a 1st approximation of how much percentage of the variance can be described with the determined correlation. After the correlation analysis the analysis of the residuals is carried out. The absolute sum of all residuals between predicted and measured values of every measurement campaign can also provide information about the applicability of a regression function. Finally, a verification of the time series is made which can be used especially to quantify possible model overfitting. After the single validation the same process is carried out for all values of both measurement campaigns.

The 3rd step is the same validation process as described before for the dry weather data. The wet weather verification is carried out on the basis of two storm events. Afterwards, by means of all validation results (correlation, residuals and time series) the three best equations of every regression method and parameter are chosen for further load calculation.

4.9.1. WEKA

Weka was developed at the University of Waikato in New Zealand. “Weka” stands for the Waikato Environment for Knowledge Analysis. The system is written in Java, an object-oriented programming language. Java allows providing a uniform interface to many different learning algorithms, along with methods for pre- and post processing and for evaluating the result of learning schemes on any given dataset.

There are several different levels at which Weka can be used. First of all, it provides implementations of state-of-the-art learning algorithms that can be applied to the dataset from the command line. It also includes a variety of tools for transforming datasets, like the algorithms for discretisation. A dataset can be pre-processed; can be fed into a learning scheme, and an analysis of the resulting classifiers and its performance can be carried out.

One way of using Weka is to apply a learning method to a dataset and analyse its output to extract information about the data. Another way is to apply several learners and compare their performance in order to choose one for prediction. The learning methods are called classifiers. They all have the same command-line interface, and there is a set of generic command-line options – as well as some scheme-specific ones. The performance of all classifiers is measured by a common evaluation module.

Implementations of actual learning schemes are the most valuable resource that Weka provides. The main focus of Weka is on classifiers and filter algorithms. However, it also includes implementations of algorithms for learning association rules and for clustering data for which no class value is specified (Witten & Frank, 2001).

The following statistical analyses were made with Weka:

- Simple linear regression (SLR)
- Least median squared linear regression (LMS)
- M5 model tree (M5)
- Support vector machine with sequential minimal optimisation algorithm (SMO)

For a better understanding of the following chapters the used statistical nomenclature will be explained. For the regression a data set is necessary for calibration and validation of the regression results. The calibration or the training of a model is determined with part of the measured lab values. The other part of the measured lab values is used for validation. The values used for training the models are so called instances. Therefore, a training set which has, for example, 20 values is a 20-th instance training set. Instances are defined with a value of certain attributes or properties. In this research project the attributes of concentrations are the absorbance spectra. The training data can be also classified in different classes which can be training data with similar properties or attributes. The dry weather lab values and storm weather lab values define two different classes for example. In statistical analysis also classifiers which make an automatically classification can be used.

4.9.2. SIMPLE LINEAR REGRESSION

The simple linear regression method (SLR) is based on the root-mean-squared error, which is given by

$$\mathrm{RMSE} = \sqrt{\frac{\sum_{i=1}^{n}\left(\hat{C}_i - C_i\right)^2}{n}}$$

where n is the number of samples taken for model calibration, C_i is the actual concentration measured in the lab and $\hat{C}_i$ Is the predicted concentration form the used wavelengths and its absorbance.

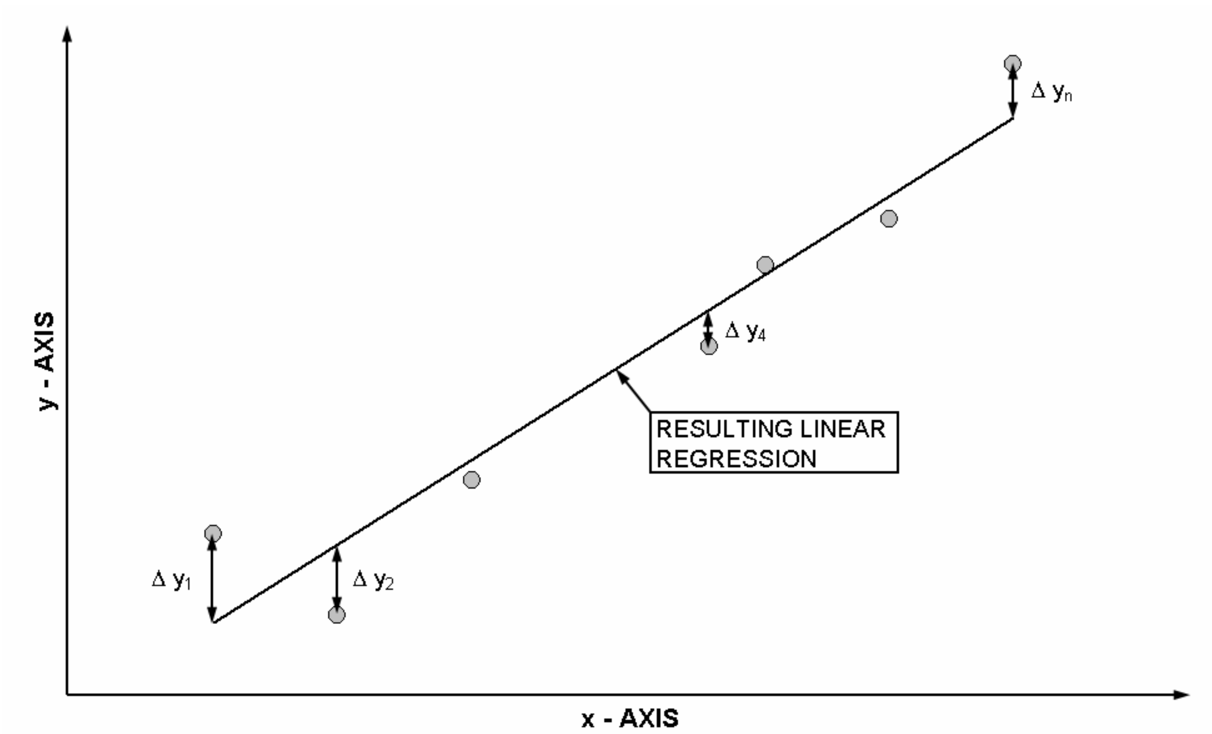

Figure 4-62 Principle of Linear Regression

Figure 4-62 more clearly displays the principle of linear regression. On the basis of the linear regression principle it is possible to calculate a linear equation. Generally, the linear regression method determines the coefficients w_j to minimise the sum of all squared differences of the training set. Assuming n training instances, where the i-th one is indicated by an (i). Hence, the sum of squared residuals can be written as:

$$\sum_{i=1}^{n}\left(x^{(i)}-\sum_{j=0}^{k}w_j\cdot a_j^{(i)}\right)^2$$

where the equation in the bracket describes the difference between actual class of i-th instance and its predicted class.

The sum of squares has to be minimised with a suitable choice of the coefficients, where x is the class, a_1, a_2, ….., a_k are the attribute values and w_0, w_1, ….. w_k are the weighing factors. The coherence can be written with following equation:

$$x = w_0 + w_1\cdot a_1 + w_2\cdot a_2 + ... + w_k\cdot a_k$$

It is also possible to write a constant factor K instead of the weighing factor w_0. The weighing factors are calculated on the basis of the training set data. Therefore, a slightly more complicated notation to express the attribute values of every trainings instance is needed. So, the first instance has the class $x^{(1)}$ with attribute values $a_1^{(1)}$, $a_2^{(1)}$, ….. $a_k^{(1)}$, where the indices (i) express the first linear regression example in this case. For a better notation it is additionally suitable to include an addition attribute a_0 with a permanent value of 1. The predicted value for the 1st instance class can therefore be written as:

$$w_0\cdot a_0^{(1)} + w_1\cdot a_1^{(1)} + w_2\cdot a_2^{(1)} + ... + w_k\cdot a_k^{(1)} = \sum_{j=0}^{k}w_j\cdot a_j^{(1)}$$

A special case of the previously described linear regression is the so-called simple linear regression. Beside the attribute a_0 which has the value zero and can be denoted as “pseudo-attribute”, only one attribute, the major influencing attribute, has to be determined. Hence, for equivalence concentrations calculation only one wavelength and its absorbance data is used.

The data pool is limited for training and validation. Thus, a definite amount of data is used for training and the rest for data validation. Usually, two third of data are for training and one third of data is for testing. This method, which was also carried out, is termed percentage split method. The used random sample for training is not representative. Generally, it is not possible to determine the representativeness of random samples without a spot check. The correct ratio of training and verification class data guarantees accurate predicted results. If all data of one definite class are not represented in the training set, it is not possible for the classifier to produce reliable results of this class. Additionally, this class is over represented in the evaluation set. Therefore, it is necessary to guarantee the right representation distribution of the samples of every class in the training and test set. This procedure is called stratification. The stratification is only a very simple “protection” against disparate representation of random samples in the training and verification set.

A more general method to compensate these representation errors is to repeat training and testing several times with different random samples. For every calculation run a definite amount of data, for example two thirds, is used for training and the rest for testing. A simple method for such statistical evaluation is cross-correlation. A precise number of partitions for cross-correlation are defined. Assuming three partitions, the data set is divided to three equal partitions. Every partition is successively used for testing and the rest for training. Hence, two third of the data are used for training and one third for testing and verification. This procedure is repeated three times, so every instance is used once for testing. This procedure is a three-fold cross correlation. If stratification is also applied, the method is called stratified three-fold cross correlation.

The standard method, which was also applied here, is a stratified 10-fold cross correlation. The data set is dissipated by random selection to ten parts. The different classes should be represented in the same distribution ratio for every part. For training nine of the parts are used and the remaining part for verification and error calculation. This calculation procedure is carried out ten times with different training sets. In practice the stratified 10-fold cross correlation has been evaluated as the most accurate method. Therefore, it has become a standard method to evaluate the error of a learning algorithm to determine a definite amount of data.

Table 4-11 Simple Linear Regression Results and its Verification Characteristics – Part 1

Parameter	Analysed Wavelength Range	Used Wavelength	Cross Correlation$^{1)}$	Percentage Split$^{2)}$	Absolute Sum of 2nd Measurement Campaign Residuals	Correlation Coefficient of 2nd Measurement Campaign
	[nm]				[mg/l]	
COD_{tot}	250 – 260	260	0.960	0.960	1 811	0.951
	270 – 280	270	0.949	0.958	1 868	0.949
	280 – 290	280	0.946	0.955	1 919	0.945
COD_{sol}	240 – 247.5, 272.5 – 290	247.5	0.803	0.664	1 050	0.839
	250 – 260	260	0.809	0.667	1 017	0.848
	270 – 280	270	0.806	0.666	1 028	0.843
TSS	600 – 647.5	622.5	0.839	0.888	1 494	0.770
	630 – 640	632.5	0.840	0.889	1 485	0.769
	680 – 690	680	0.836	0.887	1 483	0.762

1) with the training set based on 2nd and 3rd measurement campaign
2) with the training set based on 2nd and 3rd campaign (66.6% training, 33.3% testing)

To find the simple linear regression results, which reproduce the best absorbance – concentration coherence, a detail analysis with residuals, different correlation coefficients and time series curve was accomplished. Table 4-11 and Table 4-12 give an overview for the COD_{tot}, COD_{sol} and TSS parameter of these analyses. Hence, the best three results for every parameter were taken and later used for load calculation.

Table 4-11 presents the results of an in-depth analysis. Mean dry weather and storm events data are shown in the tables in the appendix. Hence, in an in-depth analysis some non-explainable results also occur. For example for the COD_{tot} and COD_{sol} parameter the correlation coefficient of the 1st analysed storm event is a negative one. Unfortunately, this can be recognised at the 1st storm event for these two parameters by all SLR approaches. Consequently, the other calculated correlation coefficients, also the one based on all storm event data, show a good coherence. The five lab values are underrepresented to verify a resulting good correlation coefficient.

Figure 4-63 shows an example of simple linear regression for the TSS parameter. The example of 600 to 647.5 analysed wavelength ranges is presented. The resulting equation for TSS_{eq} is $3.28 \cdot \lambda(622.5)+86.66$ with a corresponding correlation coefficient of the 1st storm event of 0.753. The factor of 0.753 seems to be unsatisfactory, but a closer examination of this storm event (see Figure 4-63) shows only a small range which insufficiently predicts the measured lab values. In detail it is the grey area of dilution due to thinning of the concentrations. The maximum and minimum lab values can not be reproduced so exactly by the evaluated SLR model.

Table 4-12 Simple Linear Regression Results and its Verification Characteristics – Part 2

Parameter	Analysed Wavelength Range	Absolute Sum of 3rd Measurement Campaign Residuals	Correlation Coefficient of 3rd Measurement Campaign	Absolute Aum of 1st Storm Event Residuals	Correlation Coefficient of 1st storm Event	Absolute sum of 2nd Storm Event Residuals	Correlation Coefficient of 2nd Storm Event
	[nm]	[mg/l]		[mg/l]		[mg/l]	
COD_{tot}	250 – 260	505	0.969	256	-0.626	711	0.952
	270 – 280	460	0.974	243	-0.551	676	0.954
	280 – 290	492	0.972	226	-0.484	658	0.955
COD_{sol}	240 – 247.5, 272.5 – 290	436	0.858	120	-0.890	292	0.713
	260 – 260	423	0.875	71	-0.847	374	0.692
	270 – 280	429	0.871	66	-0.808	355	0.673
TSS	600 – 647.5	434	0.981	180	0.753	690	0.848
	630 – 640	430	0.982	177	0.759	689	0.847
	680 – 690	420	0.983	192	0.758	670	0.837

The difference between maximum lab value and predicted TSS value is about 150 mg/l. Additionally, at the beginning of the storm event a remobilisation effect can be seen, characterised by the doted line. The flush effect is also reproduced by three predicted values. Interestingly, the maximum value especially for the 2nd remobilisation is approximately 700 mg/l. This value is in the same range as TSS concentration of communal waste water.

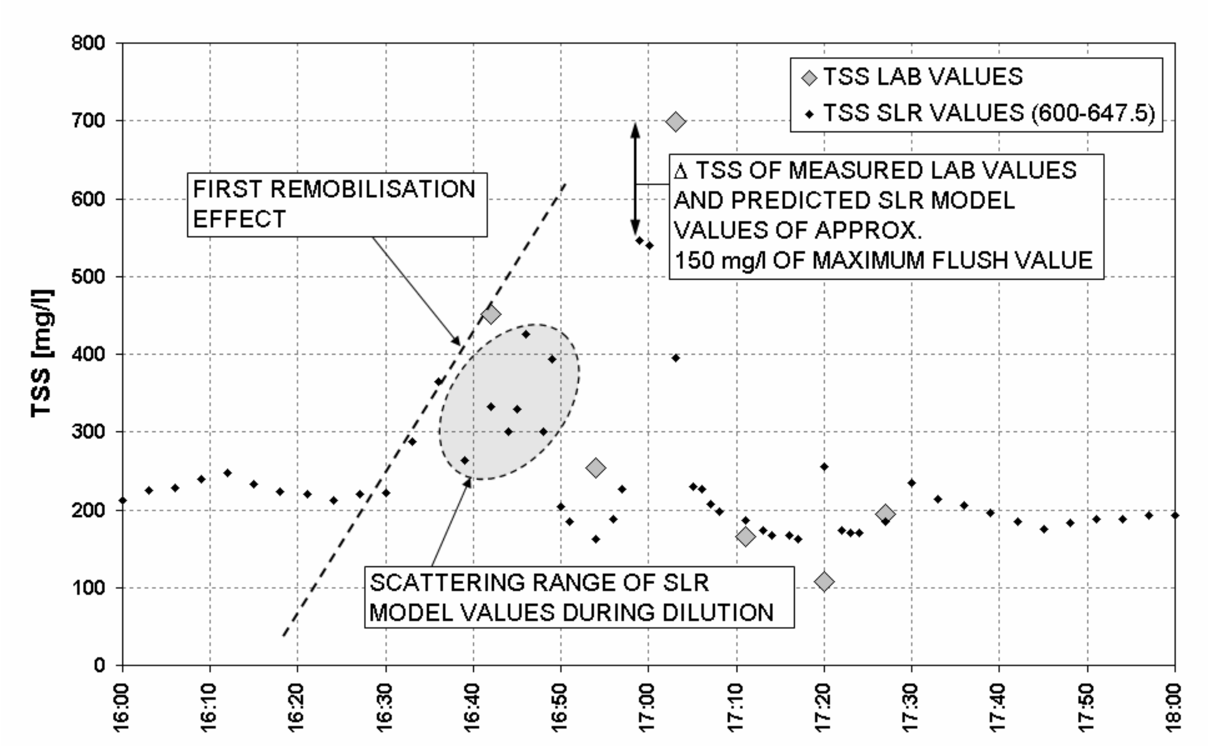

Figure 4-63 Example of SLR Model for COD_{tot} of 1st Storm Event

Hence, this figure points out the high concentrated flush effect. Unfortunately, the minimum value can only reproduced inaccurately. It was consistently recognised that low values, e.g. < 100 mg/l for TSS or COD_{sol} and < 200 mg/l for COD_{tot}, can only be predicted inadequately, regardless of which wavelength range or regression method was used. This phenomenon can be explained with too few data in the lower concentration range. An equation based on lower concentrations cannot replicate higher concentrations accurate.

Figure 4-64 shows the residual results of measured COD_{tot} lab values and predicted values based on simple linear regression. The regression was trained by the 2nd and 3rd measurement campaign of a dry weather day and resulted in an equation of $4.56 \cdot \lambda(270)-76.93$. Some values, characterised with the grey box, can be reproduced quite well with this model. The remaining values are determined as insufficient.

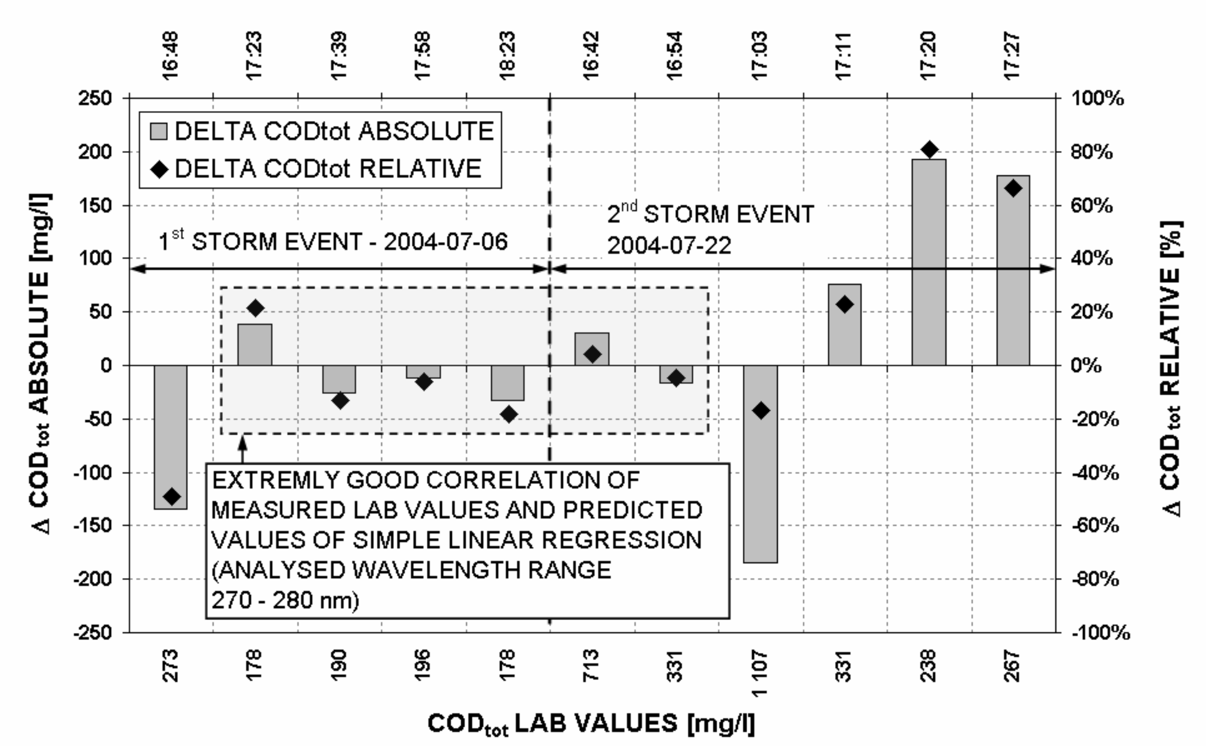

Figure 4-64 Absolute and Relative Residuals of COD_{tot} (270 – 280 nm) – Storm Event Verification

In Table 4-12, the correlation coefficient of COD_{tot} of the 1st storm event is presented with a value of -0.551, a correlation coefficient of 0.954 for the 2nd storm event and a correlation factor of 0.92 for both storms. If the 1st storm event is analysed separately, the false conclusion of an inapplicable regression can be made. A factor of only 0.551 shows the bad coherence of model and “true” values. Additionally, the minus indicates an inverted correlation behaviour, which does not reproduce the real absorbance-concentration coherence. Only the whole consideration range of both storm events equals in a satisfactory correlation coefficient. Although the correlation coefficient of the 2nd storm event shows a good coherence, the corresponding residuals show high differences. A sole analysis of the residuals for the 2nd storm event leads to the interpretation of a bad correlation regression result. These results confirm the necessity of multiple-stage verification by different correlation coefficients, residuals calculation and a time series check. Hence, the results presented in Table 4-11 and Table 4-12 are based on this multiple-stage validation.

4.9.3. LEAST MEDIAN SQUARES REGRESSION

Measured data often can include errors termed as outliers. An in-depth data check has to be carried out. The outlier detection is often made manually. Outliers can be only identified visually with the linear regression method. It is never guaranteed if an outlier is an error or if it is just a surprising but correct value. Outliers have a big influence to the general regression method based on least squares method. Far distance from the regression line points strongly influence the squared distance between these points and the regression line (residuals).

Statistical methods which consider the outlier problem are called robust. One possibility to consider this outlier problem is to use an absolute residual value instead of the standard squared one. Thus, the influence of outliers can be attenuated. Another possibility to automatically identify outliers is to eliminate, for example 10% of the data which are farthest from the regression line. These data are not considered for regression calculation. A 3rd possibility is the minimisation of the median instead of the mean value of squared residuals to the regression line. This kind of approximation is quite robust and can deal with outliers in the x-direction as well with outliers in y-direction (mostly considered with the outlier context).

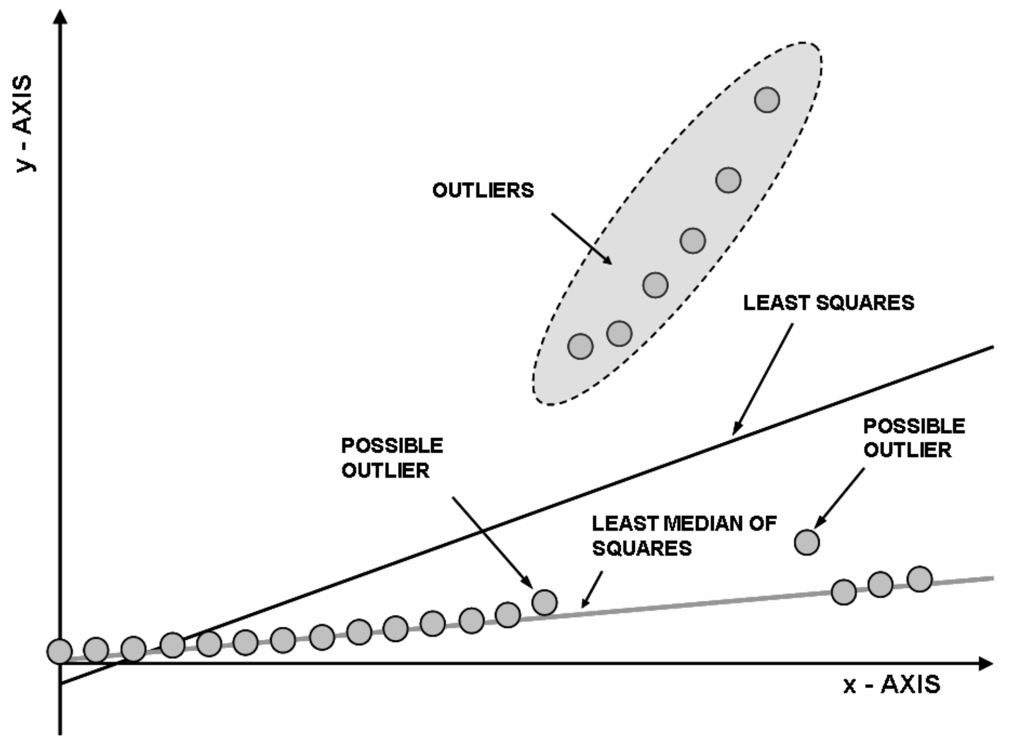

Figure 4-65 Example for Least Squared and Least Median Squared Regression

Figure 4-65 shows an artificially generated example for a regression based on least squares method and for a regression based on least median squares method. The data shows a continuously upward tendency except the points displayed in the grey area. In practice this can be due to a possible wrong unit input. Maybe two other points can also be characterised as outliers. With this example, the outliers, of course, can be identified visually, but with unfamiliar measured values this is quite more difficult like for absorbance values.

The general method based on linear regression is extremely influenced by the outliers (Figure 4-65). On the other hand the resulting line by means of least median squares regression is almost unaffected by the outliers.

For any class c (x_{i1}, y_{i1}), ……, (x_{ip}, y_{ic}), the i-th coordinate of this vector can be denoted by $\Theta_j(i_1, ..., i_c)$. The repeated median is then defined coordinatewise as

$$\hat{\Theta}_j = \underset{i1}{\text{median}}(...(\underset{ip-1}{\text{median}}(\underset{ic}{\text{median}}\ \Theta_j(i_1,.....,i_c)))...)$$

The least median of squares (LMS) estimator (Rousseeuw, 1984) is given by:

$$\min_{\hat{\Theta}} \underset{i}{\text{median}}\ r_i^2$$

This minimisation will be determined for the median of squared residuals. The residuals r_i equal $y_i - x_{i1} \cdot \hat{\Theta}_1 - ..... - x_{ip} \cdot \hat{\Theta}_p$.

LMS is not only useful for dealing with outliers; it also performs well when the y_i data are not normally distributed around their theoretical value (Massart et al., 1986). Unfortunately, median based regressions have a big disadvantage due to long calculation time and, therefore, these methods are not always applicable in practice.

The results of least median squares regression are represented in Table 4-13 and in Table 4-14. On the basis of the different correlation calculations, residuals calculations and the time series analysis the following analysed wavelength have emerged as the best regression results. The residuals of the 2nd measurement campaign for all parameters have, smaller difference than the residuals based on SLR.

Table 4-13 Least Median Squares Regression Results and its Verification Characteristics – Part 1

Parameter	Analysed Wavelength Range	Cross Correlation[1)]	Percentage Split[2)]	Absolute Sum of 2nd Measurement Campaign Residuals	Correlation Coefficient of 2nd Measurement Campaign
	[nm]			[mg/l]	
COD_{tot}	230 – 500	0.961	0.976	1 899	0.953
	254, 436	0.956	0.972	1 802	0.957
	250 – 260, 436	0.943	0.972	1 978	0.954
COD_{sol}	230 – 500	0.744	0.668	1 005	0.855
	254, 436	0.705	0.611	1 093	0.848
	250 – 260, 436	0.755	0.610	1 001	0.845
TSS	520 – 530	0.829	0.885	1 437	0.776
	590 – 600	0.865	0.889	1 429	0.772
	690 – 700	0.855	0.886	1 410	0.758

[1)] with the training set based on 2nd and 3rd measurement campaign
[2)] with the training set based on 2nd and 3rd campaign (66.6% training, 33.3% testing)

The correlation coefficients for the COD_{sol} parameter based on cross correlation as well as percentage split result for all presented regression in a value range which is unsatisfactory. It has become more and more apparent that the COD_{sol} parameter in particular is not sufficiently reproduced, regardless of which regression method. Contingently, this could be due to inaccurate measured lab values which could not be confirmed by the measured values in the lab.

Table 4-14 Least Median Squares Regression Results and its Verification Characteristics – Part 2

Parameter	Analysed Wavelength Range	Absolute Sum of 3rd Measurement Campaign Residuals	Correlation Coefficient of 3rd Measurement Campaign	Absolute Sum of 1st Storm Event Residuals	Correlation Coefficient of 1st Storm Event	Absolute Sum of 2nd Storm Event Residuals	Correlation Coefficient of 2nd Storm Event
	[nm]	[mg/l]		[mg/l]		[mg/l]	
	230 – 500	338	0.980	309	-0.246	664	0.952
COD_{tot}	254, 436	296	0.986	385	0.192	1 027	0.941
	250 – 260, 436	364	0.978	333	-0.335	729	0.951
	230 – 500	490	0.857	633	-0.601	231	0.789
COD_{sol}	254, 436	351	0.899	260	-0.154	690	0.608
	250 – 260, 436	381	0.872	58	-0.663	418	0.682
	520 – 530	377	0.980	156	0.734	695	0.866
TSS	590 – 600	369	0.981	158	0.752	669	0.851
	690 – 700	392	0.983	170	0.768	650	0.835

As already recognised in Table 4-12 with reference to the extremely bad correlation coefficient of the 1st storm event, in Table 4-14 the insufficient correlation coefficients can also be seen for the COD_{tot} and COD_{sol} parameter. Even the correlation coefficient for COD_{tot} results in 0.933 (230 – 500), 0.939 (254, 436) and 0.924 (250 – 260, 436) and for COD_{sol} it equals 0.836 (230 – 500), 0.745 (254, 436) and 0.817 (250 – 260, 436) in consideration of both storms also including the 1st storm event.

Figure 4-66 displays the COD_{tot} values of lab and predicted LMS values in the analysed wavelength range of 230 to 250 nm. This is an example of indirect discharger, although the predicted maximum value of COD_{tot} seems a little bit too high. Unfortunately, during this indirect discharging no sample was taken by the automatic sampler. Therefore, no comparison of estimated and measured values is possible. This time series plot presents a good correlation between measured and predicted values.

Figure 4-67 displays the absolute and relative residuals of COD_{sol} from measured lab values and predicted values on the basis of LMS for both analysed storm events. Some values can be reproduced quite accurately, especially the values of the 1st storm event. One value (17^{23}) has a relative difference of about 100%, whereas, at the 2nd storm event three values have a deviation between 100 and 200%. The correlation coefficient of the 1st event is -0.663, for the 2nd storm it equals 0.682. Hence, the difficulty of validation can be demonstrated.

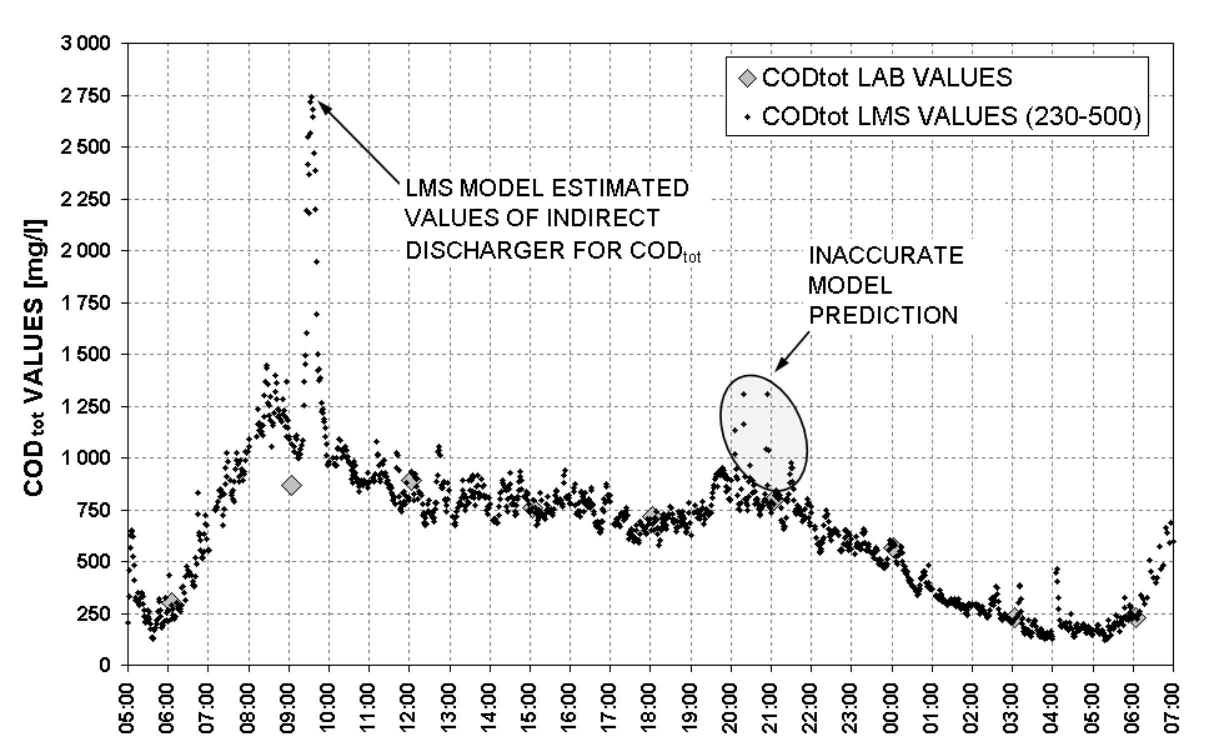

Figure 4-66 Times Series of 3rd Measurement Campaign for COD_{tot} of Lab and LMS (230-500) Values

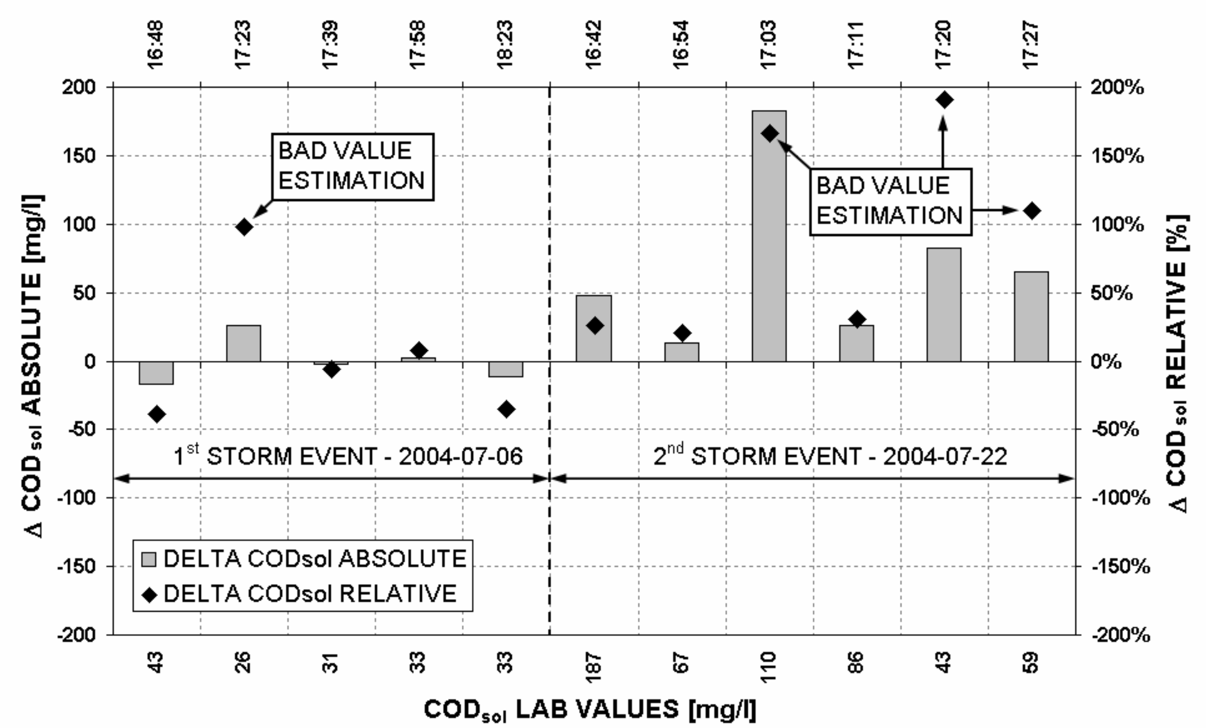

Figure 4-67 Absolute and Relative COD_{sol} (250 - 260, 436) Residuals – Storm Event Verification

4.9.4. M5 Model Tree Regression

Classification trees basically deal with discrete data. In the case of continuous data, some classification tree systems require that the data be discretised first. Regression trees can deal with both discrete and continuous data. Both kinds of trees represent learned knowledge in the form of a tree, which is very easy to understand and to use. In this thesis, only regression trees will be considered, as they are more general and can find wider use in ecology (Kompare, 1995). Indeed, regression trees can be set to mimic the behaviour of classification trees.

The problem of regression analysis is the problem of searching for the dependency between a dependent variable y, called class and independent variables x_i, called attributes and discrete (or discretised) classes. Regression trees can deal with continuous attributes and classes. Tree-structured regression is built on the assumption that the functional dependency is not uniform in the whole domain, but can be approximated as such on smaller subdomains. These subdomains are then searched for and characterised with constants or (linear) regression functions (models) of the dependent variable. The result of such an analysis is a tree-like structure, called a regression tree. A general example of such a regression tree which should predict equivalence concentrations is given in Figure 4-68.

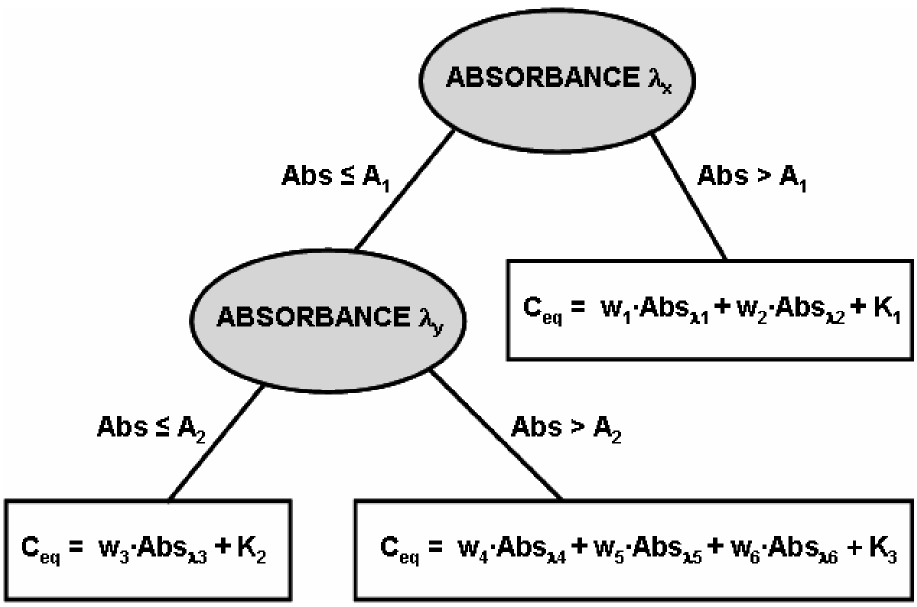

Figure 4-68 Example for M5 Model Tree Regression in UV/VIS Spectroscopy

Figure 4-68 displays the regression tree construction. A decision tree consist of internal nodes (branching points), branches (which connect branching points), and leaves (terminal nodes). An attribute is associated with each internal node. An attribute test, connected with a particular value of the attribute, is associated with each branch. The leaves contain predictions for the value of the class. These can be of three kinds: (1) a value for a discrete class: the tree is called a classification tree; (2) a value for a continuous class: the tree is called a regression tree, and (3) a (linear) model for a continuous class: the tree is called a model tree. Kompare (1995) denotes model trees as regression trees.

M5 uses recursive partitioning to build a piecewise linear model in the form of a model tree (Quinlan, 1992). The idea is to split the training cases in much the same way as when growing a decision tree, using a criterion of minimising intra-subset variation of class values rather than maximising information gain. Whereas a leaf of a decision tree contains just a class name, the corresponding leaf of a model tree is a linear model relating the class values of the training cases to their attribute values. Regression trees are based on a similar divide-and-conquer strategy, but have values rather than linear models at the leaves.

Consider a set T of training cases for which a model tree is to be constructed. Unless T contains few cases or their values vary only slightly, it is split according to the outcomes of a test. Every potential test is evaluated by determining the subset of cases associated with each outcome; let T_i denote the subset of cases that have the i-th class of the potential test. If the standard deviation $sd(T_i)$ is treated of the target values of cases in T_i as a measure of error, the expected reduction in error as a result of this test can be written (Quinlan, 1993):

$$\Delta\ \mathrm{error} = \mathrm{sd}(T) - \sum_i \frac{|T_i|}{|T|} \cdot \mathrm{sd}(T_i)$$

After examining all possible tests, M5 chooses one that maximises this expected error reduction. The major innovations of M5 come into play after the initial tree has been grown:

Error estimates: M5 often needs to estimate the accuracy of a model on unseen cases. 1st the residual of a model on a case is just the absolute difference between the actual target value of the case and the value predicted by the model. To estimate the error of a model, M5 first determines the average residual of the model on the training cases used to construct it. This will generally underestimate the error on unseen cases, so M5 multiplies the value by $(n+\nu)/(n-\nu)$, where n is the number of training cases and ν is the number of parameters in the model. The effect is to increase the estimated error of models with many parameters constructed from small numbers of cases.

Simplification of linear models: Each linear model is then simplified by eliminating parameters so as to minimise its estimated error. Even though the elimination of parameters generally causes the average residual to increase, it also reduces the multiplicative factor above, so the estimated error can decrease. M5 uses a greedy search to remove variables that contribute little to the model; in some cases, M5 removes all variables, leaving only a constant.

Pruning: Each internal node of the tree now has both a simplified model and a model subtree. The one of these with lower estimate error is chosen; if this is the linear model, the subtree at this node has been pruned to a leaf.

Smoothing: The prediction accuracy of tree-based models can be improved by a smoothing process. When the value of a case is predicted by a model tree, the values returned by the model at the appropriate leaf are adjusted to take account of models at nodes along the path from the root to that leaf. The predicted value is backed up from the leaf to the root as follows:

- The predicted value at the leaf is unchanged.
- If the case follows branch S_i of subtree S, let n_i be the number of training cases at S_i, $PV(S_i)$ the predicted value at S_i, and M(S) the value given by the model at S. The predicted value backed up to S is

$$PV(S) = \frac{n_i \cdot PV(S_i) + k \cdot M(S)}{n_i + k}$$

where k is a smoothing constant.

Smoothing has most effect when leaf models are constructed from few training cases and do not agree with models higher in the tree.

Table 4-15 M5 Model Tree Regression Results and its Verification Characteristics – Part 1

Parameter	Analysed Wavelength Range	Cross Correlation[1)]	Percentage Split[2)]	Absolute Sum of 2nd Measurement Campaign Residuals	Correlation Coefficient of 2nd Measurement Campaign
	[nm]			[mg/l]	
	254, 436	0.971	0.973	1 278	0.977
COD_{tot}	250 – 277.5,436	0.971	0.973	1 200	0.977
	310 – 320, 436	0.971	0.973	1 194	0.977
	230 – 500	0.811	0.679	1 054	0.837
COD_{sol}	240 – 250, 436	0.801	0.621	1 066	0.833
	280 – 290	0.795	0.666	1 057	0.835
	420 – 430	0.838	0.881	1 480	0.760
TSS	660 – 670	0.835	0.892	1 494	0.765
	710 – 720	0.838	0.887	1 438	0.756

1) with the training set based on 2nd and 3rd measurement campaign
2) with the training set based on 2nd and 3rd campaign (66.6% training, 33.3% testing)

Table 4-15 and Table 4-16 present the results of M5 model validation. For the COD_{tot} parameter the correlation coefficients on the basis of cross correlation and percentage split show a good coherence between predicted and measured values. Either a value of 0.971 for cross correlation or a value of 0.973 for percentage split is determined for all three chosen linear functions. Also the residuals for COD_{tot} (1 278 mg/l, 1 200 mg/l, 1 194 mg/l depending on the regression equation) of the 2nd measurement campaign show small amounts, whereas the residuals of TSS values are higher than the COD_{tot} values. Thus, the reliable and accurate reproduction of the COD_{tot} values by means of the selected M5 regression equations can be confirmed. The correlation coefficients of cross correlation and percentage split are in the same range, respectively for COD_{tot} as well as for TSS. This can not be seen for COD_{sol}, where the cross correlation factors show a higher correlation than the factors on the basis of percentage split method. This possibility indicates a moderate or even a bad distribution of data in the training and validation set.

Table 4-16 presents the validation results of the 3rd measurement campaign, 1st storm event and the 2nd storm event. Every regression equals in a very good correlation especially for COD_{tot} and TSS of the 3rd measurement campaign. These are expressed in values of 0.996 to 0.997 for COD_{tot}. The values for correlation of TSS result in a range from 0.966 to 0.982. Even the values of COD_{sol} of the 3rd campaign are acceptable. The residuals sums of COD_{tot} are quite a lot lower than the sum for COD_{sol} and TSS, in spite of the fact that the COD_{tot} parameter is in a higher value range than the values of COD_{sol} and TSS. The correlation coefficients of the 1st storm event show negative coherence as has already been seen with SLR and LMS methods. However, a consideration of both storms together equals in a correlation coefficient of 0.933 (254, 436), 0.932 (250 – 277.5, 436) and 0.929 (310 – 320, 436) for the COD_{tot} parameter. The calculation coefficients of both storms together are 0.830 (230 – 500), 0.831 (240 – 250, 436) and 0.802 (280 – 290) for the COD_{sol} parameter.

Table 4-16 M5 Model Tree Regression Results and its Verification Characteristics – Part 2

Parameter	Analysed Wavelength Range	Absolute Sum of 3rd Measurement Campaign Residuals	Correlation Coefficient of 3rd Measurement Campaign	Absolute Sum of 1st Storm Event Residuals	Correlation Coefficient of 1st Storm Event	Absolute Sum of 2nd Storm Event Residuals	Correlation Coefficient of 2nd Storm Event
	[nm]	[mg/l]		[mg/l]		[mg/l]	
	254, 436	295	0.996	515	-0.701	620	0.950
COD_{tot}	250–277.5,436	222	0.997	542	-0.737	616	0.951
	310 – 320, 436	234	0.997	236	-0.088	822	0.936
	230 – 500	453	0.853	282	-0.869	212	0.722
COD_{sol}	240 – 250, 436	441	0.848	190	-0.906	249	0.717
	280 – 290	418	0.864	59	-0.735	348	0.655
	420 – 430	350	0.969	168	0.657	843	0.778
TSS	660 – 670	433	0.982	179	0.767	680	0.843
	710 – 720	367	0.970	167	0.828	888	0.499

Figure 4-69 displays an example of an insufficient M5 model due to M5 model simplification. The removal of variables has already been described before.

Therefore it is possible that all variables are removed by the model, and this results in a constant value.

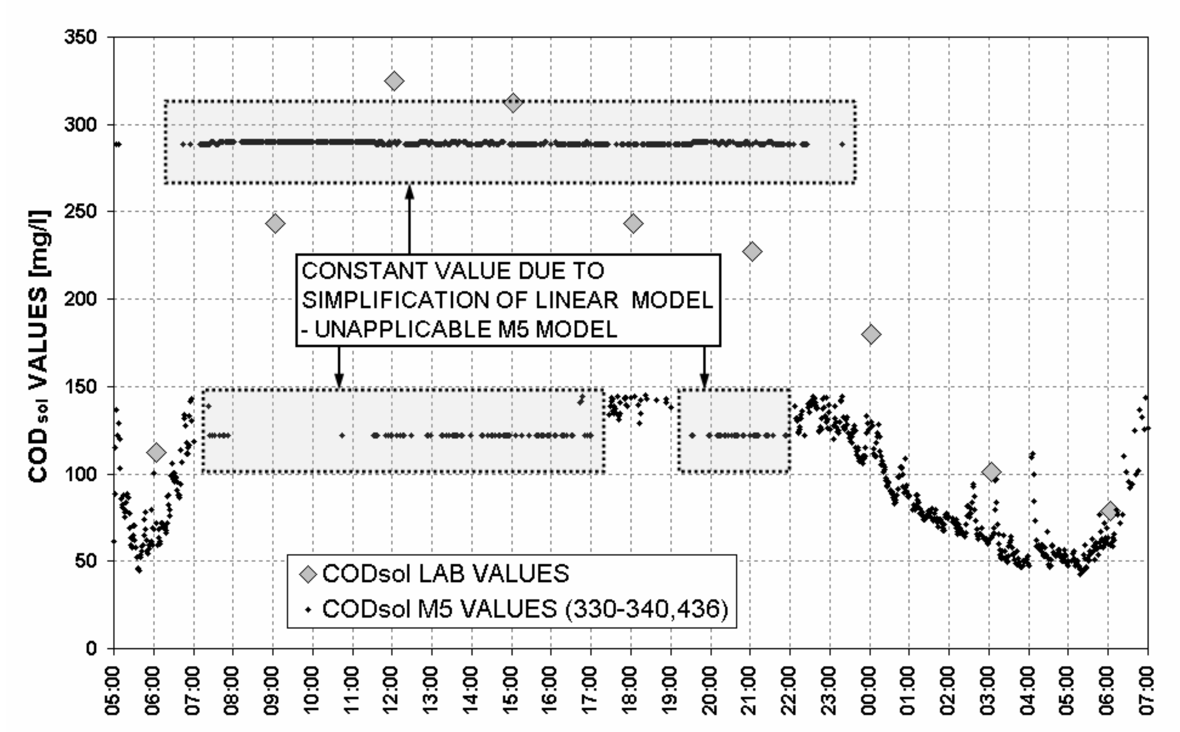

Figure 4-69 Example of Inapplicable M5 Model of COD_{sol} due to Extreme Model Simplification

The figure shows that two leaves of the M5 model result in a constant value. A constant value as a model can, of course, not predict the real concentrations. Hence, this regression equation has to be eliminated.

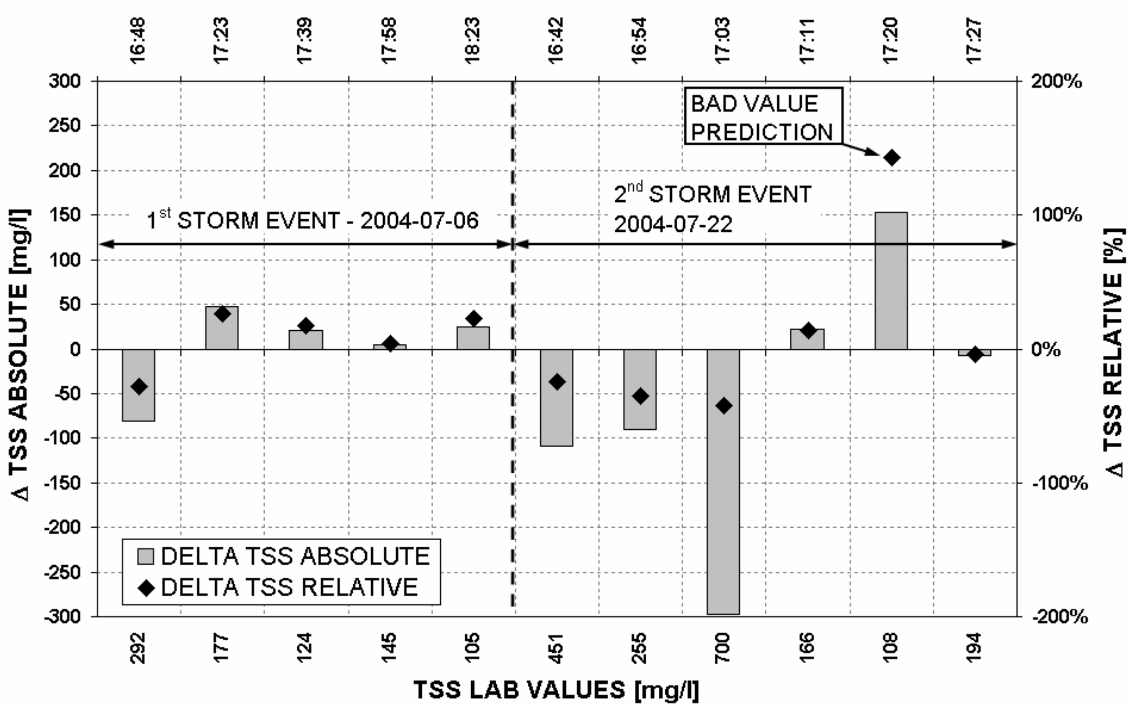

Figure 4-70 Absolute and Relative TSS (660 – 670) Residuals – Storm Event Verification

Figure 4-70 also displays an accurate and sufficient M5 model for the TSS parameter. For the 1st storm event the absolute and relative differences are in an acceptable range. Two worse TSS value predictions can be seen for the 2nd storm event. One prediction has a value of an absolute residual of -270 mg/l and a corresponding relative difference of 42.4%. The second bad estimation is expressed in a relative deviation of 143% and 154 mg/l.

4.9.5. SUPPORT VECTOR MACHINES USING SEQUENTIAL MINIMAL OPTIMISATION

Support vector machines (SVM) are starting to enjoy increasing adoption in machine learning and computer vision research communities. However, SVMs have not yet enjoyed widespread adoption in the engineering community. There are two possible reasons for their limited use by engineers. First, SVM training is slow, especially for large problems. Second, SVM training algorithms are complex, subtle, and sometimes difficult to implement (Platt, 1999).

SVMs are a range of classification and regression algorithms that have been formulated from the principles of statistical learning theory (Boser et al., 1992). This theoretical framework develops a link between the empirical performance of a learning algorithm, when trained from a finite data sample, and the “true” performance when used in practice. It has been shown that the rate of convergence of the empirical estimate to the true value is a function of the algorithm’s Vapnik-Cherronenkis (VC) dimension. The VC-dimension of a model or classifier is, effectively, a measure of its flexibility and by minimising the model’s flexibility as part of the learning process (structural risk minimisation) the risk of over-fitting the training set is reduced (Brown et al., 1999).

SVMs choose the parameters for the 1st layer to be the training input vectors, because this minimises the VC-dimension. It is assumed that there are as many nodes in this layer as there are training points. A selection procedure is then used to calculate the weights in the 2nd layer and this generally sets many of the weights to zero, which has the effect of dropping the corresponding training point from the overall calculation (Sánchez, 2003). This selection procedure attempts to minimise the VC-dimension of the final solution.

Consider a data set that contains two classes that are separable. For the pure pixels containing these classes, shown in Figure 4-71, there are an infinite number of lines (hyperplanes) that will separate the data. Figure 4-71 displays a linear SVM for two inputs and two classes. The stars and crosses represent the labelled training data and the circles denote the selected support vectors which determine the linear margin’s boundaries and the contours, b^0, for the 2nd model are labelled.

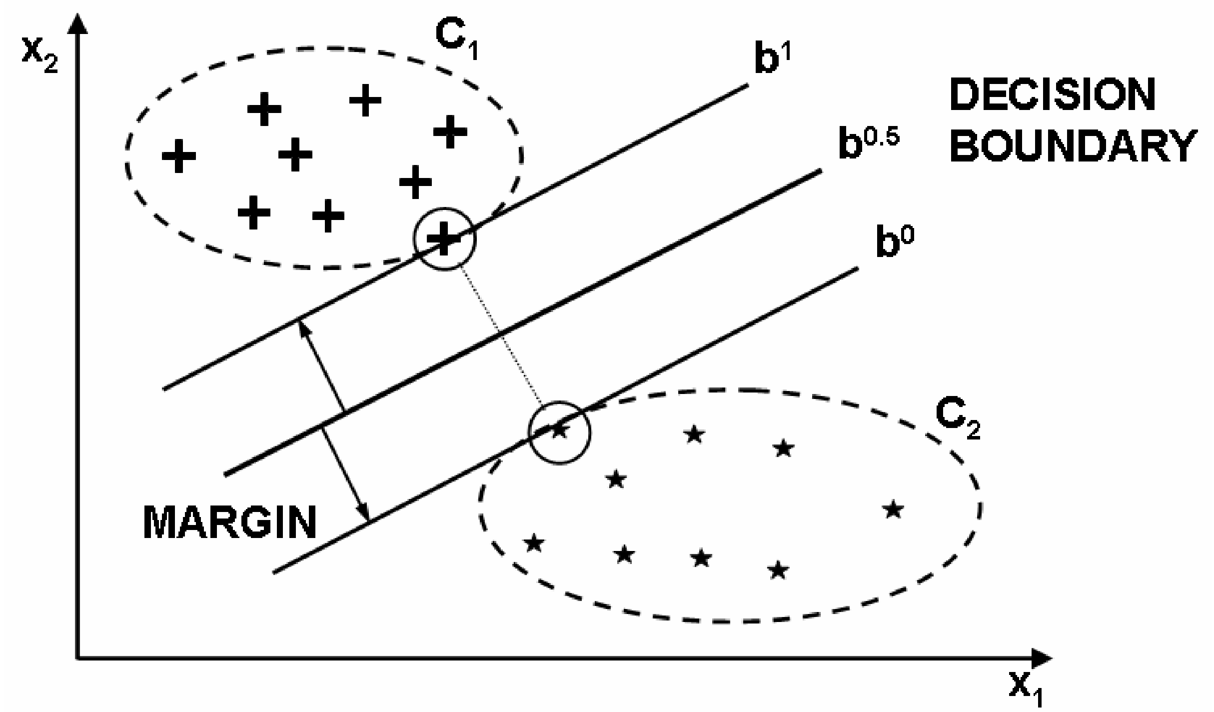

Figure 4-71 Linear SVM for Two Classes (Brown et al., 1999)

The linear SVM is based on the principle of selecting the one that maximises the minimum distance of the hyperplane from each class (the margin). This is because the VC dimension of a linear classifier is related to both to the number of inputs and to the size of the calculated weights (Vapnik, 1995). Minimising the size of the weight vector produces a solution that maximally separates the classes and this is often known as the optimal separating hyperplane (OSH). As only the data points which lie on the class boundary closest to the hyperplane are involved in determining the minimum distance, effectively, all of the other data points in the training set are discarded from the calculation (Brown et al., 1999).

Maximising the margin and correctly classifying all the training data can be formulated as:

$$\min \Phi(w) = \frac{1}{2} \cdot \|w\|_2^2$$

subject to

$$\left(x^i \cdot w + w_0\right) \cdot t^i \geq 1$$

for the model:

$$y^i = w^T \cdot x^i + w_0$$

where $\{y^i\}_{i=1}^{l}$ are the output mixing proportions, $w = (w_1,.....w_n)$ is the weight vector associated with the linear decision boundary, w_0 is the corresponding bias term and $\{x^i, t^i\}_{i=1}^{l}$ is the labelled data set containing the spectral feature vector x^i and the target mixture proportion t^i for the i-th data point. This can be formulated as a Lagrange functional producing a quadratic program (QP) with a global optimum.

Platt (1998) describes the sequential minimal optimisation (SMO) which uses an analytic QP step. SMO does particularly well for sparse data sets, with either binary or non-binary input data. SMO is a simple algorithm that quickly solves the SVM QP problem without any extra matrix storage and without an iterative numerical routine for each sub-problem. SMO decomposes the overall QP problem into QP sub-problems. SMO chooses to solve the smallest possible optimisation problem at every step. For the standard SVM QP problem, the smallest possible optimisation problem involves two Lagrange multipliers because the Lagrange multipliers must obey a linear equality constraint. At every step, SMO chooses two Lagrange multipliers to jointly optimise, finds the optimal values for these multipliers, and updates the SVM to reflect the new optimal values.

The advantage of SMO lies in the fact that solving for two Lagrange multipliers can be done analytically. Thus, an entire inner iteration due to numerical QP optimisation is avoided.

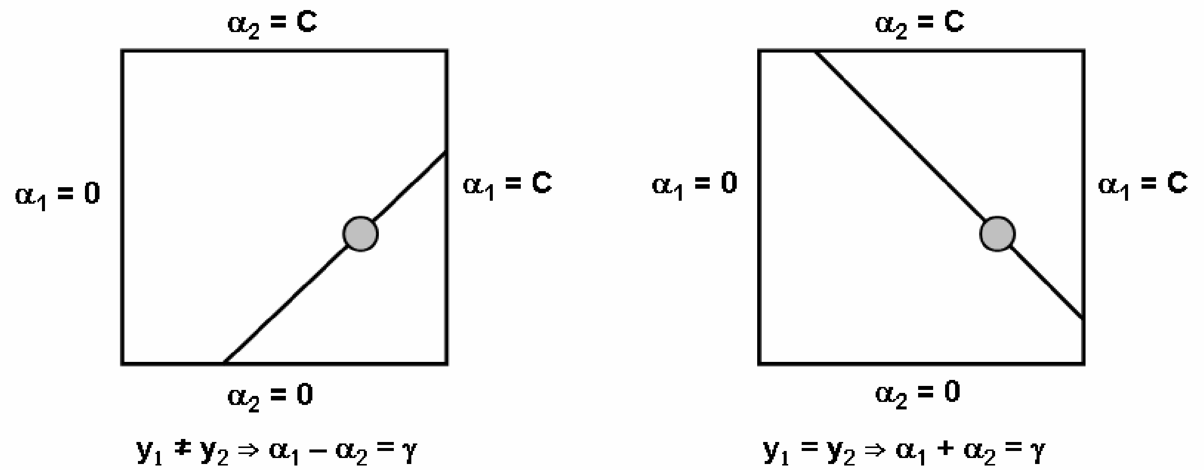

Figure 4-72 Example of Two Lagrange Multipliers (Platt, 1998)

The two Lagrange multipliers must fulfil all of the constraints of the full problems (Figure 4-72). The inequality constraints cause Lagrange multipliers to lie in the box. The linear equality constraint causes them to lie on a diagonal line. Therefore, one step of SMO must find an optimum of the objective function on a diagonal line segment. In Figure 4-72, $\gamma = \alpha_1^{old} + s \cdot \alpha_2^{old}$, is a constant that depends on the previous values of α_1 and α_2, and $s = y_1 \cdot y_2$.

Table 4-17 SMO Results and its Verification Characteristics – Part 1

Parameter	Analysed Wavelength Range	Cross Correlation[1)]	Percentage Split[2)]	Absolute Sum of 2nd Measurement Campaign Residuals	Correlation Coefficient of 2nd Measurement Campaign
	[nm]			[mg/l]	
COD_{tot}	240 – 250	0.956	0.967	1 633	0.959
	250 – 260	0.955	0.965	1 719	0.956
	290 – 300	0.948	0.960	1 835	0.950
COD_{sol}	250 – 260	0.790	0.660	962	0.847
	260 – 270, 436	0.819	0.692	903	0.867
	270 – 280, 436	0.787	0.656	964	0.846
TSS	620 – 630	0.848	0.887	1 389	0.770
	670 – 680	0.845	0.886	1 385	0.764
	720 – 730	0.841	0.887	1 400	0.758

1) with the training set based on 2nd and 3rd measurement campaign
2) with the training set based on 2nd and 3rd campaign (66.6% training, 33.3% testing)

Table 4-17 and Table 4-18 present the results of the profound validation. The correlation coefficients for the 2nd and 3rd measurement campaign demonstrate an exceptionally good correlation for the COD_{tot} parameter between the measured lab values and the predicted values by the SMO models. A bad coherence can be recognised for the 1st storm event expressed in a negative correlation coefficient, which was already identified by the other regression methods. The correlation coefficient of the COD_{sol} parameter results in poor values. Interestingly, the COD_{sol} parameter can not be reproduced as accurately as the COD_{tot} and TSS parameters.

Table 4-18 SMO Results and its Verification Characteristics – Part 2

Parameter	Analysed Wavelength Range	Absolute Sum of 3rd Measurement Campaign Residuals	Correlation Coefficient of 3rd Measurement Campaign	Absolute Sum of 1st Storm Event Residuals	Correlation Coefficient of 1st Storm Event	Absolute Sum of 2nd Storm Event Residuals	Correlation Coefficient of 2nd Storm Event
	[nm]	[mg/l]		[mg/l]		[mg/l]	
COD_{tot}	240 – 250	336	0.980	249	-0.214	895	0.953
	250 – 260	324	0.981	256	-0.570	736	0.954
	290 – 300	318	0.978	215	-0.133	687	0.952
COD_{sol}	250 – 260	372	0.873	58	-0.882	408	0.695
	260–270,436	365	0.889	60	-0.856	453	0.773
	270–280,436	393	0.872	70	-0.901	368	0.698
TSS	620 – 630	443	0.981	160	0.753	699	0.849
	670 – 680	447	0.981	160	0.771	688	0.841
	720 – 730	426	0.983	180	0.765	661	0.830

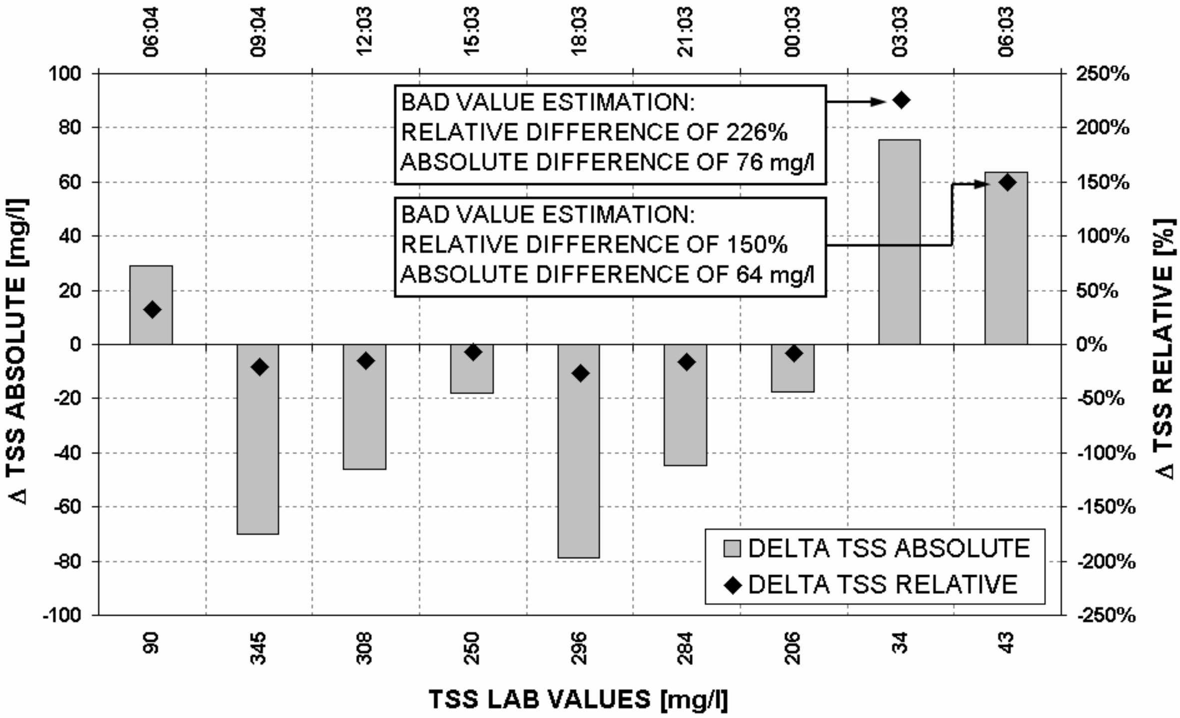

Figure 4-73 Absolute and Relative TSS Residuals of SMO (620 -630) Regression – 3rd Measurement Campaign

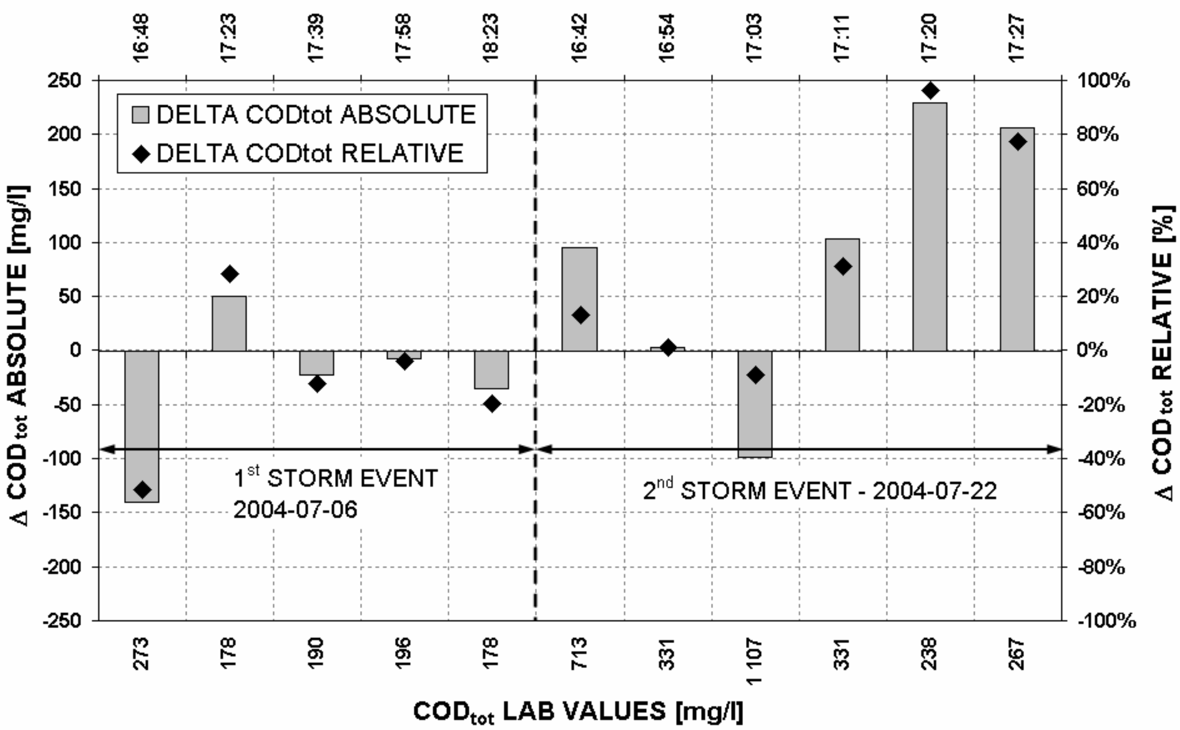

Figure 4-74 Absolute and Relative COD_{tot} (250 – 260) Residuals – SMO – Storm Event Verification

Figure 4-73 displays an example of TSS residuals on the basis of SMO regression with an analysed wavelength range from 620 to 630 nm. The first seven values can be estimated accurately; the maximum positive difference equals in a relative deviation of 28.9% and the minimum negative difference is -26.7%. This range seems to be acceptable, but the last two values show the problem in detail. The relative differences are 226% and 150%. The problem is the bad estimation of low concentration values for every parameter due to the under-representation of low concentration data in the training and calibration set, respectively.

Figure 4-74 displays the storms validation results for the COD_{tot} parameter. Again well and poorly predicted values can be seen. The maximum flush value for the 2nd storm event of 1 107 mg/l can be estimated with only a relative difference of -8.9% and an absolute difference -98.5 mg/l.

4.9.6. PARTIAL LEAST SQUARES REGRESSION

PLS regression is a recent technique that generalises and combines features from principal component analysis and multiple regressions. It is particularly useful when a set of dependent variables from a large set of independent variables need to be predicted (Abdi, 2003). The PLS regression offers an alternative to regression on principal components. It gives a solution to the problems of multicollinearity of predictors and when the number of observations is smaller than the number of predictor variables (Preda & Saporta, 2005).

Classical partial least squares regression (PLS) is directly linked to the usual procedures for simple and multiple regressions and is therefore enriched by the classical testing procedures of such methods (Bastien et al., 2005).

In its simplest terms, PLS comprises modelling techniques that rely upon decomposing the original measurement (i.e. spectra) and the response (i.e. concentration) into a new smaller set of latent variables that best describe all the variance in the data. These new latent variables are then used to produce a calibration that relates the measurement to the response (Haswell & Walmsley, 1999).

One of the main features of multivariate regression techniques such as PLS is the generation of a model that will minimise the influence of variables that do not positively contribute to the model, whilst maximising the contribution of variables that provide useful information. Selection of such variables is important as the presence of a large number of unwanted variables in spectral data will contribute considerably to the error component and hence the predictive capability of the model. This situation is common with spectral data, where a large number of variables (e.g. wavelengths) exist, of which a large subset contains little or no real information (e.g. regions of no spectral response). One possible approach to such a situation is to simply remove the variables that are information poor. However, manual deletion of variables suffers from two main flaws: (i) there is no certainty that exactly the same section of the data will be removed every time and (ii) removed sections may not be optimal from the point of view of the model (e.g. parts of a spectra may not look to the eye to be information rich, but for the model, they contain useful information). Thus, when using this manual approach, there is a tendency to remove sections that contain either high noise or low detector response; however, such an approach can prove to be counter-productive in terms of robust model building. For example, information in the background noise can be extremely useful for establishing a robust calibration model as noise free spectra often has a large source of predictive errors due to collinearity between neighbouring wavelengths in a single peak. The presence of a high degree of collinearity between variables in a model will tend to influence the matrix towards singularity, and this in turn will have a large influence on the coefficients generated. Furthermore, removing variables from a multivariate system can have a large impact on the corresponding coefficients.

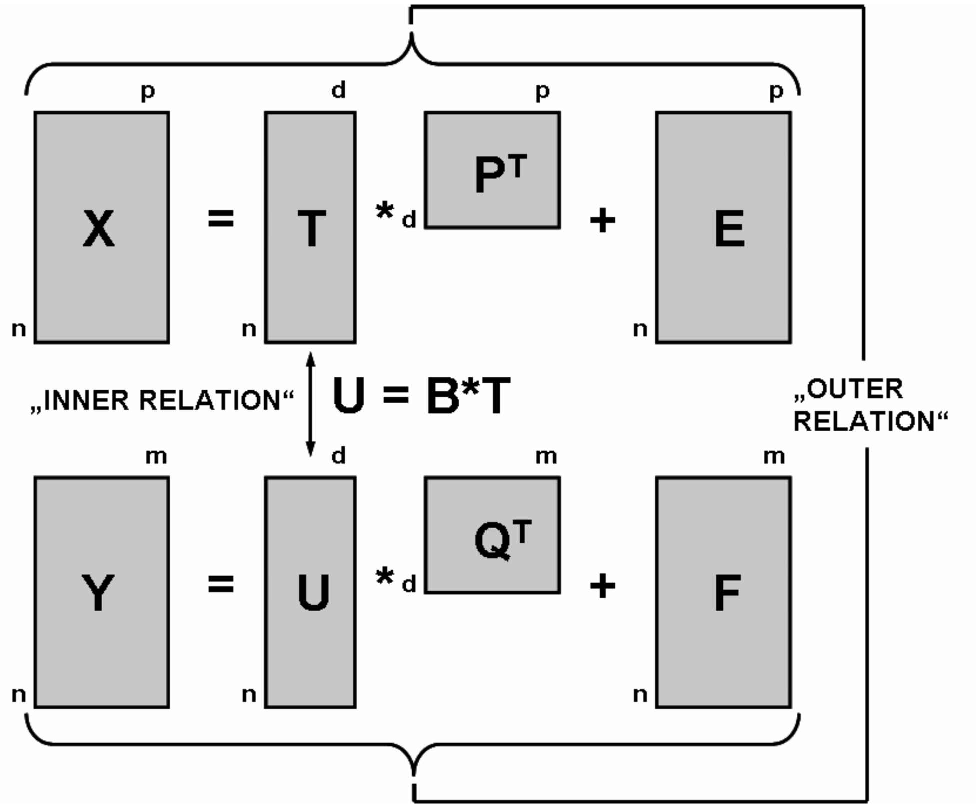

Figure 4-75 Overview of the PLS Algorithm

Consider a data set representing the “normal” operating conditions of a process. $X_{n \times p}$ represents the data matrix of process variables and $Y_{n \times m}$ the data matrix of quality (response) variables, which are recorded for n time points. The objective of linear PLS is to project the data down onto a number of latent variables, say T_i and U_i (i = 1,….., A), where A is the number of the latent variables, and then to develop a regression model (Geladi & Kowalski, 1986; Otto, 1999) between (for the calculation algorithm see also Figure 4-75) T_i and U_i, which can be written as:

$$U_i = B_i \cdot T_i + E_i \qquad i = 1,....., A$$

where E_i is a vector of errors and B_i is an unknown parameter estimated by:

$$\hat{B}_i = \frac{T_i^T \cdot U_i}{T_i^T \cdot T_i}$$

The latent variables are computed by $T_i = X_i \cdot P_i$ and $U_i = Y_i \cdot Q_i$ where both P_i and Q_i have unit length and are determined by maximising the covariance between T_i and U_i.

$X_{i+1} = X_i - T_i \cdot P_i^T$ where $X_1 = X$ and $P_i = (X_i^T \cdot T_i)/(T_i^T \cdot T_i)$ and $Y_{i+1} = Y_i - B_i \cdot T_i \cdot Q_i^T$ where $Y_1 = Y$. Letting $\hat{U}_i = \hat{B}_i \cdot T_i$ be the prediction of U_i, the matrices X and Y can be decomposed as the sum of the following outer products (Figure 4-75):

$$X = \sum_{i=1}^{A} T_i \cdot P_i^T + E \quad \text{and} \quad Y = \sum_{i=1}^{A} \hat{U}_i \cdot Q_i^T + F$$

where E and F are the residuals of X and Y after extracting the first A pairs of latent variables (Li et al., 2002).

Table 4-19 PLS Results and its Verification Characteristics – Part 1

Parameter	Analysed Wavelength Range	Number of Used Wavelength	K-Finder	Absolute Sum of 2nd Measurement Campaign Residuals	Correlation Coefficient of 2nd Measurement Campaign
	[nm]			[mg/l]	
COD_{tot}	240 – 270	5	10	966	0.978
	240 – 270	3	5	1 004	0.977
	240 – 500	50	6	756	0.985
	245 – 265	9	-	1 859	0.949
	250 – 277.5 1)	12	-	4 552	0.949
	257.5 – 290 2)	3	-	2 251	0.974
COD_{sol}	230 – 380	7	10	489	0.948
	240 – 500	7	6	472	0.953
	240 – 500	5	6	477	0.952
	250 – 270	9	-	5 571	0.845
	245 – 265	9	-	3 096	0.844
	240 – 290 1)	12	-	6 150	0.837
	250 – 282.5 2)	4	-	38 937	0.863
TSS	380 – 750	3	6	793	0.904
	380 – 750	2	6	1 218	0.765
	380 – 750	50	6	802	0.912
	550 – 600	3	6	1 204	0.803
	550 – 600	2	6	1 210	0.795
	600 – 647.5 1)	20	-	1 450	0.770

1) provided by the manufacturer – PLS global calibration
2) determined by the manufacturer on the basis of 3rd measurement campaign – PLS global gruber

Table 4-19 and Table 4-20 present the result of the PLS regression validation. In addition to the selected regression equations, the PLS regression functions provided by the manufacturer are also shown. Interestingly, the correlation coefficients of the 2nd and of the 3rd measurement campaign show a high coherence between measured and predicted values, respectively. The correlation coefficients also have a high value for the COD_{sol} parameter, which before could only be estimated insufficiently. These values would indicate the PLS regression as the best model of all analysed and used regressions.

Table 4-20 PLS Results and its Verification Characteristics – Part 2

Parameter	Analysed Wavelength Range	Absolute Sum of 3rd Measurement Campaign Residuals	Correlation Coefficient of 3rd Measurement Campaign	Absolute Sum of 1st Storm Event Residuals	Correlation Coefficient of 1st Storm Event	Absolute Sum of 2nd Storm Event Residuals	Correlation Coefficient of 2nd Storm Event
	[nm]	[mg/l]		[mg/l]		[mg/l]	
COD_{tot}	240 – 270	353	0.985	698	-0.941	1 663	0.883
	240 – 270	379	0.983	699	-0.849	1 532	0.808
	240 – 500	221	0.994	315	0.324	2 200	0.836
	245 – 265	480	0.972	288	-0.699	709	0.950
	250 – 277.5 1)	1 278	0.973	225	-0.623	854	0.952
	257.5 – 290 2)	387	0.989	331	-0.555	1 985	0.902
COD_{sol}	230 – 380	184	0.954	137	-0.283	816	0.905
	240 – 500	221	0.939	100	0.319	757	0.840
	240 – 500	218	0.940	109	0.074	742	0.848
	250 – 270	1 772	0.871	876	-0.862	1 717	0.690
	245 – 265	971	0.868	619	-0.878	1 193	0.699
	240 – 290 1)	1 846	0.861	557	-0.838	1 646	0.680
	250 – 282.5 2)	12 576	0.917	2 648	-0.948	11 100	0.614
TSS	380 – 750	334	0.933	951	-0.508	1 589	0.912
	380 – 750	358	0.983	235	0.779	700	0.841
	380 – 750	312	0.928	1 052	-0.944	1 781	0.806
	550 – 600	296	0.951	646	-0.866	1 202	0.904
	550 – 600	279	0.968	450	0.394	939	0.917
	600 – 647.5 1)	278	0.981	258	0.755	632	0.847

1) provided by the manufacturer – PLS global calibration
2) determined by the manufacturer on the basis of 3rd measurement campaign – PLS global gruber

The PLS regression for all parameters which is characterised with 1) gives a general waste water absorbance and concentration correlation for “typical” waste water. Of course, such an equation has its deficits. The correlation coefficient indicates a quite good absorbance – concentration behaviour reproduction. Although, the “true” value can only be estimated fairly, this is expressed by the residual sums. This does not hold for the TSS parameter. TSS results in small residuals and equals in poor correlation coefficients. The TSS parameter can be predicted almost independent from the waste water matrix. The only influence is from the turbidity in the visible range.

The manufacturer also provided a 2nd calibration for the monitoring station for the COD_{tot} and COD_{sol} parameter on the basis of the measured lab values of the 3rd measurement campaign. Unfortunately, the accuracy of the determined equation by means of PLS regression is poor. Even, for example, the residuals of COD_{tot} for the 3rd campaign are low; the residuals of 2nd campaign may indicate a possible model over-fitting and an insufficient prediction for dry weather values. The calibration of COD_{sol} is totally useless. It has to be emphasised, that the user in practice has a tool to improve and adapt the default calibration to the local waste water via reference measurements as already described in chapter 4.8.3, respectively.

Figure 4-76 shows the absolute residuals and relative differences of the COD_{tot} parameter for measured lab values and predicted values on the basis of PLS regression. In this case, a wavelength range from 240 to 270 nm was analysed considering the seven most effecting wavelengths. The exact equation is given in the appendix. The absolute sum of the residuals of the 2nd measurement campaign equals 1 002 mg/l, which indicates an extremely good correlation between measured and predicted data.

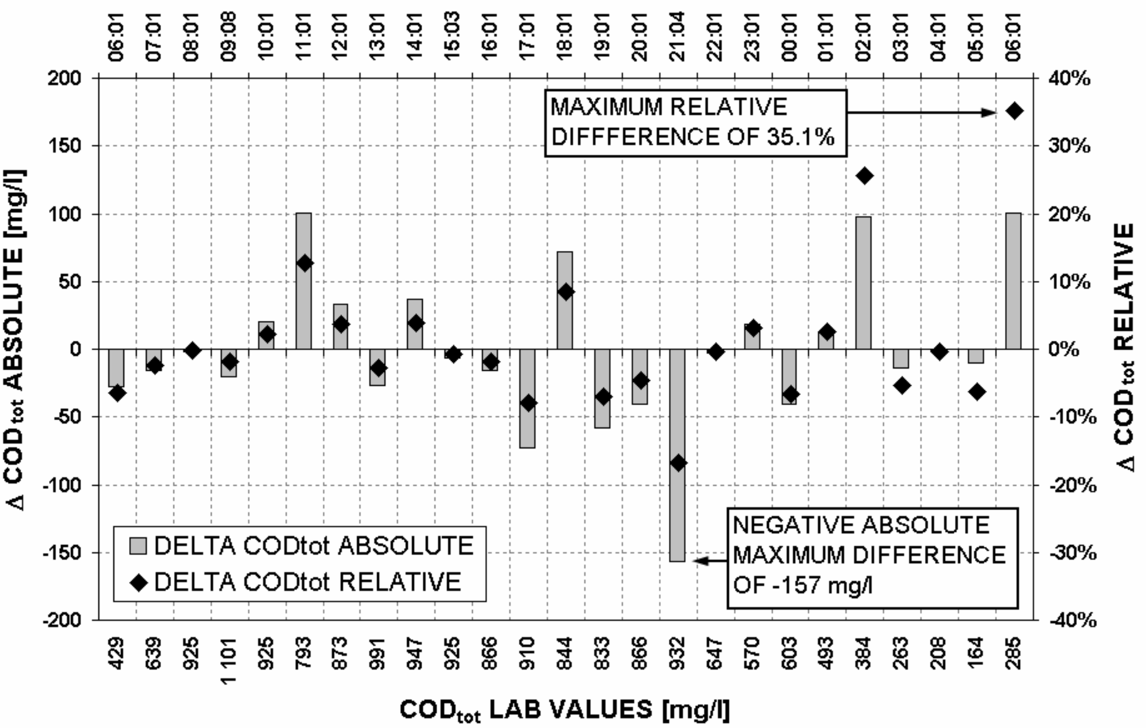

Figure 4-76 Absolute and Relative COD_{tot} Differences of Measured Lab Values and Predicted PLS Regression Values on the Basis of an Analysed Wavelength Range between 240 to 270 nm and 7 Applied Wavelength in the Equation for the 2nd Measurement Campaign

The resulting correlation coefficient of 0.979 of the 2nd measurement campaign for COD_{tot} also demonstrates a good absorbance – concentration coherence. A further analysis of the other correlation coefficients of 0.980 (2nd + 3rd measurement campaign) and of 0.804 (both storm events together) confirms the previous assumption. Figure 4-77 disproves this assumption and displays a typical example for model overfitting. Overfitting for PLS regression was sometimes recognised. It seems that PLS regression is susceptible for model overfitting. This example also demonstrates the necessity of a multi-stage validation process.

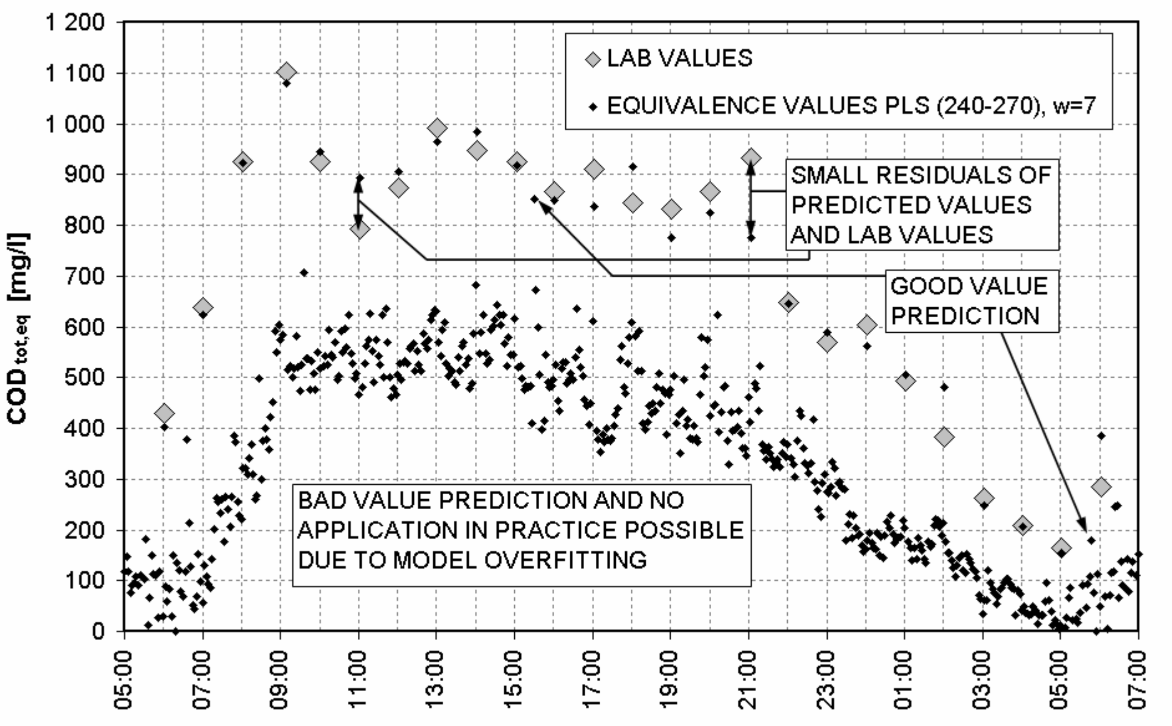

Figure 4-77 Example for Model Overfitting for the COD_{tot} Parameter

4.9.7. Comparison of Different Regression Methods

Figure 4-78 shows the cumulative frequency of the COD_{tot} parameter for different regression methods by means of the 2^{nd} measurement campaign.

The default settings to determine the equivalence concentrations are based on PLS regression. Of course, this equation can only reproduce a general behaviour of absorbance and equivalence concentrations. 80% of the cumulative frequency results in a relative deviation of about 33%. This calibration setting should be adapted to the waste matrix and, therefore, be improved. This default setting was improved on the basis of the measured COD_{tot} lab values (Figure 4-78). The improved PLS regression results in relative difference of approximately 15% by a cumulative frequency of 80%. The other regression methods equal for 80% cumulative frequency in about 22% for LMS (230-250) regression, in 16% for PLS (240-260) regression, in 15% for SLR (200-750), in 14% for SVM (250-260) using SMO, and 11% for M5 model tree regression. Figure 4-78 demonstrates the necessity of the global calibration adaptation to the waste water matrix.

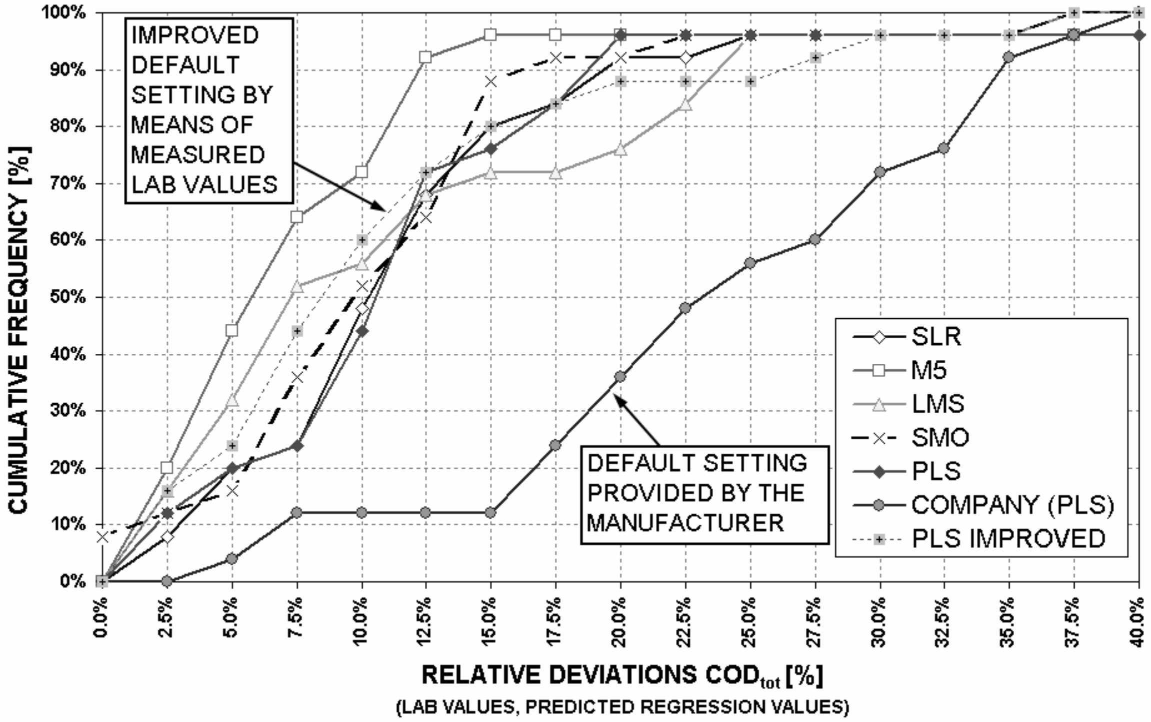

Figure 4-78 Cumulative Frequency of Different Regression Methods for COD_{tot} on the Basis of the 2nd Measurement Campaign

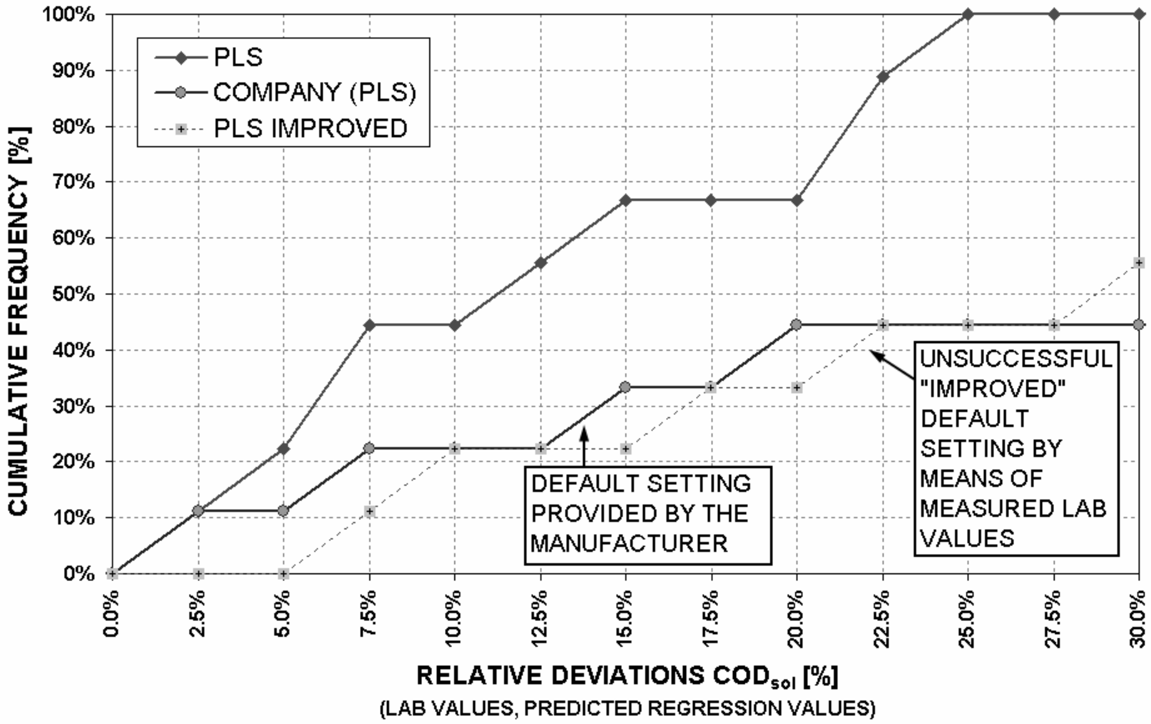

Figure 4-79 Cumulative Frequency of Different PLS Regressions for COD_{sol} on the Basis of the 3rd Measurement Campaign

Figure 4-79 displays the different PLS regression for the COD_{sol} parameter by means of the 3rd measurement campaign. Again it can be seen that the default setting can inaccurately reproduces equivalence parameters. Unfortunately, the “improvement” for the COD_{sol} parameter did not work. The figure demonstrates that even the measured lab values are reliable; it is not always possible to achieve an improvement and adaptation to the waste matrix. The self-developed PLS regression with an analysed wavelength range from 240 to 500 nm and 5 used wavelengths in the regression equation gives improved results. All regression analyses show that the COD_{sol} parameter can not be reproduced as accurately as the results for the COD_{tot} and TSS parameters.

Figure 4-80 shows the cumulative frequency of the TSS parameter on the basis of the two measurement campaigns. All the displayed regression methods show a similar results behaviour. Interesting, the PLS model provided by the manufacturer is the model which has the best results. An improvement by means of the measured lab values does not yield the expected results. The default setting for the TSS parameter provides sufficient values. Thus, in this case of the TSS parameter an improvement is not implicitly necessary. The absorbance for TSS is in the visible range indicated by solids and turbidity, respectively.

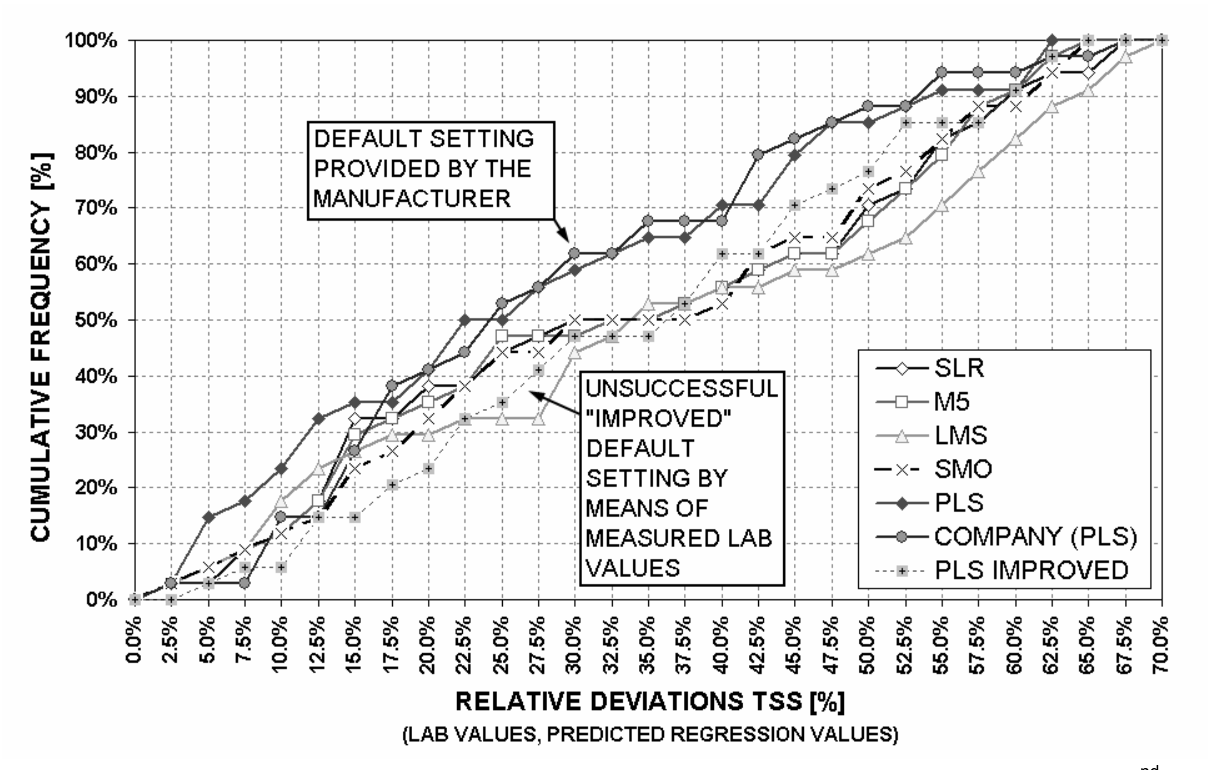

Figure 4-80 Cumulative Frequency of Different Regression Methods for TSS on the Basis of 2nd and 3rd Measurement Campaign

4.10. DRY WEATHER TIME SERIES

A mean value does not always represent the “real” flow or concentration behaviour in a sewer during a whole day. Therefore, typical dry weather curves of flow and concentrations are determined. These curves are also needed as input data for quality modelling (in the software an average value and the depending ratio of actual and daily mean value is needed).

4.10.1. FLOW DRY WEATHER CURVES FOR THE GRAZ-WEST CSO

On the basis of the corrected flow data a typical dry weather flow curve for the CSO Graz-West was created for a weekday, Saturday and Sunday. The results of this calculation are presented in Figure 4-81.

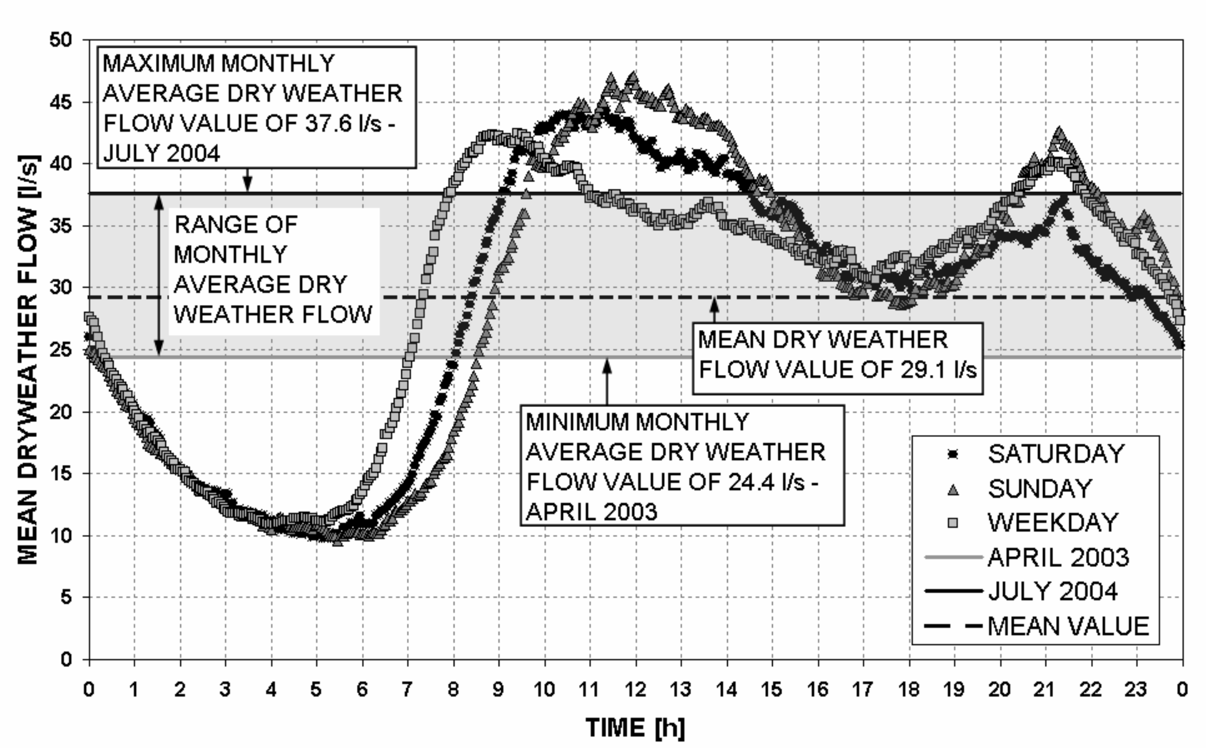

Figure 4-81 Mean Dry Weather Flow Curves and Mean Values by Means of the Corrected Flow Data

The maximum flow value of a weekday is reached at about 9^{00} with a value of about 42 l/s and the minimum about between 4^{00} and 5^{00} of about 11 l/s. The rise in the Saturday and Sunday curve is similar to the weekday curve, but the curves are time-shifted. Interestingly, the maximum value of Saturday and Sunday is higher than the maximum of a weekday. Additionally, monthly mean values are displayed in the figure. The mean value of all dry weather flows equals 19.1 l/s. The grey box presents the whole range of monthly mean values. The minimum mean value in April 2003 results in 24.4 l/s and the maximum in July 2004 in 37.6 l/s.

4.10.2. MEAN DRY WEATHER TSS CONCENTRATION CURVE FOR THE GRAZ-WEST CSO

Figure 4-82 displays a typical DW TSS concentration curve for a weekday and for Saturday on the basis of PLS regression. In this case a wavelength range from 550 to 600 nm was analysed. The resulting equation has 3 used wavelengths. The accuracy of this regression had already been proved and is also given in Figure 4-80.

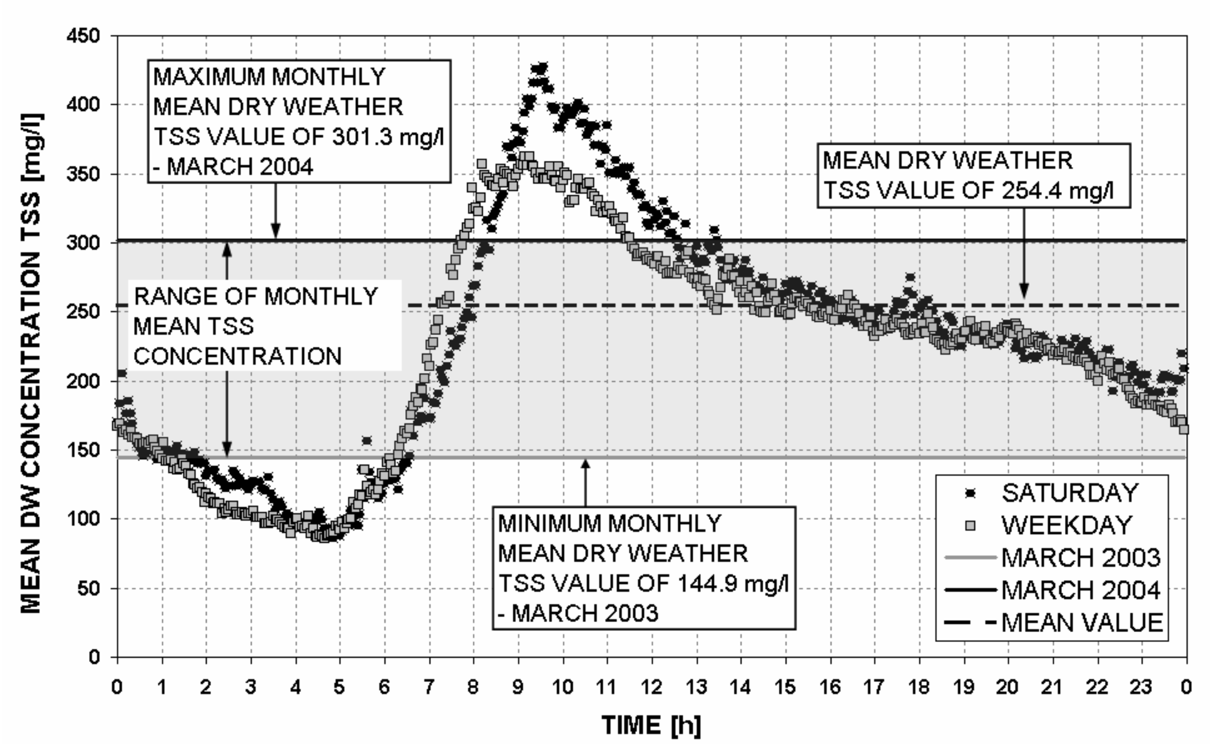

Figure 4-82 Mean Dry Weather TSS Concentration Curves and Mean Values by Means of PLS Regression (550 – 600 nm, 3 Wavelengths)

The resulting monthly mean dry weather value of TSS equals 254.5 mg/l. The range of all monthly mean values is from 144.6 mg/l (March 2003) to 301.3 mg/l (March 2004). A slightly time-shifted curve can be recognised between Saturday and the weekday curve.

4.10.3. MEAN DRY WEATHER COD_{TOT} CONCENTRATION CURVE

Typical mean dry weather concentration curves for Saturday and weekday are displayed in Figure 4-83. The results are based on support vector machines using sequential minimal optimisation algorithm (analysed wavelength range 250 to 260 nm). Again, the grey box indicates the monthly mean DW COD_{tot} concentration range from 495.1 mg/l (minimum – March 2003) to 1 154 mg/l (maximum – October 2003). The mean dry weather value of months results in 930.1 mg/l for COD_{tot}. Until about 8 o'clock both curves (Saturday and weekday) have similar trends; from 10^{00} until about 24^{00} a nearly constant offset of about 100 mg/l can be recognised.

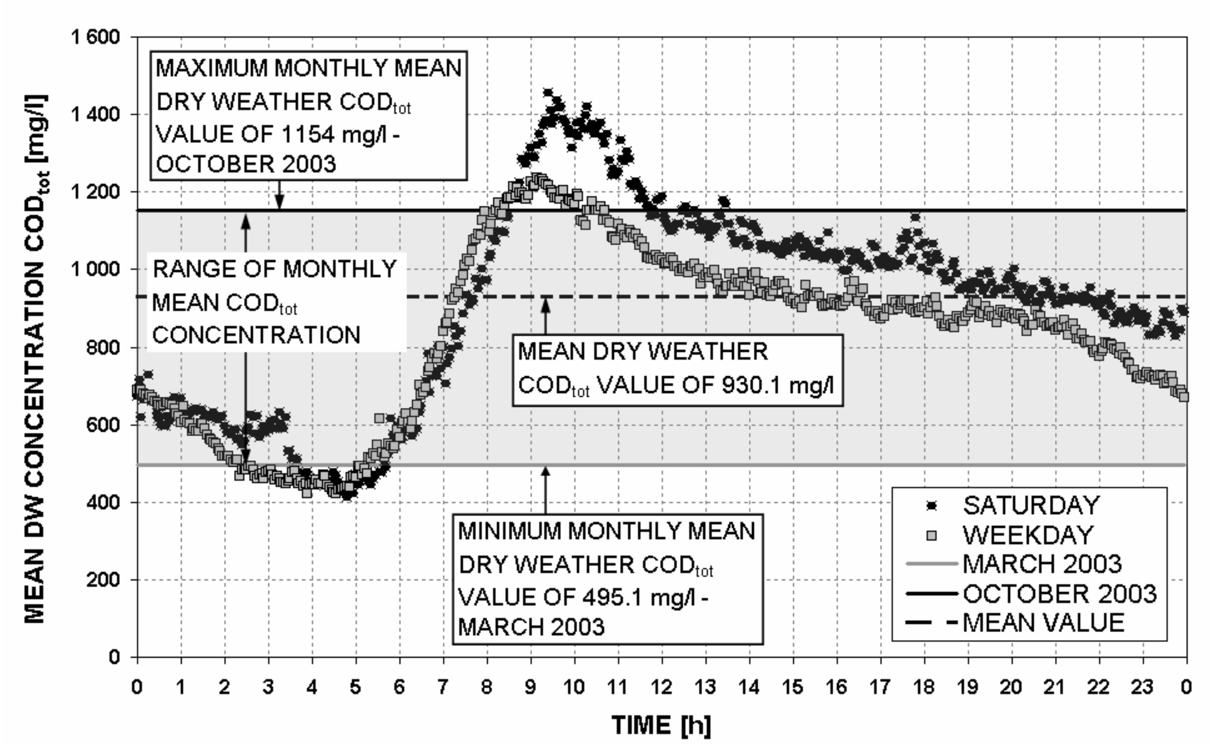

Figure 4-83 Mean Dry Weather COD$_{tot}$ Concentration Curves and Mean Values by Means of SVM using SMO (250 – 260 nm)

4.10.4. MEAN DRY WEATHER COD$_{SOL}$ CONCENTRATION CURVE

The mean dry weather curves of the COD$_{sol}$ parameter can be seen in Figure 4-84. These curves are based on the result of PLS regression with an analysed wavelength range from 240 to 500 nm with 5 wavelengths considered. The displayed curves are for typical Saturdays and weekdays. Unfortunately, both curves do not have such a smooth trend as the other determined mean dry weather concentration curves. This also demonstrates the harder reproduction of the absorbance concentration behaviour of this parameter.

The monthly mean concentration range is from the minimum in March 2003 with a value of 152.7 mg/l to the maximum in February 2003 with a value of 349.1 mg/l. The mean dry weather concentration over the whole analysed period is 261.1 mg/l. A time shift as recognised in the other curves can not be seen here. This is not implicitly due not existing of a time shift. Maybe, the more vague calculation results reproduce a higher scattering range and therefore a “fuzzy” mean dry weather curve for Saturdays and weekdays, respectively.

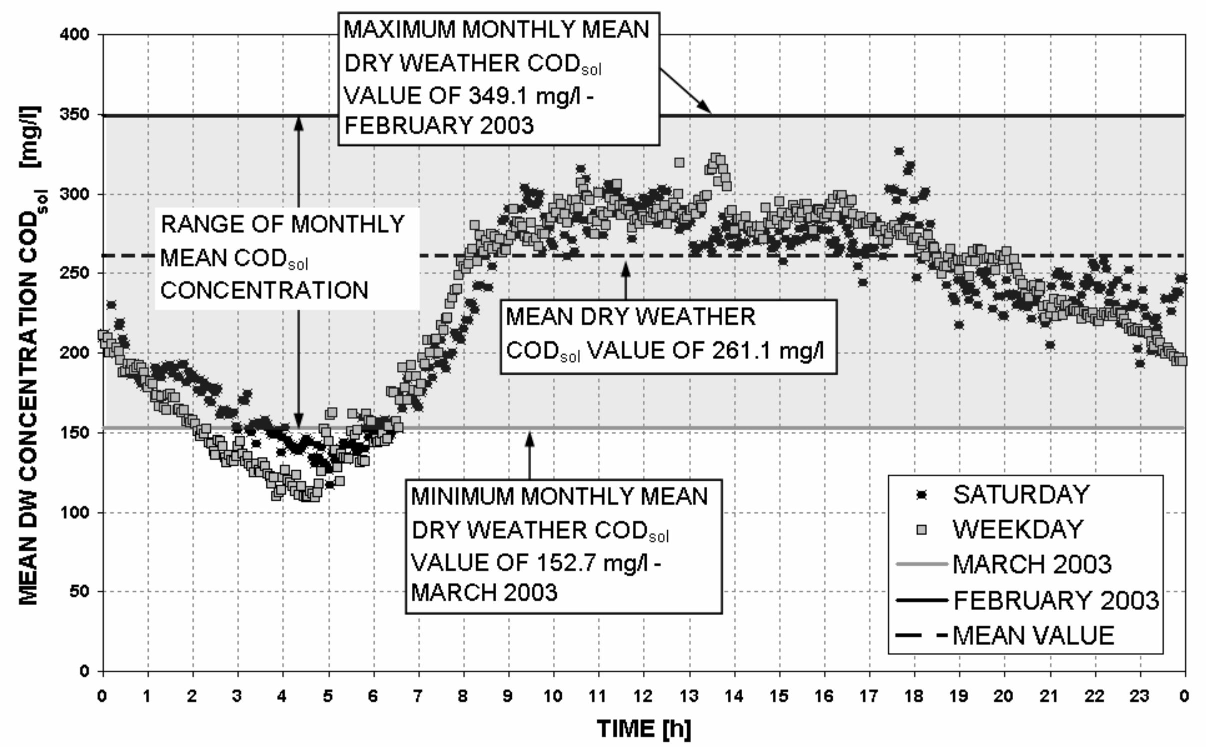

Figure 4-84 Mean Dry Weather COD$_{sol}$ Concentration Curves and Mean Values by Means of PLS Regression (240 – 500 nm, 5 Wavelengths)

4.11. Pollution Load Calculation

This chapter describes the procedure of load calculation and its different calculation methods. The later calculated mean concentrations for dry weather and rain weather are input parameters for load quality modelling.

4.11.1. Methods

For a quantification of the catchment specific dry weather part (Schulz, 1995) of storm water loads, different kind of approaches for dry weather concentrations and rain weather concentrations are usually used. The storm water load is a superposition of the two components dry weather and rain weather load. The storm load is calculated with the following equation of the two components method (Macke et al., 2002):

$$\text{storm weather load} = \text{dry weather load} + \text{rain weather load}$$

Generally, a comparison between different kinds of pollution is made by mean pollution concentration by means of the online data in this thesis. Table 4-21 describes the different methods for concentration calculation.

For the determination of the pollution load potential flow and load weighted mean values are especially useful. The values are calculated from the ratio of load sum to flow sum. Some concentration values in the literature are based on the arithmetic mean (mean sample value) or mean values over a definite period (temporal mean value). Compared with the results from the temporal mean, the result from flow weighted concentrations on the same data basis can result in higher values. This effect can be explained due to the simultaneous superposition of flow and concentration maxima and minima, respectively.

Table 4-21 Concentration Calculation Methods (Schulz, 1995)

Notation	Method of Calculation	Equation	Remarks
Mean Sample Value	Arithmetic mean of single samples and its concentrations	$C = \frac{1}{n} \cdot \sum_{i=1}^{n} C_i$	Comparability only by constant time intervals of sampling
Temporal Mean	Mean value over a period of Δt	$C = \frac{1}{\Delta t} \cdot \int C(t)\, dt$	Common used analysis to determine from 24 hours measured mean dry weather concentration
Flow- and Load Weighted Mean	Mean value from the ration of load sum to flow sum	$C = \frac{\int \left(C(t) \cdot Q(t)\right) dt}{\int Q(t)\, dt}$	Appropriate for comparison of different catchment areas due to easy calculation of exactly load sums by known rain volume

The pollution load for every analysed parameter is calculated with this superposition of flow and concentration time series and an assumed linear concentration trend between two waste water samples. On the basis of this approach, it is possible to determine the temporal load developing at the monitoring station for dry weather as well as for storm weather.

The elimination of the dry weather part for storm water flow and storm water load is made on the basis of the two components method (Macke et al., 2002):

$$C_{RW} = \frac{C_{SW} \cdot VQ_{SW} - C_{DW} \cdot VQ_{DW}}{VQ_{SW} - VQ_{DW}} \quad [\mathrm{mg/l}]$$

where C_{RW} is the rainwater concentration; C_{SW} is the storm water concentration; C_{DW} is the dry weather concentration, VQ_{SW} is the storm water flow volume and VQ_{DW} is the dry weather flow volume.

The two components method can only reproduce one value and, therefore, the real concentration developing can not be reproduced. This can be also clearly seen in Figure 4-82, Figure 4-83 and Figure 4-84. Time dependent the real concentrations are under and over estimated, respectively.

4.11.2. MEAN DRY WEATHER CONCENTRATIONS

The results and the range of the different regressions methods of the mean dry weather concentrations calculation of COD_{tot} and TSS are displayed in Figure 4-85. The black dots indicate an outlier and extreme value, respectively. The grey box is the range from the lower and upper quartile. The maximum and minimum value is given by the lines.

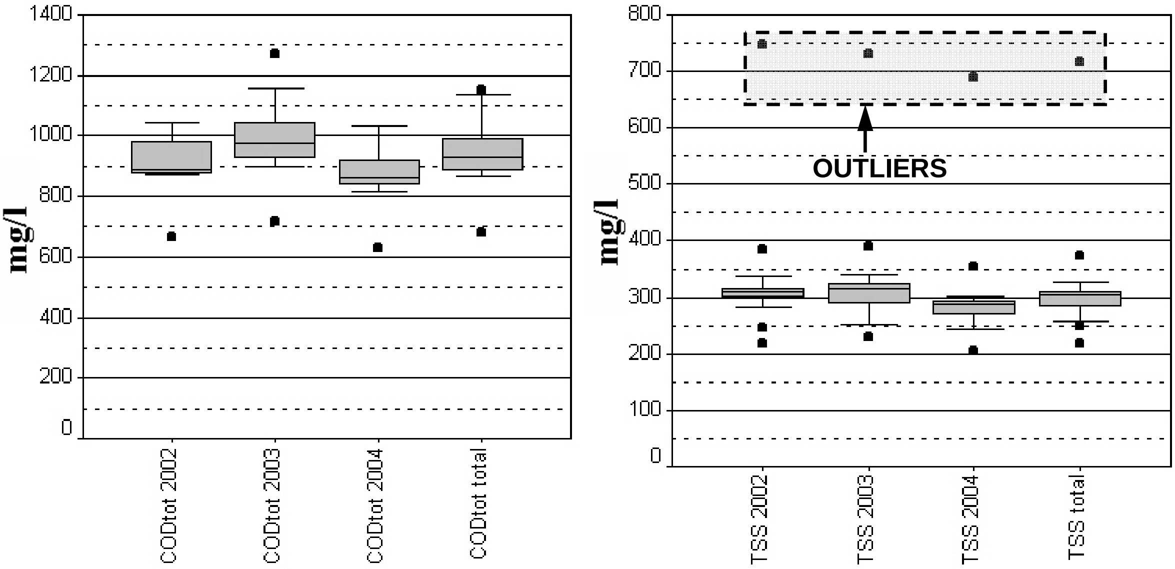

Figure 4-85 Box Plot Figures of Annual and Total Mean Dry Weather Concentrations of COD_{tot} (Left Figure) and TSS (Right Figure)

The results over the whole analysed period (total results) have almost the same range as the results of the year 2002. The year 2004 with lower concentration values demonstrates the influence of more annual precipitation and the resulting higher ground water infiltration as in the year 2002 and 2003. The ranges of the lower and upper quartile are between 100 to 150 mg/l. The average mean dry weather concentrations result in values of approximately 900 to 950 mg/l (median) for COD_{tot}. Hence, with this quite high concentration of COD_{tot}, the ground water infiltrations seem to be minor.

The TSS results are presented in Figure 4-85 in the right figure. The results from the PLS regression with an analysed wavelength range from 380 to 750 nm and three used wavelengths can be indicated as outliers. Also, for TSS the higher ground water infiltration for the year 2004 can be seen. The TSS mean dry weather concentrations result approximately in values of 300 mg/l (median).

Table 4-22 gives an overview of mean dry weather concentrations for the parameter COD_{tot} by means of different regression methods. The detail results (COD_{tot}, COD_{sol} and TSS) with all tables are displayed in the appendix. Two values are shown for every regression method. One value is the result for the calculation method based on the two component method and the other value is the arithmetic mean (average).

Table 4-22 Overview of COD_{tot} Mean Dry Weather Concentrations for Different Regression Methods

Year	Month	SLR		LMS		M5		SVM u. SMO		PLS	
		250-260		230-500		250-277.5,436		240-250		240-270,w3	
		2-CM [mg/l]	av. [mg/l]	2-CM [mg/l]	av. [mg/l]	2-CM [mg/l]	av. [mg/l]	2-CM [mg/l]	av. [mg/l]	2-CM [mg/l]	av. [mg/l]
2002	October	898	854	1043	995	986	957	941	886	831	775
	November	941	857	1035	933	902	828	905	815	939	855
	December	811	727	868	766	771	696	806	718	843	759
2003	January	-	-	-	-	-	-	-	-	-	-
	February	871	794	920	833	803	752	821	737	1036	943
	March	759	820	811	871	727	782	724	778	865	948
	April	982	867	1079	949	920	833	955	841	1053	923
	May	961	880	1050	953	903	837	935	851	1044	958
	June	919	851	1018	936	904	844	889	816	970	902
	July	971	909	1060	987	910	861	939	876	1101	1035
	August	944	861	1030	929	881	811	920	830	1105	1022
	September	929	848	1006	907	868	797	922	836	1092	1007
	October	1095	1033	1232	1157	1028	984	1046	977	1179	1118
	November	1093	1010	1181	1082	992	932	1033	945	1216	1136
	December	1097	1023	1118	1033	1000	946	1050	968	1207	1147
2004	January	1060	986	1144	1054	966	910	1000	918	1216	1145
	February	1007	931	1109	1015	934	874	967	881	1132	1055
	March	865	786	947	851	845	773	837	754	977	885
	April	811	722	880	772	808	721	815	720	804	711
	May	874	766	951	821	869	764	876	762	850	758
	June	670	616	709	643	665	607	680	623	688	633
	July	564	552	589	569	547	534	579	566	580	570
	August	971	887	1045	954	909	843	971	881	1004	911
	2002	883	813	982	898	886	827	884	806	871	796
	2003	966	900	1046	967	903	853	930	860	1079	1013
	2004	853	781	922	835	818	753	841	763	906	834
	total	913	845	992	910	870	813	891	817	988	918

4.11.3. MEAN RAIN WEATHER CONCENTRATIONS

The mean rain weather concentrations are one of the important input parameter for load quality modelling. Therefore, accurate and reliable mean rain weather concentration values are of great importance. Figure 4-86 displays the mean rain weather concentrations of COD_{tot} (left figure) and TSS (right figure). The values are extremely scattered. The mean rain weather concentrations result in a value range of approximately 300 to 400 mg/l (2003, 2004 and total). The year 2003 yields higher values from about 400 to 480 mg/l (upper and lower quartile). These concentrations depend on the dry weather periods and the 1st flush behaviour. The TSS values result for 2003, 2004 and total in approximately 200 mg/l. Only the year 2002 has a value range of about 150 to 175 mg/l (upper and lower quartile).

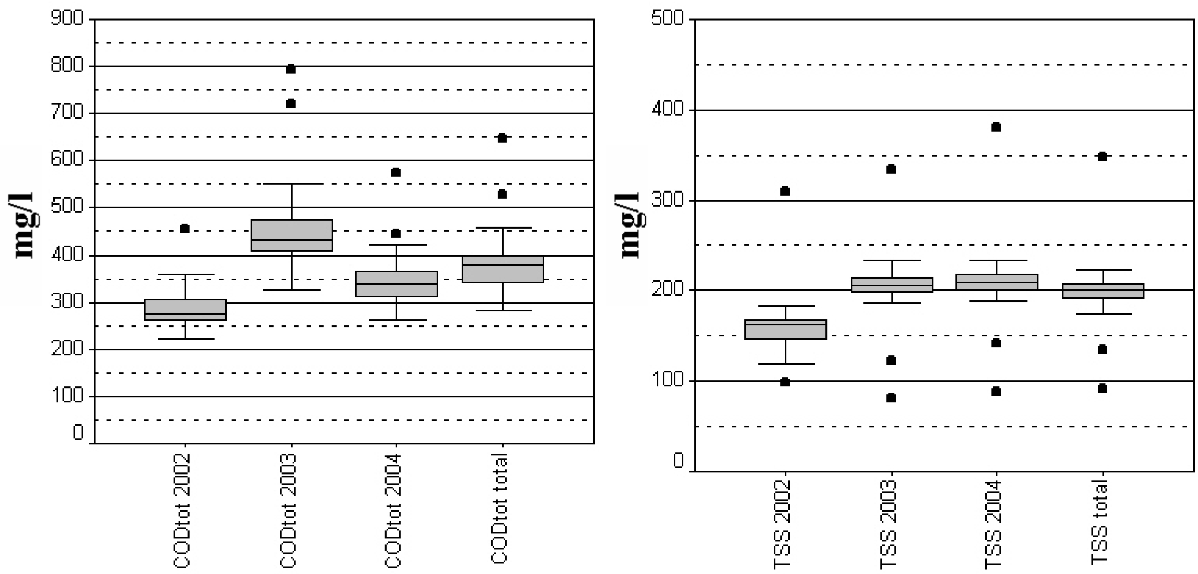

Figure 4-86 Box Plot Figures of Annual and Total Mean Rain Weather Concentrations of COD_{tot} (Left Figure) and TSS (Right Figure)

Table 4-23 Overview COD_{tot} Mean Rain Weather Concentrations for Different Regression Methods

Year	Month	SLR 250-260 [mg/l]	LMS 230-500 [mg/l]	M5 250-277.5,436 [mg/l]	SVM u. SMO 240-250 [mg/l]	PLS 240-270,w3 [mg/l]
2002	October	452	518	630	557	411
	November	284	292	274	324	290
	December	55	22	9	79	54
2003	January	-	-	-	-	-
	February	-	-	-	-	-
	March	-	-	-	-	-
	April	-	-	-	-	-
	May	640	707	699	672	797
	June	395	426	442	437	474
	July	316	327	333	360	420
	August	541	564	527	581	783
	September	303	303	289	346	448
	October	212	203	198	243	334
	November	443	489	507	471	610
	December	-	-	-	-	-
2004	January	-	-	-	-	-
	February	-	-	-	-	-
	March	448	526	548	488	464
	April	350	393	441	411	263
	May	238	243	229	295	202
	June	164	157	136	219	125
	July	114	105	98	167	80
	August	540	609	691	561	618
	2002	264	277	304	223	252
	2003	407	431	428	444	552
	2004	309	339	357	350	292
	total	343	368	378	386	398

Table 4-23 displays the mean rain weather concentrations for the COD_{tot} parameter for different regression methods based on the two components method. The detailed results (COD_{tot}, COD_{sol} and TSS) with all tables are shown in the appendix. The values are calculated on the two component method. The results of December 2002 are interesting. These low concentrations can be explained by storm events with no remobilisation effect. High concentrations indicate the high influence of the "first flush".

4.11.4. COMPARISON OF RAIN WEATHER CONCENTRATIONS WITH OTHER PROJECTS

The German standard A 128E (1992) is based on the results of Geiger (1984) and Krauth (1970). This standard gives an average rain weather concentration for COD_{tot} of 107 mg/l. The use of higher concentrations yields after the calculation of A 128E (1992) for higher overflow loads under same conditions.

Table 4-24 Comparison of COD_{tot} concentrations from different research projects

Research Project	Graz	Stuttgart*	Munich**	Braunschweig***
Catchment Area [ha]	351	31.4	540	636
Mean Sewer Slope [%]	1.6	1-3	0.6	0.3
Mean Flow Time [min]	~75	~7	10-50	127
Mean Dry Weather Flow [l/s]	24.4-37.6[1)]	~4	78	484
Av. COD_{tot} DW Conc. [mg/l]	583-1272[2)]	443	440	679
Av. COD_{tot} RW Conc. [mg/l]	223-444[3)]	-	163	288

*Krauth, 1970; **Geiger, 1984; ***Macke et al., 2002; Schulz, 1995

[1)]dry weather flow range of corrected flow data based on monthly mean dry weather flows

[2)]dry weather concentration range of COD_{tot} of annual mean concentrations based on different regressions

[3)]rain weather concentration range of COD_{tot} of annual mean concentrations based on different regressions

Sztruhár et al. (2002) presented an event mean concentration (EMC) of 445 mg/l for COD_{tot} on the basis of eight storm events at a CSO. Brezonik & Stadelmann (2002) achieved EMC values for TSS of 134 mg/l in winter, 118 mg/l in spring, 80 mg/l in summer, 62 mg/l in autumn and, for COD_{tot} of 196 mg/l in winter, 129 mg/l in spring, 82 mg/l in summer and 70 mg/l in autumn of stormwater runoff based on 499 rainfall events for an urban watershed. Ruan (1999) displayed results from a quality continuous simulation of a combined sewer system with an area of 56.5 ha. In one case study the CSO emission in terms of TSS was 187 kg/ha per year. The mean CSO concentration of TSS was calculated as CSO emission divided by CSO volume times a factor of 100, which resulted in 216 mg/l.

Macke et al. (2002) shows an average concentration of rainwater for COD_{tot} in the range of 200 to 300 mg/l for sewer systems with low slopes. The results of the project for COD_{tot} in Graz are, of course, dependent on the used statistical regression method. The value range, which is displayed in Table 4-24, shows concentrations between 223 to 444 mg/l. These results are about two to four times higher than the value given by the standard. These values present the same concentration range compared with Macke et al. (2002) for sewer systems with high slopes. The equation in A 128E (1992) for load calculation has only one factor which considers the remobilisation of sewer deposits. The influence of this factor on this equation is insignificant and does not reproduce the real "first flush" behaviour (Macke et al., 2002). This conclusion can also be seen for sewer systems with steep slopes. In practice the real mean rain weather concentrations should be determined by measurements for an assumption of overflow loads. The results of A 128E equations underestimates the overflow loads in most cases.

4.11.5. RESULTS OF LOAD CALCULATION

The load calculation results of the Graz-West CSO are displayed in Figure 4-87 for COD_{tot} and TSS. Of course, the itemised loads from every year can not be compared due to different observation periods and data losses in the year 2003. The high resulting range can be seen in the result for COD_{tot} and TSS parameter (Figure 4-87).

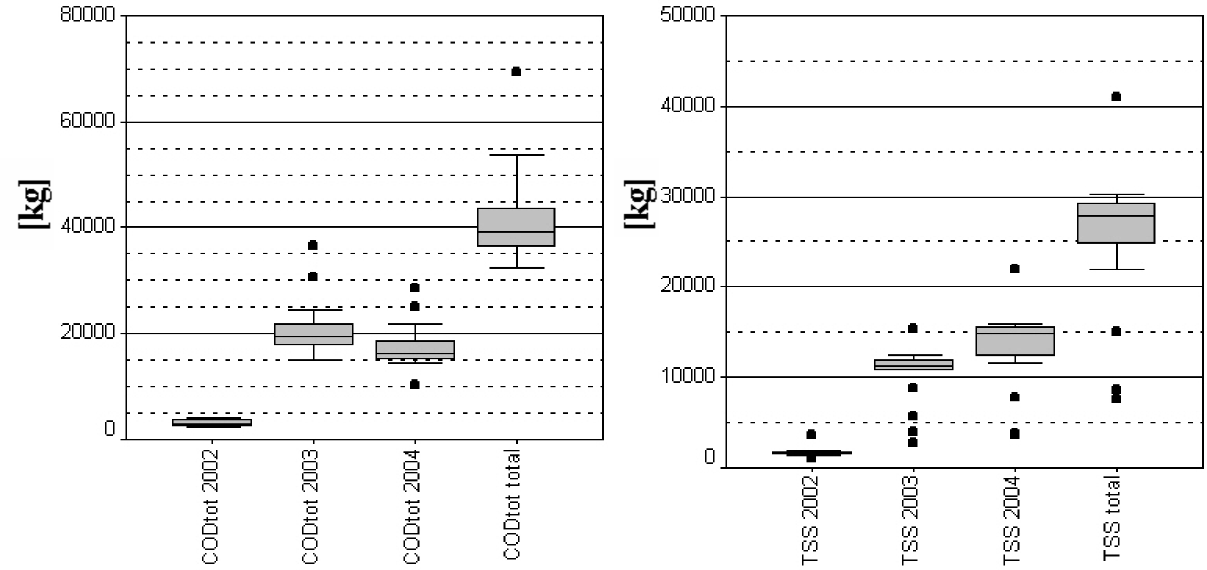

Figure 4-87 Box Plots of Annual and Total Overflow Loads of COD_{tot} (Left Figure) and TSS (Right Figure) and the Scattering Range

Table 4-25 shows the exact overflow loads for COD_{tot}, dependent on selective regression methods. A difference of about 25% can be recognised between the total lowest load for PLS regression of 34 789 kg/year and the total highest load for SVM of 43 761 kg/year. This difference shows the necessity of a longer statistical analysis for an easier assessment of the "best" fitting regression model for the Graz-West CSO.

The TSS results, which are displayed in the right figure, show a quite low resulting value range for the single year. Some extreme values, as well as outliers indicated by the black dots, can be recognised. The TSS overflow loads of the year 2004 are higher than of the year 2003. This trend can not be recognised for COD_{tot} loads.

For the COD_{sol} parameter the detail overflow results are displayed in the tables in the appendix. The exact results for COD_{tot} and TSS and the depending different regression methods can also be seen in the appendix.

Table 4-25 Overview of Overflow Loads of COD_{tot} Based on Different Regression Methods

Year	Month	SLR 250-260 [kg/a]	LMS 230-500 [kg/a]	M5 250-277.5,436 [kg/a]	SVM u. SMO 240-250 [kg/a]	PLS 240-270,w3 [kg/a]
2002	October	2 405	2 771	3 477	3 013	2 154
	November	244	403	314	445	411
	December	63	42	24	81	62
2003	January	-	-	-	-	-
	February	-	-	-	-	-
	March	-	-	-	-	-
	April	-	-	-	-	-
	May	155	174	218	162	186
	June	5 771	6 391	6 640	6 397	6 135
	July	8 242	8 751	8 795	9 261	10 258
	August	293	318	304	320	367
	September[1)]	223	216	164	262	303
	October	2 206	2 087	1 755	2 573	3 244
	November	1 132	1 257	1 280	1 173	1 414
	December	-	-	-	-	-
2004	January	-	-	-	-	-
	February	-	-	-	-	-
	March	247	289	287	272	238
	April	432	527	666	490	345
	May	2 488	2 462	2 199	3 205	1 635
	June	6 557	6 415	5 824	8 900	4 166
	July	3 111	3 1357	3 333	4 607	1 620
	August	2 579	3 139	3 844	2 600	2 251
	2002	2 712	3 216	3 815	3 539	2 627
	2003	18 022	19 194	19 156	20 148	21 907
	2004	15 414	15 989	16 153	20 074	10 255
	total	36 148	38 399	39 124	43 761	34 789

[1)] 14 days malfunction of process unit – data loss

5. MODELLING OF OVERFLOW LOADS

Modelling became an important tool for the urban drainage engineer and for the researcher a long time ago. Computer modelling of sewer systems emerged several decades ago. Although, in this thesis, only emission modelling was carried out, the consideration of an integrated model for an urban catchment is exceptionally important. The historical development of municipal drainage systems has led to a separate design and operation of the three main components of the system, these being the sewer system, the wastewater treatment and receiving water. However, sewage drainage result in effects and interactions with the total system and, consequently, should not be seen from the point of view of each individual subsystem alone (Rauch et al., 1999). The system boundaries of the model to be set up have to be chosen. However, urban wastewater systems do not stop at the boundaries of the three subsystems – sewer system, wastewater treatment plant, receiving water – but also include groundwater interactions and many others (Schütze & Alex, 2004).

Some of the core issues of (integrated) modelling and the related problems have been summarised by the Central European Researchers' Simulation Group meeting by the triangle shown in Figure 5-1.

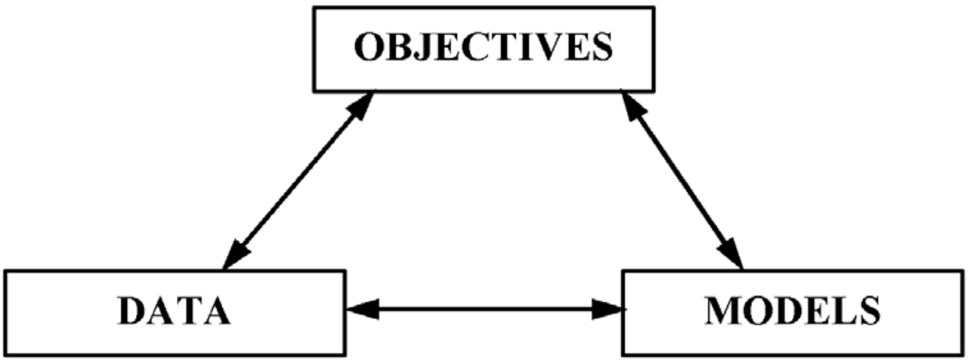

Figure 5-1 The Three Driving Forces of Modelling Studies (Schütze & Alex, 2004)

It is obvious that the availability of data and models influence each other and that everything else is governed by the overall objectives of the study. The objectives of the study will determine which modelling approaches are to be considered. The objectives will also determine the system boundaries to be considered in the study. The interrelation between data and models is obvious: models require data for model structure and model parameter estimation. They may also give hints as to what type of data are missing or erroneous. Often, scarcity of appropriate data constitutes a major obstacle to the successful set up and application of models. Finally, the availability of data and models may also lead to a redefinition of the objectives of the study (Schütze & Alex, 2004).

Various authors (see for example Rauch et al. 2002, Erbe & Schütze 2004, Seggelke 2002 and Leinweber 2002) have already incorporated this approach of integrated modelling in their research work.

Deterministic models to simulate rainfall-runoff processes as well for integrated modelling in urban drainage systems are generally accepted as being state of the art (Rauch et al., 2002). They are used, for example, to indicate the efficiency of planned or existing sewer systems or storage tanks. Scholz (1997) presented a stochastic-hydrological model for pollutant wash-off on the basis of effective precipitation and a wash-off coefficient.

Hauger et al. (2002) showed the results of integrated modelling considering a cost benefit risk. Cost-benefit risk is a useful method for the integrated analysis of urban wastewater systems. It opens up the opportunity to take into account risk and uncertainty. The major disadvantage of such kind of modelling is the problem with converting intangible benefits into monetary terms. Hauger et al. (2002) left out all problematic benefits. Attempts to assign a value to the benefit failed. The consequences of failure were difficult to predict or estimate. The sum of costs, benefits and risk is expressed as the Net Present Cost.

While under dynamic loading from rain, the flow in the pipe system, the release of stormwater from storage tanks and the loading and operation of the treatment plant can be regulated by pumps and gates according to an appropriate control strategy on the basis of on-line measurements in the system, including on-line gauging of the environment. Linear programming is the classical tool for solving the real-time control optimisation problem in the urban drainage field. However, this technique requires rigorous linearisation, which is a severe simplification, but this is may be acceptable for the runoff process in the sewer system. The possibilities of the genetic algorithm as an optimisation procedure for real-time control of urban wastewater systems were explored by Rauch & Harremoës (1999). The main strength of Rauch & Harremoës (1999) research methods was seen in the freedom in the formulation of deterministic model and the reliability of the search algorithm.

5.1. QUALITY MODELLING

When modelling of the urban water system is carried out there are a number of phenomena that the modeller has to be aware of in order to produce good modelling results and to be able to interpret the result. Thus, there it is not always possible to distinguish between variation and uncertainty (Hauger et al., 2002).

The level of uncertainty is a measure of errors that are made when reality is simplified into a model. Model parameters are estimated based on measurements or deduced somehow from prior knowledge. The measurements provide limited information about the parameter on a single or a few spots and the value is then extrapolated to represent the whole area. This simplification, of course, introduces an error, but the measurement itself is also an error source which was presented in chapters 3 and 4.

Quality models simulate the run-off and pollutant transport within the pipe network. Precipitation-runoff models reproduce sewer transport processes by determining the effective precipitation and the concentration until the inflow into the sewer system. Generally, two kinds of sewer transport calculation are possible: a hydrologic and a hydrodynamic calculation. The latter one is an exact solution of Saint-Venant equations. The hydrologic approach of flow calculation is a simple function which describes the changing of the flow wave from two positions. A combination of continuity load and storage behaviour is used. The approach of linear reservoir cascade is implemented in the software KOSIM (ITWH, 2002) which is used in this thesis for quality modelling. The non-linearity sewer flow function due to possible backwater or flow direction changing can not be described with a hydrologic approach (Seggelke, 2002). In this case a hydrodynamic simulation should be carried out. Cabtree et al. (1995) proposed sewer sediment depositing and pollutant behaviour into a sewer system hydraulic analysis package.

Quality models consider the precipitation run-off process and the sewer flow ingredients. Sedimentation, degradation and deposit remobilisation are complex processes that are hard to describe in simulation programs. Thus, a conservative substance process is assumed and no degradation process is considered. The quality calculation is based on the dry weather and rain weather load mixture. Hence, the mean concentration of resulting loads is calculable with the components method.

5.1.1. PHENOMENA OF STORM WATER FLOW

Storm events cause a distinct dynamic on the surface and in the sewer system which can be seen in large flows and the pollution load behaviour. During dry weather periods, particulate matter is deposited on the surface as well as in the sewer system. During a storm, the removal of matter from the surface and a remobilisation of deposits (first flush) in the sewer system can be recognised (Leinweber, 2002).

First flushes have most often been observed in small watersheds, particularly if the imperviousness is high. Large watersheds have a longer time to travel, so that the early runoff from areas far from the sample location is mixed with later runoff from areas adjacent to the sample location.

If the first flush is frequent, then the structures do not need large capacities: They can merely intercept the first part of the event to intercept most of the pollution load, and protect the receiving waters (Saget et al., 1996).

The concept of seasonal first flush also exists in regions with extended dry periods (Kim et al., 2004; Lee et al., 2004). Under such conditions, storms that mark the end of the dry season have disproportionably larger mass discharges.

The behaviour of dissolved compounds during a storm has been given by Krebs et al. (1999). The wave front travels faster than the water body, rainwater inflow causes a first flush type effect in combined sewers. The wave front is formed from the sewage and thus maintains the original concentrations of the dissolved compounds in the sewage while the flow rate is increased. Whereas the first flush originating from erosion of sewer sediments increases the concentration of particulate matter, the wash-out effect of dissolved compounds creates a load increase proportional to the flow-rate increase in the worst case.

One definition of the first flush is when the slope of normalised cumulative mass emission plotted against normalised cumulative volume is higher than 45 degrees. A lot of researchers have used this definition in their projects (e.g. Larsen et al., 1998; Gupta & Saul, 1996; Lee & Bang, 2000). A more restrictive definition is given by Geiger (1984); the definition is based on the analysis of pollutant mass distribution vs. volume curves. A first flush is identified after Geiger (1984) if the gap between the mass-volume curve and the bisector (45 degree line) is greater than 0.2. Saget et al. (1995) and Bertrand-Krajewski et al. (1998) defined a first flush as occurring when at least 80% of the pollutant load is emitted in the first 30% of the runoff volume. Sansalone & Buchberger (1997) used a 20/80 first flush in their research as well as a 25/50 first flush definition. Kim et al. (2005) analysed the existence of the first flush as a function of site-specific variables as well as storm characteristics and classified two kind of first flushes. Kim et al. (2005) used two kinds of flush criteria; the “high” first flush and “medium” first flush, as 50% of the mass in the first 30% of the volume, and 30 to 50% in the first 30% volume. The difficulty of a first flush identification was also shown by Deletic (1998). In this research the first flush values were calculated as the total load of pollutant transported by the first 20% of runoff.

The generalisation of the median pollutant mass distribution vs. volume curves of Geiger (1984) and the transposition of this curve to other sites have, in fact, different characteristics. This definition after Geiger (1984) has sometimes led to inadequate or wrongly designed detention facilities (Bertrand-Krajewski et al., 1998).

Dorfer (2005) analysed 45 storms in terms of normalised pollutant mass distribution vs. volume curves on the basis of the improved company PLS regression for Graz-West CSO. Unfortunately, these analyses are not based on corrected flow data. However, an in-depth analysis showed that the influence of flow is minor due to the normalised mass and volume. The major influence is from concentration measurements (Figure 5-2 and Figure 5-3). Dorfer (2005) could not identify a first flush after the 30/80 first flush definition. Bertrand-Krajewski’s (1998) definition is a very restrictive one. The Graz-West catchment is a too large to identify extreme first flushes; the 30/80 definition will be kept by distinct first flushes which occur in small catchments.

Figure 5-2 shows the results of COD_{tot} for normalised cumulative mass emission plotted against normalised cumulative volume, so-called M(V)-diagram for the 9th of September 2003. The scattering range can be clearly seen in these curves based on different regression. All the curves are above the bisector and therefore fulfil the definition of the first flush above the bisector. The 80/30 flush can not be identified. Analyses after Geiger's definition reproduce interesting results. Different results occur depending on the regression method used. Geiger (1984) defined the first flush as the gap between mass-volume curve and the bisector greater than 0.2. The improved company PLS regression used produces a very clear first flush with a maximum value of 0.253.

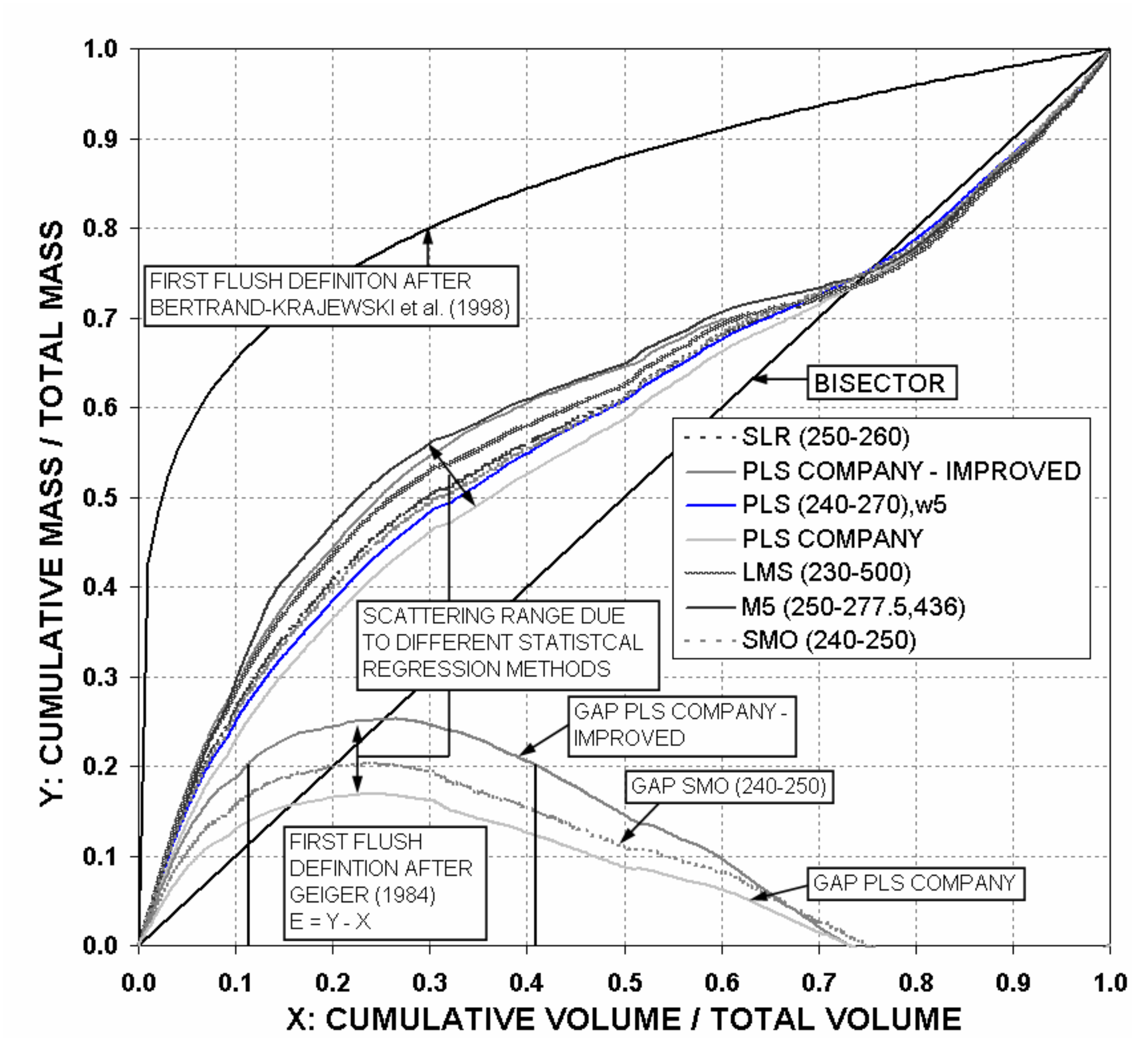

Figure 5-2 M(V) Diagram of COD_{tot} from the 9th of September 2003 Based on Different Regressions

On the basis of the SMO regression for the COD_{tot} parameter a flush of only 0.203 can be identified. The PLS regression, provided by the manufacturer, results in no first flush using Geiger's definition.

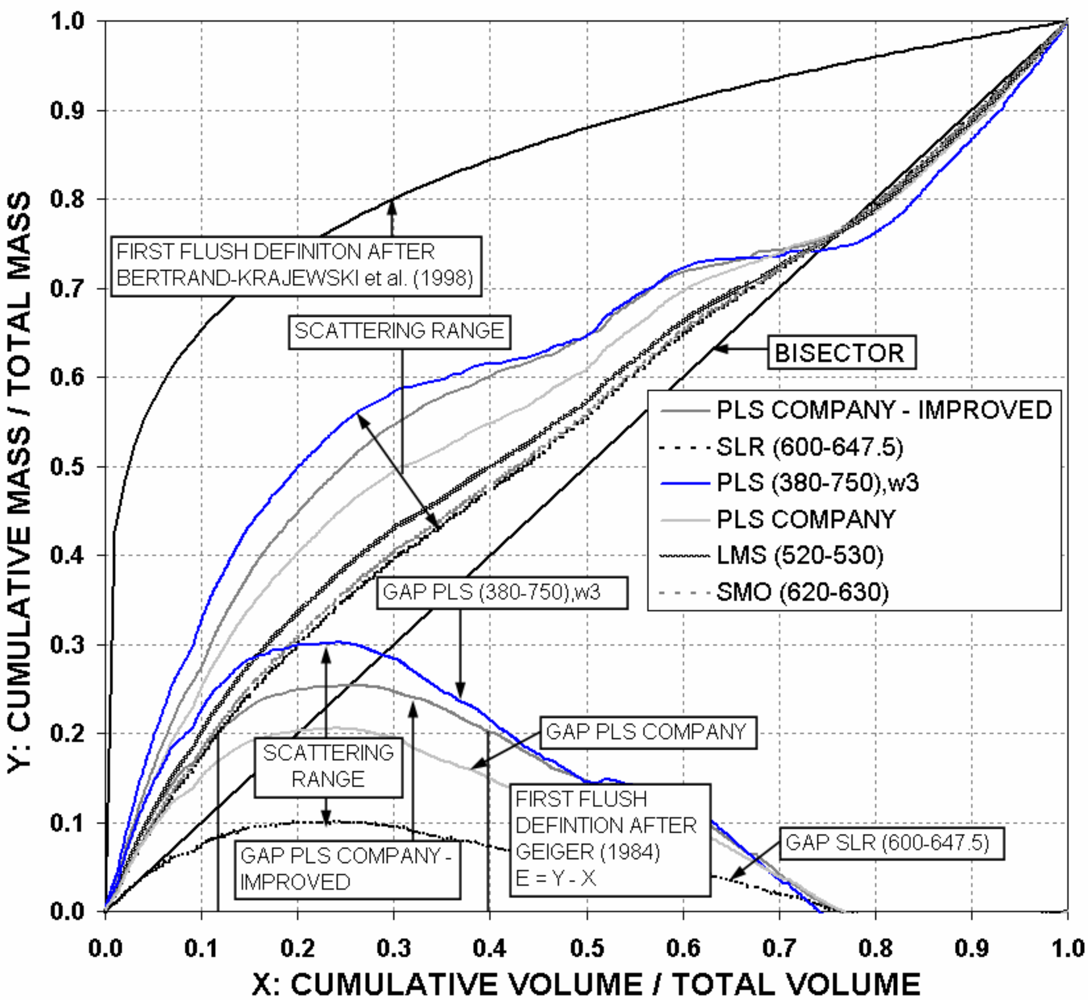

Figure 5-3 M(V) Diagram of TSS from the 9th of September 2003 Based on Different Regressions

The results of TSS (Figure 5-3) also demonstrate the concentration influence of first flush analyses. The scattering range of TSS for the different M(V) diagrams is larger than for COD_{tot}. A very large scattering range can be seen from the first flush curves using Geiger's definition. The gap curve based on PLS (380-750) regression results in an "extreme" first flush with a value of 0.302. The SLR gap curve does not result in a first flush using Geiger's definition with a value of 0.1. The two figures demonstrates the high influence of concentration measurements for M(V) diagrams.

5.1.2. DESCRIPTION OF QUALITY MODEL

The KOSIM hydrological quality modelling software was used in this thesis . Thus, a consideration of backwater or flow direction changing is not possible. The transport in the sewer system is calculated after Kalinin-Miljukov's approach. The rain flow pollution is determined on the basis of surface pollution potential and the rain weather and dry weather load components. Hence, the rain weather concentration is constant and no variation is considered. The following chapters will give a short description of the software approaches.

5.1.1.1. PRECIPITATION

Precipitation is a load parameter for urban drainage systems. Hence, the temporal and spatial rainfall distribution is of high importance. The high temporal precipitation change extremely influences transporting process in the sewer system. 5-minute discretised precipitation intervals were the rainfall input data for the simulation. Rainfall was considered as uniform over the whole catchment area. But applying a spatial rainfall model, the rainfall input can be improved and, consequently, the accuracy of model simulations can be increased (Willems, 1999). However, in KOSIM it is possible to assign every part-catchment its precipitation gauge when considering the spatial rainfall. Thus, a constant rainfall distribution for every part-catchment is possible. But this was not considered in this research due to inexistence of spatial precipitation data.

5.1.1.2. SURFACE RUNOFF MODEL

The runoff from unpaved areas is not considered, which is standard for quality modelling. The runoff approach of paved areas considers evaporation loss and depression storage. The approach is given by ATV (1986) using a temporal changing runoff coefficient and is also displayed in Figure 5-4.

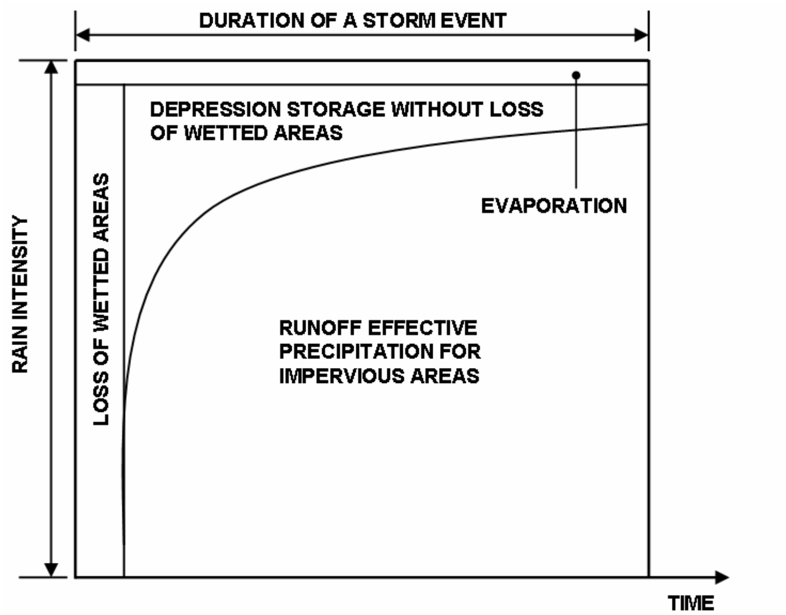

Figure 5-4 Overview of the Surface Runoff Model for Quality Modelling (ATV, 1986)

5.1.1.3. POLLUTION CONCENTRATION

The pollution concentration is calculated on the basis of unit hydrographs with regards to the runoff effective precipitation. Hence, a cascade of linear reservoir model is used to simulate lag and retention (ATV, 1987). The reservoir term is determined by means of surface runoff duration as well as the sewer travel time.

5.1.1.4. Flow Calculation in the Sewer System

The two parts of flow – dry weather and rain weather – are collected in the sewer system and simultaneously superposed. The transport leads to a lag and an attenuation of the flow wave. However, at least the flow which is simulated has the same value as the runoff effective precipitation volume. The sum of inflow and discharge is equal. The calculation is based on the Kalinin-Miljukov-approach. Every sewer reach is simulated as a reservoir.

5.1.1.5. Surface Pollution

An accumulation and removal of surface deposits is not considered in the simulation. KOSIM is based on pollution surface potential and the resulting constant rain weather concentration. This leads to different surface load with different precipitation volume. Hence, an increasing effective runoff precipitation results in increasing pollution loads.

5.1.1.6. Load Transport and Pollution Concentration

A synchronic superposition of rain weather and dry weather load is calculated for every part of the catchment. The resulting storm load can be determined assuming a complete intermixture of rain and dry weather load. A conservative matter behaviour and no biological removal is considered. The remobilisation of deposits is also not included in the simulation model.

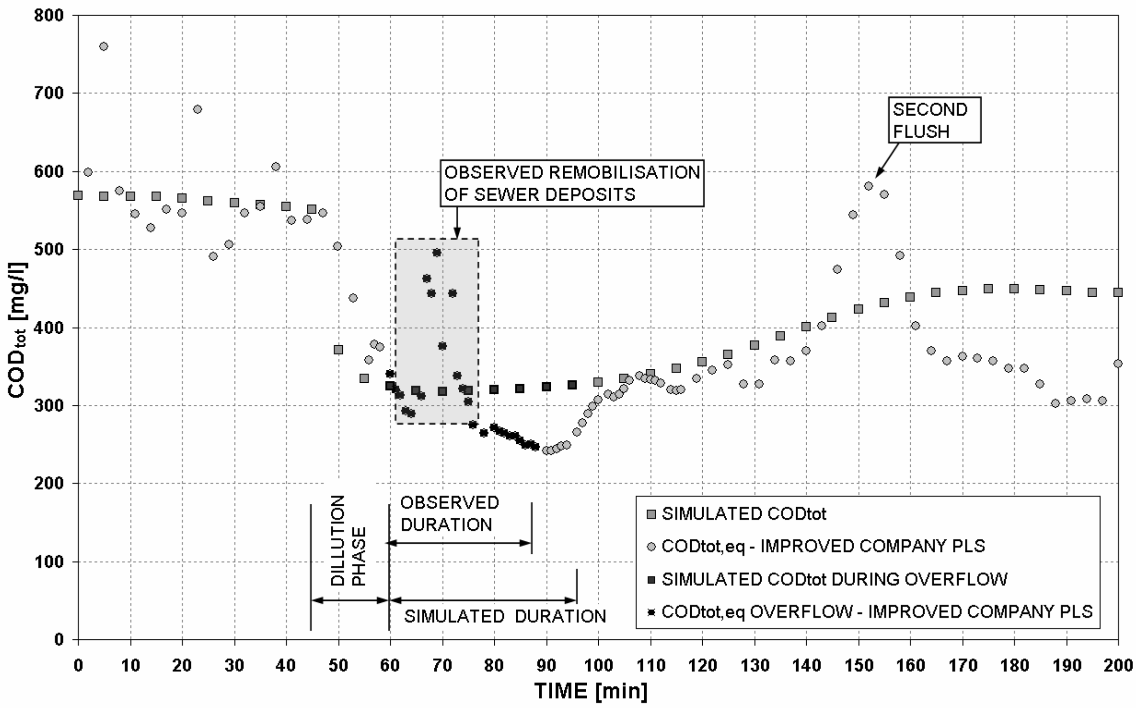

Figure 5-5 Impossible Flush Simulation of Quality Model vs. Measured $COD_{tot,eq}$ Concentrations Based on Improved PLS Regression – 16th June 2003

Figure 5-5 demonstrates the weakness of the quality model. For the example of the 16th of June 2003, a mean rain weather concentration of 310 m/l and the dry weather data based on the improved PLS regression of the company were used The model can not reproduce the real concentration behaviour due to sewer sediment remobilisation. Hence, a first flush can never be exactly simulated.

5.1.3. MODEL CALIBRATION

The input data for model calibration are the improved values described in chapter 3 and 4. Thus, corrected precipitation data, corrected flow data and 24-hour flow dry weather curves and pollution curves were used. A seasonal behaviour of flow and pollution was not considered.

On the basis of the mean dry weather flow curve described in chapter 3.7.1, relative dry weather curves of weekdays and weekends were produced. These relative curves are used in the simulation programme for a daily and weekly flow behaviour consideration (Figure 5-6). This relative dry weather curve creation was also made for the pollution parameters.

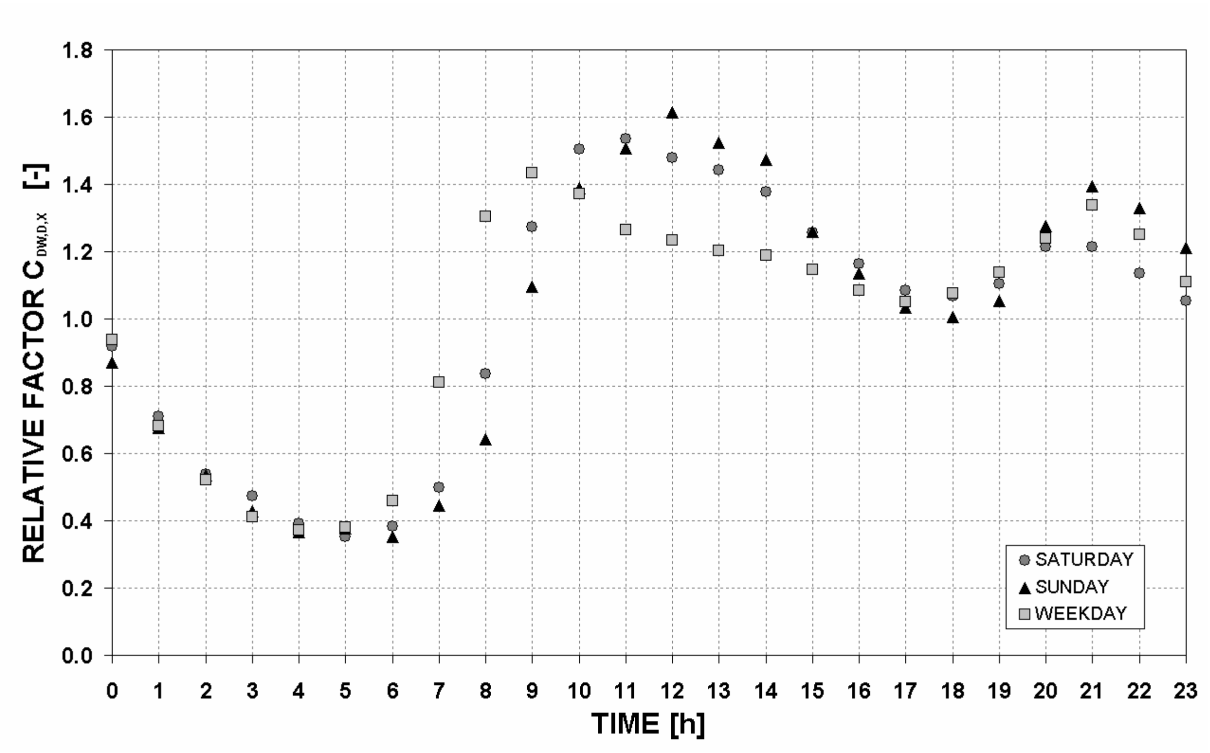

Figure 5-6 Generated Relative Dry Weather Flow Curves (modified after Haring, 2004)

The Graz-West CSO has a quite short throttle length of about 3 m and a throttle diameter of 600 mm and leads into the right Graz main sewer collector. The "challenge" of this CSO is the curved weir which could not be reproduced in a satisfactory way by the simulation program. All trials to simulate the CSO overflow by means with the CSO geometry failed. Therefore the second possibility with a characteristic inflow-overflow curve was used. This curve defines the critical inflow when the overflow starts and then value pairs of inflow and overflow. This determination for the “best” fitting inflow-overflow curve was an iterative process. The first analysis of measured inflow and overflow values resulted in the 1st trial inflow-overflow curve (see Figure 5-7). This curve can be formulated with a fifth power function. Unfortunately, this curve did not result in reliable simulation results. Therefore a new inflow-overflow approximation was made resulting in the 2nd trial curve displayed in Figure 5-7 and can be written as:

$$\mathrm{OVERFLOW} = 0.0004 \cdot \mathrm{INFLOW}^2 - 0.2742 \cdot \mathrm{INFLOW} - 30$$

Even this equation does not give the real flow behaviour as exactly as the 1st trial curve. The second simulation was “better”: to be more exact, closer to the measured values. Thus, the overflow volumes and loads can be better reproduced.

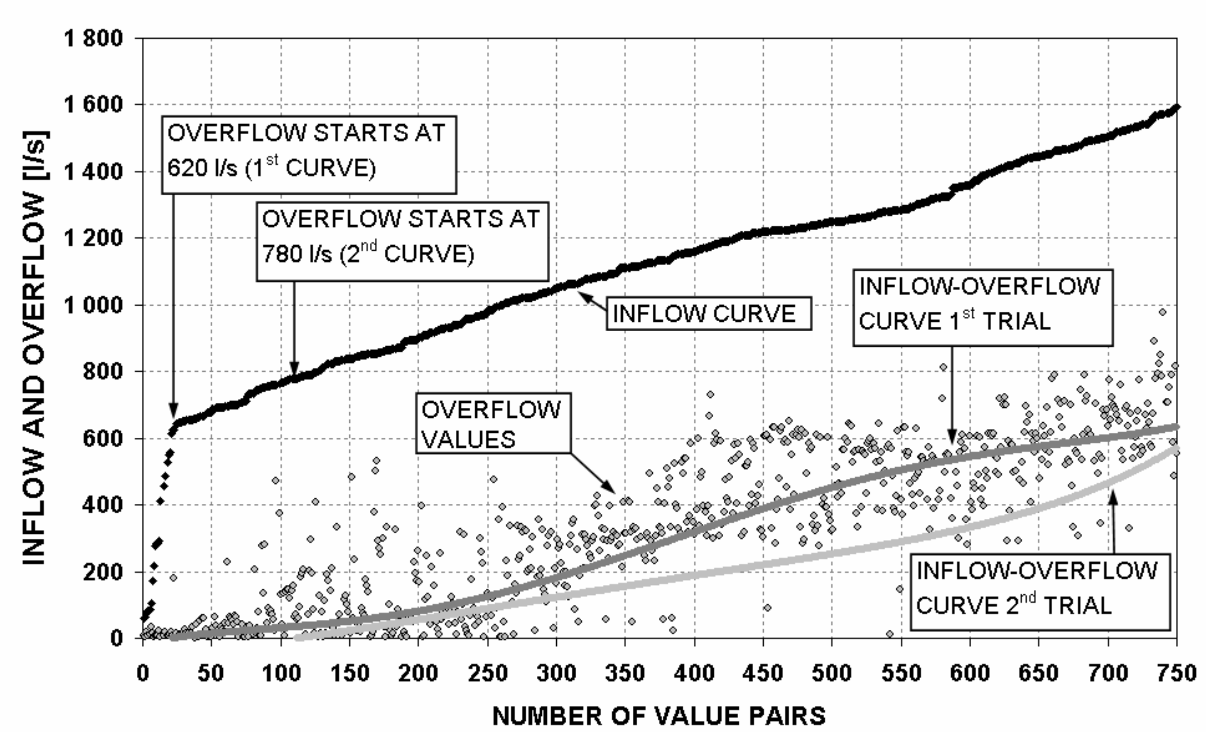

Figure 5-7 Determination of the Inflow-Overflow Curve for Quality Modelling Programme (modified after Haring, 2004)

14 overflow events were used to get the right “set up” to calibrate the quality model. The results of this calibration are presented in Table 5-1 and were carried out for flow and COD_{tot} and TSS parameter.

First the inflow and then the inflow rain weather (RW), inflow dry weather (DW) and storm weather (SW) volume were calibrated. It was possible to achieve results with minor differences between measured and simulated volumes. The pollution parameters also resulted in small differences of, at most -6.8% for COD_{tot} rain weather volume and -7.7% for TSS dry weather volume. The overflow volume and loads were also calibrated which resulted for the volume of 3.2%, for COD_{tot} overflow load in 10.3% and for TSS overflow load in 2.5%. This calibration seems to be in a satisfactory range.

Table 5-1 Calibration Results of Quality Modelling

		Volume			COD_{tot}*)			TSS**)		
		Measured	Model	Diff.	Measured	Model	Diff.	Measured	Model	Diff.
		[10³·m³]	[10³·m³]	[%]	[10³·kg]	[10³·kg]	[%]	[10³·kg]	[10³·kg]	[%]
Inflow	RW Volume or Load	134.0	133.9	-0.1	44.5	41.5	-6.8	26.8	26.1	-2.6
	DW Volume or Load	432.3	444.3	2.8	306.0	302.2	-1.3	146.9	135.5	-7.7
	SW Volume or Load	566.4	578.2	2.1	350.5	343.7	-2.0	173.7	161.6	-7.0
Overflow	Overflow Events	16	19	-	16	19	-	16	19	-
	Used Overflow Events for Model Calibration	14	14	-	14	14	-	14	14	-
	Overflow Duration [min]	932	885	-5.0	932	885	-5.0	932	885	-5.0
	Overflow Volume or Overflow Load	23.8	24.6	3.2	7.1	7.9	10.3	4.8	4.9	2.5

*) Based on a mean rain weather concentration of 285 mg/l and on a dry weather concentration of 682 mg/l
**) Based on a mean rain weather concentration of 195 mg/l and on a dry weather concentration of 304 mg/l

5.1.4. Model Validation of a Single Overflow Event

A validation was also undertaken for single storm events. The next figures present the results of the storm event from 16th of June 2003. A possible existing time shift between measurements and simulation was corrected for a better curve comparison.

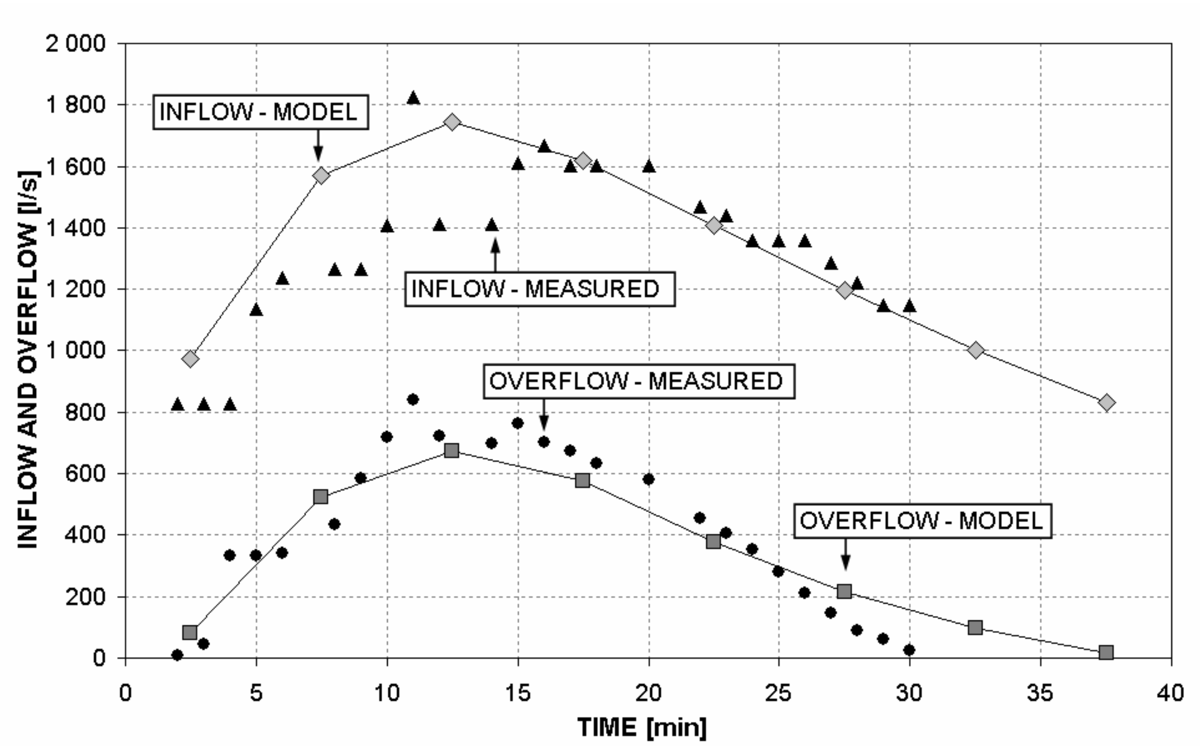

Figure 5-8 Inflow and Overflow Curves of the Overflow Event from 16th June 2003

The overflow event from 16th of June 2003 is an example of rather good reproducibility of a single storm event. The start of the overflow event was simulated 71 minutes too early, but the difference of the overflow duration resulted only in 7 minutes. The overflow volume was simulated in a value 2% too high compared with the measurements. The difference of overflow load was higher; for COD_{tot} it equals in a difference of -12% and -27% for TSS.

Figure 5-8 presents the compared results of measured and simulated inflow and overflow curves. The inflow as well as the overflow could be reproduced accurately with the simulation. Other events with longer duration resulted in worse simulation results.

Figure 5-9 displays the TSS concentration curves. Before the overflow, the dilution phase can be clearly seen which is caused by the starting of the storm event. It is also possible to model this dilution effect with the used quality model program. This could also be recognised with other storms.

The flush effect (Figure 5-9) can not be modelled with a quality model program. The program results in a “blurred” concentration. The following conclusion can be made, assuming an accurate reproducibility of inflow and overflow by the quality model (which often does not hold in practice). The inflow and overflow load curve is the result of concentration and flow curve multiplication. Hence, during short overflow events after the “first flush” this result in underestimation. Long overflow events result in overestimation. The decreasing of the load curves after rain event start can also be seen in Figure 5-10. The results of simulated load curves are in an acceptable range.

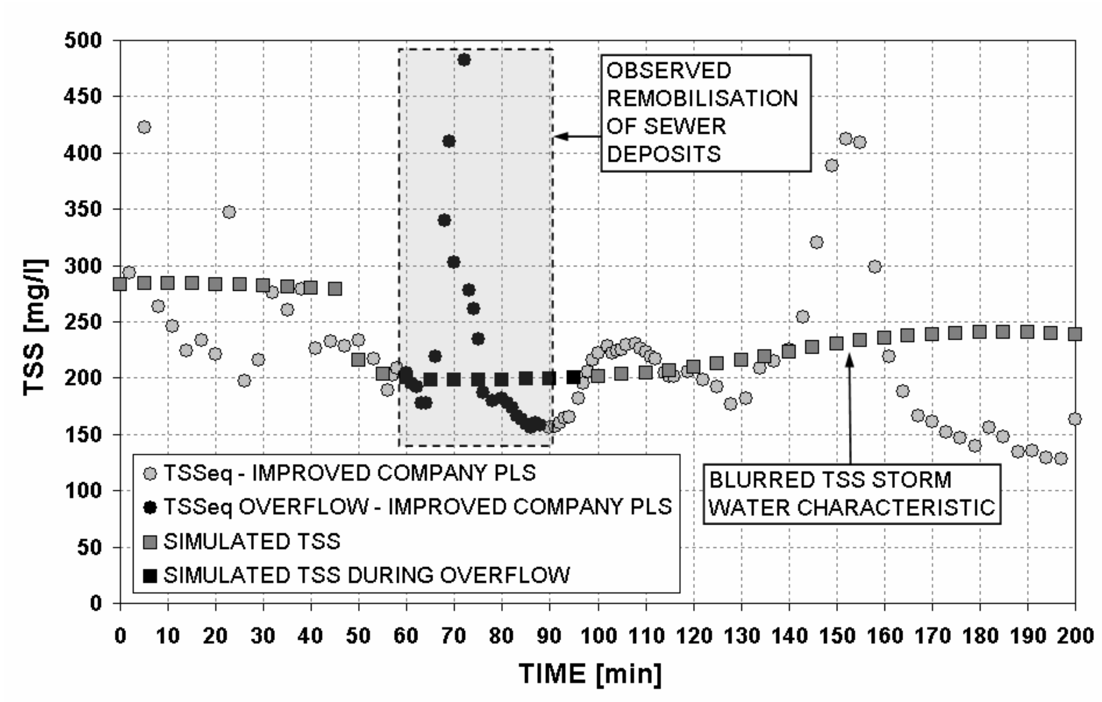

Figure 5-9 TSS Measured and Simulated Concentrations Curves of 16th June 2003

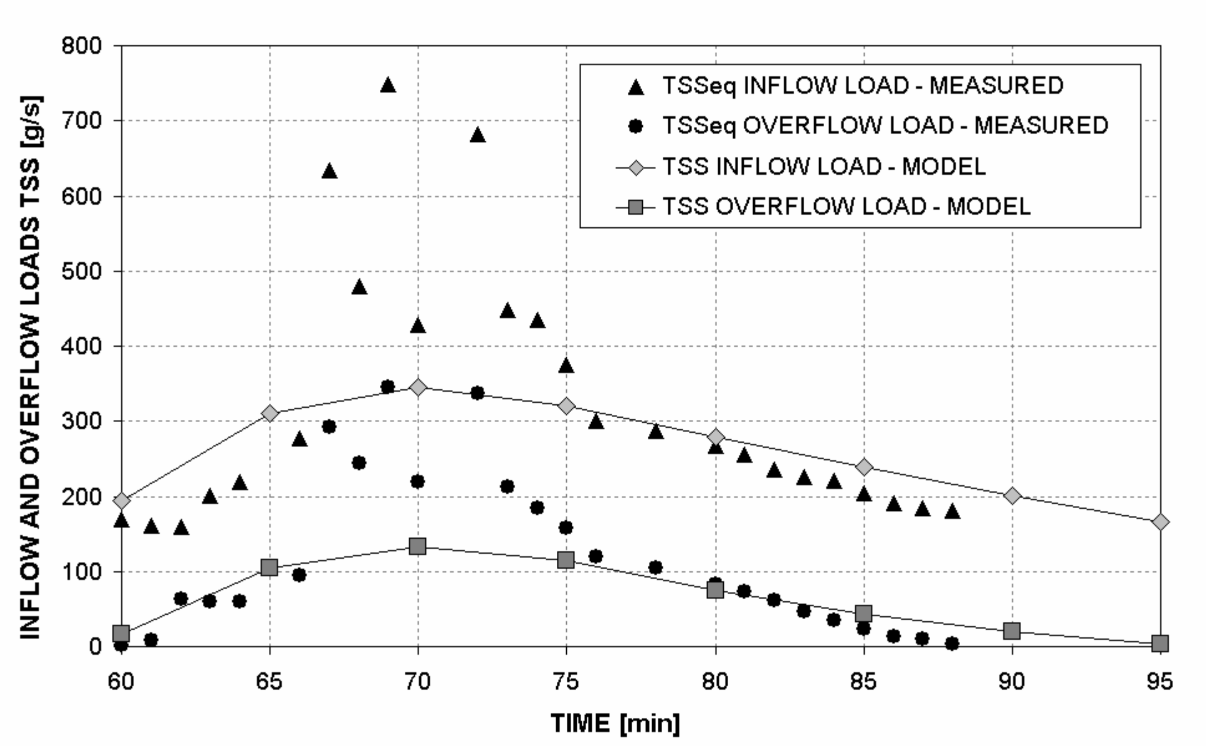

Figure 5-10 TSS Inflow and Overflow Load Curves of 16th June 2003

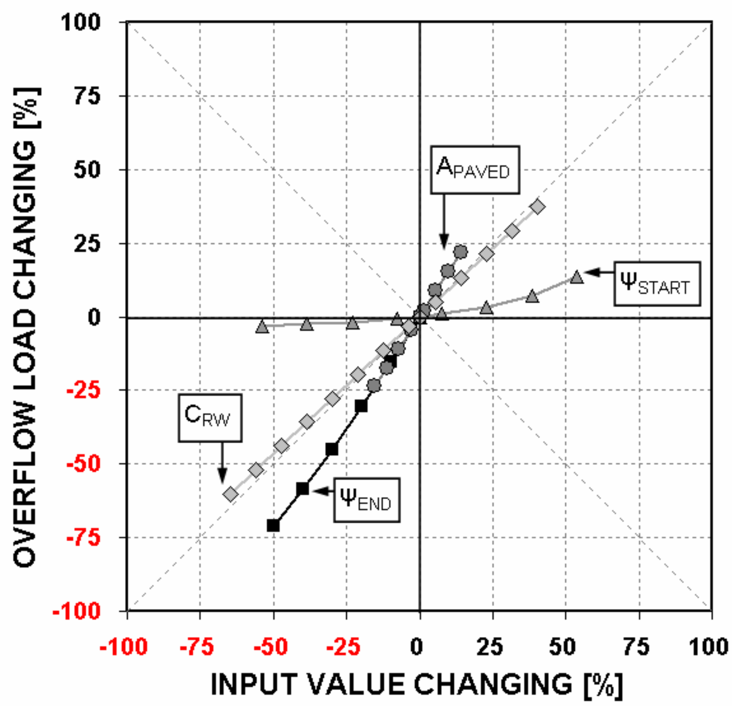

Figure 5-11 Results of a Relative Sensitive Analysis for Graz-West CSO – Overflow Pollution Load Changing vs. Input Parameter Value Changing Diagram

The paved area, the runoff coefficient and the mean rain weather concentrations have the most influence on the results of overflow loads. These results are confirmed by means of a relative sensitive analysis for Graz-West CSO. Only one input parameter was changed and the resulting overflow loads compared. Hence, the major influence parameter could be detected. The results are displayed in Figure 5-11. The runoff coefficient is expressed in two different runoff coefficients, the runoff coefficient at a beginning of a storm and the runoff coefficient at the end. The paved area as well as the runoff coefficient and the end of a storm influence the overflow load results disproportionately. The rain weather concentration has a linear influence on the results. Other input parameters like depression storage, dry weather concentrations or mean daily flow have only a minor influence on the simulated overflow results.

5.1.5. LONG-TERM SIMULATION

The basis for the long-term simulation is the calibrated model of chapter 5.1.3. It was not possible to calculate with data from Klusemanngasse tipping bucket gauge due to the existence of only three years of precipitation data. Hence, the precipitation from TU Graz tipping bucket gauge was used and therefore a 9 year long-term simulation was carried out. This gauge is located about 2 km from the Graz-West CSO and the spatial rainfall is certainly a little bit different. The TU Graz tipping bucket gauge has been measuring data since 1983, but due to data loss, only nine years (1996-2004) are accurate and reliable. Generally, a long-term simulation of 10 years is recommended.

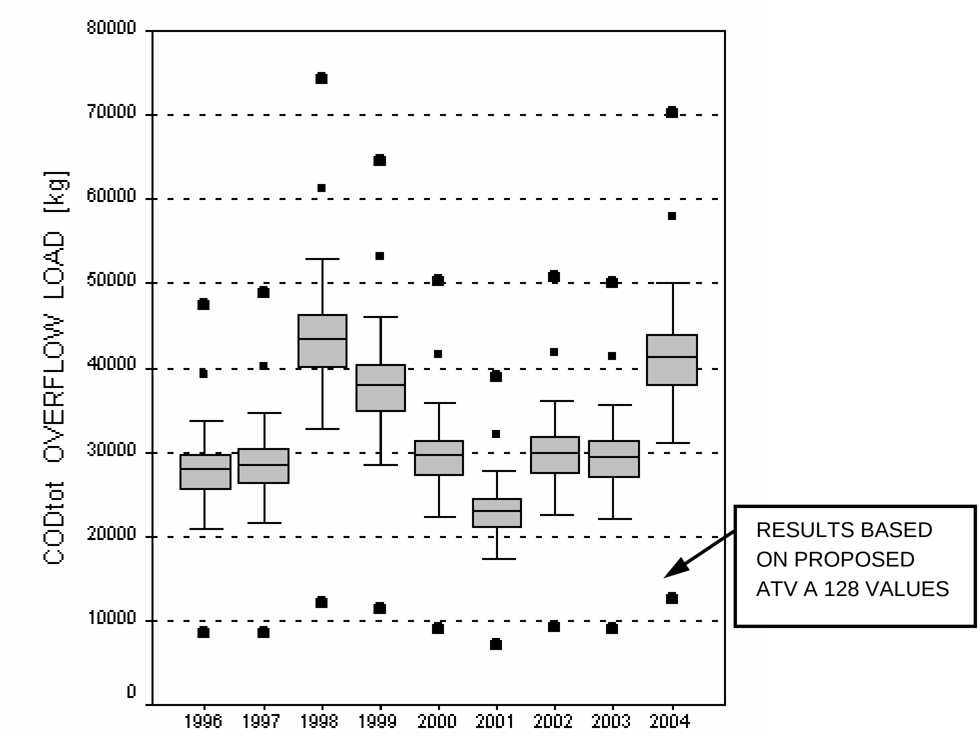

Figure 5-12 COD_{tot} Overflow Loads of Long-Term Simulation

The COD_{tot} overflow loads from the long-term simulation are displayed in Figure 5-12. The results are presented in box-plot format. The grey box shows the lower and upper quartile of all results. The lines indicate the minimum and maximum values.

The small dots are extreme result values, the big dots are outliers. The results are based on the proposed input values for rain weather (107 mg/l) and dry weather concentrations (600 mg/l) of the ATV A 128 German standard which also can be seen in the figure. Hence, the other results, which are based on different regression methods, are about three to four times higher than the A 128 results. This evidences the necessity of measurements for the input data of quality modelling. Of course, it is difficult to calculate and forecast and exact value. Only a result range can give a serious conclusion. The other outlier, which provides values that are too high, is the result based on PLS regression from the manufacturer. The indicated extreme values result from the PLS (240-270, 5 used wavelengths) regression. A coherence between annual spilled overflow loads and the annual precipitation depth could not be found.

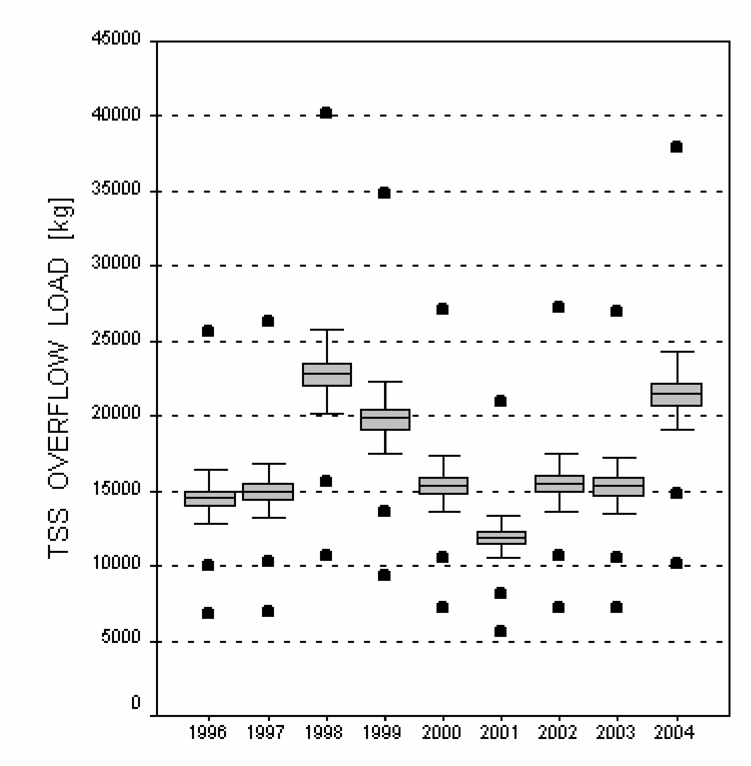

Figure 5-13 TSS Overflow Loads of Long-Term Simulation

The results of TSS over loads from the long-term simulation are plotted in Figure 5-13. The format is the same as for the COD_{tot} figure. The scattering range of the results is lower than of COD_{tot} which also depends on the lower input concentration values of TSS. Three regression methods are identified as outliers. These are PLS regression (550-600, 3 used wavelengths) with the lowest resulting overflow load values, PLS (550-600, 2 used wavelengths) and the PLS regression (380-750, 3 used wavelengths) with the highest result values. The PLS regression provided by the manufacturer achieves accurate and reliable results for TSS. The results also evidences the accurateness of simple models like SLR for the TSS parameter. All results for COD_{tot} and TSS are presented in tables A-73 to A-77 in the appendix.

6. CONCLUSION

The assessment of the combined sewer overflow emissions was the main aim of this thesis under consideration of measurement errors and its corrections. The behaviour of different pollution concentrations and flows in combined sewer systems during a storm are complex. Measurements data provide knowledge about these processes, but great efforts often have to be made to achieve reliable and accurate measurements values. The difficulty in sewer monitoring is the high variability of the flow and concentrations. Therefore, the detection of the influence and scattering range on calculated or simulated overflow loads by means of the different regression methods was also be analysed. The results of this thesis and its used methodology can be summarised as follows:

- Precipitation is a main input data for quality modelling. In this thesis the precipitation data are measured from a tipping bucket gauge and from a weighing gauge. The correction of tipping bucket gauge data for accurate precipitation input data in quality modelling is not absolutely necessary for long-term simulations, a comparison of a six month period resulted in difference of only about 4% for COD_{tot} on the basis of corrected and uncorrected tipping bucket gauge data. Modelling analysis demonstrated the higher influence of corrected and uncorrected precipitation data at storms with high intensities. A simulation of a single storm event resulted in a COD_{tot} overflow load differences of about 10% between corrected and uncorrected precipitation data, although, the differences of rain depth equalled about 18%. A correction of tipping bucket gauge data is recommended for short-term modelling.

- The inflow measurements are determined by means of a radar system. On the basis of a 24 hours measurement campaign with three different methods the radar system was validated. Due to a false area input a wrong dry weather flow measurement resulted in a difference of almost 100% of corrected and uncorrected flows. However, after the validation and the correction accurate and reliable flow data result which are further used for overflow load calculation and quality modelling.

- For absorbance measurement an UV/VIS spectrometer is used to achieve absorbance data and to calculate the equivalence concentration parameters by means of different regression methods. The company gives a default coherence equation between absorbance and concentrations which has to be adapted to the existing waste water properties. This can be done with an improvement of the default calibration by means of measurements. Therefore, three measurements campaigns were carried out to assess all kind of measurement errors and to achieve data for the default calibration improvement. The calibration provided by the company for the parameter TSS produces already accurate results. But this does not hold for the COD_{tot} and COD_{sol} parameter. The COD_{tot} parameter differences between the values by means of the default calibration and the lab values equals for the 2nd measurement campaign in a maximum value of about 60% and for the 3rd measurement campaign in a maximum value of about 50%. A cumulative frequency analysis resulted for COD_{tot} parameter in relative deviations of 33% by means of the default PLS calibration and in 14% relative deviations by means of the improved PLS calibration of the company at a cumulative frequency of 80%. The TSS parameter equals in 42.5% relative differences on basis of the default PLS calibration, which is provided by the company, for 80% cumulative frequency. Every trial to improve this calibration resulted in worse values, and therefore in higher relative differences.

- On the basis of five different regression methods (simple linear regression, least median squares regression, M5 model tree regression, support vector machine using sequential optimisation algorithm, partial least squares regression) absorbance concentration equations (local calibration) for the Graz-West combined sewer overflow were developed for the parameters COD_{tot}, COD_{sol} and TSS. A multi-stage validation process was carried out to guarantee accurate and reliable regression equations. With this validation process poor and accurate regression equations were determined and verified. Complex regression methods (partial least squares regression) deliver mostly accurate equations; but complex models are susceptible for model overfitting. The COD_{sol} parameter could be reproduced with all kind of regressions insufficient. For TSS parameter a very simple model is sufficient to deliver accurate concentration values.

- The mean rain weather concentration, which is an important input parameter in quality modelling, was also analysed and compared with other research projects. The results of Macke et al. (2002) were circumstantiated for steep sewer systems in this research work. The mean COD_{tot} rain weather concentrations of 223 to 444 mg/l are two-times to four-times higher than the value after the ATV A 128 German standard with 107 mg/l. This value influences linear the overflow load results. In quality modelling, meaning, for example, a three-times higher mean rain weather concentration also results in three-time higher overflow loads. However, the value given in the standard seems to be for this research catchment too low.

- The load calculation which is based on the different linear regression methods also shows a high scattering range. The COD_{tot} parameter results for the annual overflow load of 2003 in a difference between the minimum and the maximum value of 39%. For the total $CODt_{ot}$ load, which was calculated for the duration from September 2002 to August 2004, also a high scattering range can be recognised, resulting in a difference between minimum and maximum loads of 40%. The total TSS load equals for the same duration in a difference between minimum and maximum value of 27%.

- The quality model was calibrated on 14 overflow events and resulted in a difference between measured and simulated overflows of 3% for all overflows together. The differences between measured and simulated values equal for COD_{tot} loads in 10% and for TSS in 2.5%. The scattering range of long-term simulation on the basis of the different regression methods, used for concentration calculation, resulted in a deviation of 38% for COD_{tot} and 22% for TSS. Although the correlation between absorbance and concentration is only a very small link in the input data of quality modelling, absorbance concentration coherences have a major influence on overflow load results.

- The first flush analysis demonstrated the influence of the different regressions used for the first flush analysis. The calculation of the first flush after Geiger's (1984) definition extremely pointed out the scattering range depending on different regressions.

6.1. OUTLOOK AND FUTURE RESEARCH

To further improve the CSO Graz-West monitoring station an automatic or semi-automatic detection and validation of recorded data should be implemented in the process unit. Mourrad & Bertrand Krajewski (2002) and Thomann (2004) give possible solutions regarding how to manage data checks. These two researches can be basis for the implementation of data checking in Graz. The verification of the overflow device has not been evaluated up to now. Even when the measurement data seem to be reliable and accurate a validation measurement has to be carried out. Of course, this requirement seems to be almost impossible to fulfil due to the extremely dangerous situation during a storm in the CSO chamber. Most of the regression methods produced satisfactory results, but the M5 model tree regression in particular can determine better results and also detect and divide functions considered on sewer process behaviour (dry weather, wet weather, night with higher groundwater infiltration rate). Two to three more campaigns should result in even more accurate regression equations of M5 model tree regression. Additionally, data during a storm are needed; these kinds of measurements have been under represented up to now. Finally, the absorbance-concentration coherence, for example for dry weather and wet weather, can be implemented. The results of this thesis are based on 3 years measurement data, but this period seems to be too short for a detail statistical analysis. Therefore, the monitoring station should be operated further to achieve data for future statistical analysis.

The integrated view of the whole urban drainage system (sewer system, WWTP and receiving water) or integrated modelling is only realisable when the model can be calibrated by accurate measuring data. This thesis delivers these values from the sewer system, and therefore, can also be implemented in a future possible integrated model.

The results of this thesis are also base knowledge for future sewer real time control with pollution reduction aim. However, this only can be carried by means of accurate sewer measurements and a combination of quality and quantity model.

REFERENCES

Aalderink, R.H. & Lijklema, L. (1985): Water quality effects in surface waters receiving stormwater discharges, *Water in Urban Areas*, TNO Committee on Hydrological Research, Proceedings and Information No. 33, pp. 143 – 159.

Abdi, H. (2003): Partial Least Squares (PLS) Regression, in: *Encyclopaedia of Social Sciences Research Methods*, Lewis-Beck, M.; Bryman, A.; Futing, T. (Eds.), Sage Publications, Thousand Oaks, California, USA.

Adams, B.J. & Papa, F. (2000): Urban Stormwater Management Planning with Analytical Probabilistic Models, Jon Wiley & Sons, Inc., New York, USA, ISBN 0-471-33217-9.

Arnbjerg-Nielsen, K.; Madsen, H. & Harremoës, P. (1998): Formulating and Testing a Rain Series Generator Based on Tipping Bucket Gauges, *Water Science and Technology*, Vol. 37, No. 11, pp. 47 – 55.

ATV (1986): Die Berechnung des Oberflächenabflusses in Kanalnetzmodellen – Teil I – Abflussbildung, in German, Report of the ATV-Arbeitsgruppe 1.2.6. „Hydrologie der Stadtentwässerung“ gemeinsam mit dem DVWK, *Korrespondenz Abwasser*, No. 2, pp. 157 – 162.

ATV-DVWK-A 110E (2001): Hydraulic Dimensioning and Performance Verification of Sewers, German Standard, St. Augustin, Germany.

ATV-DVWK-A 128E (1992): Dimensioning and Design of Stormwater Structures in Combined Sewer, German Standard, St. Augustin, Germany.

ATV-DVWK-A 131E (2000): Dimensioning of Single-Stage Activated Sludge Plants, German Standard, St. Augustin, Germany.

Bastien, P.; Vinzi, V.E.; Tenenhaus, M. (2005): PLS generalised linear regression, *Computational Statistics & Data Analysis*, Vol. 48, pp. 17 – 46.

Barraud, S.; Gibert, J.; Winiarski, T. & Bertrand-Krajewski, J.-L. (2001): Impact of a storm infiltration drainage system on soil and groundwater: Presentation of the OTHU project; *Proceedings of INTERUBA II,* 19 – 22 February 2001, Lisbon, Portugal.

Baurés, E. Berho, C.; Pouet, M.F. & Thomas O. (2004): In situ UV monitoring of wastewater: a response to sample aging, *Water Science and Technology*, Vol. 49, No. 1, pp. 47 – 52.

Bertrand-Krajewski, J.-L.; Chebbo, G. & Saget, A. (1998): Distribution of pollutant mass vs. volume in stormwater discharges and the first flush phenomenon, *Water Research*, Vol. 32, pp. 2341 - 2356.

Bertrand-Krajewski, J.-L.; Laplace, D.; Joannis, C. & Chebbo, G. (2000a) : Mesures en hydrologie urbaine et assainissement, in French, Tec et Doc Edition, Paris, France, ISBN 2-7430-0380-4.

Bertrand-Krajewski, J.-L.; Barraud, S. & Chocat, B. (2000b): La mesure de l'impact environnemental des systèmes d'assainissement: exemple de l'Observatoire de Terrain en Hydrologie Urbaine (OTHU), in French, *Actes du 3° Congrès Universitaire de Génie Civil AUGC*, pp. 35 – 42, 27 – 28 June 2000, Lyon, France.

BMLFUW (2001) : Verordnung des Bundesministers für Land- und Forstwirtschaft, Umwelt und Wasserwirtschaft über die Begrenzung von Emissionen aus Mischwasserentlastungen in Mischkanalisationen (AEV Mischwasser), in German, Regulation Draft for CSO Emissions Federal Ministry for Agriculture, Forestry, Environment and Water Management, March 2001, CELEX-No.: 376L0464, 391L0271.

Boser, B. ; Guyon, I.M. ; Vapnik, V.N. (1992): A Training Algorithm for Optimal Margin Classifiers, Proceedings of Fifth Annual Workshop on Computational Learning Theory, pp. 144 – 152, Pittsburgh, ACM, USA.

Butler, D. & Davies, J.W. (2000): Urban Drainage, E & FN Spon publishing, London, United Kingdom, ISBN 0-419-22340-1.

Brezonik, P.L & Stadelmann T.H. (2002): Analysis and predictive models of stormwater runoff volumes, loads and pollutant concentrations from watersheds in the Twin Cities metropolitan area, Minnesota, USA, *Water Research*, Vol. 36, pp. 1743 – 1757.

Brown, M.; Gunn, S.R.; Lewis, H.G. (1999): Support vector machines for optimal classification and spectral unmixing, *Ecological Modelling*, Vol. 120, pp. 167 – 179.

Cabtree. R.W.; Ashley, R. & Gent, R. (1995): Mousetrap: Modelling of real sewer sediment characteristics and attached pollutants, *Water Science and Technology*, Vol. 31, No. 7, pp. 43 – 50.

Chebbo, G.; Gromaire, M.C.; Ahyerre, M. & Granaud, S. (2001): Production and transport of urban wet weather pollution in combined sewer systems: the "Marais" experimental urban catchment in Paris, *Urban Water*, Vol. 3, pp. 3 – 15.

Chebbo. G. & Gromaire, M.C. (2004): The experimental urban catchment "Le Marais" in Paris: what lessons can be learned from it?, *Journal of Hydrology*, Vol. 299, pp. 312 – 323.

Daniel, M.; Janicki, M.; Wroblewski, W.; Dybko, A.; Brzozka, Z. & Napieralski, A. (2004): Ion selective transistor modelling for behavioural simulations, Proceedings of 2nd International IWA Conference on Automation in Water Quality Monitoring, pp. 37 – 44, 19 – 20 April 2004, Vienna, Austria.

Deletic, A. (1998): The First Flush Load of Urban Surface Runoff, *Water Research*, Vol. 32, No. 8, pp. 2462 – 2470.

Dorfer, C. (2005): Transportvorgänge in Mischwasserkanälen auf Basis von Online-Messungen, in German (Transportation Proccesses in Combined Sewer Systems Based on On-Line Measurements), Diploma Thesis, Institute of Urban Water Management and Landscape Water Engineering, University of Technology Graz.

Eichler, H.J.; Gobrecht, H.; Hahn, D.; Niedrig, H.; Richter, M.; Schoenebeck, H.; Weber, H. & Weber, K. (1974): Bergmann-Schaefer – Lehrbuch der Experimentalphysik – Band III Optik, in German, Walter de Gruyter publishing, Berlin, Germany, ISBN 3-11-004366-1.

Emerson, K.; Russo. R.C.; Lund, R.E. & Thurston, R.V. (1975): Aqueous ammonia equilibrium calculations: Effect of pH and temperature, *Journal of the Fisheries Research Board of Canada*, Vol. 32, pp. 2379 – 2383.

Erbe, V. & Schütze M. (2004): An integrated modelling concept for immission-based management of sewer system, WWTP and river, *Proceedings of 6th International Conference on Urban Drainage Modelling – UDM '04*, 15 – 17 September, Dresden, Germany.

EU (2000) Directive 2000/60/EC of the European Parliament and of the Council of 23 October 2000 Establishing a Framework for Community Action in the Field of Water Policy, Official Journal of the European Communities, L 327.

Fankhauser, R. (1998): Influence of systematic errors from tipping bucket rain gauges on recorded rainfall data, *Water Science and Technology*, Vol. 37, No. 11, pp. 121 – 129.

Felder, A. & Siedschlag, S. (2004): Fließgeschwindigkeitserfassung an Flüssen mit dem Radarsensor Kalesto, in German, *Proceedings of the workshop „Neue Entwicklungen in der Durchflussmessung in natürlichen und künstlichen Gerinnen",* 11 – 12 March 2004, Munich, Germany.

Fenz, R. & Nowak, O. (1998): Wechselwirkung zwischen Kanal, Kläranlage und Gewässer bei Regenwetter, in German, *Wiener Mitteilungen*, Vol. 145, pp. 1 – 44.

Fenz, R. (1999): Gewässerschutz bei Entlastungsbauwerken der Mischkanalisation - Ein Beitrag zur Verknüpfung von Emissions- und Immissionsanforderungen, PhD Thesis, Institute for Water Quality, Resources and Waste, Management, University of Technology Vienna.

Fenz, R. & Rauch, W. (2004): Ermittlung von Bemessungsgrundlagen für Mischwasserentlastungen, in German, *Wiener Mitteilungen*, Vol. 187, pp. 409 – 424.

FWR (1998): A planning guide for the management of urban wastewater discharges during wet weather, *Urban Pollution Management Manual (UPM)*, Foundation for Water Research, 2nd Edition, FR/CL0009, Marlow, United Kingdom.

Gammeter, S. & Krejci, V. (1998): Auswirkungen von Mischwassereinleitungen auf den Stoffhaushalt und die Biozönose von Fließgewässern: Fallbeispiel Luppmen und Rohrbach, Schweiz, in German, *GWF Wasser-Abwasser*, Vol. 139, No. 6, pp. 343 – 348.

Geladi, P.; Kowalski, B.R. (1986): Partial Least-Squares Regression: A Tutorial, *Analytica Chimica Acta*, Vol. 185, pp. 1 – 17.

Geiger, W.F. (1984): Mischwasserabfluss und dessen Beschaffenheit – ein Beitrag zur Kanalnetzplanung, in German, *Berichte aus Wassergütewirtschaft und Gesundheitsingenieurwesen*, Vol. 50, TU Munich.

Gromaire, M.C.; Garnaud, S.; Ahyerre, M. & Ghebbo, G. (2000): The quality of street cleaning waters: comparison with dry and wet weather flows in a Parisian combined sewer system, *Urban Water*, Vol. 2, pp. 39 – 46.

Gruber, G.; Pressl, A.; Winkler, S. & M. Ecker (2003): Innovative Messtechnik in der Wasserwirtschaft, Quantifizierung von Schmutzfrachten im Bereich von Mischwasserentlastungen in Österreich, in German (Quantification of Pollution Loads at CSOs in Austria), *Wiener Mitteilungen*, Vol. 182, pp. R1 – R14.

Gruber, G.; Winkler, S. & Pressl, A. (2004a): Quantification of pollution loads from CSO´s into surface water bodies by means of online techniques, *Proceedings of AutMoNet – 2nd International IWA Conference on Automation in Water Quality Monitoring*, Vienna, 19. – 20. April 2004, Austria.

Gruber, G; Fuchs, R.; Gerhold, H.; Stojanovic, B. & Fischer-Colbrie, A. (2004b): Kanal-Messstation: Aufbau und Betriebserfahrungen, in German, ÖWAV-Conference „Innovative Technology for Integrated Water Quality Measurement", *Schriftenreihe zur Wasserwirtschaft*, University of Technology Graz. Vol. 42, E1-E28.

Gruber, G.; Hochedlinger, M.; Kainz, H.; Winkler, S. & Pressl A. (2005): Sewer online monitoring and quantification of pollution loads from combined sewer overflows, *Proceedings of 1st International Conference on Environmental Science and Technology*, New Orleans, 23. – 26. January 2005, USA.

Gujer, W. (2002): Siedlungswasserwirtschaft, Springer, Berlin, Germany, ISBN 3-540-43404-6, in German.

Gupta, K. & Saul, A.J. (1996): Specific Relationships for the First Flush Load in Combined Sewer Flows, *Water Research*, Vol. 30, No. 5, pp. 1244 – 1252.

Haas, G. (2005): Vergleich und Kalibration von unterschiedlichen Durchflussmessmethoden, in German (Comparison and Calibration of Different Discharge Measurement Methods), Diploma thesis, Institute of Urban Water Management and Landscape Water Engineering, University of Technology Graz.

Haring, P. (2004): Modellierung von Entlastungsfrachten an einem Mischwasserüberlaufbauwerk am Beispiel Graz-West, in German (Combined Sewer Overflow Emissions Modelling for the Sewer Catchment Area Graz-West), Diploma thesis, Institute of Urban Water Management and Landscape Water Engineering, University of Technology Graz.

Hauger, M.B.; Rauch, W.; Linde, J.J. & Mikkelsen, P.S. (2002): Cost benefit risk – a concept for management of integrated urban wastewater systems?, *Water Science and Technology*, Vol. 45, No. 3, pp. 185 – 193.

Haswell, S.J.; Walmsley, A.D. (1999): Chemometrics: the issues of measurement and modelling, *Analytica Chimica Acta*, Vol. 400, pp. 399 – 412.

Hochedlinger, M.; Sprung, W.: Gruber, G.; Wedenig, M. & Haring, P. (2004a): Ergebnisse des Kanal-Monitorings an einem Mischwasserüberlaufbauwerk in Graz und deren Anwendung bei Rechenmodellen, in German, ÖWAV-Conference „Innovative Technology for Integrated Water Quality Measurement", *Schriftenreihe zur Wasserwirtschaft*, University of Technology Graz. Vol. 42, K1 - K41.

Hochedlinger, M.; Gruber, G. & Kainz, H. (2004b): Variability of combined sewer overflow emissions measured by means of online techniques, *Proceedings of 4th International Symposium on Environmental Hydraulics and 14th Congress of Asia and Pacific Division, International Association of Hydraulic Engineering and Research*, pp. 1463 – 1469, 15 – 18 December 2004, Hong Kong, China.

Hochedlinger, M; Kainz, H. & Rauch, W. (2005a): Assessment of CSO Loads – Based on UV/VIS-Spectroscopy by Means of Different Regression Methods, accepted paper for *10th International Conference on Urban Drainage*, 21-26 August 2005, Copenhagen, Denmark.

Hochedlinger, M; Gruber, G. & Kainz, H. (2005b): Assessment of spill flow emission on the basis of measured precipitation and waste water data, *Atmospheric Research*, Article in Press.

House, M.; Ellis, J.; Herricks, E.; Hvitved-Jacobsen, T.; Seager, J.; Liklema, L.; Aalderink, R.H. & Clifforde, I. (1993): Urban drainage – impacts on receiving water quality, *Water Science and Technology*, Vol. 27, No. 12, pp. 117 – 158.

Huber, E. & Frost, M. (1998): Light scattering by small particles, *J Water SRT – Aqua*, Vol. 47, No. 2, pp. 87 – 94.

ITWH (2002): Kontinuierliche Simulation zur Bemessung von Speicherbauwerken in urbanen Entwässerungssystemen, in German, User Manual KOSIM 6.3, ITWH Institut für technisch-wissenschaftliche Hydrologie GmbH, Hannover, Germany.

Kim, L.-H.; Kahyanian, M. & Stenstrom, M.K. (2004): Event mean concentration and loading of litter from highways during storms, *Science of the Total Environment*, Vol. 330, pp. 101 – 113.

Kim, L.-H.; Kayhanian, M.; Zoh, K.-D. & Stenstrom, M.K. (2005): Modeling of highway stormwater runoff, *Science of the Total Environment*, Article in Press.

Kölling, C. (2000): SIMK – Kalibrierung von Durchflussmessanlagen – Durchflussmessung an Regenüberlaufbecken, in German, *ATV-DVWK Schriftenreihe*, Vol. 19, pp. 35 – 47, Hennef, Germany.

Kölling, C. (2004): SIMK - Calibration of Streamflow - Gauging Stations in Rivers and Canals, *Proceedings of Fifth International Conference IGHEM 2004 – "Innovation in Hydraulic Efficiency Measurement"*, 14 – 16 July, Lucerne, Switzerland.

Kompare B. (1995) The use of artificial intelligence in ecological modelling, PhD thesis, University of Ljubljana, FGG – Department of Hydroengineering, Institute of Sanitary Engineering, Ljubljana, Slovenia, ISBN 961-6167-05-7.

Krauth, K. (1970): Der Regenabfluss und seine Behandlung im Mischverfahren, in German, Stuttgarter Berichte zur Siedlungswasserwirtschaft, University of Stuttgart, Vol. 45.

Krebs, P; Holzer, P.; Huisman, J.L. & Rauch, W. (1999): First Flush of Dissolved Compounds, *Water Science and Technology*, Vol. 39, No. 9, pp. 55 – 62.

La Barbera, P.; Lanza, L.G. & Stagi, L. (2002): Tipping bucket mechanical errors and their influence on rainfall statistics and extremes, *Water Science and Technology*, Vol. 45, No. 2, pp. 1 – 9.

Langergraber, G.; Fleischmann, N. & Hofstädter, F. (2003): A multivariate calibration procedure for UV-VIS spectrometric quantification of organic matter and nitrate in wastewater, *Water Science and Technology*, Vol. 47, No. 2, pp. 63 – 71.

Langergraber, G. (2004): What to do with spectral data? or: Deriving information from absorption measurements, *Oral presentation at the Workshop "On-line spectroscopy"*, Scientific pre-event AutMoNet 2004, 18 April 2004, Vienna, Austra.

Langergraber, G.; Fleischmann, N.; Hofstädter, F. & Weingartner, A. (2004): Monitoring of a paper mill wastewater treatment plant using UV-VIS spectroscopy, *Water Science and Technology*, Vol. 49, No. 1, pp. 9 – 14.

Larsen, T.; Broch, K. & Andersen, M.R. (1998): First Flush Effects in an Urban Catchment Area in Aaalborg, *Water Science and Technology*, Vol. 37, No. 1, pp. 251 – 257.

Lee, J.H. & Bang, K.W. (2000): Characterization of Urban Stormwater Runoff, *Water Research*, Vol. 34, No. 6., pp. 1773 – 1780.

Lee, H.; Lau, S.-L.; Kayhanian, M. & Stenstrom, M.K. (2004): Seasonal first flush phenomenon of urban stormwater discharges, *Water Research*, Vol. 38, pp. 4153 – 4163.

Leinweber, U. (2002): Anforderungen an die integrierte Modellierung von Entwässerungssystem und Kläranlage, in German, *Schriftenreihe Siedlungswasserwirtschaft Universität Kaiserslautern*, PhD Thesis, Vol. 16 University of Kaiserslautern.

Li, B.; Morris, J.; Martin, E.B. (2002): Model selection for partial least squares regression, *Chemometrics and Intelligent Laboratory Systems*, Vol. 64, pp. 79 – 89.

Macke, E.; von Koerber, N. & Sander, T. (1987): Schmutzfrachtuntersuchungen im Mischwassernetz der Stadt Braunschweig, in German (Investigations of pollution loads in the combined sewerage system of the city of Braunschweig), *Mitteilungen des Leichtweiß-Institutes für Wasserbau*, Technical University Braunschweig, Vol. 94, pp. 377 – 402.

Macke, E.; Hartmann, A. & von Koerber, N (2002): Zur Schmutzfracht von Regenwasser in großen, flach verlegten Mischwassernetzen, in German (The Pollution Load of Stormwater in Large Horizontal Combined Sewer Systems), *KA-Abwasser, Abfall*, Vol. 1, pp. 40 -48.

Massart, D. L; Kaufman, L.; Rousseeuw, P.J. and Leroy A. (1986): Least median of squares: A robust method for outlier and model error detection in regression and calibration, *Analytica Chimica Acta*, Vol. 187, pp. 171 – 179.

Matsché, N. & Ruider, E. (1982): UV-Absorption, ein aussagekräftiger Parameter zur Erfassung der Restverschmutzung von biologisch gereinigtem Abwasser, in German, *Wiener Mitteilungen*, Vol. 49, pp. 239 – 260.

Matsché, N.; Winkler, S.; Saracevic, E. & Sturmwöhrer, K. (2002): History of the application of spectral absorption coefficient (SAC) measurement to the field of wastewater analysis, *Proceedings of 1st International IWA Conference on Automation in Water Quality Monitoring*, pp. 9 – 16, 21 – 22 May 2002, Vienna, Austria.

Marsalek, J. (1981): Calibration of the tipping-bucket raingage. *Journal of Hdrology*, Vol. 53, No. 3-4, pp. 343 – 354.

Marsalek, J.; Brownlee, B.; Mayer, T.; Lawal, S. & Larkin, G.A. (1997): Heavy Metals and PAHs in Stormwater Runoff from Skyway Bridge, Burlington, Ontario, *Water Quality Research Journal of Canada*, Vol. 32, No. 4, pp. 815 – 827.

Moilleron, R.; Gonzalez, A.; Chebbo, G.; & Thévenot, D.R. (2002): Determination of aliphatic hydrocarbons in urban runoff samples from the “Le Marais” experimental catchment in Paris centre, *Water Research*, Vol. 36, pp. 1275 -1285.

Mourad, M. & Bertrand Krajewski, J.-L. (2002): A method for automatic validation of long time series of data in urban hydrology, *Water Science and Technology*, Vol. 45, No. 4-5, pp. 263 – 270.

Niemczynowicz, J. (1986) The dynamic calibration of tipping bucket raingauges. Nordic Hydrology, Vol. 17, pp. 203 – 214.

Otto, M. (1999): Chemometrics – Statistics and Computer Application in Analytical Chemistry, WILEY-VCH Verlag, Weinheim, Germany, ISBN 3-527-29628-X.

Overgaard S., El-Shaarawi, A.H. & Arnbjerg-Nielsen, K. (1998): Calibration of Tipping Bucket Raing Gauges, *Water Science and Technology*, Vol. 37, No. 11, pp. 139 – 145.

ÖWAV (2003): ÖWAV-Regelblatt 19 – Richtlinien für die Bemessung von Regenentlastungen in Mischwasserkanälen, in German, Austrian Guideline, Österreichischer Wasser- und Abfallwirtschaftsverband, Vienna, Draft 10.2003.

Perkampus, H.-H. (1986): UV-VIS-Spektroskopie und ihre Anwendungen, Springer Verlag, Berlin, Germany, ISBN 3-540-15467-1.

Perkampus, H.-H. (1992): UV VIS atlas of organic compounds, Wiley-VCH publishing, ISBN 3-527-29628-X.

Platt, J.C. (1998): Fast training of support vector machines using sequential minimal optimization, in *Advances in Kernel Methods – Support Vector learning*, chapter 12, (Eds.) B. Scholkopf, C. Burges, and A.J. Smola, pp. 185 – 208, MIT Press, Cambridge, Massachusetts, USA, ISBN 0-262-19416-3.

Pons, M.-N.; Le Bonté, S.; Portier, O. (2004): Spectral analysis and fingerprinting for biomedia characterisation, *Journal of Biotechnology*, Vol. 113, pp. 211 – 230.

Preda, C; Saporta, G. (2005): PLS regression on a stochastic process, *Computational Statistics & Data Analysis*, Vol. 48, pp. 149 – 158.

Quinlan, J. R. (1992): Learning with continuous classes. in Adams & Sterling (Eds.), *Proceedings AI'92* (Australian Conference on AI), Singapore, World Scientific, pp. 343 – 348.

Quinlan, J. R. (1993): Combining Instance-Based and Model-Based Learning, *Proceedings of the 10th International Conference on Machine Learning*, Amherst, Massachusetts, 27 – 29 June 1993, Morgan Kaufman Publishing, San Mateo, California, pp. 236 – 243.

Rauch, W. & Harremoës, P. (1996): The importance of the treatment plant performance during rain to acute water pollution, *Water Science and Technology*, Vol. 34, No. 3 – 4, pp. 1 – 8.

Rauch, W.; Thurner, N. & Harremoës, P. (1998): Required Accuracy of Rainfall Data for Integrated Urban Drainage Modeling, *Water Science and Technology*, Vol. 37, No. 11, pp. 81 – 89.

Rauch, W. & Harremoës, P. (1999): Genetic Algorithms in Real Time Control applied to Minimize Transient Pollution from Urban Wastewater systems, *Water Research*, Vol. 33, No. 5, pp. 1265 – 1277.

Rauch, W., Brøndholt Nielsen, H.; Hauger, M. & Mikkelsen, P.S. (1999): Urban Drainage Management - An Integrated Assessment of Options, *Proceedings of 8th International Conference on Urban Storm Drainage*, 30 August – 3 September, Sydney, Australia.

Rauch, W.; Bertrand-Krajewski, J.-L.; Krebs, P.; Mark, O.; Schilling, W.; Schütze, M. & Vanrolleghem, P.A. (2002): Deterministic modelling of integrated urban drainage systems, *Water Science and Technology*, Vol. 45, No. 3, pp. 81 – 94.

Reiff, H. (1992): Wachstum und Abtrag der Sielhaut in Mischwasserkanälen, *Schriftenreihe des Fachgebietes Siedlungswasserwirtschaft*, University of Kassel, Vol. 9.

Rousseeuw, P.J. (1984): Least Median of Squares Regression, *Journal of the American Statistical Association*, Vol. 79, No. 388, pp. 871 – 880.

Ruan, M. (1999): Continuous simulation of CSO emissions, *Urban Water*, Vol. 1, pp 201 – 205.

Saget, A.; Chebbo, G. & Bertrand-Krajewski, J.-L. (1996): The First Flush in Sewer Systems, *Water Science and Technology*, Vol. 33, No. 9, pp. 101 – 108.

Sánchez, V. D. (2003): Advanced support vector machines and kernel methods, *Neurocomputing*, Vol. 55, pp. 5 – 20.

Sansalone, J.J. & Buchberger, S.G. (1997): Partitioning and First Flush of Metals in Urban Roadway Storm Water, *Journal of Environmental Engineering*, Vol. 123, No. 2, pp. 134 – 143.

S::can (2005): UV/VIS spectrometer manual of spectro::lyser, www.s-can.at, hompage of the s::can company, visited on 1st March 2005.

Scheer, M. & Schilling, W. (2003): Einsatz von Online-Messgeräten zur Beurteilung der Mischwasserqualität im Kanal, in German (Use of Online Measurement Equipment to Assess the Quality of Combined Sewage in Sewers), *KA-Abwasser, Abfall*, No. 5, pp. 585 – 595.

Scholz, K. (1997): Stochastic Simulation of Urbanhydrological Processes, *Water Science and Technology*, Vol. 36, No. 8-9, pp. 25 – 31.

Schulz, O. (1995): Gebietsspezifische Schmutzfrachtpotenziale flach verlegter und vorentlasteter Mischwassernetze, in German, Mitteilungen des Leichtweiß-Institutes für Wasserbau der TU Braunschweig, Vol. 137, pp. 1 – 172.

Schütze, M. & Alex, J. (2004): Suitable Integrated Modelling – based on simplified models, *Proceedings of 6th International Conference on Urban Drainage Modelling – UDM '04*, 15 – 17 September 2004, Dresden, Germany.

Seggelke, K. (2002): Integrierte Bewirtschaftung von Kanalnetz und Kläranlage zur Reduzierung der Gewässbelastung, in German, *Veröffentlichung des Institutes für Siedlungswasserwirtschaft und Abfalltechnik der Universität Hannover*, PhD Thesis, Vol. 124, University of Hannover.

Seibert, J & Morén, A.-S. (1999): Reducing systematic errors in rainfall measurements using a new type of gauge, *Agricultural and Forest Meteorology*, Vol. 98-99, pp. 341 – 348.

Sévar, J.-M-; Warmbier, G. & Wagner, L. (2004): Geschwindigkeits-Radar-Durchflusssensoren im Abwasserkanal, in German, *Proceedings of the workshop „Neue Entwicklungen in der Durchflussmessung in natürlichen und künstlichen Gerinnen",* 11 – 12 March 2004, Munich, Germany.

Skripalle, J. (2004): Ultaschall-Laufzeit-Verfahren in Flüssen, in German, *Proceedings of the workshop „Neue Entwicklungen in der Durchflussmessung in natürlichen und künstlichen Gerinnen",* 11 – 12 March 2004, Munich, Germany.

Sprung, W. (2004): Strategien einer nachhaltigen Mischwasserbewirtschaftung der Stadt Graz, in German, Oral Presentation at the Institute of Urban Water Management and Landscape Water Enginnering, University of Technology Graz, Held for the Austrian Hydrological Communitie, 30 March 2004.

Sztruhár, D; Sokáč, M; Holienčin, A. & Markovič, A (2002); Comprehensive assessment of combined sewer overflows in Slovakia, *Urban Water*, Vol. 4, pp. 237 – 243.

Tekusová, M.; Stástny, P & Chvíla, B. (2003): Comparison of recording precipitation gauges: weighing, tipping bucket and float types, *Proceedings of 3rd International Conference on Experiences of Automatic Meterogical Stations*, Malaga, Spain.

Teufel, M. (2004): Doppler-Verfahren, Pulsdoppler und Kreuzkorrelation bei Ultraschallmessungen, in German, *Proceedings of the workshop „Neue Entwicklungen in der Durchflussmessung in natürlichen und künstlichen Gerinnen",* 11 – 12 March 2004, Munich, Germany.

Thaler, M. (2004): Fehler bei der Messung und Kalibrierung von Niederschlagswippen, in German (Measurement's and Calibration's Errors of Tipping Bucket Raing Gauge), Diploma thesis, Institute of Urban Water Management and Landscape Water Engineering, University of Technology Graz.

Thomann, M. (2004): Qualitätskontrolle der Betriebsdaten von Kläranlagen, in German, *Wiener Mitteilungen*, Vol. 187, pp. 295 – 318.

Uhl, M. (2000): Messbereiche und Messfehler – Durchflussmessung an Regenüberlaufbecken, in German, *ATV-DVWK Schriftenreihe*, Vol. 19, pp. 111 – 132, Hennef, Germany.

Vapnik, V.N. (1995): The Nature of Statistical Learning Theory, Springer-Verlag, New York, USA, ISB 0-387-94559-8.

Vasvari, V. (1995): Kontrollmessungen zur Eichung der mit Wippe ausgestatteten Niederschlagsmessgeräte, in German, Mitteilungsblatt des Hydrographischen Dienstes in Österreich, Vol. 73, pp. 55 – 66.

Vasvári, V. (2005): Calibration of tipping bucket rain gauges in the Graz urban research area, *Atmospheric Research*, submitted and accepted paper.

Vasvári, V.; Hochedlinger, M. & Sprung, W. (2005): Erfahrung mit der Kalibrierung von Wippengeräten am Beispiel des Grazer Versuchsgebietes, in German (Experience in calibration of tipping bucket gauges by means of the research area Graz), submitted and accepted paper for Mitteilungsblatt des hydrographischen Dienstes in Österreich.

de Vries, J.M. (1993): Bestimmung des Schmutzfrachtpotentials in flach verlegten Misch- und Tennnetzen infolge abfließenden Niederschlagswassers, in German (Determination of the Pollution Potential in Flat-Layed, Combined Sewage and Seperate Sewage Systems as a Result of Precipitation Runoff), *Mitteilungen des Leichtweiß-Institutes für Wasserbau*, Technical University Braunschweig, Vol. 125, pp. 1 – 132.

VSA (2003): Messtechnik in der Siedlungsentwässerung – Fachdokumentation für die Planung, die Einrichtung und den Betrieb von Messstellen in Kanalisationen und Kläranlagen, in German, VSA – Verband Schweizer Abwasser- und Gewässerfachleute, Chapter 10, Messungen von N-, P- und C-Komponenten, Zurich, Switzerland.

Wedenig, M. (2004): Quantifizierung von abgeschlagenen Schmutzfrachten aus einer Mischwasserentlastung in einen Vorfluter, in German (Quantification of Pollution Loads from a Combined Sewer Overflow into a Receiving Water), Diploma thesis, Institute of Urban Water Management and Landscape Water Engineering, University of Technology Graz.

Weyand, M. (2001): Messungen in Kanalnetzen – Anwendungsspektrum, Zielsetzung und Nutzen, Online-Messung in Kanalisationsnetzen – Erfahrungen und Möglichkeiten zur Abfluss- und Parametermessung, *Schriftenreihe Siedlungswasserwirtschaft Bochum*, Vol. 40, pp. 89 – 113, in German.

Willems, P. (1999): Stochastic Generation of Spatial Rainfall for Urban Drainage Areas, *Water Science and Technology*, Vol. 39, No. 9, pp. 23 – 30.

Willems, P. & Berlamont, J. (1999): Probabilistic Modelling of Sewer System Overflow Emissions, *Water Science and Technology*, Vol. 39, No. 9, pp. 47 – 54.

Winkler, S. (2004): Entwicklung auf dem Gebiet der Messtechnik für Abwasserreinigung, in German, Proceedings of ÖWAV-Workshop „Datengewinnung, -verwaltung und –nutzung in der Wassergütewirtschaft“, *Wiener Mitteilungen*, Vol. 187, pp. 119 – 143, 3 – 4 March 2004, Vienna, Austria.

Winkler, S. & Fleischmann, N. (2004): Konzept des IMW-Wasserqualitätsmessnetzes, in German, Proceedings of ÖWAV-Workshop „Innovative Messtechnik in der Wasserwirtschaft – Konzeption und Praxiserfahrungen mit einem modularen Monitoringnetzwerk zur universellen Anwendung in der Wasserwirtschaft“, *Schriftenreihe zur Wasserwirtschaft,* University of Technology Graz, Vol. 42, pp. C1 – C23, 29 June 2004, Graz, Austria.

Winkler, S., Rieger, L., Pressl, A., Gruber, G. & Saracevic, E. (2004): Application of ion-sensitive sensors in water quality monitoring, Proceedings of 2nd International IWA Conference on Automation in Water Quality Monitoring, pp. 45 – 54, 19 – 20 April 2004, Vienna, Austria.

Witten, I.H. & Frank, E (2001): Data Mining – Praktische Werkzeuge und Techniken für das maschinelle Lernen, in German, Carl Hanser publishing, Munich, Germany, ISBN 3-446-21553-6.

Wöhrle, C. & Brombach, H. (1991): Probennahme im Abwasserkanal, in German (Sampling in Sewers), *Wasser-Wirtschaft*, Vol. 2, pp. 60 – 65.

CONTENT OF FIGURES

CONTENT OF TABLES

APPENDIX

FIGURES OF UV-VIS AND LAB VALUES COMPARISONS OF OVERFLOW EVENTS

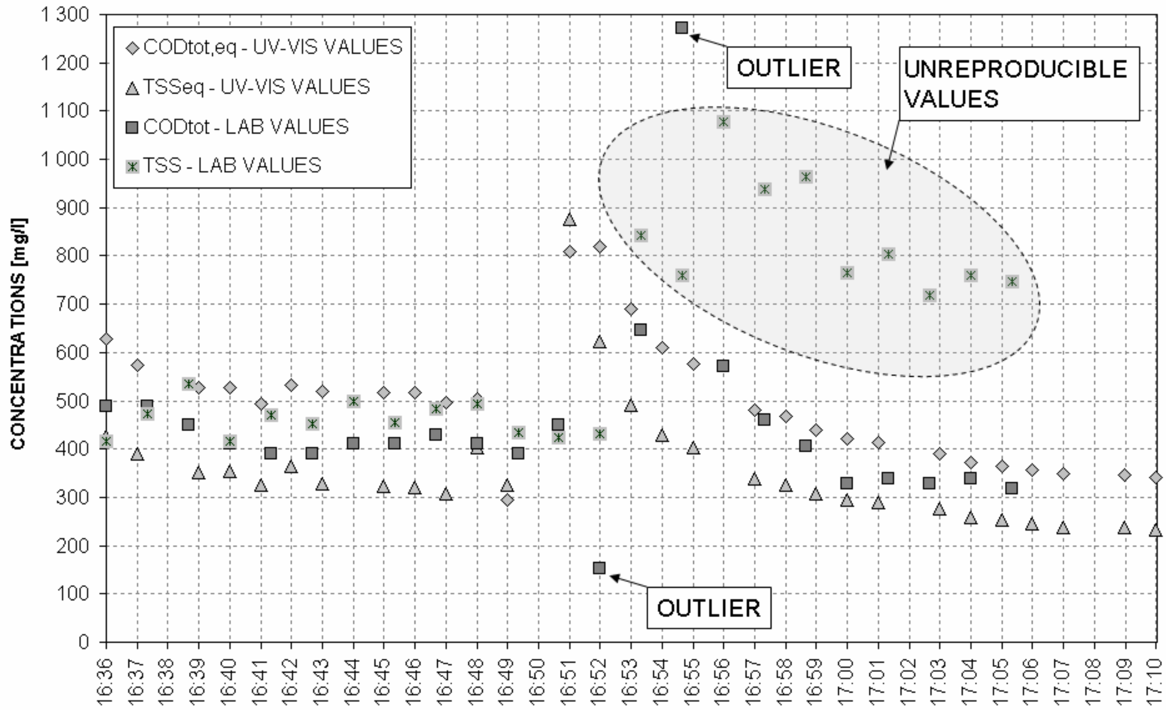

Figure A- 1 Overflow Event – 13th June 2003

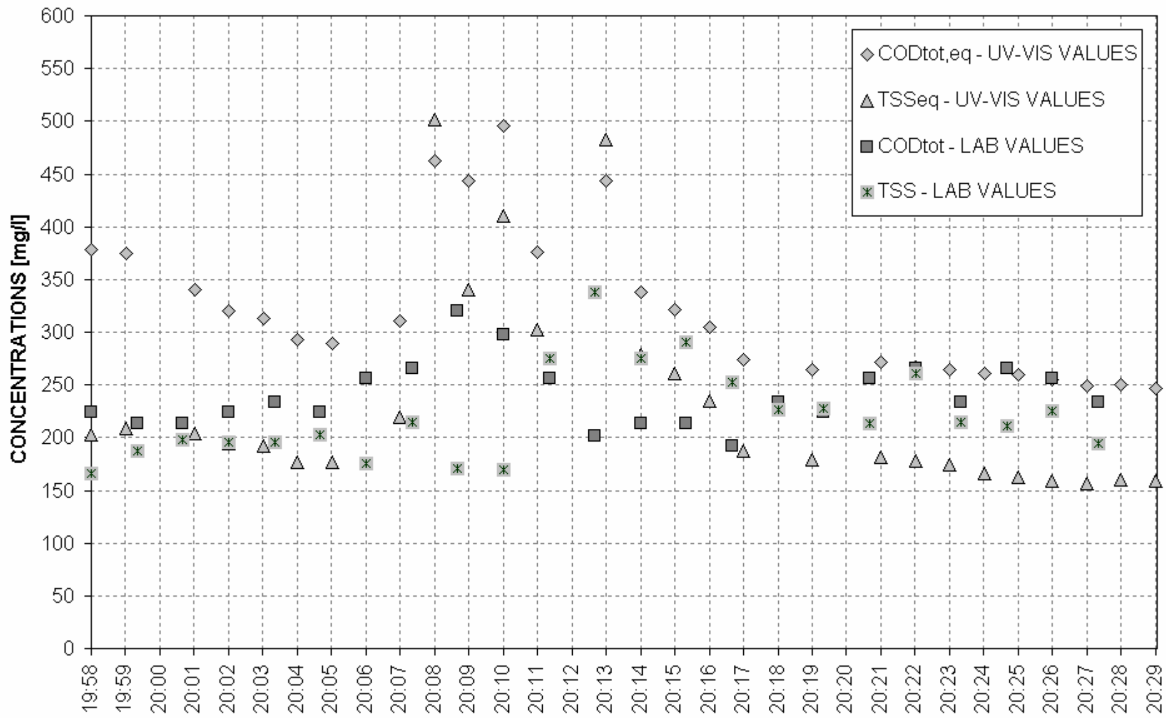

Figure A- 2 Overflow Event – 16th June 2003

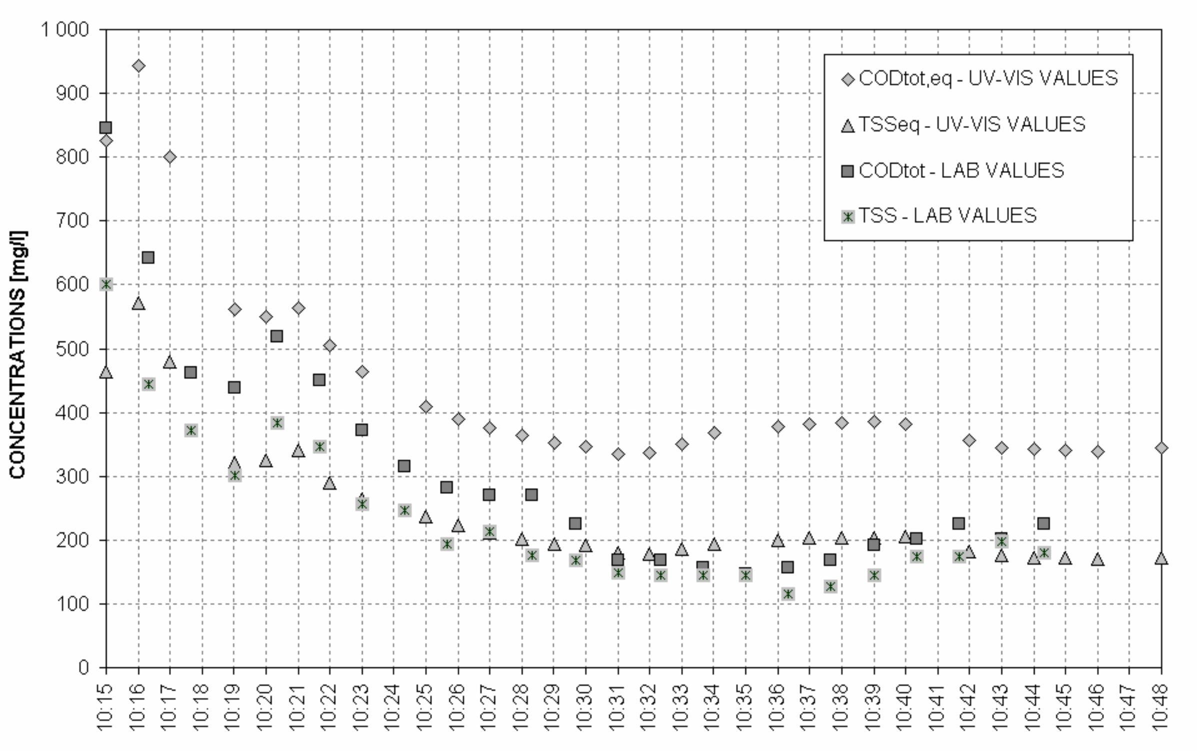

Figure A- 3 Overflow Event – 18th June 2003 – Nr. 1

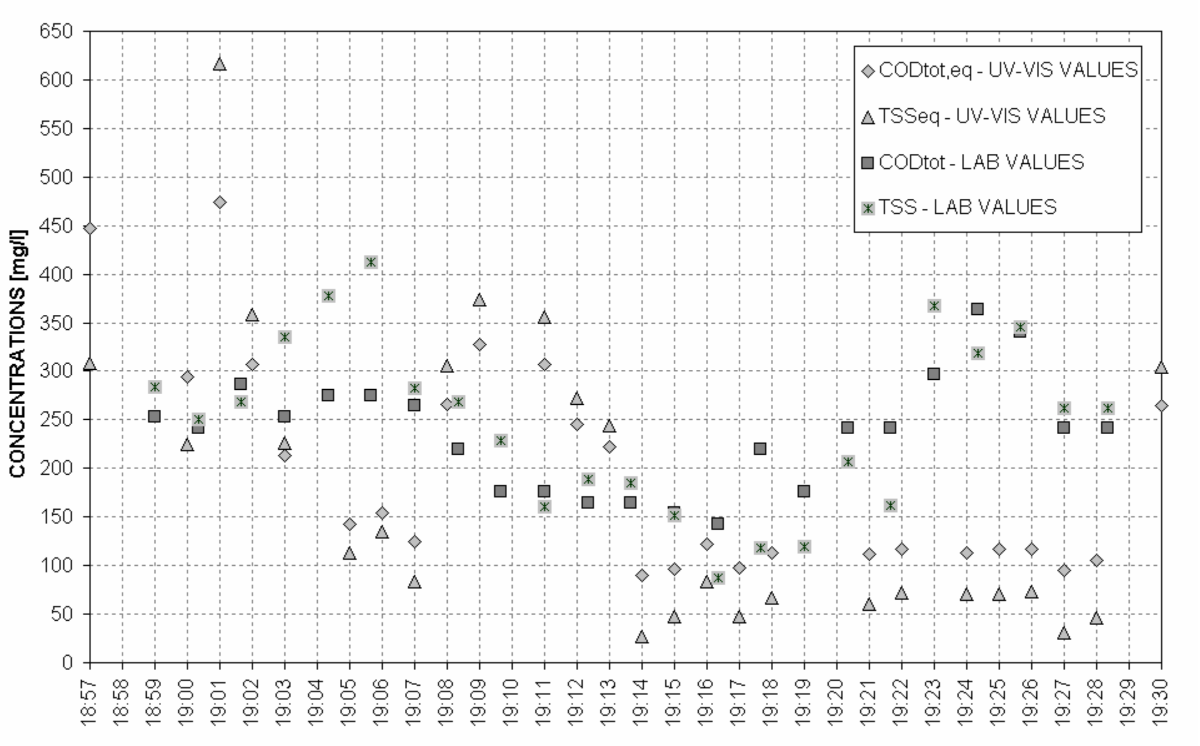

Figure A- 4 Overflow Event – 18th June 2003 – Nr. 2

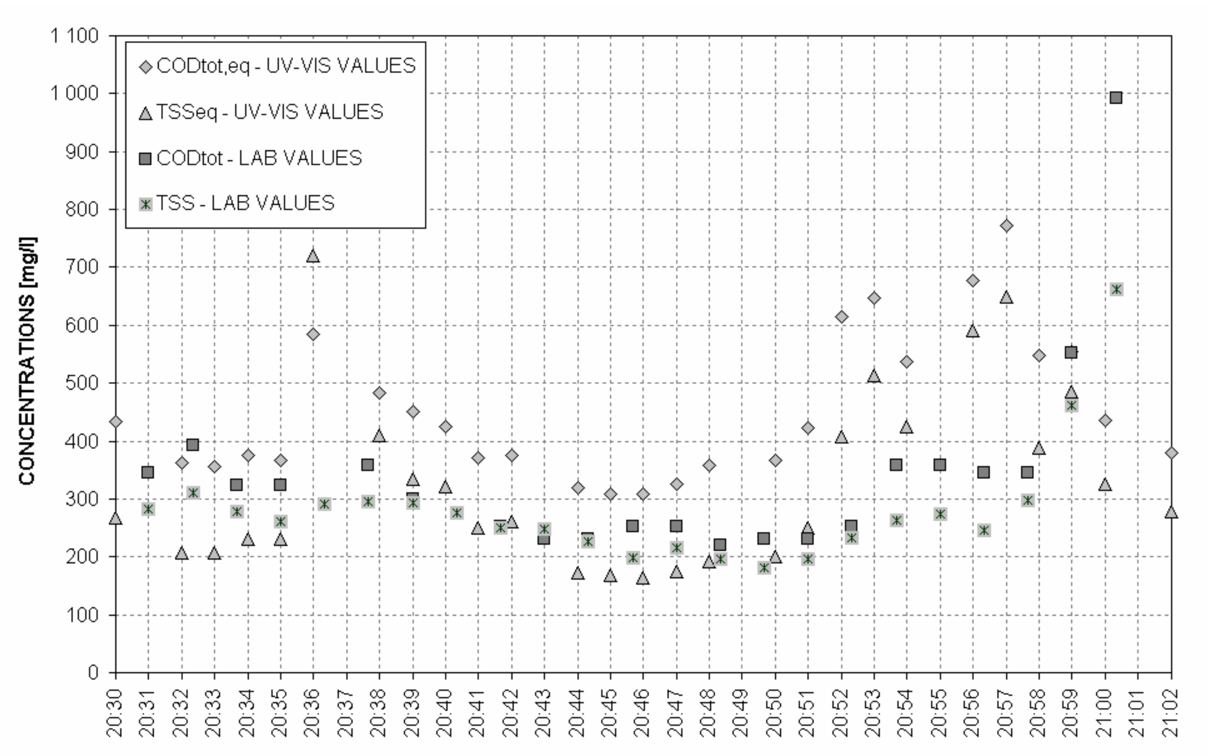

Figure A- 5 Overflow Event – 24th June 2003

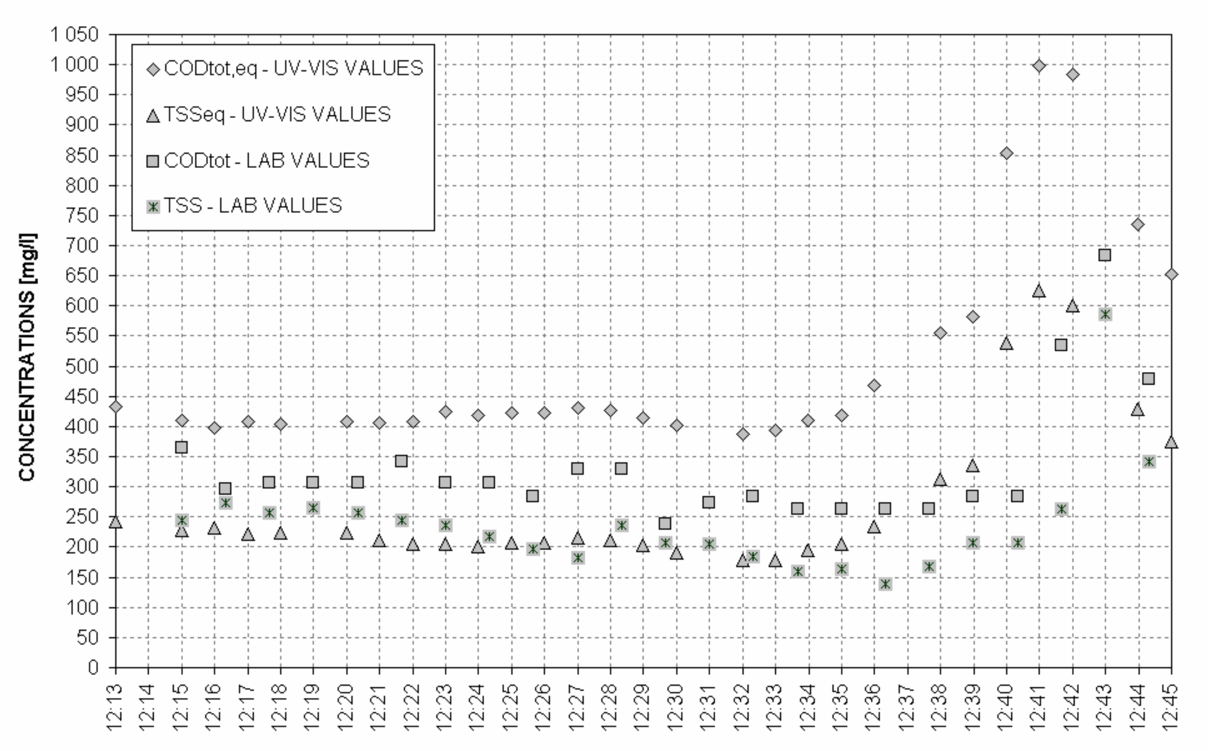

Figure A- 6 Overflow Event – 27th June 2003

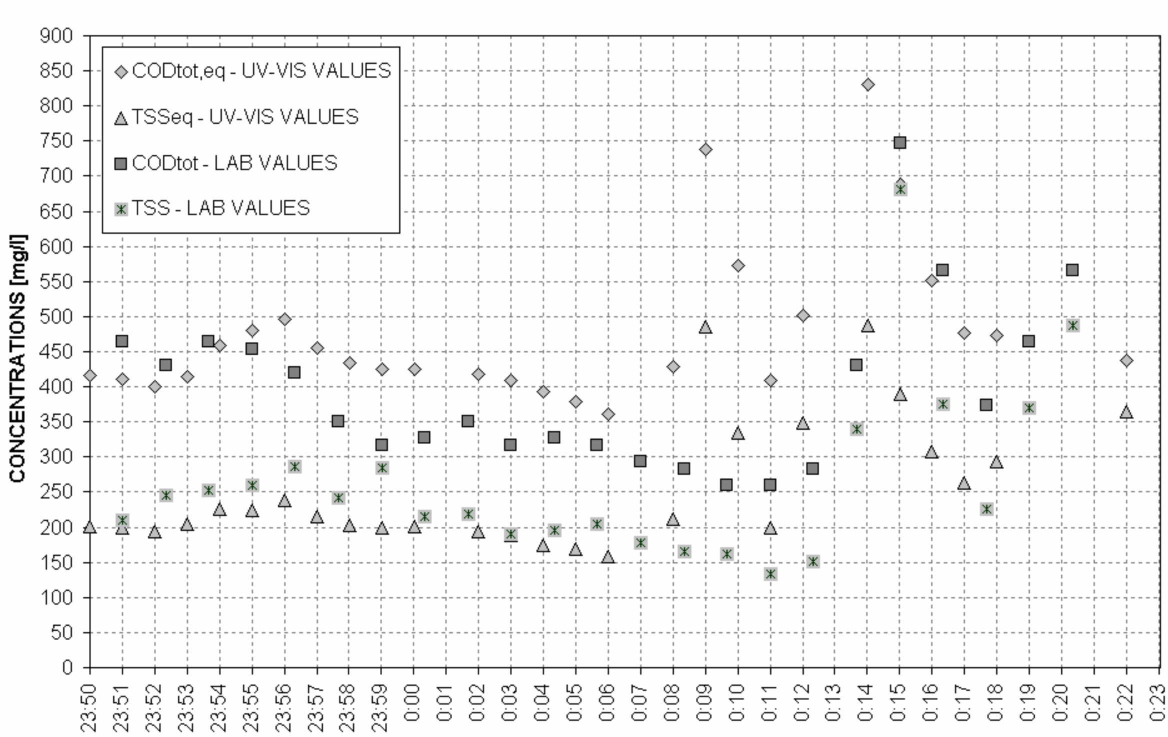

Figure A- 7 Overflow Event – 1st July 2003

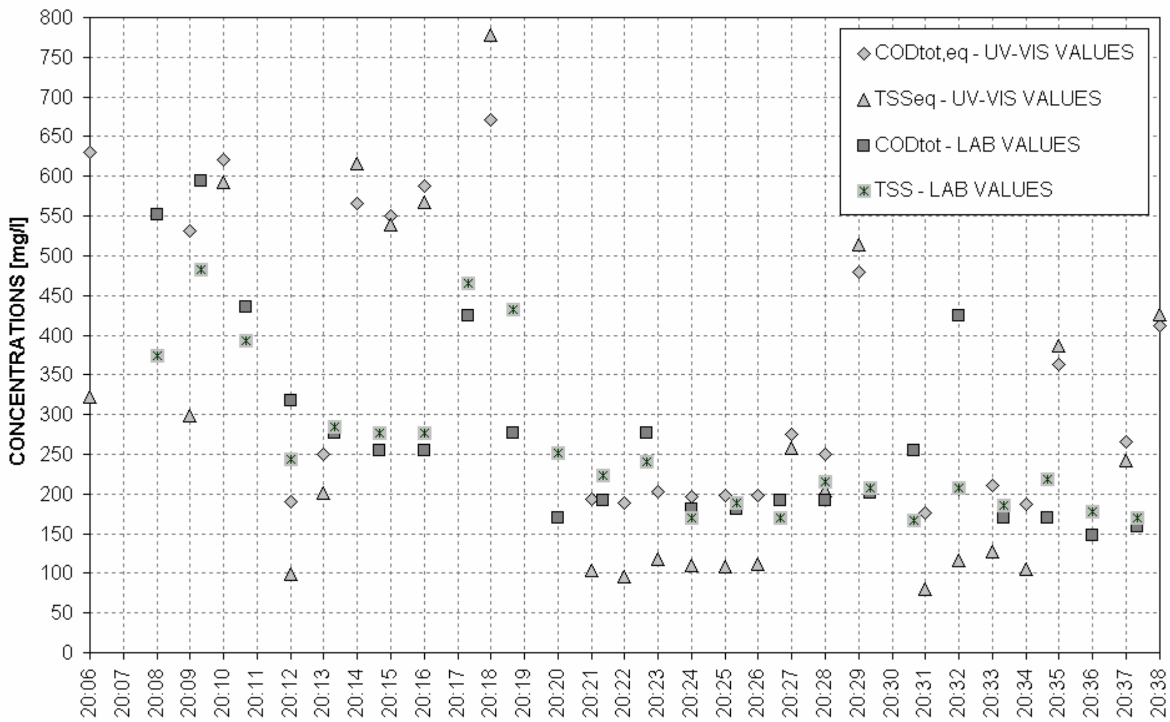

Figure A- 8 Overflow Event – 17th July 2003

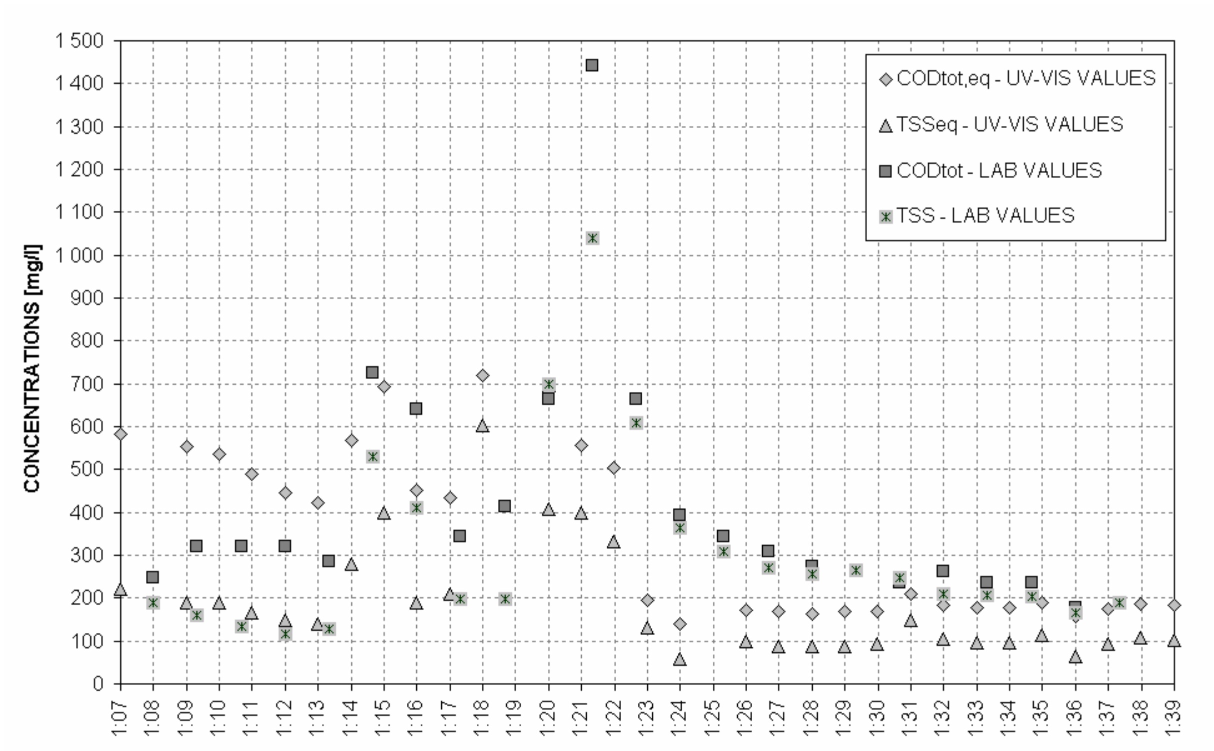

Figure A- 9 Overflow Event – 23rd July 2003 – Nr. 1

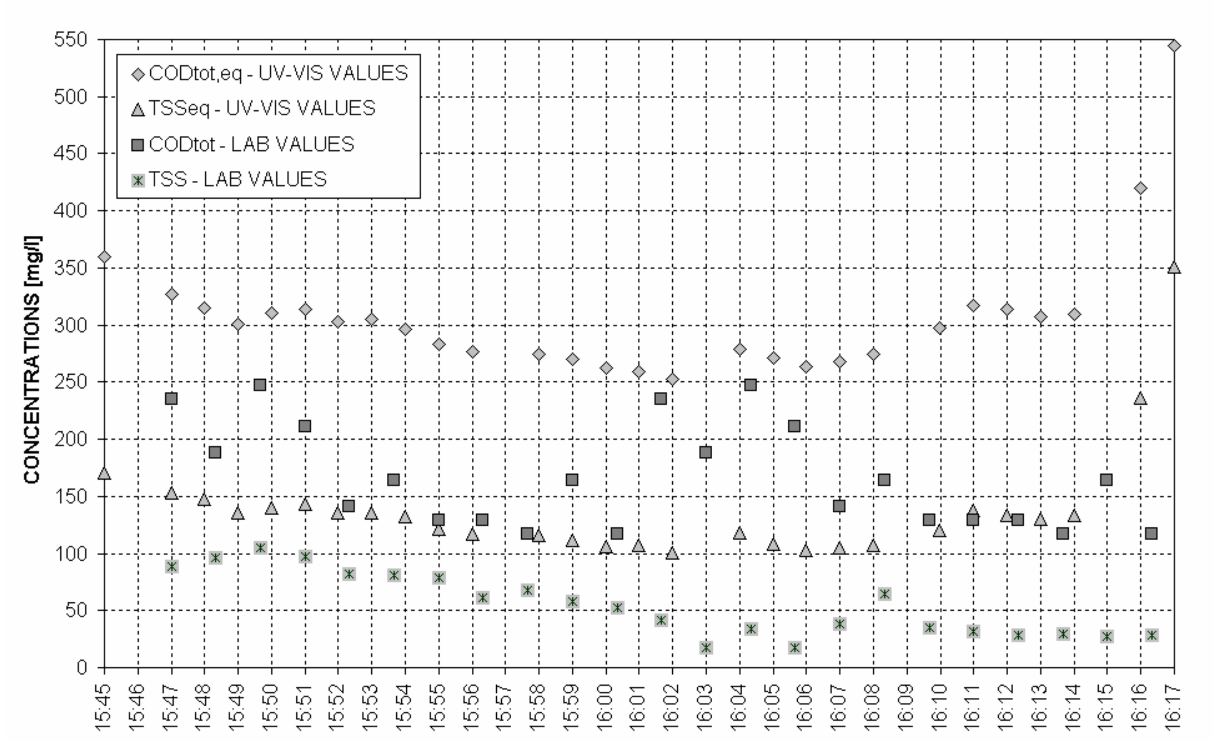

Figure A- 10 Overflow Event – 23rd July 2003 – Nr. 2

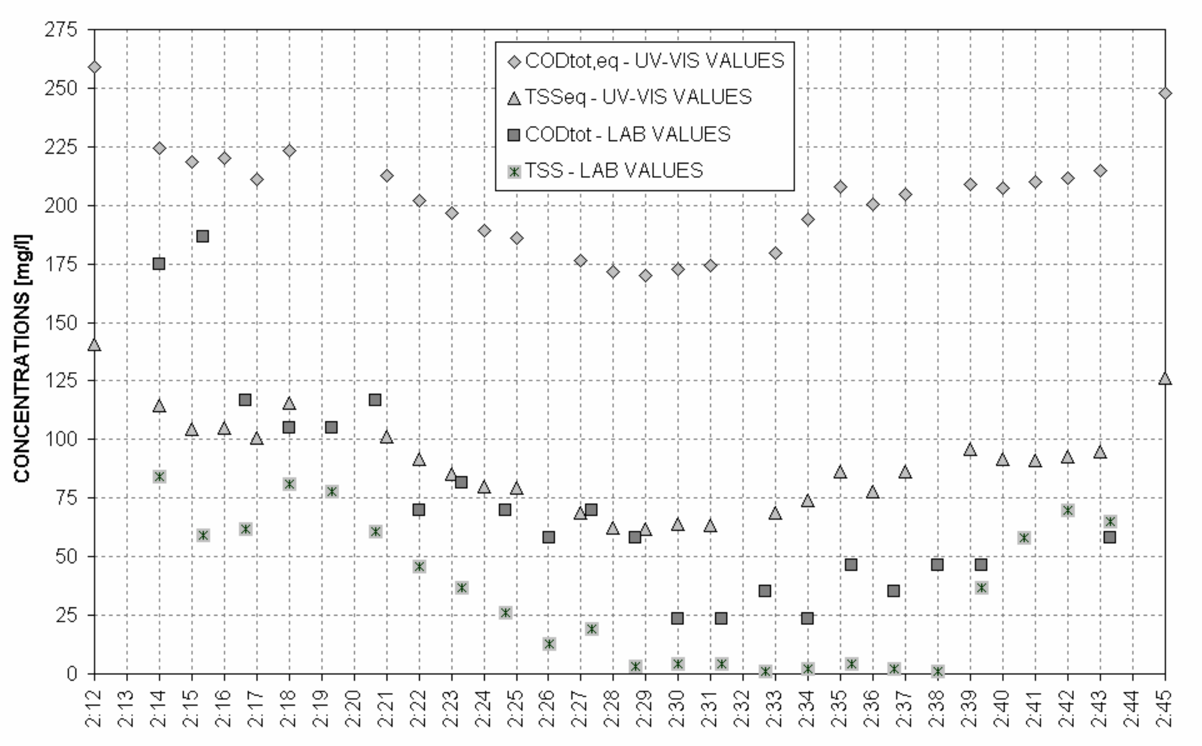

Figure A- 11 Overflow Event – 25th July 2003

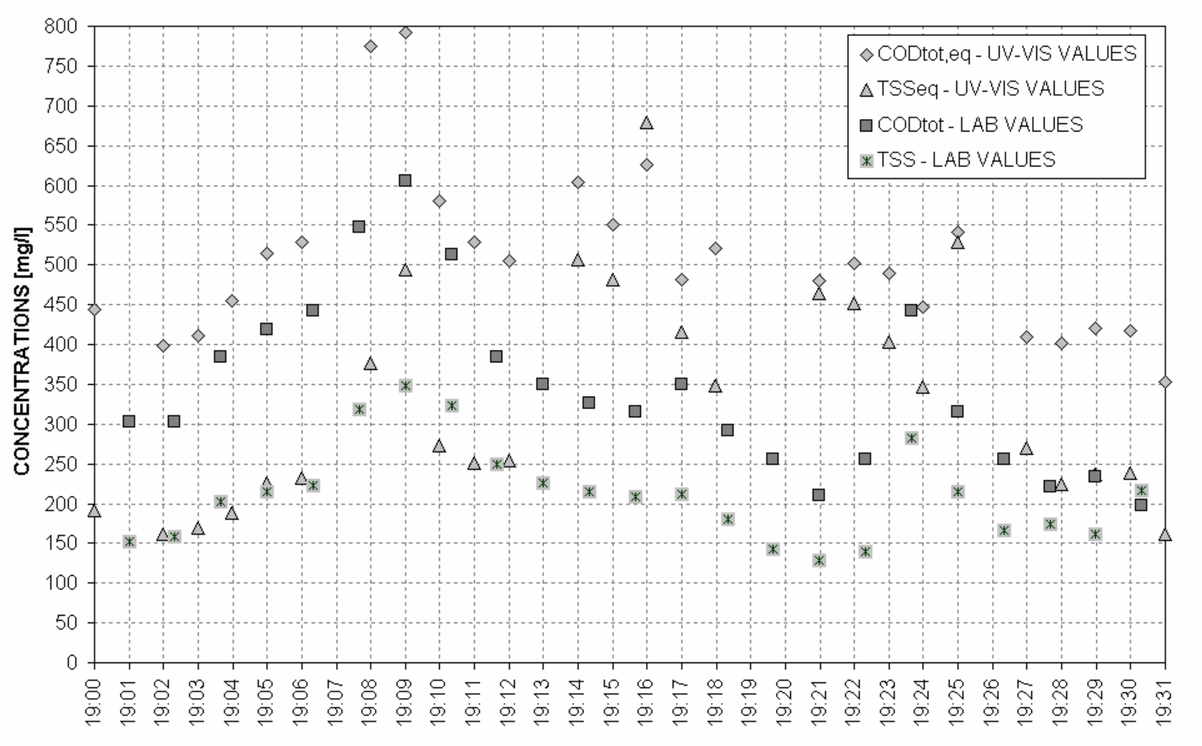

Figure A- 12 Overflow Event – 28th July 2003

TABLES OF UV-VIS AND LAB VALUES OF OVERFLOW EVENTS

Table A- 1 Overflow Event – 13th June 2003

Date	Time	$COD_{tot,eq}$ UV-VIS Values	COD_{tot} Lab Values	TSS_{eq} UV-VIS Values	TSS_{eq} Lab Values
[dd.mm.yy]	[hh:mm:ss]		[mg/l]		
13.06.03	16:36:00	629	488	425	417
13.06.03	16:37:00	573	-	389	-
13.06.03	16:37:20	-	488	-	473
13.06.03	16:38:40	-	449	-	535
13.06.03	16:39:00	527	-	353	-
13.06.03	16:40:00	527	410	353	417
13.06.03	16:41:00	493	-	325	-
13.06.03	16:41:20	-	390	-	471
13.06.03	16:42:00	534	-	363	-
13.06.03	16:42:40	-	390	-	453
13.06.03	16:43:00	519	-	328	-
13.06.03	16:44:00	-	410	-	500
13.06.03	16:45:00	518	-	323	-
13.06.03	16:45:20	-	410	-	454
13.06.03	16:46:00	516	-	322	-
13.06.03	16:46:40	-	429	-	483
13.06.03	16:47:00	497	-	309	-
13.06.03	16:48:00	504	410	402	493
13.06.03	16:49:00	295	-	325	-
13.06.03	16:49:20	-	390	-	435
13.06.03	16:50:40	-	449	-	425
13.06.03	16:51:00	810	-	876	-
13.06.03	16:52:00	820	153*	622	431
13.06.03	16:53:00	689	-	491	-
13.06.03	16:53:20	-	647	-	843**
13.06.03	16:54:00	610	-	402	-
13.06.03	16:54:40	-	1 271*	-	761
13.06.03	16:55:00	576	-	402	-
13.06.03	16:56:00	-	570	-	1 078**
13.06.03	16:57:00	482	-	338	-
13.06.03	16:57:20	-	460	-	938
13.06.03	16:58:00	467	-	325	-
13.06.03	16:58:40	-	405	-	963
13.06.03	16:59:00	439	-	307	-
13.06.03	17:00:00	420	328	294	766**
13.06.03	17:01:00	415	-	290	-
13.06.03	17:01:20	-	339	-	803**
13.06.03	17:02:40	-	328	-	719**
13.06.03	17:03:00	391	-	278	-
13.06.03	17:04:00	372	339	258	759**
13.06.03	17:05:00	365	-	252	-
13.06.03	17:06:00	358	-	247	-
13.06.03	17:07:00	349	-	237	-
13.06.03	17:09:00	345	-	237	-
13.06.03	17:10:00	341	-	233	-

* outlier

** unreproducible values

Table A- 2 Overflow Event – 16th June 2003

Date	Time	$COD_{tot,eq}$ UV-VIS Values	COD_{tot} Lab Values	TSS_{eq} UV-VIS Values	TSS_{eq} Lab Values
[dd.mm.yy]	[hh:mm:ss]	[mg/l]			
16.06.03	19:58:00	378	224	202	166
16.06.03	19:59:00	375	-	209	-
16.06.03	19:59:20	-	213	-	187
16.06.03	20:00:40	-	213	-	198
16.06.03	20:01:00	340	-	204	-
16.06.03	20:02:00	320	224	195	196
16.06.03	20:03:00	313	-	192	-
16.06.03	20:03:20	-	234	-	196
16.06.03	20:04:00	293	-	177	-
16.06.03	20:04:40	-	224	-	203
16.06.03	20:05:00	290	-	177	-
16.06.03	20:06:00	-	256	-	176
16.06.03	20:07:00	311	-	219	-
16.06.03	20:07:20	-	266	-	215
16.06.03	20:08:00	462	-	502	-
16.06.03	20:08:40	-	320	-	171
16.06.03	20:09:00	444	-	340	-
16.06.03	20:10:00	495	298	410	170
16.06.03	20:11:00	376	-	303	-
16.06.03	20:11:20	-	256	-	275
16.06.03	20:12:40	-	202	-	338
16.06.03	20:13:00	443	-	482	-
16.06.03	20:14:00	338	213	278	275
16.06.03	20:15:00	321	-	261	-
16.06.03	20:15:20	-	213	-	290
16.06.03	20:16:00	304	-	234	-
16.06.03	20:16:40	-	192	-	253
16.06.03	20:17:00	274	-	187	-
16.06.03	20:18:00	-	234	-	227
16.06.03	20:19:00	264	-	179	-
16.06.03	20:19:20	-	224	-	228
16.06.03	20:20:40	-	256	-	214
16.06.03	20:21:00	271	-	182	-
16.06.03	20:22:00	267	266	178	261
16.06.03	20:23:00	264	-	174	-
16.06.03	20:23:20	-	234	-	215
16.06.03	20:24:00	261	-	166	-
16.06.03	20:24:40	-	266	-	211
16.06.03	20:25:00	260	-	163	-
16.06.03	20:26:00	255	256	159	225
16.06.03	20:27:00	249	-	156	-
16.06.03	20:27:20	-	234	-	195
16.06.03	20:28:00	250	-	160	-
16.06.03	20:29:00	246	-	158	-

Table A- 3 Overflow Event – 18th June 2003

Date	Time	$COD_{tot,eq}$ UV-VIS Values	COD_{tot} Lab Values	TSS_{eq} UV-VIS Values	TSS_{eq} Lab Values
[dd.mm.yy]	[hh:mm:ss]	[mg/l]			
18.06.03	18:57:00	447	-	308	-
18.06.03	18:59:00	-	253	-	284
18.06.03	19:00:00	294	-	225	-
18.06.03	19:00:20	-	242	-	250
18.06.03	19:01:00	474	-	617	-
18.06.03	19:01:40	-	286	-	268
18.06.03	19:02:00	307	-	358	-
18.06.03	19:03:00	213	253	226	335
18.06.03	19:04:20	-	275	-	378
18.06.03	19:05:00	142	-	113	-
18.06.03	19:05:40	-	275	-	412
18.06.03	19:06:00	155	-	134	-
18.06.03	19:07:00	124	264	84	283
18.06.03	19:08:00	267	-	305	-
18.06.03	19:08:20	-	220	-	269
18.06.03	19:09:00	328	-	374	-
18.06.03	19:09:40	-	176	-	229
18.06.03	19:11:00	307	176	355	161
18.06.03	19:12:00	245	-	273	-
18.06.03	19:12:20	-	165	-	189
18.06.03	19:13:00	222	-	244	-
18.06.03	19:13:40	-	165	-	185
18.06.03	19:14:00	90	-	27	-
18.06.03	19:15:00	97	154	48	152
18.06.03	19:16:00	121	-	84	-
18.06.03	19:16:20	-	143	-	87
18.06.03	19:17:00	98	-	47	-
18.06.03	19:17:40	-	220	-	118
18.06.03	19:18:00	114	-	66	-
18.06.03	19:19:00	-	176	-	120
18.06.03	19:20:20	-	242	-	207
18.06.03	19:21:00	111	-	60	-
18.06.03	19:21:40	-	242	-	162
18.06.03	19:22:00	117	-	72	-
18.06.03	19:23:00	-	297	-	367
18.06.03	19:24:00	113	-	70	-
18.06.03	19:24:20	-	363	-	318
18.06.03	19:25:00	117	-	71	-
18.06.03	19:25:40	-	341	-	346
18.06.03	19:26:00	117	-	74	-
18.06.03	19:27:00	95	242	31	262
18.06.03	19:28:00	105	-	46	-
18.06.03	19:28:20	-	242	-	262
18.06.03	19:30:00	264	-	305	-

Table A- 4 Overflow Event – 24th June 2003

Date	Time	$COD_{tot,eq}$ UV-VIS Values	COD_{tot} Lab Values	TSS_{eq} UV-VIS Values	TSS_{eq} Lab Values
[dd.mm.yy]	[hh:mm:ss]	[mg/l]			
24.06.03	20:30:00	433	-	267	-
24.06.03	20:31:00	-	346	-	283
24.06.03	20:32:00	362	-	207	-
24.06.03	20:32:20	-	392	-	311
24.06.03	20:33:00	357	-	206	-
24.06.03	20:33:40	-	323	-	278
24.06.03	20:34:00	376	-	231	-
24.06.03	20:35:00	366	323	231	262
24.06.03	20:36:00	584	-	720	-
24.06.03	20:36:20	-	288	-	291
24.06.03	20:37:40	-	357	-	296
24.06.03	20:38:00	483	-	409	-
24.06.03	20:39:00	450	300	334	293
24.06.03	20:40:00	424	-	322	-
24.06.03	20:40:20	-	276	-	276
24.06.03	20:41:00	371	-	250	-
24.06.03	20:41:40	-	253	-	251
24.06.03	20:42:00	375	-	261	-
24.06.03	20:43:00	-	230	-	247
24.06.03	20:44:00	320	-	173	-
24.06.03	20:44:20	-	230	-	226
24.06.03	20:45:00	308	-	168	-
24.06.03	20:45:40	-	253	-	199
24.06.03	20:46:00	308	-	165	-
24.06.03	20:47:00	325	253	176	216
24.06.03	20:48:00	357	-	193	-
24.06.03	20:48:20	-	219	-	196
24.06.03	20:49:40	-	230	-	182
24.06.03	20:50:00	366	-	200	-
24.06.03	20:51:00	422	230	250	196
24.06.03	20:52:00	614	-	408	-
24.06.03	20:52:20	-	253	-	234
24.06.03	20:53:00	648	-	512	-
24.06.03	20:53:40	-	357	-	264
24.06.03	20:54:00	537	-	425	-
24.06.03	20:55:00	-	357	-	275
24.06.03	20:56:00	678	-	591	-
24.06.03	20:56:20	-	346	-	245
24.06.03	20:57:00	772	-	648	-
24.06.03	20:57:40	-	346	-	297
24.06.03	20:58:00	548	-	388	-
24.06.03	20:59:00	554	553	485	461
24.06.03	21:00:00	435	-	325	-
24.06.03	21:00:20	-	992	-	662
24.06.03	21:02:00	380	-	278	-

Table A- 5 Overflow Event – 27th June 2003

Date	Time	$COD_{tot,eq}$ UV-VIS Values	COD_{tot} Lab Values	TSS_{eq} UV-VIS Values	TSS_{eq} Lab Values
[dd.mm.yy]	[hh:mm:ss]		[mg/l]		
27.06.03	12:13:00	434	-	243	-
27.06.03	12:15:00	409	364	227	245
27.06.03	12:16:00	398	-	232	-
27.06.03	12:16:20	-	296	-	274
27.06.03	12:17:00	408	-	221	-
27.06.03	12:17:40	-	307	-	256
27.06.03	12:18:00	404	-	223	-
27.06.03	12:19:00	-	307	-	265
27.06.03	12:20:00	407	-	224	-
27.06.03	12:20:20	-	307	-	256
27.06.03	12:21:00	407	-	211	-
27.06.03	12:21:40	-	341	-	244
27.06.03	12:22:00	409	-	204	-
27.06.03	12:23:00	425	307	206	237
27.06.03	12:24:00	419	-	202	-
27.06.03	12:24:20	-	307	-	217
27.06.03	12:25:00	422	-	208	-
27.06.03	12:25:40	-	284	-	196
27.06.03	12:26:00	423	-	207	-
27.06.03	12:27:00	432	330	216	183
27.06.03	12:28:00	426	-	211	-
27.06.03	12:28:20	-	330	-	236
27.06.03	12:29:00	415	-	202	-
27.06.03	12:29:40	-	239	-	207
27.06.03	12:30:00	403	-	190	-
27.06.03	12:31:00	-	273	-	206
27.06.03	12:32:00	386	-	178	-
27.06.03	12:32:20	-	284	-	185
27.06.03	12:33:00	394	-	179	-
27.06.03	12:33:40	-	262	-	160
27.06.03	12:34:00	410	-	196	-
27.06.03	12:35:00	418	262	205	163
27.06.03	12:36:00	467	-	235	-
27.06.03	12:36:20	-	262	-	138
27.06.03	12:37:40	-	262	-	167
27.06.03	12:38:00	554	-	313	-
27.06.03	12:39:00	583	284	336	207
27.06.03	12:40:00	854	-	538	-
27.06.03	12:40:20	-	284	-	207
27.06.03	12:41:00	999	-	626	-
27.06.03	12:41:40	-	535	-	264
27.06.03	12:42:00	983	-	600	-
27.06.03	12:43:00	-	683	-	587
27.06.03	12:44:00	735	-	429	-
27.06.03	12:44:20	-	478	-	342
27.06.03	12:45:00	653	-	376	-

Table A- 6 Overflow Event – 1st July 2003

Date	Time	$COD_{tot,eq}$ UV-VIS Values	COD_{tot} Lab Values	TSS_{eq} UV-VIS Values	TSS_{eq} Lab Values
[dd.mm.yy]	[hh:mm:ss]	[mg/l]			
01.07.03	23:50:00	417	-	201	-
01.07.03	23:51:00	410	464	199	209
01.07.03	23:52:00	400	-	194	-
01.07.03	23:52:20	-	430	-	246
01.07.03	23:53:00	415	-	205	-
01.07.03	23:53:40	-	464	-	252
01.07.03	23:54:00	459	-	226	-
01.07.03	23:55:00	480	453	224	259
01.07.03	23:56:00	497	-	238	-
01.07.03	23:56:20	-	419	-	286
01.07.03	23:57:00	455	-	216	-
01.07.03	23:57:40	-	350	-	242
01.07.03	23:58:00	434	-	202	-
01.07.03	23:59:00	426	317	199	284
02.07.03	00:00:00	424	-	201	-
02.07.03	00:00:20	-	328	-	215
02.07.03	00:01:40	-	350	-	219
02.07.03	00:02:00	417	-	195	-
02.07.03	00:03:00	410	317	188	190
02.07.03	00:04:00	393	-	175	-
02.07.03	00:04:20	-	328	-	195
02.07.03	00:05:00	378	-	168	-
02.07.03	00:05:40	-	317	-	205
02.07.03	00:06:00	361	-	158	-
02.07.03	00:07:00	-	294	-	177
02.07.03	00:08:00	428	-	212	-
02.07.03	00:08:20	-	283	-	165
02.07.03	00:09:00	737	-	485	-
02.07.03	00:09:40	-	260	-	161
02.07.03	00:10:00	573	-	335	-
02.07.03	00:11:00	410	260	199	133
02.07.03	00:12:00	502	-	348	-
02.07.03	00:12:20	-	283	-	152
02.07.03	00:13:40	-	430	-	339
02.07.03	00:14:00	830	-	488	-
02.07.03	00:15:00	689	747	390	681
02.07.03	00:16:00	551	-	308	-
02.07.03	00:16:20	-	566	-	376
02.07.03	00:17:00	477	-	263	-
02.07.03	00:17:40	-	373	-	226
02.07.03	00:18:00	474	-	293	-
02.07.03	00:19:00	-	464	-	370
02.07.03	00:20:20	-	566	-	487
02.07.03	00:22:00	438	-	365	-

Table A- 7 Overflow Event – 17th July 2003

Date	Time	$COD_{tot,eq}$ UV-VIS Values	COD_{tot} Lab Values	TSS_{eq} UV-VIS Values	TSS_{eq} Lab Values
[dd.mm.yy]	[hh:mm:ss]	[mg/l]			
17.07.03	20:06:00	631	-	323	-
17.07.03	20:08:00	-	552	-	374
17.07.03	20:09:00	531	-	299	-
17.07.03	20:09:20	-	594	-	483
17.07.03	20:10:00	621	-	593	-
17.07.03	20:10:40	-	435	-	393
17.07.03	20:12:00	190	318	99	243
17.07.03	20:13:00	250	-	202	-
17.07.03	20:13:20	-	276	-	285
17.07.03	20:14:00	566	-	616	-
17.07.03	20:14:40	-	254	-	276
17.07.03	20:15:00	551	-	538	-
17.07.03	20:16:00	588	254	568	276
17.07.03	20:17:20	-	424	-	466
17.07.03	20:18:00	671	-	778	-
17.07.03	20:18:40	-	276	-	432
17.07.03	20:20:00	-	169	-	251
17.07.03	20:21:00	193	-	104	-
17.07.03	20:21:20	-	191	-	223
17.07.03	20:22:00	188	-	96	-
17.07.03	20:22:40	-	276	-	241
17.07.03	20:23:00	202	-	117	-
17.07.03	20:24:00	197	180	110	169
17.07.03	20:25:00	198	-	109	-
17.07.03	20:25:20	-	180	-	189
17.07.03	20:26:00	197	-	112	-
17.07.03	20:26:40	-	191	-	170
17.07.03	20:27:00	276	-	257	-
17.07.03	20:28:00	250	191	204	216
17.07.03	20:29:00	479	-	514	-
17.07.03	20:29:20	-	201	-	208
17.07.03	20:30:40	-	254	-	166
17.07.03	20:31:00	176	-	81	-
17.07.03	20:32:00	205	424	116	208
17.07.03	20:33:00	210	-	128	-
17.07.03	20:33:20	-	169	-	186
17.07.03	20:34:00	187	-	105	-
17.07.03	20:34:40	-	169	-	218
17.07.03	20:35:00	363	-	387	-
17.07.03	20:36:00	-	148	-	178
17.07.03	20:37:00	266	-	242	-
17.07.03	20:37:20	-	159	-	170
17.07.03	20:38:00	411	-	426	-

Table A- 8 Overflow Event – 23rd July 2003 – Part 1

date	Time	$COD_{tot,eq}$ UV-VIS Values	COD_{tot} Lab Values	TSS_{eq} UV-VIS Values	TSS_{eq} Lab Values
[dd.mm.yy]	[hh:mm:ss]		[mg/l]		
23.07.03	01:07:00	582	-	220	-
23.07.03	01:08:00	-	249	-	188
23.07.03	01:09:00	552	-	190	-
23.07.03	01:09:20	-	320	-	161
23.07.03	01:10:00	537	-	190	-
23.07.03	01:10:40	-	320	-	135
23.07.03	01:11:00	490	-	165	-
23.07.03	01:12:00	446	320	147	117
23.07.03	01:13:00	422	-	140	-
23.07.03	01:13:20	-	285	-	127
23.07.03	01:14:00	569	-	279	-
23.07.03	01:14:40	-	724	-	530
23.07.03	01:15:00	692	-	398	-
23.07.03	01:16:00	453	641	190	411
23.07.03	01:17:00	433	-	209	-
23.07.03	01:17:20	-	344	-	199
23.07.03	01:18:00	719	-	603	-
23.07.03	01:18:40	-	415	-	199
23.07.03	01:20:00	682	665	408	700
23.07.03	01:21:00	558	-	398	-
23.07.03	01:21:20	-	1 443	-	1 040
23.07.03	01:22:00	504	-	333	-
23.07.03	01:22:40	-	665	_	610
23.07.03	01:23:00	196	-	131	-
23.07.03	01:24:00	139	392	57	365
23.07.03	01:25:20	-	344	-	310
23.07.03	01:26:00	172	-	98	-
23.07.03	01:26:40	-	308	-	272
23.07.03	01:27:00	168	-	87	-
23.07.03	01:28:00	163	273	86	256
23.07.03	01:29:00	170	-	88	-
23.07.03	01:29:20	-	261	-	264
23.07.03	01:30:00	169	-	93	-
23.07.03	01:30:40	-	237	-	248
23.07.03	01:31:00	209	-	149	-
23.07.03	01:32:00	182	261	105	210
23.07.03	01:33:00	178	-	96	-
23.07.03	01:33:20	-	237	-	206
23.07.03	01:34:00	177	-	97	-
23.07.03	01:34:40	-	237	-	205
23.07.03	01:35:00	189	-	114	-
23.07.03	01:36:00	157	178	66	166
23.07.03	01:37:00	175	-	93	-
23.07.03	01:37:20	-	190	-	189
23.07.03	01:38:00	186	-	108	-
23.07.03	01:39:00	183	-	101	-

Table A- 9 Overflow Event – 23rd July 2003 – Part 2

Date	Time	$COD_{tot,eq}$ UV-VIS Values	COD_{tot} Lab Values	TSS_{eq} UV-VIS Values	TSS_{eq} Lab Values
[dd.mm.yy]	[hh:mm:ss]	[mg/l]			
23.07.03	15:45:00	359	-	171	-
23.07.03	15:47:00	327	235	153	89
23.07.03	15:48:00	315	-	148	-
23.07.03	15:48:20	-	188	-	96
23.07.03	15:49:00	301	-	136	-
23.07.03	15:49:40	-	247	-	105
23.07.03	15:50:00	310	-	140	-
23.07.03	15:51:00	314	211	144	97
23.07.03	15:52:00	303	-	135	-
23.07.03	15:52:20	-	141	-	82
23.07.03	15:53:00	305	-	135	-
23.07.03	15:53:40	-	164	-	81
23.07.03	15:54:00	297	-	132	-
23.07.03	15:55:00	284	129	122	79
23.07.03	15:56:00	277	-	117	-
23.07.03	15:56:20	-	129	-	61
23.07.03	15:57:40	-	117	-	68
23.07.03	15:58:00	274	-	116	-
23.07.03	15:59:00	270	164	112	58
23.07.03	16:00:00	263	-	106	-
23.07.03	16:00:20	-	117	-	53
23.07.03	16:01:00	260	-	108	-
23.07.03	16:01:40	-	235	-	42
23.07.03	16:02:00	253	-	101	-
23.07.03	16:03:00	-	188	-	18
23.07.03	16:04:00	279	-	118	-
23.07.03	16:04:20	-	247	-	34
23.07.03	16:05:00	271	-	109	-
23.07.03	16:05:40	-	211	-	18
23.07.03	16:06:00	263	-	103	-
23.07.03	16:07:00	268	141	105	38
23.07.03	16:08:00	274	-	107	-
23.07.03	16:08:20	-	164	-	64
23.07.03	16:09:40	-	129	-	35
23.07.03	16:10:00	298	-	120	-
23.07.03	16:11:00	317	129	137	32
23.07.03	16:12:00	313	-	134	-
23.07.03	16:12:20	-	129	-	28
23.07.03	16:13:00	307	-	130	-
23.07.03	16:13:40	-	117	-	30
23.07.03	16:14:00	309	-	133	-
23.07.03	16:15:00	-	164	-	27
23.07.03	16:16:00	420	-	236	-
23.07.03	16:16:20	-	117	-	28
23.07.03	16:17:00	544	-	350	-

Table A- 10 Overflow Event – 25th July 2003

date	Time	$COD_{tot,eq}$ UV-VIS Values	COD_{tot} Lab Values	TSS_{eq} UV-VIS Values	TSS_{eq} Lab Values
[dd.mm.yy]	[hh:mm:ss]		[mg/l]		
25.07.03	02:12:00	259	-	141	-
25.07.03	02:14:00	224	175	115	84
25.07.03	02:15:00	219	-	104	-
25.07.03	02:15:20	-	186	-	59
25.07.03	02:16:00	220	-	105	-
25.07.03	02:16:40	-	117	-	62
25.07.03	02:17:00	211	-	101	-
25.07.03	02:18:00	223	105	116	81
25.07.03	02:19:20	-	105	-	78
25.07.03	02:20:40	-	117	-	61
25.07.03	02:21:00	213	-	101	-
25.07.03	02:22:00	202	70	92	46
25.07.03	02:23:00	197	-	85	-
25.07.03	02:23:20	-	82	-	37
25.07.03	02:24:00	189	-	80	-
25.07.03	02:24:40	-	70	-	26
25.07.03	02:25:00	186	-	79	-
25.07.03	02:26:00	-	58	-	13
25.07.03	02:27:00	177	-	69	-
25.07.03	02:27:20	-	70	-	19
25.07.03	02:28:00	171	-	63	-
25.07.03	02:28:40	-	58	-	3
25.07.03	02:29:00	170	-	62	-
25.07.03	02:30:00	173	23	64	4
25.07.03	02:31:00	174	-	63	-
25.07.03	02:31:20	-	23	-	4
25.07.03	02:32:40	-	35	-	1
25.07.03	02:33:00	180	-	69	-
25.07.03	02:34:00	194	23	74	2
25.07.03	02:35:00	208	-	86	-
25.07.03	02:35:20	-	47	-	4
25.07.03	02:36:00	200	-	78	-
25.07.03	02:36:40	-	35	-	2
25.07.03	02:37:00	204	-	86	-
25.07.03	02:38:00	-	47	-	1
25.07.03	02:39:00	209	-	96	-
25.07.03	02:39:20	-	47	-	37
25.07.03	02:40:00	208	-	92	-
25.07.03	02:40:40	-	58	-	58
25.07.03	02:41:00	210	-	91	-
25.07.03	02:42:00	211	70	92	70
25.07.03	02:43:00	215	-	95	-
25.07.03	02:43:20	-	58	-	65
25.07.03	02:45:00	248	-	127	-

Table A- 11 Overflow Event – 28th July 2003

Date	Time	$COD_{tot,eq}$ UV-VIS Values	COD_{tot} Lab Values	TSS_{eq} UV-VIS Values	TSS_{eq} Lab Values
[dd.mm.yy]	[hh:mm:ss]	[mg/l]			
28.07.03	19:00:00	444	-	192	-
28.07.03	19:01:00	-	303	-	152
28.07.03	19:02:00	398	-	162	-
28.07.03	19:02:20	-	303	-	159
28.07.03	19:03:00	411	-	169	-
28.07.03	19:03:40	-	385	-	203
28.07.03	19:04:00	454	-	189	-
28.07.03	19:05:00	515	419	225	215
28.07.03	19:06:00	528	-	232	-
28.07.03	19:06:20	-	443	-	222
28.07.03	19:07:40	-	548	-	318
28.07.03	19:08:00	775	-	377	-
28.07.03	19:09:00	793	606	494	348
28.07.03	19:10:00	581	-	273	-
28.07.03	19:10:20	-	513	-	323
28.07.03	19:11:00	528	-	251	-
28.07.03	19:11:40	-	385	-	249
28.07.03	19:12:00	506	-	255	-
28.07.03	19:13:00	-	350	-	226
28.07.03	19:14:00	603	-	507	-
28.07.03	19:14:20	-	326	-	215
28.07.03	19:15:00	550	-	481	-
28.07.03	19:15:40	-	315	-	209
28.07.03	19:16:00	626	-	679	-
28.07.03	19:17:00	481	350	416	212
28.07.03	19:18:00	521	-	349	-
28.07.03	19:18:20	-	291	-	181
28.07.03	19:19:40	-	256	-	142
28.07.03	19:21:00	480	210	464	128
28.07.03	19:22:00	501	-	453	-
28.07.03	19:22:20	-	256	-	139
28.07.03	19:23:00	489	-	403	-
28.07.03	19:23:40	-	443	-	282
28.07.03	19:24:00	446	-	346	-
28.07.03	19:25:00	541	315	529	215
28.07.03	19:26:20	-	256	-	167
28.07.03	19:27:00	410	-	269	-
28.07.03	19:27:40	-	221	-	174
28.07.03	19:28:00	402	-	225	-
28.07.03	19:29:00	420	233	237	162
28.07.03	19:30:00	418	-	238	-
28.07.03	19:30:20	-	198	-	216
28.07.03	19:31:00	353	-	162	-

DATA OF 2ND AND 3RD MEASUREMENT CAMPAIGN

Table A- 12 Overview of 2nd Measurement Campaign

Date	Sampling Time	$COD_{eq,tot}$ UV-VIS values	COD_{tot} lab values	TSS_{eq} UV-VIS values	TSS lab values
[dd.mm.yy]	[hh:mm]	[mg/l]			
03.09.2003	06:00	382	429	86	106
03.09.2003	07:00	600	639	202	254
03.09.2003	08:00	844	925	344	278
03.09.2003	09:00	912	1 101	422	306
03.09.2003	10:00	818	925	355	292
03.09.2003	11:00	721	793	300	250
03.09.2003	12:00	729	873	335	292
03.09.2003	13:00	710	991	311	310
03.09.2003	14:00	699	947	319	262
03.09.2003	15:00	724	925	321	370
03.09.2003	16:00	648	866	263	360
03.09.2003	17:00	661	910	285	266
03.09.2003	18:00	742	844	373	200
03.09.2003	19:00	639	833	280	140
03.09.2003	20:00	632	866	271	108
03.09.2003	21:00	637	932	297	118
03.09.2003	22:00	542	647	215	108
03.09.2003	23:00	514	570	201	114
04.09.2003	00:00	494	603	176	102
04.09.2003	01:00	464	493	147	106
04.09.2003	02:00	427	384	129	78
04.09.2003	03:00	327	263	79	70
04.09.2003	04:00	293	208	64	60
04.09.2003	05:00	263	164	59	48
04.09.2003	06:00	408	285	104	118

Table A- 13 COD_{tot} of 3rd Measurement Campaign

	$COD_{tot,eq}$ Pontoon	$COD_{tot,eq}$ Sampler	$COD_{tot,eq}$ Scooping	COD_{tot} Sampler	COD_{tot} Scooping	COD_{tot} Sampler	COD_{tot} Scooping
	1st UV-VIS Probe	2nd UV-VIS Probe	2nd UV-VIS Probe	Lab	Lab	Lab After Defrost	Lab After Defrost
				[mg/l]			
06:00	274	269	264	293	304	-	-
07:00	432	435	419	-	-	546	466
08:00	757	721	692	-	-	773	784
09:00	716	726	695	833	890	-	-
10:00	681	652	636	-	-	717	739
11:00	598	592	580	-	-	739	784
12:00	623	633	616	946	890	-	-
13:00	562	571	555	-	-	785	1 032
14:00	502	522	500	-	-	684	751
15:00	528	559	548	789	833	-	-
16:00	551	555	541	-	-	830	1 110
17:00	516	521	508	-	-	785	830
18:00	487	517	480	789	732	-	-
19:00	477	494	476	-	-	554	796
20:00	721	707	694	-	-	1 154	1 280
21:00	541	551	535	811	823	-	-
22:00	493	522	493	-	-	853	784
23:00	409	424	400	-	-	669	669
00:00	446	460	438	568	568	-	-
01:00	318	419	308	-	-	415	427
02:00	269	263	257	-	-	346	335
03:00	230	221	214	239	257	-	-
04:00	203	185	189	-	-	91	80
05:00	205	193	188	-	-	68	57
06:00	232	220	215	236	236	-	-

Table A- 14 TSS of 3rd Measurement Campaign

	TSS_{eq} Pontoon	TSS_{eq} Sampler	TSS_{eq} Scooping	TSS Sampler	TSS Scooping	TSS Sampler	TSS Scooping
	1st UV-VIS Probe	2nd UV-VIS Probe	2nd UV-VIS Probe	Lab	Lab	Lab After Defrost	Lab After Defrost
	[mg/l]						
06:00	68	84	82	90	63	-	-
07:00	148	168	161	-	-	20	10
08:00	333	316	305	-	-	32	28
09:00	302	323	308	349	345	-	-
10:00	299	299	292	-	-	212	206
11:00	282	292	286	-	-	418	420
12:00	282	308	298	275	283	-	-
13:00	249	273	264	-	-	256	262
14:00	215	247	232	-	-	244	256
15:00	238	272	265	251	266	-	-
16:00	243	256	248	-	-	308	300
17:00	218	235	228	-	-	212	240
18:00	215	255	227	288	288	-	-
19:00	198	223	213	-	-	184	212
20:00	373	374	368	-	-	398	334
21:00	249	268	262	279	282	-	-
22:00	219	251	237	-	-	324	334
23:00	160	182	167	-	-	238	246
00:00	173	197	181	199	221	-	-
01:00	90	327	98	-	-	70	62
02:00	71	80	75	-	-	68	62
03:00	54	64	58	33	38	-	-
04:00	53	53	59	-	-	46	64
05:00	39	49	45	-	-	68	64
06:00	50	58	54	40	54	-	-

Table A- 15 COD_{sol} of 3rd Measurement Campaign

	$COD_{sol,eq}$ Pontoon	$COD_{sol,eq}$ Sampler	$COD_{sol,eq}$ Scooping	COD_{sol} Sampler	COD_{sol} Scooping	COD_{sol} Sampler	COD_{sol} Scooping
	1st UV-VIS Probe	2nd UV-VIS Probe	2nd UV-VIS Probe	Lab	Lab	Lab After Defrost	Lab After Defrost
				[mg/l]			
06:00	151	138	138	117	117	-	-
07:00	202	190	190	-	-	168	168
08:00	282	266	264	-	-	250	259
09:00	253	247	245	239	241	-	-
10:00	232	200	199	-	-	232	220
11:00	187	176	176	-	-	269	294
12:00	196	184	183	325	343	-	-
13:00	184	174	173	-	-	278	366
14:00	181	174	171	-	-	296	290
15:00	190	187	187	310	308	-	-
16:00	204	196	195	-	-	314	322
17:00	192	184	182	-	-	327	327
18:00	181	176	172	243	241	-	-
19:00	180	173	171	-	-	286	287
20:00	217	205	205	-	-	342	355
21:00	191	183	181	225	230	-	-
22:00	182	179	174	-	-	323	316
23:00	173	166	163	-	-	214	212
00:00	191	184	183	180	178	-	-
01:00	163	118	153	-	-	164	175
02:00	141	131	131	-	-	150	146
03:00	121	108	107	103	97	-	-
04:00	104	92	92	-	-	113	113
05:00	123	110	110	-	-	109	125
06:00	139	125	126	77	70	-	-

TABLES OF DIFFERENT REGRESSION METHODS AND ITS VERIFICATIONS

Table A- 16 COD_{tot} – Simple Linear Regression (SLR)

Analysed Wavelength Range	Resulting Equation	Correlation Coefficient Based on 2nd and 3rd Measurement Campaign	Sum of Residuals of 2nd and 3rd Measurement Campaign	Correlation Coefficient of Storm Events[1)]	Sum of Residuals of Storm Events[1)]
[nm]			[mg/l]		[mg/l]
200 - 750	13.02·λ(625)+156.6	0.968	1 876	0.894	3 295
230 - 500	10.4·λ(492.5)+127.16	0.967	1 988	0.920	2 548
250 - 277.5	4.4·λ(260)-84.03	0.958	2 250	0.912	967
254, 436	9.11·λ(436)+110.94	0.966	2 051	0.932	2 090
(254-436)	7.46·λ(254-436)-250.43	0.935	2 929	0.781	2 184
250 - 277.5, 436	9.11·λ(436)+110.94	0.966	2 051	0.932	2 090
230 - 240	3.24·λ(230)-263.44	0.950	2 444	0.871	1 823
230 - 240, 436	9.11·λ(436)+110.94	0.966	2 051	0.932	2 090
240 - 250	4.03·λ(250)-115.8	0.954	2 348	0.902	1 048
240 - 250, 436	9.11·λ(436)+110.94	0.966	2 051	0.932	2 090
250 - 260	4.4·λ(260)-84.03	0.958	2 250	0.912	967
250 - 260, 436	9.11·λ(436)+110.94	0.966	2 051	0.932	2 090
260 - 270	4.4·λ(260)-84.03	0.958	2 250	0.912	967
260 - 270, 436	9.11·λ(436)+110.94	0.966	2 051	0.932	2 090
270 - 280	4.56·λ(270)-76.93	0.956	2 328	0.920	919
270 - 280, 436	9.11·λ(436)+110.94	0.966	2 051	0.932	2 090
280 - 290	4.71·λ(280)-68.1	0.953	2 411	0.924	884
280 - 290, 436	9.11·λ(436)+110.94	0.966	2 051	0.932	2 090
290 - 300	5.41·λ(300)-28.61	0.956	2 345	0.933	935
290 - 300, 436	9.11·λ(436)+110.94	0.966	2 051	0.932	2 090
300 - 310	5.89·λ(310)+7.64	0.961	2 190	0.939	1 140
300 - 310, 436	9.11·λ(436)+110.94	0.966	2 051	0.932	2 090
310 - 320	6.22·λ(320)+30.04	0.963	2 128	0.941	1 251
310 - 320, 436	6.22·λ(320)+30.04	0.963	2 128	0.941	1 251
320 - 330	6.49·λ(330)+44.39	0.963	2 121	0.944	1 325
320 - 330, 436	9.11·λ(436)+110.94	0.966	2 051	0.932	2 090
330 - 340	6.63·λ(335)+51.22	0.963	2 118	0.944	1 367
330 - 340, 436	9.11·λ(436)+110.94	0.966	2 051	0.932	2 090
340 - 350	6.77·λ(340)+56.89	0.963	2 120	0.945	1 406
340 - 350, 436	9.11·λ(436)+110.94	0.966	2 051	0.932	2 090
350 - 360	7.28·λ(360)+74.14	0.963	2 123	0.944	1 534
350 - 360, 436	9.11·λ(436)+110.94	0.966	2 051	0.932	2 090
360 - 370	7.54·λ(370)+82.6	0.963	2 121	0.943	1 609
360 - 370, 436	9.11·λ(436)+110.94	0.966	2 051	0.932	2 090
370 - 380	7.66·λ(375)+81.32	0.963	2 116	0.942	1 634
370 - 380, 436	9.11·λ(436)+110.94	0.966	2 051	0.932	2 090

[1)] 2 storm events, 2004-07-06: 16^{48} – 18^{23} (5 samples), 2004-07-22: 16^{42} – 17^{27} (6 samples)

Table A- 17 COD_{sol} – Simple Linear Regression (SLR)

Analysed Wavelength Range	Resulting Equation	Correlation Coefficient Based on 2nd and 3rd Measurement Campaign	Sum of Residuals of 2nd and 3rd Measurement Campaign	Correlation Coefficient of Storm Events[1)]	Sum of Residuals of Storm Events[1)]
[nm]			[mg/l]		[mg/l]
200 - 750	1.83·λ(202.5)-475.42	0.859	1 478	0.774	1 561
230 - 500	1.1·λ(230)-123.25	0.851	1 482	0.833	566
240 - 247.5, 272.5 - 290	1.32·λ(247.5)-72.79	0.842	1 486	0.831	412
240 - 247.5, 272.5 - 290, 436	1.32·λ(247.5)-72.79	0.842	1 486	0.831	412
254, 436	1.4·λ(254)-64.9	0.852	1 598	0.823	411
(254-436)	2.56·λ(254-436)-122.17	0.831	1 802	0.817	609
230 - 240	1.1·λ(230)-123.25	0.851	1 482	0.833	566
230 - 240, 436	1.1·λ(230)-123.25	0.851	1 482	0.833	566
240 - 250	1.35·λ(250)-69.82	0.845	1 469	0.829	419
240 - 250, 436	1.35·λ(250)-69.82	0.845	1 469	0.829	419
250 - 260	1.47·λ(260)-58.39	0.854	1 441	0.822	444
250 - 260, 436	1.47·λ(260)-58.39	0.854	1 441	0.822	444
260 - 270	1.47·λ(260)-58.39	0.854	1 441	0.822	444
260 - 270, 436	1.47·λ(260)-58.39	0.854	1 441	0.822	444
270 - 280	1.52·λ(270)-55.74	0.849	1 457	0.812	421
270 - 280, 436	1.52·λ(270)-55.74	0.849	1 457	0.812	421
280 - 290	1.67·λ(290)-48.43	0.840	1 471	0.799	419
280 - 290, 436	1.67·λ(290)-48.43	0.840	1 471	0.799	419
290 - 300	1.7·λ(292.5)-46.66	0.841	1 476	0.797	427
290 - 300, 436	1.7·λ(292.5)-46.66	0.841	1 476	0.797	427
300 - 310	1.8·λ(300)-39.4	0.847	1 462	0.793	475
300 - 310, 436	1.8·λ(300)-39.4	0.847	1 462	0.793	475
310 - 320	1.95·λ(310)-25.72	0.858	1 429	0.782	615
310 - 320, 436	1.95·λ(310)-25.72	0.858	1 429	0.782	615
320 - 330	2.05·λ(320)-17.87	0.861	1 424	0.772	673
320 - 330, 436	2.05·λ(320)-17.87	0.861	1 424	0.772	673
330 - 340	2.19·λ(335)-10.73	0.861	1 419	0.757	729
330 - 340, 436	2.19·λ(335)-10.73	0.861	1 419	0.757	729
340 - 350	2.32·λ(350)-5.06	0.861	1 422	0.747	777
340 - 350, 436	2.32·λ(350)-5.06	0.861	1 422	0.747	777
350 - 360	2.32·λ(350)-5.06	0.861	1 422	0.747	777
350 - 360, 436	2.32·λ(350)-5.06	0.861	1 422	0.747	777
360 - 370	2.46·λ(367.5)-0.43	0.860	1 418	0.737	822
360 - 370, 436	2.46·λ(367.5)-0.43	0.860	1 418	0.737	822
370 - 380	2.48·λ(370)+0.21	0.860	1 415	0.736	831
370 - 380, 436	2.48·λ(370)+0.21	0.860	1 415	0.736	831

[1)] 2 storm events, 2004-07-06: 16^{48} – 18^{23} (5 samples), 2004-07-22: 16^{42} – 17^{27} (6 samples)

Table A- 18 TSS – Simple Linear Regression (SLR)

Analysed Wavelength Range	Resulting Equation	Correlation Coefficient Based on 2nd and 3rd Measurement Campaign	Sum of Residuals of 2nd and 3rd Measurement Campaign	Correlation Coefficient of Storm Events[1)]	Sum of Residuals of Storm Events[1)]
[nm]			[mg/l]		[mg/l]
200 - 750	1.62·λ(325)+55.73	0.822	1 951	0.873	1 040
380 - 750	2.75·λ(512.5)+79.81	0.808	1 942	0.879	896
600 - 647.5	3.28·λ(622.5)+86.66	0.804	1 927	0.865	870
380 - 390	2.04·λ(390)+68.68	0.818	1 948	0.888	960
390 - 400	2.04·λ(390)+68.68	0.818	1 948	0.888	960
400 - 410	2.1·λ(400)+70.33	0.817	1 952	0.888	950
410 - 420	2.19·λ(415)+72.21	0.816	1 950	0.888	935
420 - 430	2.27·λ(430)+74.58	0.814	1 945	0.887	924
430 - 440	2.33·λ(440)+74.67	0.813	1 949	0.887	921
440 - 450	2.39·λ(450)+75.62	0.812	1 948	0.887	916
450 - 460	2.42·λ(455)+77.23	0.812	1 944	0.886	914
460 - 470	2.46·λ(460)+76.69	0.812	1 945	0.886	912
470 - 480	2.52·λ(472.5)+78.26	0.811	1 943	0.884	909
480 - 490	2.61·λ(487.5)+78.18	0.811	1 937	0.884	901
490 - 500	2.66·λ(497.5)+80.61	0.810	1 938	0.881	900
500 - 510	2.69·λ(502.5)+80.4	0.809	1 939	0.880	898
510 - 520	2.75·λ(512.5)+79.81	0.808	1 942	0.879	896
520 - 530	2.82·λ(525)+81.81	0.809	1 934	0.878	889
530 - 540	2.87·λ(535)+81.28	0.808	1 935	0.877	886
540 - 550	2.92·λ(545)+82.43	0.807	1 937	0.876	885
550 - 560	2.98·λ(557.5)+83.44	0.807	1 933	0.873	882
560 - 570	3.04·λ(570)+83.83	0.807	1 930	0.872	879
570 - 580	3.04·λ(570)+83.83	0.807	1 930	0.872	879
580 - 590	3.13·λ(587.5)+84.19	0.807	1 924	0.870	874
590 - 600	3.15·λ(592.5)+85.66	0.807	1 921	0.869	875
600 - 610	3.22·λ(607.5)+86.31	0.807	1 919	0.867	875
610 - 620	3.23·λ(610)+87.19	0.806	1 921	0.867	873
620 - 630	3.28·λ(622.5)+86.66	0.804	1 927	0.865	870
630 - 640	3.33·λ(632.5)+87.48	0.806	1 915	0.864	865
640 - 650	3.38·λ(642.5)+89.07	0.806	1 915	0.862	866
650 - 660	3.41·λ(650)+87.75	0.805	1 916	0.861	863
660 - 670	3.47·λ(662.5)+89.58	0.805	1 913	0.861	859
670 - 680	3.5·λ(672.5)+91.14	0.803	1 917	0.860	860
680 - 690	3.54·λ(680)+92.45	0.805	1 903	0.857	862
690 - 700	3.57·λ(690)+94.51	0.803	1 909	0.855	863
700 - 710	3.66·λ(710)+96.44	0.802	1 907	0.855	860
710 - 720	3.67·λ(712.5)+95.39	0.803	1 898	0.854	854
720 - 730	3.72·λ(722.5)+98.32	0.803	1 899	0.852	858
730 - 740	3.75·λ(730)+98.74	0.805	1 882	0.851	859
740 - 750	3.81·λ(750)+100	0.801	1 893	0.851	861

[1)] 2 storm events, 2004-07-06: 16^{48} – 18^{23} (5 samples), 2004-07-22: 16^{42} – 17^{27} (6 samples)

Table A- 19 COD_{tot} – Least Median Squared Linear Regression (LMS)

Analysed Wavelength Range	Resulting Equation	Correlation Coefficient Based on 2nd and 3rd Measurement Campaign	Sum of Residuals of 2nd and 3rd Measurement Campaign	Correlation Coefficient of Storm Events[1)]	Sum of Residuals of Storm Events[1)]
[nm]			[mg/l]		[mg/l]
200 - 750	-0.592·λ(200)-3.8861·λ(210)+ 0.7499·λ(215)+3.0989·λ(22.5)+ 2.2458·λ(277.5)-1.5882·λ(337.5)- 7.7411·λ(747.5)+20.9904·λ(750)+454.3166	0.961	3 014	0.827	3 942
230 - 500	0.52·λ(230)+0.7579·λ(237.5)+ 5.2096·λ(327.5)-136.0443	0.961	2 237	0.933	973
250 - 277.5	4.325·λ(250)-3.6141·λ(260)+4.61·λ(277.5) -230.7933	0.950	2 624	0.914	1 266
254, 436	1.5819·λ(254)+7.4524·λ(436)-39.9939	0.965	2 097	0.939	1 411
(254-436)	9.0933·λ(254-436)-407.1355	0.935	2 904	0.781	2 820
250 - 277.5, 436	6.3775·λ(257.5)-2.2846·λ(272.5)+ 2.0154·λ(436)-150.3444	0.962	2 292	0.919	1 103
230 - 240	2.1857·λ(230)-3.6095·λ(235)+ 5.9734·λ(240)-315.8809	0.949	2 608	0.891	1 662
230 - 240, 436	0.4048·λ(230)+2.7359·λ(240)+ 3.2931·λ(436)-209.9011	0.957	2 441	0.921	1 165
240 - 250	0.5361·λ(240)+4.3526·λ(250)-245.4022	0.953	2 532	0.901	1 399
240 - 250, 436	3.7188·λ(250)+2.6341·λ(436)-166.8778	0.959	2 383	0.924	1 086
250 - 260	4.9299·λ(250)-0.0051·λ(260)-237.4541	0.954	2 514	0.902	1 368
250 - 260, 436	4.4505·λ(250)+1.7152·λ(436)-148.9255	0.961	2 341	0.924	1 063
260 - 270	5.298·λ(260)-187.2384	0.958	2 401	0.912	1 171
260 - 270, 436	4.4505·λ(260)+1.7152·λ(436)-148.9255	0.961	2 341	0.924	1 063
270 - 280	3.0719·λ(270)+2.5956·λ(280)-185.9633	0.955	2 515	0.922	1 087
270 - 280, 436	3.4378·λ(270)+1.5131·λ(280)+ 1.292·λ(436)-157.4674	0.957	2 443	0.928	1 033
280 - 290	8.3905·λ(280)-2.6939·λ(287.5)-189.5193	0.954	2 551	0.923	1 085
280 - 290, 436	5.4652·λ(290)+1.2113·λ(436)-143.5051	0.955	2 549	0.933	992
290 - 300	3.9712·λ(290)+2.3472·λ(300)-154.8677	0.954	2 571	0.930	1 011
290 - 300, 436	7.2643·λ(290)-7.3561·λ(300)+ 10.0816·λ(436)-12.2105	0.964	2 251	0.937	1 668
300 - 310	6.756·λ(302.5)-128.7648	0.958	2 413	0.934	964
300 - 310, 436	5.2902·λ(302.5)-4.5987·λ(310)+ 9.3283·λ(436)-4.8197	0.964	2 241	0.936	1 774
310 - 320	7.2232·λ(310)-103.5211	0.961	2 368	0.939	1 032
310 - 320, 436	0.2436·λ(310)+10.307·λ(436)+36.788	0.966	2 055	0.933	2 116
320 - 330	7.5878·λ(320)-73.3513	0.963	2 310	0.941	1 131
320 - 330, 436	-1.6761·λ(330)+12.9964·λ(436)+59.7399	0.966	2 045	0.926	2 377
330 - 340	-3.7447·λ(330)+11.922·λ(335)-43.8367	0.963	2 307	0.945	1 290
330 - 340, 436	-1.6761·λ(330)+12.9964·λ(436)+59.7399	0.966	2 045	0.926	2 377
340 - 350	5.1916·λ(340)+2.9368·λ(350)-21.9102	0.963	2 177	0.945	1 347
340 - 350, 436	-3.6259·λ(340)+15.826·λ(436)+60.2853	0.966	2 190	0.922	2 592
350 - 360	8.5556·λ(357.5)-7.1747	0.963	2 169	0.944	1 505
350 - 360, 436	8.4181·λ(352.5)-9.9736	0.963	2 172	0.944	1 449
360 - 370	8.8477·λ(367.5)+2.0685	0.963	2 171	0.943	1 579
360 - 370, 436	8.327·λ(360)+9.9533	0.963	2 096	0.944	1 507
370 - 380	-1.3194·λ(377.5)+10.5298·λ(380)+2.7739	0.963	2 151	0.942	1 670
370 - 380, 436	8.9888·λ(372.5)+3.6096	0.963	2 154	0.942	1 608

[1)] 2 storm events, 2004-07-06: 16^{48} – 18^{23} (5 samples), 2004-07-22: 16^{42} – 17^{27} (6 samples)

Table A- 20 COD_{sol} – Least Median Squared Linear Regression (LMS)

Analysed Wavelength Range	Resulting Equation	Correlation Coefficient Based on 2nd and 3rd Measurement Campaign	Sum of Residuals of 2nd and 3rd Measurement Campaign	Correlation Coefficient of Storm Events[1)]	Sum of Residuals of Storm Events[1)]
[nm]			[mg/l]		[mg/l]
200 - 750	0.9432·λ(200)+1.3301·λ(202.5)+ 0.2785·λ(215)-0.3099·λ(257.5)+ 0.7863·λ(367.5)-7.0945·λ(670)+ 4.8925·λ(675)-643.9902	0.848	1 490	0.726	2 239
230 - 500	1.9423·λ(230)-1.4221·λ(295)+ 0.3187·λ(490)-178.6094	0.853	1 496	0.836	864
240 - 247.5, 272.5 - 290	0.1513·λ(240)+2.6155·λ(272.5)- 1.3384·λ(290)-64.8303	0.851	1 387	0.822	442
240 - 247.5, 272.5 - 290, 436	2.2505·λ(272.5)-0.9993·λ(290)+ 0.4768·λ(436)-49.8658	0.854	1 364	0.809	485
254, 436	0.3123·λ(254)+2.8471·λ(436)-20.3329	0.860	1 444	0.745	949
(254-436)	2.4372·λ(254-436)-118.6066	0.831	2 001	0.817	614
230 - 240	1.181·λ(240)-82.9713	0.835	1 654	0.831	411
230 - 240, 436	0.771·λ(240)+1.2405·λ(436)-48.5815	0.849	1 377	0.804	493
240 - 250	0.6654·λ(240)+0.5595·λ(250)-76.4798	0.840	1 638	0.830	395
240 - 250, 436	0.771·λ(240)+1.2405·λ(436)-48.5815	0.849	1 377	0.804	493
250 - 260	1.142·λ(250)+0.1512·λ(260)-66.7314	0.846	1 622	0.829	378
250 - 260, 436	1.1011·λ(250)+0.6427·λ(436)-53.9638	0.850	1 382	0.817	476
260 - 270	1.5414·λ(270)-55.5137	0.849	1 421	0.812	436
260 - 270, 436	1.5908·λ(267.5)-0.0707·λ(436)-57.6498	0.850	1 388	0.815	459
270 - 280	1.6161·λ(280)-52.9894	0.843	1 408	0.805	439
270 - 280, 436	1.2275·λ(280)+0.7513·λ(436)-38.0268	0.848	1 373	0.790	535
280 - 290	1.6161·λ(280)-52.9894	0.843	1 408	0.805	439
280 - 290, 436	-1.4415·λ(280)+2.8418·λ(290)+ 0.7193·λ(436)-30.2229	0.844	1 384	0.778	591
290 - 300	0.5289·λ(290)+1.2525·λ(300)-41.7392	0.845	1 425	0.795	477
290 - 300, 436	0.446·λ(290)+2.4296·λ(436)-9.3762	0.857	1 369	0.743	909
300 - 310	0.3847·λ(300)+1.5934·λ(310)-28.4399	0.856	1 356	0.784	635
300 - 310, 436	0.5818·λ(300)-0.8319·λ(310)+ 3.8414·λ(436)-4.823	0.858	1 439	0.716	1 164
310 - 320	2.0525·λ(320)-17.8669	0.861	1 421	0.772	675
310 - 320, 436	2.9113·λ(436)+10.5402	0.860	1 445	0.718	955
320 - 330	-0.8721·λ(320)+2.9821·λ(327.5)-12.98	0.861	1 467	0.761	681
320 - 330, 436	2.9606·λ(436)+11.7239	0.860	1 392	0.718	994
330 - 340	2.2302·λ(340)-8.6424	0.861	1 420	0.753	745
330 - 340, 436	2.9606·λ(436)+11.7239	0.860	1 392	0.718	994
340 - 350	2.2763·λ(345)-7.0598	0.861	1 420	0.750	761
340 - 350, 436	2.9606·λ(436)+11.7239	0.860	1 392	0.718	994
350 - 360	2.3449·λ(352.5)-4.1114	0.861	1 419	0.745	785
350 - 360, 436	3.0317·λ(436)+11.0892	0.860	1 358	0.718	1 025
360 - 370	2.5296·λ(370)-0.1634	0.860	1 380	0.736	858
360 - 370, 436	3.0799·λ(436)+11.9263	0.860	1 331	0.718	1 060
370 - 380	2.6463·λ(380)+0.5328	0.860	1 344	0.732	910
370 - 380, 436	3.0799·λ(436)+11.9263	0.860	1 331	0.718	1 060

[1)] 2 storm events, 2004-07-06: 16^{48} – 18^{23} (5 samples), 2004-07-22: 16^{42} – 17^{27} (6 samples)

Table A- 21 TSS – Least Median Squared Linear Regression (LMS)

Analysed Wavelength Range	Resulting Equation	Correlation Coefficient Based on 2nd and 3rd Measurement Campaign	Sum of Residuals of 2nd and 3rd Measurement Campaign	Correlation Coefficient of Storm Events[1)]	Sum of Residuals of Storm Events[1)]
[nm]			[mg/l]		[mg/l]
200 - 750	-0.5893·λ(207.5)+0.634·λ(212.5)-0.6836·λ(235)+3.3586·λ(377.5)+0.2478·λ(725)+127.1068	0.800	1 907	0.875	963
380 - 750	0.552·λ(380)+2.748·λ(697.5)+79.334	0.809	1 866	0.867	856
600 - 647.5	3.7926·λ(647.5)+76.9881	0.806	1 853	0.861	821
380 - 390	2.0358·λ(382.5)+62.3041	0.820	1 901	0.887	982
390 - 400	2.0839·λ(390)+62.8792	0.818	1 906	0.888	975
400 - 410	2.2078·λ(410)+64.8985	0.815	1 912	0.888	952
410 - 420	2.4204·λ(412.5)-0.1981·λ(417.5)+65.2264	0.815	1 912	0.888	949
420 - 430	-0.44·λ(422.5)+2.7815·λ(430)+68.8657	0.815	1 902	0.887	924
430 - 440	2.3325·λ(430)+68.5246	0.814	1 904	0.887	926
440 - 450	2.3977·λ(440)+68.4693	0.813	1 907	0.887	917
450 - 460	2.4766·λ(452.5)+70.155	0.813	1 898	0.886	911
460 - 470	2.5692·λ(467.5)+71.1803	0.811	1 901	0.884	906
470 - 480	2.5339·λ(472.5)+73.3743	0.811	1 898	0.884	912
480 - 490	2.9627·λ(487.5)+58.2334	0.811	1 828	0.884	870
490 - 500	3.0082·λ(495)+60.1411	0.811	1 826	0.881	868
500 - 510	3.0768·λ(505)+60.6494	0.810	1 822	0.880	865
510 - 520	3.1613·λ(517.5)+60.813	0.809	1 825	0.879	859
520 - 530	3.2438·λ(530)+61.4856	0.809	1 814	0.878	851
530 - 540	3.098·λ(540)+69.6316	0.809	1 839	0.876	869
540 - 550	3.0497·λ(550)+76.1392	0.809	1 881	0.874	874
550 - 560	3.1047·λ(560)+76.9429	0.808	1 883	0.873	871
560 - 570	3.1152·λ(562.5)+77.0311	0.810	1 872	0.873	870
570 - 580	3.201·λ(580)+77.5277	0.807	1 883	0.871	863
580 - 590	3.201·λ(580)+77.5277	0.807	1 883	0.871	863
590 - 600	3.641·λ(600)+66.661	0.808	1 798	0.868	827
600 - 610	3.6658·λ(605)+65.4125	0.807	1 802	0.867	826
610 - 620	3.4652·λ(610)+74.0963	0.806	1 829	0.867	844
620 - 630	3.7988·λ(630)+68.457	0.807	1 794	0.864	819
630 - 640	3.4468·λ(630)+81.3881	0.807	1 867	0.864	851
640 - 650	-1.2966·λ(642.5)+4.8507·λ(650)+80.4596	0.804	1 870	0.860	845
650 - 660	3.5419·λ(650)+80.9966	0.805	1 869	0.861	845
660 - 670	3.622·λ(665)+83.7951	0.807	1 847	0.860	841
670 - 680	3.7361·λ(680)+85.8368	0.805	1 863	0.857	839
680 - 690	4.3439·λ(680)-0.525·λ(687.5)+78.5912	0.805	1 803	0.857	827
690 - 700	3.9204·λ(700)+82.4525	0.803	1 803	0.856	820
700 - 710	4.0233·λ(710)+83.1949	0.802	1 818	0.855	814
710 - 720	5.1064·λ(710)-1.0932·λ(717.5)+82.8862	0.802	1 824	0.855	814
720 - 730	4.3925·λ(720)-0.3189·λ(730)+84.0677	0.803	1 810	0.853	815
730 - 740	3.6597·λ(737.5)+0.5113·λ(740)+86.1803	0.805	1 784	0.850	809
740 - 750	4.2039·λ(750)+89.8984	0.804	1 787	0.849	817

[1)] 2 storm events, 2004-07-06: 16^{48} – 18^{23} (5 samples), 2004-07-22: 16^{42} – 17^{27} (6 samples)

Table A- 22 COD_{tot} – M5 Model Tree – Part 1

Analysed Wavelength Range	Resulting Equation	Correlation Coefficient Based on 2nd and 3rd Measurement Campaign	Sum of Residuals of 2nd and 3rd Measurement Campaign	Correlation Coefficient of Storm Events[1)]	Sum of Residuals of Storm Events[1)]
[nm]			[mg/l]		[mg/l]
200 - 750	13.6562·λ(660)+163.0562	0.968	1 876	0.888	3 438
230 - 500	λ(315)≤104.713:3.804·λ(242.5)-177.2878 λ(315)>104.713:4.2207·λ(402.5)+487.0871	0.980	1 469	0.932	1 251
250 - 277.5	λ(257.5)≤183.321:4.3094·λ(250)-176.4109 λ(257.5)>183.321:1.5481·λ(250)+511.3758	0.979	1 457	0.897	1 311
254, 436	λ(436)≤59.399:4.3291·λ(254)-146.2961 λ(436)>59.399:4.7327·λ(436)+486.5013	0.981	1 573	0.933	1 135
(254-436)	λ(254-436)≤116.228:7.8521·λ(254-436)-322.3207 λ(254-436)>116.228:3.0839·λ(254-436)+417.8024	0.965	2 230	0.781	2 645
250-277.5,436	λ(436)≤59.399:4.1198·λ(250)-156.2482 λ(436)>59.399:4.7327·λ(436)+486.5013	0.981	1 422	0.932	1 158
230 - 240	λ(230)≤272.778:3.8328·λ(232.5)-365.1993 λ(230)>272.778:1.6394·λ(235)+362.2693	0.972	1 689	0.882	2 058
230-240,436	9.1123·λ(436)+110.9439	0.966	2 051	0.932	2 091
240 - 250	λ(240)≤213.238:4.048·λ(240)-240.0302 λ(240)>213.238:1.7395·λ(240)+394.5551	0.973	1 625	0.891	1 541
240-250,436	λ(436)≤59.399:3.7045·λ(240)-192.5718 λ(436)>59.399:4.7327·λ(436)+486.5013	0.980	1 625	0.934	1 311
250 - 260	λ(257.5)≤183.321:4.3094·λ(250)-176.4109 λ(257.5)>183.321:1.5481·λ(250)+511.3758	0.979	1 457	0.897	1 311
250-260,436	λ(436)≤59.399:4.1198·λ(250)-156.2482 λ(436)>59.399:4.7327·λ(436)+486.5013	0.981	1 422	0.932	1 158
260 - 270	λ(260)≤179.256:4.8289·λ(260)-151.8255 λ(260)>179.256:1.7956·λ(260)+499.7104	0.981	1 414	0.896	1 202
260-270,436	λ(436)≤59.399:4.6409·λ(260)-134.6248 λ(436)>59.399:4.7327·λ(436)+486.5013	0.981	1 405	0.929	1 071
270 - 280	λ(270)≤171.213:5.0209·λ(270)-147.2737 λ(270)>171.213:1.81·λ(270)+513.8062	0.980	1 430	0.903	1 150
270-280,436	λ(436)≤59.399:4.8197·λ(270)-129.8082 λ(436)>59.399:4.7327·λ(436)+486.5013	0.981	1 411	0.933	1 030
280 - 290	λ(280)≤148.853:5.2981·λ(280)-150.5327 λ(280)>148.853:2.4227·λ(285)+409.9741	0.974	1 581	0.907	1 117
280-290,436	λ(436)≤59.399:4.9726·λ(280)-121.9874 λ(436)>59.399:2.0845·λ(285)+483.0954	0.979	1 477	0.913	1 071
290 - 300	λ(292.5)≤148.543:5.4674·λ(290)-121.6859 λ(292.5)>148.543:1.8568·λ(290)+546.2947	0.979	1 470	0.909	1 097
290-300,436	9.1123·λ(436)+110.9439	0.966	2 051	0.932	2 092
300 - 310	λ(300)≤134.978:6.0088·λ(300)-98.1952 λ(300)>134.978:2.1117·λ(300)+538.3533	0.980	1 428	0.908	1 063
300-310,436	λ(436)≤59.399:5.8021·λ(300)-84.6391 λ(436)>59.399:4.7327·λ(436)+486.5013	0.981	1 405	0.935	966
310 - 320	λ(315)≤104.713:6.5257·λ(310)-54.8014 λ(315)>104.713:2.8331·λ(310)+486.1852	0.980	1 442	0.912	1 097
310-320,436	λ(315)≤104.713:6.5257·λ(310)-54.8014 λ(315)>104.713:4.7327·λ(436)+486.5013	0.981	1 429	0.929	1 058
320 - 330	λ(320)≤100.107:7.2841·λ(327.5)-25.0024 λ(320)>100.107:3.0636·λ(320)+468.4864	0.980	1 439	0.912	1 247
320-330,436	λ(320)≤100.107:7.2841·λ(327.5)-25.0024 λ(320)>100.107:3.0636·λ(320)+468.4864	0.980	1 439	0.927	1 217

[1)] 2 storm events, 2004-07-06: 16^{48} – 18^{23} (5 samples), 2004-07-22: 16^{42} – 17^{27} (6 samples)

Table A- 23 COD_{tot} – M5 Model Tree – Part 2

Analysed Wavelength Range	Resulting Equation	Correlation Coefficient Based on 2nd and 3rd Measurement Campaign	Sum of Residuals of 2nd and 3rd Measurement Campaign	Correlation Coefficient of Storm Events[1)]	Sum of Residuals of Storm Events[1)]
[nm]			[mg/l]		[mg/l]
330 - 340	λ(330)≤93.471:7.359·λ(330)-20.7639 λ(330)>93.471:3.2426·λ(332.5)+475.7769	0.980	1 439	0.914	1 261
330-340,436	λ(330)≤93.471:7.359·λ(330)-20.7639 λ(330)>93.471:3.2426·λ(332.5)+475.7769	0.980	1 439	0.914	1 261
340 - 350	λ(340)≤87.747:7.7327·λ(340)-9.0266 λ(340)>87.747:3.3446·λ(340)+480.1622	0.980	1 437	0.913	1 362
340-350,436	λ(340)≤87.747:7.7327·λ(340)-9.0266 λ(340)>87.747:3.3446·λ(340)+480.1622	0.980	1 437	0.913	1 362
350 - 360	λ(350)≤82.826:8.0988·λ(350)+2.2835 λ(350)>82.826:3.4815·λ(350)+485.3959	0.980	1 439	0.910	1 455
350-360,436	λ(350)≤82.826:8.0988·λ(350)+2.2835 λ(350)>82.826:3.4815·λ(350)+485.3959	0.980	1 439	0.910	1 455
360 - 370	λ(360)≤79.125:8.3924·λ(360)+8.2619 λ(360)>79.125:3.6142·λ(360)+486.7266	0.980	1 439	0.909	1 523
360-370,436	λ(360)≤79.125:8.3924·λ(360)+8.2619 λ(360)>79.125:3.6142·λ(360)+486.7266	0.980	1 439	0.909	1 523
370 -380	λ(370)≤75.382:8.6994·λ(370)+17.728 λ(370)>75.382:3.7502·λ(370)+489.7739	0.980	1 442	0.906	1 582
370-380,436	λ(370)≤75.382:8.6994·λ(370)+17.728 λ(370)>75.382:3.7502·λ(370)+489.7739	0.980	1 442	0.906	1 582

[1)] 2 storm events, 2004-07-06: 16^{48} – 18^{23} (5 samples), 2004-07-22: 16^{42} – 17^{27} (6 samples)

Table A- 24 COD_{sol} – M5 Model Tree – Part 1

Analysed Wavelength Range	Resulting Equation	Correlation Coefficient Based on 2nd and 3rd Measurement Campaign	Sum of Residuals of 2nd and 3rd Measurement Campaign	Correlation Coefficient of Storm Events[1)]	Sum of Residuals of Storm Events[1)]
[nm]			[mg/l]		[mg/l]
200 - 750	λ(200)≤379.122 λ(200)≤356.904:0.6263·λ(235)-28.0321 λ(200)>356.904:-10.3678·λ(200)+ 4038.0195 λ(200)>379.122:1.8712·λ(255)- 4.5534·λ(450)+234.1023	0.846	1 717	0.916	211
230 - 500	1.1614·λ(235)-104.888	0.840	1 506	0.830	494
240 - 247.5, 272.5 - 290	1.2416·λ(240)-85.1011	0.835	1 507	0.831	439
240 - 247.5, 272.5-290,436	1.2416·λ(240)-85.1011	0.835	1 507	0.831	439
254, 436	1.3987·λ(254)-64.9045	0.852	1 602	0.823	410
(254-436)	2.559·λ(254-436)-122.165	0.831	1 804	0.817	609
230 - 240	1.1614·λ(235)-104.888	0.840	1 506	0.830	494
230-240,436	1.1614·λ(235)-104.888	0.840	1 506	0.830	494
240 - 250	1.2416·λ(240)-85.1011	0.835	1 507	0.831	439
240-250,436	1.2416·λ(240)-85.1011	0.835	1 507	0.831	439
250 - 260	1.4697·λ(260)-58.3921	0.854	1 441	0.822	444
250-260,436	1.4697·λ(260)-58.3921	0.854	1 441	0.822	444
260 - 270	1.4697·λ(260)-58.3921	0.854	1 441	0.822	444
260-270,436	1.4697·λ(260)-58.3921	0.854	1 441	0.822	444
270 - 280	1.5305·λ(272.5)-55.5583	0.847	1 457	0.811	415
270-280,436	1.5305·λ(272.5)-55.5583	0.847	1 457	0.811	415
280 - 290	1.6108·λ(285)-51.1165	0.841	1 475	0.802	407
280-290,436	1.6108·λ(285)-51.1165	0.841	1 475	0.802	407
290 - 300	1.6665·λ(290)-48.4294	0.840	1 476	0.799	417
290-300,436	1.6665·λ(290)-48.4294	0.840	1 476	0.799	417
300 - 310	1.8394·λ(302.5)-36.0505	0.850	1 453	0.302	666
300-310,436	1.8394·λ(302.5)-36.0505	0.850	1 453	0.790	503
310 - 320	2.027·λ(317.5)-19.5	0.861	1 422	0.774	664
310-320,436	2.9606·λ(436)+11.7239	0.860	1 392	0.718	994
320 - 330	2.1208·λ(327.5)-14.3456	0.861	1 420	0.764	701
320-330,436	2.9606·λ(436)+11.7239	0.860	1 392	0.718	994
330 - 340	2.1389·λ(330)-12.8182	0.861	1 420	0.762	709
330-340,436	λ(330)≤90.769:1.4836·λ(330)+10.3311 λ(330)>90.769 λ(330)≤116.098 λ(436)≤71.517: 288.7 λ(436)>71.517: 122 λ(330)>116.098: 289.875	0.848	1 654	0.875	632
340 - 350	2.2302·λ(340)-8.6424	0.861	1 420	0.753	745
340-350,436	λ(340)≤84.807:1.5548·λ(340)+12.8694 λ(340)>84.807 λ(340)≤109.552 λ(436)≤71.517: 288.7 λ(436)>71.517: 122 λ(340)>109.552: 289.875	0.848	1 654	0.871	653
350 - 360	2.3229·λ(350)-5.0632	0.861	1 420	0.747	779

[1)] 2 storm events, 2004-07-06: 16^{48} – 18^{23} (5 samples), 2004-07-22: 16^{42} – 17^{27} (6 samples)

Table A- 25 COD_{sol} – M5 Model Tree – Part 2

Analysed Wavelength Range	Resulting Equation	Correlation Coefficient Based on 2nd and 3rd Measurement Campaign	Sum of Residuals of 2nd and 3rd Measurement Campaign	Correlation Coefficient of Storm Events[1)]	Sum of Residuals of Storm Events[1)]
[nm]			[mg/l]		[mg/l]

350-360,436	λ(350)≤79.473:1.6299·λ(350)+15.0374
	λ(350)>79.473
	  λ(350)≤103.624
	    λ(436)≤71.517: 288.7
	    λ(436)>71.517: 122
	λ(350)>103.624: 289.875
		0.821	1 776	0.469	634

360 - 370	2.3972·λ(360)-2.7338	0.860	1 417	0.741	806

360-370,436	λ(360)≤75.936:1.6809·λ(360)+16.5708
	λ(360)>75.936
	  λ(360)≤99.602
	    λ(436)≤71.517: 288.7
	    λ(436)>71.517: 122
	λ(360)>99.602: 289.875
		0.848	1 654	0.864	686

370 -380	2.4789·λ(370)+0.2062	0.860	1 416	0.736	830

370-380,436	λ(370)≤72.139:1.7421·λ(370)+18.4633
	λ(370)>72.139
	  λ(370)≤95.263
	    λ(436)≤71.517: 288.7
	    λ(436)>71.517: 122
	λ(370)>95.263: 289.875
		0.847	1 654	0.861	698

[1)] 2 storm events, 2004-07-06: 16^{48} – 18^{23} (5 samples), 2004-07-22: 16^{42} – 17^{27} (6 samples)

Table A- 26 TSS – M5 Model Tree – Part 1

Analysed Wavelength Range	Resulting Equation	Correlation Coefficient Based on 2nd and 3rd Measurement Campaign	Sum of Residuals of 2nd and 3rd Measurement Campaign	Correlation Coefficient of Storm Events 1)	Sum of Residuals of Storm Events 1)
[nm]			[mg/l]		[mg/l]
200 - 750	λ(200)≤373.505:3.1365·λ(597.5)+78.8778 λ(200)>373.505 λ(212.5)≤355.641:237.9 λ(212.5)>355.641: λ(235)≤317.259: 316.9286 λ(235)>317.259: 259.6429	0.859	1 789	0.795	943
380 - 750	λ(380)≤73.105:3.1365·λ(597.5)+78.8778 λ(380)>73.105:275.0263	0.815	1 790	0.720	1 028
600 - 647.5	λ(600)≤40.718:3.2998·λ(640)+82.6165 λ(600)>40.718:275.0263	0.815	1 789	0.538	1 121
380 - 390	λ(380)≤73.105:2.0113·λ(380)+56.9888 λ(380)>73.105:275.0263	0.819	1 785	0.824	1 058
390 - 400	λ(390)≤70.153:2.0734·λ(390)+58.3743 λ(390)>70.153:275.0263	0.819	1 786	0.822	1 051
400 - 410	λ(400)≤67.423:2.1323·λ(400)+60.0614 λ(400)>67.423:275.0263	0.818	1 787	0.819	1 045
410 - 420	λ(410)≤65.302:2.1919·λ(410)+60.6672 λ(410)>65.302:275.0263	0.818	1 788	0.816	1 038
420 - 430	λ(420)≤62.809:2.3061·λ(430)+64.8219 λ(420)>62.809:275.0263	0.818	1 830	0.804	1 012
430 - 440	λ(430)≤60.593:2.3061·λ(430)+64.8219 λ(430)>60.593:275.0263	0.818	1 788	0.809	1 021
440 - 450	λ(440)≤59.007:2.3918·λ(445)+65.8347 λ(440)>59.007:275.0263	0.817	1 806	0.628	1 078
450 - 460	λ(450)≤57.235:2.4216·λ(450)+66.1542 λ(450)>57.235:275.0263	0.817	1 790	0.629	1 075
460 - 470	λ(460)≤55.504:2.4812·λ(460)+67.4728 λ(460)>55.504:275.0263	0.817	1 790	0.629	1 070
470 - 480	λ(470)≤53.969:2.5323·λ(470)+68.6398 λ(470)>53.969:275.0263	0.816	1 791	0.629	1 069
480 - 490	λ(480)≤52.441:2.5848·λ(480)+70.0429 λ(480)>52.441:275.0263	0.816	1 791	0.629	1 066
490 - 500	λ(490)≤51.376:2.6366·λ(490)+70.0762 λ(490)>51.376:275.0263	0.816	1 791	0.630	1 064
500 - 510	λ(500)≤49.822:2.6905·λ(500)+71.7985 λ(500)>49.822:275.0263	0.816	1 791	0.629	1 065
510 - 520	λ(510)≤48.886:2.7451·λ(510)+71.6283 λ(510)>48.886:275.0263	0.816	1 791	0.630	1 065
520 - 530	λ(520)≤47.877:2.7921·λ(520)+72.3726 λ(520)>47.877:275.0263	0.816	1 792	0.630	1 063
530 - 540	λ(530)≤46.862:2.8368·λ(530)+73.5903 λ(530)>46.862:275.0263	0.816	1 790	0.630	1 063
540 - 550	λ(540)≤45.673:2.8869·λ(540)+74.75 λ(540)>45.673:275.0263	0.816	1 790	0.629	1 063
550 - 560	λ(550)≤44.883:2.938·λ(550)+74.872 λ(550)>44.883:275.0263	0.816	1 790	0.629	1 063
560 - 570	λ(560)≤43.829:2.9923·λ(560)+75.6461 λ(560)>43.829:275.0263	0.816	1 790	0.628	1 063
570 - 580	λ(570)≤43.182:3.024·λ(570)+76.2095 λ(570)>43.182:275.0263	0.815	1 791	0.629	1 062

1) 2 storm events, 2004-07-06: 16^{48} – 18^{23} (5 samples), 2004-07-22: 16^{42} – 17^{27} (6 samples)

Table A- 27 TSS – M5 Model Tree – Part 2

Analysed Wavelength Range	Resulting Equation	Correlation Coefficient Based on 2nd and 3rd Measurement Campaign	Sum of Residuals of 2nd and 3rd Measurement Campaign	Correlation Coefficient of Storm Events[1)]	Sum of Residuals of Storm Events[1)]
[nm]			[mg/l]		[mg/l]
580 - 590	λ(580)≤42.465:3.0686·λ(580)+76.6178 λ(580)>42.465:275.0263	0.815	1 791	0.628	1 061
590 - 600	λ(590)≤41.635:3.1365·λ(597.5)+78.8778 λ(590)>41.635:275.0263	0.815	1 790	0.627	1 061
600 - 610	λ(600)≤40.718:3.1448·λ(600)+79.2094 λ(600)>40.718:275.0263	0.815	1 790	0.535	1 129
610 - 620	λ(610)≤39.964:3.1766·λ(610)+80.2637 λ(610)>39.964:275.0263	0.815	1 791	0.536	1 125
620 - 630	λ(620)≤39.534:3.2601·λ(630)+81.2872 λ(620)>39.534:275.0263	0.815	1 791	0.537	1 124
630 - 640	λ(630)≤38.801:3.2998·λ(640)+82.6165 λ(630)>38.801:275.0263	0.815	1 789	0.538	1 121
640 - 650	λ(640)≤37.912:3.2998·λ(640)+82.6165 λ(640)>37.912:275.0263	0.815	1 789	0.538	1 121
650 - 660	λ(650)≤37.852:3.3438·λ(650)+81.0465 λ(650)>37.852:275.0263	0.815	1 791	0.538	1 121
660 - 670	3.4481·λ(660)+88.8612	0.802	1 927	0.862	859
670 - 680	λ(670)≤36.212:3.41·λ(677.5)+85.2996 λ(670)>36.212:275.0263	0.815	1 788	0.539	1 119
680 - 690	λ(680)≤35.53:3.4285·λ(680)+86.1721 λ(680)>35.53:275.0263	0.815	1 788	0.540	1 116
690 - 700	λ(690)≤34.585:3.477·λ(690)+87.8996 λ(690)>34.585:275.0263	0.814	1 790	0.535	1 051
700 - 710	λ(700)≤33.749:3.5011·λ(700)+89.6589 λ(700)>33.749:275.0263	0.814	1 790	0.536	1 051
710 -720	λ((710)≤33.285:3.5566·λ(710)+89.7787 λ(710)>33.285:275.0263	0.815	1 805	0.536	1 055
720 - 730	λ(720)≤32.56:3.5753·λ(720)+91.2078 λ(720)>32.56:275.0263	0.814	1 791	0.536	1 054
730 - 740	λ(730)≤31.794:3.5595·λ(730)+93.2014 λ(730)>31.794:275.0263	0.814	1 791	0.536	1 054
740 - 750	λ(740)≤31.046:3.6037·λ(740)+94.0983 λ(740)>31.046:275.0263	0.814	1 790	0.536	1 056

[1)] 2 storm events, 2004-07-06: 16^{48} – 18^{23} (5 samples), 2004-07-22: 16^{42} – 17^{27} (6 samples)

Table A- 28 COD_{tot} – Support Vector Machine with Sequential Minimal Optimisation Algorithm (SMO) – Part 1

Analysed Wavelength Range	Resulting Equation	Correlation Coefficient Based on 2nd and 3rd Measurement Campaign	Sum of Residuals of 2nd and 3rd Measurement Campaign	Correlation Coefficient of Storm Events 1)	Sum of Residuals of Storm Events 1)
[nm]			[mg/l]		[mg/l]
200 - 750	-1.7503·λ(200)+5.0566·λ(202.5)+5.2202·λ(205)-2.7465·λ(207.5)-1.5279·λ(210)-2.0075·λ(212.5)-1.3597·λ(215)-0.1635·λ(217.5)-1.5024·λ(220)+0.1943·λ(222.5)+2.0663·λ(225)+1.6167·λ(227.5)+1.2495·λ(230)+0.3503·λ(232.5)-0.1574·λ(235)+0.1354·λ(237.5)+0.1382·λ(240)+0.2837·λ(242.5)+0.8227·λ(245)+1.2848·λ(247.5)+1.5376·λ(250)+1.9839·λ(252.5)+2.4626·λ(255)+2.6405·λ(257.5)+2.2828·λ(260)+1.9458·λ(262.5)+1.7368·λ(265)+1.493·λ(267.5)+0.7514·λ(270)-0.1187·λ(272.5)-0.531·λ(275)-1.1733·λ(277.5)-1.9181·λ(280)-2.4339·λ(282.5)-2.6061·λ(285)-2.9753·λ(287.5)-3.1922·λ(290)-3.1057·λ(292.5)-2.8766·λ(295)-2.3943·λ(297.5)-1.9572·λ(300)-1.5175·λ(302.5)-0.9811·λ(305)-0.5635·λ(307.5)-0.1756·λ(310)+0.0752·λ(312.5)+0.2039·λ(315)+0.1634·λ(317.5)+0.0088·λ(320)+0.1269·λ(322.5)-0.0256·λ(325)-0.135·λ(327.5)-0.2291·λ(330)-0.2303·λ(332.5)-0.1369·λ(335)-0.3993·λ(337.5)-0.2447·λ(340)-0.2522·λ(342.5)-0.4146·λ(345)-0.4739·λ(347.5)-0.4515·λ(350)-0.5285·λ(352.5)-0.4126·λ(355)-0.5214·λ(357.5)-0.6139·λ(360)-0.5668·λ(362.5)-0.6318·λ(365)-0.7053·λ(367.5)-0.6835·λ(370)-0.5302·λ(372.5)-0.6088·λ(375)-0.9124·λ(377.5)-0.8493·λ(380)-0.8389·λ(382.5)-0.7955·λ(385)-0.5575·λ(387.5)-0.6523·λ(390)-0.6286·λ(392.5)-0.6313·λ(395)-0.6959·λ(397.5)-0.5643·λ(400)-0.2566·λ(402.5)-0.1216·λ(405)-0.4228·λ(407.5)-0.3953·λ(410)-0.1884·λ(412.5)-0.3406·λ(415)-0.5612·λ(417.5)-0.088·λ(420)-0.0966·λ(422.5)-0.2207·λ(425)-0.0736·λ(427.5)-0.0427·λ(430)+0.107·λ(432.5)+0.0178·λ(435)+0.1982·λ(437.5)+0.2214·λ(440)+0.2265·λ(442.5)+0.195·λ(445)+0.1824·λ(447.5)+0.4049·λ(450)+0.3365·λ(452.5)+0.3932·λ(455)+0.3977·λ(457.5)+0.3568·λ(460)+0.4585·λ(462.5)+0.4927·λ(465)+0.2077·λ(467.5)+0.3641·λ(470)+0.6152·λ(472.5)+0.5042·λ(475)+0.2905·λ(477.5)+0.2685·λ(480)+0.2118·λ(482.5)+0.206·λ(485)+0.3099·λ(487.5)+0.5837·λ(490)+0.5382·λ(492.5)+0.4458·λ(495)+0.5145·λ(497.5)+0.641·λ(500)+0.6196·λ(502.5)+0.1061·λ(505)+0.4107·λ(507.5)+0.781·λ(510)+0.7338·λ(512.5)+0.5601·λ(515)+0.566·λ(517.5)+0.976·λ(520)+0.9616·λ(522.5)+0.521·λ(525)+0.2206·λ(527.5)+0.3279·λ(530)+0.5636·λ(532.5)+0.5402·λ(535)+0.4053·λ(537.5)+0.7224·λ(540)+0.9226·λ(542.5)+0.646·λ(545)+0.4827·λ(547.5)+0.4405·λ(550)+0.4602·λ(552.5)+0.64·λ(555)+0.7351·λ(557.5)+0.7751·λ(560)+1.0016·λ(562.5)+1.051·λ(565)+0.807·λ(567.5)+0.9475·λ(570)+1.2069·λ(572.5)+0.9106·λ(575)+0.7268·λ(577.5)+1.1865·λ(580)+1.1334·λ(582.5)+0.9704·λ(585)+1.0828·λ(587.5)+0.9152·λ(590)+1.2173·λ(592.5)+0.908·λ(595)+0.6005·λ(597.5)+0.6782·λ(600)+0.7925·λ(602.5)+0.628·λ(605)+1.0386·λ(607.5)+0.8084·λ(610)+0.887·λ(612.5)+0.6792·λ(615)+0.7898·λ(617.5)+1.1271·λ(620)+1.2472·λ(622.5)+1.3471·λ(625)+1.1223·λ(627.5)+0.8106·λ(630)+1.2319·λ(632.5)+0.8786·λ(635)+0.6089·λ(637.5)+0.5862·λ(640)+1.0684·λ(642.5)+0.275·λ(645)+0.4404·λ(647.5)+0.1445·λ(650)+0.1659·λ(652.5)+0.2609·λ(655)-0.4136·λ(657.5)-0.0407·λ(660)-0.3288·λ(662.5)-0.4341·λ(665)+0.1039·λ(667.5)+0.8787·λ(670)+1.0491·λ(672.5)-0.2152·λ(675)-0.6689·λ(677.5)+0.0399·λ(680)-0.0649·λ(682.5)-0.3483·λ(685)-0.5492·λ(687.5)-0.147·λ(690)-0.6099·λ(692.5)-0.6555·λ(695)-0.149·λ(697.5)-0.5906·λ(700)-0.4751·λ(702.5)-1.0258·λ(705)-1.236·λ(707.5)-1.3621·λ(710)-0.6372·λ(712.5)-0.2622·λ(715)-0.837·λ(717.5)-0.8754·λ(720)-1.2455·λ(722.5)-0.9946·λ(725)-0.795·λ(727.5)-0.579·λ(730)-0.5073·λ(732.5)-1.6637·λ(735)-1.4794·λ(737.5)-0.7231·λ(740)-1.5824·λ(742.5)-1.1314·λ(745)-2.0195·λ(747.5)-0.8991·λ(750)-728.1575	0.989	784	0.821	2 830
230 – 500	-1.1445·λ(230)-0.9712·λ(232.5)+0.712·λ(235)+1.2857·λ(237.5)+0.6755·λ(240)+1.0127·λ(242.5)+1.6706·λ(245)+2.1625·λ(247.5)+2.7885·λ(250)+4.2815·λ(252.5)+5.2049·λ(255)+5.0449·λ(257.5)+4.5743·λ(260)+4.0433·λ(262.5)+3.5055·λ(265)+2.0993·λ(267.5)+0.0188·λ(270)-1.3683·λ(272.5)-1.916·λ(275)-2.8266·λ(277.5)-3.5237·λ(280)-4.0702·λ(282.5)-4.0045·λ(285)-4.0794·λ(287.5)-3.9734·λ(290)-3.415·λ(292.5)-3.2096·λ(295)-3.0282·λ(297.5)-2.5887·λ(300)-1.8896·λ(302.5)-1.1914·λ(305)-0.8477·λ(307.5)-0.6597·λ(310)-0.5322·λ(312.5)-0.1543·λ(315)-0.0824·λ(317.5)+0.2454·λ(320)+0.3512·λ(322.5)+0.1103·λ(325)+0.1316·λ(327.5)-0.1116·λ(330)-0.3502·λ(332.5)+0.1506·λ(335)-0.147·λ(337.5)-0.4856·λ(340)-0.2321·λ(342.5)-0.4985·λ(345)-0.6352·λ(347.5)-0.165·λ(350)-0.4246·λ(352.5)-0.7023·λ(355)-0.9689·λ(357.5)-1.2243·λ(360)-1.2162·λ(362.5)-1.0674·λ(365)-1.0243·λ(367.5)-1.1679·λ(370)-0.9936·λ(372.5)-0.8901·λ(375)-1.3971·λ(377.5)-1.0458·λ(380)-0.6959·λ(382.5)-1.0667·λ(385)-1.118·λ(387.5)-0.9733·λ(390)-0.9523·λ(392.5)-0.8748·λ(395)-0.8281·λ(397.5)-0.881·λ(400)-0.7115·λ(402.5)-1.1269·λ(405)-1.1223·λ(407.5)-0.9773·λ(410)-0.5263·λ(412.5)-0.2554·λ(415)-0.3654·λ(417.5)-0.4848·λ(420)-0.212·λ(422.5)-0.1914·λ(425)-0.0507·λ(427.5)+0.3342·λ(430)+0.2275·λ(432.5)+0.1757·λ(435)+0.4066·λ(437.5)+0.5098·λ(440)+0.4545·λ(442.5)+0.6427·λ(445)+0.7418·λ(447.5)+0.9532·λ(450)+1.5189·λ(452.5)+1.4273·λ(455)+1.6014·λ(457.5)+1.4641·λ(460)1.4483·λ(462.5)+1.5143·λ(465)+1.5217·λ(467.5)+1.4505·λ(470)+1.9643·λ(472.5)+2.0087·λ(475)+1.9927·λ(477.5)+1.9893·λ(480)+2.1441·λ(482.5)+2.2936·λ(485)+2.5008·λ(487.5)+2.4181·λ(490)+2.4718·λ(492.5)+2.8812·λ(495)+2.8837·λ(497.5)+2.7047·λ(500)-97.8814	0.986	784	0.858	2 622

1) 2 storm events, 2004-07-06: 16^{48} – 18^{23} (5 samples), 2004-07-22: 16^{42} – 17^{27} (6 samples)

Table A- 29 COD_{tot} – Support Vector Machine with Sequential Minimal Optimisation Algorithm (SMO) – Part 2

Analysed Wavelength Range	Resulting Equation	Correlation Coefficient Based on 2nd and 3rd Measurement Campaign	Sum of Residuals of 2nd and 3rd Measurement Campaign	Correlation Coefficient of Storm Events 1)	Sum of Residuals of Storm Events 1)
[nm]			[mg/l]		[mg/l]
250 - 277.5	-1.8357·λ(250)+2.7257·λ(252.5)+6.5466·λ(255)+ 7.8928·λ(257.5)+7.2061·λ(260)+5.5878·λ(262.5)+ 3.2416·λ(265)+0.0374·λ(267.5)-3.404·λ(270)- 6.0635·λ(272.5)-8.3408·λ(275)-10.7983·λ(277.5)- 174.8762	0.972	1 670	0.827	1 772
254, 436	1.0878·λ(254)+7.5963·λ(436)+5.9453	0.966	1 967	0.938	1 410
(254 - 436)	8.0196·λ(254-436)-310.891	0.935	2 956	0.781	2 463
250-277.5, 436	2.3589·λ(250)+4.7972·λ(252.5)+6.68·λ(255)+ 6.7198·λ(257.5)+4.9371·λ(260)+3.1684·λ(262.5)+ 1.2626·λ(265)-1.3406·λ(267.5)-4.0634·λ(270)- 6.3143·λ(272.5)-11.484·λ(277.5)+8.4428·λ(436)- 60.3448	0.979	1 495	0.891	1 463
230 - 240	2.3081·λ(230)-0.3217·λ(232.5)-1.7537·λ(235)- 0.3774·λ(237.5)+4.179·λ(240)-285.844	0.949	2 338	0.886	1 670
230 - 240, 436	-0.228·λ(230)-0.472·λ(232.5)+0.2302·λ(235)+ 0.5815·λ(237.5)+0.5122·λ(240)+8.536·λ(436)+ 34.4694	0.965	1 936	0.936	1 699
240 - 250	-8.7154·λ(240)-3.9994·λ(242.5)+1.1714·λ(245)+ 6.2114·λ(247.5)+10.4334·λ(250)-44.6183	0.965	1 968	0.927	1 144
240 - 250, 436	-3.1728·λ(240)-1.2223·λ(242.5)+0.8324·λ(245)+ 2.3688·λ(247.5)+3.1242·λ(250)+6.0449·λ(436)+ 15.7609	0.966	1 918	0.940	1 486
250 - 260	-6.4298·λ(250)-0.836·λ(252.5)+3.4726·λ(255)+ 4.5139·λ(257.5)+4.3881·λ(260)-87.5703	0.963	2 043	0.918	992
250 - 260, 436	-1.2892·λ(250)+1.0838·λ(252.5)+2.0227·λ(255)+ 0.6165·λ(257.5)-1.2348·λ(260)+7.379·λ(436)+ 4.8667	0.966	1 928	0.938	1 452
260 - 270	6.4796·λ(260)+4.7715·λ(262.5)+2.0651·λ(265)- 2.0583·λ(267.5)-6.7283·λ(270)-143.5111	0.962	1 019	0.902	1 136
260 - 270, 436	4.7109·λ(260)+2.6608·λ(262.5)+0.8076·λ(265)- 1.8945·λ(267.5)-4.8429·λ(270)+6.4768·λ(436)- 11.7976	0.967	1 890	0.937	1 309
270 - 280	6.3933·λ(270)+2.8655·λ(272.5)+0.6229·λ(275)- 1.6885·λ(277.5)-3.3686·λ(280)-140.9829	0.958	2 160	0.916	1 029
270 - 280, 436	3.7678·λ(270)+1.7902·λ(272.5)+0.2544·λ(275)- 1.7195·λ(277.5)-3.6338·λ(280)+8.5209·λ(436)+ 40.0732	0.967	1 911	0.937	1 729
280 - 290	4.2379·λ(280)+1.6185·λ(282.5)-0.0702·λ(285)- 0.8079·λ(287.5)+0.2399·λ(290)-139.6606	0.953	2 263	0.925	984
280 - 290, 436	1.1576·λ(280)+0.253·λ(282.5)-0.1379·λ(285)- 0.7282·λ(287.5)-0.8648·λ(290)+10.3073·λ(436)+ 69.7646	0.966	1 926	0.931	2 040
290 - 300	-3.6101·λ(290)-1.4079·λ(292.5)+0.7401·λ(295)+ 3.4024·λ(297.5)+7.1374·λ(300)-78.3841	0.958	2 152	0.935	902
290 - 300, 436	-0.7592·λ(290)-0.3521·λ(292.5)-0.1461·λ(295)+ 0.3722·λ(297.5)+0.7332·λ(300)+10.2448·λ(436)+ 74.7776	0.966	1 927	0.930	2 095
300 - 310	-3.988·λ(300)-1.1238·λ(302.5)+1.9221·λ(305)+ 4.1846·λ(307.5)+5.4999·λ(310)-66.1233	0.963	2 054	0.941	1 145

1) 2 storm events, 2004-07-06: 16^{48} – 18^{23} (5 samples), 2004-07-22: 16^{42} – 17^{27} (6 samples)

Table A- 30 COD_{tot} – Support Vector Machine with Sequential Minimal Optimisation Algorithm (SMO) – Part 3

Analysed Wavelength Range	Resulting Equation	Correlation Coefficient Based on 2nd and 3rd Measurement Campaign	Sum of Residuals of 2nd and 3rd Measurement Campaign	Correlation Coefficient of Storm Events[1)]	Sum of Residuals of Storm Events[1)]
[nm]			[mg/l]		[mg/l]
300 - 310, 436	-0.5344·λ(300)+0.0146·λ(302.5)+0.171·λ(305)+ 0.0862·λ(307.5)+0.361·λ(310)+9.7685·λ(436)+ 64.9198	0.966	1 933	0.932	1 988
310 - 320	-1.3308·λ(310)-0.4443·λ(312.5)+1.1646·λ(315)+ 2.684·λ(317.5)+4.5836·λ(320)-8.4811	0.963	2 047	0.942	1 092
310 - 320, 436	-0.2096·λ(310)-0.0064·λ(312.5)+0.2724·λ(315)+ 0.2172·λ(317.5)+0.1776·λ(320)+9.2164·λ(436)+ 57.0233	0.966	1 939	0.933	1 903
320 - 330	0.7849·λ(320)+1.1342·λ(322.5)+1.2587·λ(325)+ 1.9165·λ(327.5)+1.7178·λ(330)-3.4946	0.963	2 043	0.943	1 103
320 - 330, 436	0.3371·λ(320)+0.5238·λ(322.5)+0.099·λ(325)- -0.2835·λ(327.5)-0.1996·λ(330)+9.1625·λ(436)+ 55.9789	0.966	1 939	0.933	1 892
330 - 340	1.0144·λ(330)+1.3016·λ(332.5)+1.9496·λ(335)+ 1.451·λ(337.5)+1.3236·λ(340)+15.1869	0.963	2 037	0.944	1 207
330 - 340, 436	0.5236·λ(330)+0.518·λ(332.5)+0.1868·λ(335)- 0.5145·λ(337.5)-0.2764·λ(340)+9.2339·λ(436)+ 57.2873	0.966	1 939	0.933	1 902
340 - 350	1.3605·λ(340)+1.6059·λ(342.5)+1.3649·λ(345)+ 1.3278·λ(347.5)+1.7126·λ(350)+22.5536	0.963	2 037	0.945	1 284
340 - 350, 436	0.5159·λ(340)+0.3222·λ(342.5)-0.0548·λ(345)- 0.2905·λ(347.5)-0.2686·λ(350)+9.5493·λ(436)+ 60.3948	0.966	1 936	0.932	1 939
350 - 360	1.6132·λ(350)+1.6802·λ(352.5)+1.4645·λ(355)+ 1.4507·λ(357.5)+1.5009·λ(360)+25.9977	0.963	2 035	0.944	1 355
350 - 360, 436	0.0157·λ(350)+0.0169·λ(352.5)-0.0543·λ(355)- 0.0545·λ(357.5)+0.1585·λ(360)+9.7697·λ(436)+ 62.8323	0.966	1 935	0.932	1 967
360 - 370	1.2793·λ(360)+1.5083·λ(362.5)+1.679·λ(365)+ 1.5938·λ(367.5)+1.9532·λ(370)+31.5698	0.963	2 033	0.943	1 435
360 - 370; 436	-0.028·λ(360)+0.1649·λ(362.5)+0.0545·λ(365)- 0.2669·λ(367.5)+0.2828·λ(370)+9.6198·λ(436)+ 62.3222	0.966	1 936	0.932	1 960
370 - 380	0.8615·λ(370)+1.6161·λ(372.5)+2.0927·λ(375)+ 1.6726·λ(377.5)+2.0829·λ(380)+31.0682	0.963	2 022	0.942	1 485
370 - 380, 436	-0.5646·λ(370)+0.3125·λ(372.5)+0.5642·λ(375)+ 0.1853·λ(377.5)+0.324·λ(380)+8.915·λ(436+ 59.7824	0.966	1 942	0.933	1 927

1) 2 storm events, 2004-07-06: 16^{48} – 18^{23} (5 samples), 2004-07-22: 16^{42} – 17^{27} (6 samples)

Table A- 31 COD_{sol} – Support Vector Machine with Sequential Minimal Optimisation Algorithm (SMO) – Part 1

Analysed Wavelength Range	Resulting Equation	Correlation Coefficient Based on 2nd and 3rd Measurement Campaign	Sum of Residuals of 2nd and 3rd Measurement Campaign	Correlation Coefficient of Storm Events[1)]	Sum of Residuals of Storm Events[1)]
[nm]			[mg/l]		[mg/l]
200 - 750		0.893	1 395	0.606	4 375
	4.0552·λ(200)+2.1136·λ(202.5)-2.8456·λ(205)-3.3396·λ(207.5)+3.1503·λ(210)+2.7989·λ(212.5)-1.5785·λ(215)-3.7042·λ(217.5)-0.7493·λ(220)+2.3543·λ(222.5)+2.4566·λ(225)+2.5212·λ(227.5)+1.7547·λ(230)-1.3692·λ(232.5)-4.0003·λ(235)-4.216·λ(237.5)-2.7798·λ(240)-1.9052·λ(242.5)-0.9446·λ(245)-0.1172·λ(247.5)+0.37·λ(250)+0.5816·λ(252.5)+0.833·λ(255)+1.7385·λ(257.5)+2.456·λ(260)+2.2366·λ(262.5)+1.8464·λ(265)+1.6317·λ(267.5)+1.4762·λ(270)+1.1157·λ(272.5)+0.8585·λ(275)+0.579·λ(277.5)+0.7597·λ(280)+0.4269·λ(282.5)+0.2667·λ(285)+0.3337·λ(287.5)+0.4518·λ(290)+0.4487·λ(292.5)+0.3054·λ(295)+0.4705·λ(297.5)+0.3725·λ(300)+0.2343·λ(302.5)+0.3731·λ(305)+0.4421·λ(307.5)+0.5098·λ(310)+0.4842·λ(312.5)+0.4091·λ(315)+0.4422·λ(317.5)+0.26·λ(320)+0.141·λ(322.5)+0.2984·λ(325)+0.1079·λ(327.5)-0.51·λ(330)-0.3963·λ(332.5)-0.454·λ(335)-0.573·λ(337.5)-0.6467·λ(340)-0.5822·λ(342.5)-0.5928·λ(345)-0.4414·λ(347.5)-0.3489·λ(350)-0.5159·λ(352.5)-0.5167·λ(355)-0.5993·λ(357.5)-0.6658·λ(360)-0.6481·λ(362.5)-0.7568·λ(365)-0.5212·λ(367.5)-0.7283·λ(370)-0.9838·λ(372.5)-1.0057·λ(375)-1.0164·λ(377.5)-1.0409·λ(380)-1.0187·λ(382.5)-0.8976·λ(385)-0.6988·λ(387.5)-0.9041·λ(390)-0.7452·λ(392.5)-0.7787·λ(395)-0.6722·λ(397.5)-0.5893·λ(400)-0.512·λ(402.5)-0.1892·λ(405)-0.3395·λ(407.5)-0.3906·λ(410)-0.1554·λ(412.5)-0.2117·λ(415)-0.163·λ(417.5)-0.0877·λ(420)-0.3179·λ(422.5)+0.0838·λ(425)+0.199·λ(427.5)+0.0595·λ(430)-0.1506·λ(432.5)-0.1914·λ(435)-0.0963·λ(437.5)+0.0925·λ(440)+0.0839·λ(442.5)+0.1308·λ(445)+0.1595·λ(447.5)+0.156·λ(450)+0.3605·λ(452.5)-0.0023·λ(455)-0.1542·λ(457.5)+0.2357·λ(460)+0.2123·λ(462.5)-0.0974·λ(465)+0.0027·λ(467.5)+0.083·λ(470)+0.0101·λ(472.5)-0.0253·λ(475)-0.0153·λ(477.5)-0.067·λ(480)-0.0429·λ(482.5)-0.0147·λ(485)+0.1902·λ(487.5)-0.1775·λ(490)-0.2599·λ(492.5)+0.0451·λ(495)-0.1555·λ(497.5)-0.1618·λ(500)-0.2543·λ(502.5)-0.2838·λ(505)-0.4077·λ(507.5)-0.174·λ(510)-0.1794·λ(512.5)-0.2958·λ(515)-0.1748·λ(517.5)-0.2366·λ(520)-0.2826·λ(522.5)-0.074·λ(525)-0.1813·λ(527.5)+0.0279·λ(530)-0.0054·λ(532.5)-0.0942·λ(535)+0.1504·λ(537.5)+0.1133·λ(540)+0.2313·λ(542.5)+0.0111·λ(545)-0.2464·λ(547.5)+0.1219·λ(550)+0.1433·λ(552.5)-0.0542·λ(555)-0.0721·λ(557.5)+0.133·λ(560)+0.5839·λ(562.5)+0.5435·λ(565)+0.028·λ(567.5)+0.1523·λ(570)+0.497·λ(572.5)+0.1706·λ(575)+0.2782·λ(577.5)+0.3007·λ(580)+0.3343·λ(582.5)+0.291·λ(585)+0.0929·λ(587.5)+0.2872·λ(590)+0.3101·λ(592.5)+0.7013·λ(595)+0.4897·λ(597.5)+0.2773·λ(600)+0.7291·λ(602.5)+0.6329·λ(605)+0.1394·λ(607.5)+0.5369·λ(610)+0.8407·λ(612.5)+0.8402·λ(615)+0.7154·λ(617.5)+0.4069·λ(620)+0.1521·λ(622.5)+0.2385·λ(625)+0.4953·λ(627.5)+0.2546·λ(630)+0.5983·λ(632.5)+0.8579·λ(635)+0.0445·λ(637.5)+0.2286·λ(640)+0.7619·λ(642.5)+0.1736·λ(645)-0.0368·λ(647.5)-0.1179·λ(650)-0.5937·λ(652.5)+0.168·λ(655)+0.4672·λ(657.5)-0.5583·λ(660)-0.0933·λ(662.5)+0.4031·λ(665)+0.6756·λ(667.5)+0.0789·λ(670)-0.3595·λ(672.5)+0.3818·λ(675)+0.6203·λ(677.5)-0.1672·λ(680)-0.4416·λ(682.5)+0.2808·λ(685)-0.1966·λ(687.5)-1.2265·λ(690)-2.2327·λ(692.5)-0.8319·λ(695)-0.1624·λ(697.5)-0.8087·λ(700)-1.2421·λ(702.5)-0.9724·λ(705)-0.2199·λ(707.5)-0.673·λ(710)-0.4078·λ(712.5)-0.7082·λ(715)-0.5805·λ(717.5)-0.0056·λ(720)-0.6316·λ(722.5)-0.0228·λ(725)+0.5973·λ(727.5)+0.1859·λ(730)-0.2061·λ(732.5)-0.1427·λ(735)+0.561·λ(737.5)+0.2461·λ(740)-1.2481·λ(742.5)-1.0408·λ(745)-0.5803·λ(747.5)+0.3063·λ(750)-1002.7089				
230 – 500		0.875	1 554	0.756	1 414
	4.7775·λ(230)-0.3742·λ(232.5)-2.5505·λ(235)-2.7546·λ(237.5)-1.6262·λ(240)-0.3883·λ(242.5)+0.1742·λ(245)+0.7757·λ(247.5)+1.1516·λ(250)+2.1674·λ(252.5)+2.6074·λ(255)+2.6699·λ(257.5)+3.6198·λ(260)+2.8839·λ(262.5)+2.0674·λ(265)+0.4614·λ(267.5)-2.1102·λ(270)-3.4216·λ(272.5)-3.2811·λ(275)-2.9612·λ(277.5)-1.9829·λ(280)-2.0488·λ(282.5)-1.4867·λ(285)-0.0165·λ(287.5)+1.6231·λ(290)+2.6093·λ(292.5)+2.2752·λ(295)+1.4095·λ(297.5)+0.7777·λ(300)+0.2205·λ(302.5)+0.0403·λ(305)-0.4296·λ(307.5)-1.5258·λ(310)-2.5523·λ(312.5)-2.5233·λ(315)-1.5473·λ(317.5)-0.5264·λ(320)-0.9417·λ(322.5)-0.5805·λ(325)-0.1701·λ(327.5)-1.439·λ(330)-1.2781·λ(332.5)+0.4251·λ(335)+0.6736·λ(337.5)-0.3397·λ(340)+0.7087·λ(342.5)+1.0112·λ(345)+1.6473·λ(347.5)+2.7153·λ(350)+2.513·λ(352.5)+1.8194·λ(355)+1.6077·λ(357.5)+0.95·λ(360)+0.6905·λ(362.5)+1.2254·λ(365)+2.3298·λ(367.5)+1.2126·λ(370)+0.1336·λ(372.5)+0.6419·λ(375)+0.3136·λ(377.5)+0.6707·λ(380)+1.6281·λ(382.5)+0.6084·λ(385)-0.204·λ(387.5)-0.0792·λ(390)-0.1351·λ(392.5)-0.5199·λ(395)-0.1877·λ(397.5)-0.8257·λ(400)-1.7528·λ(402.5)-2.6627·λ(405)-2.0291·λ(407.5)-2.0331·λ(410)-1.7028·λ(412.5)-0.5615·λ(415)+0.0645·λ(417.5)-2.2468·λ(420)-2.6248·λ(422.5)-1.1135·λ(425)-0.8054·λ(427.5)+0.1064·λ(430)-1.2407·λ(432.5)-1.1605·λ(435)-1.093·λ(437.5)-1.0568·λ(440)-1.3842·λ(442.5)-0.8932·λ(445)-0.4765·λ(447.5)-0.9675·λ(450)+1.2872·λ(452.5)+0.2876·λ(455)-0.0888·λ(457.5)+0.3015·λ(460)-0.3047·λ(462.5)-1.1307·λ(465)+0.1896·λ(467.5)-0.0826·λ(470)+0.0704·λ(472.5)+0.0566·λ(475)+0.6578·λ(477.5)+0.6899·λ(480)+1.09·λ(482.5)+0.899·λ(485)+1.5149·λ(487.5)-0.186·λ(490)-0.1101·λ(492.5)+1.7336·λ(495)+1.213·λ(497.5)+0.6056·λ(500)-245.9711				

1) 2 storm events, 2004-07-06: 16^{48} – 18^{23} (5 samples), 2004-07-22: 16^{42} – 17^{27} (6 samples)

Table A- 32 COD_{sol} – Support Vector Machine with Sequential Minimal Optimisation Algorithm (SMO) – Part 2

Analysed Wavelength Range	Resulting Equation	Correlation Coefficient Based on 2nd and 3rd Measurement Campaign	Sum of Residuals of 2nd and 3rd Measurement Campaign	Correlation Coefficient of Storm Events[1)]	Sum of Residuals of Storm Events[1)]
[nm]			[mg/l]		[mg/l]
240-247.5, 272.5-290	-1.0772·λ(240)-0.8348·λ(242.5)+0.5092·λ(245)+ 2.673·λ(247.5)+0.8161·λ(272.5)+0.0984·λ(275)- 0.6758·λ(277.5)-0.4419·λ(280)-1.0912·λ(282.5)- 1.034·λ(285)+0.3363·λ(287.5)+2.2164·λ(290)- 39.8681	0.851	1 316	0.826	504
240-247.5, 272.5-290, 436	0.5546·λ(240)+0.3608·λ(242.5)+1.104·λ(245)+ 2.6453·λ(247.5)-0.5295·λ(272.5)-1.0665·λ(275)- 1.6194·λ(277.5)-1.1978·λ(280)-1.7477·λ(282.5)- 1.5932·λ(285)-0.1876·λ(287.5)+1.6176·λ(290)+ 4.2924·λ(436)-22.6701	0.866	1 251	0.821	747
254, 436	1.3087·λ(254)+0.1525·λ(436)-50.5788	0.853	1 421	0.820	435
(254-436)	2.3179·λ(254-436)-103.4121	0.831	1 922	0.817	537
230 - 240	3.8277·λ(230)-1.4865·λ(232.5)-2.4811·λ(235)- 0.9316·λ(237.5)+2.6121·λ(240)-1.1099·λ(436)- 158.3324	0.864	1 521	0.840	582
230 - 240, 436	3.8277·λ(230)-1.4865·λ(232.5)-2.4811·λ(235)- 0.9316·λ(237.5)+2.6121·λ(240)-1.1099·λ(436)- 158.3324	0.851	1 484	0.835	757
240 - 250	-0..8738·λ(240)-0.7605·λ(242.5)-0.1474·λ(245)+ 1.0582·λ(247.5)+2.1347·λ(250)-40.4626	0.854	1 313	0.827	498
240 - 250, 436	-1.0383·λ(240)-0.9014·λ(242.5)-0.176·λ(245)+ 1.1758·λ(247.5)+2.4085·λ(250)-0.0931·λ(436)- 39.0941	0.856	1 309	0.828	507
250 - 260	-0.4291·λ(250)+0.6651·λ(252.5)+0.7936·λ(255)+ 0.0243·λ(257.5)+0.3596·λ(260)-50.9857	0.852	1 334	0.822	466
250 - 260, 436	-2.6742·λ(250)-0.272·λ(252.5)+1.2618·λ(255)+ 1.6191·λ(257.5)+2.496·λ(260)-1.6421·λ(436)- 67.076	0.860	1 350	0.823	495
260 - 270	4.4841·λ(260)+3.0543·λ(262.5)+1.3118·λ(265)- 1.7325·λ(267.5)-5.9455·λ(270)-48.0877	0.875	1 269	0.851	530
260 - 270, 436	4.2137·λ(260)+3.1217·λ(262.5)+1.4775·λ(265)- 1.5818·λ(267.5)-5.8981·λ(270)-0.2974·λ(436)- 54.276	0.873	1 268	0.851	512
270 - 280	2.7236·λ(270)+0.4299·λ(272.5)-0.2221·λ(275)- 0.8992·λ(277.5)-0.5612·λ(280)-50.1162	0.853	1 350	0.818	457
270 - 280, 436	2.973·λ(270)+0.5931·λ(272.5)-0.1805·λ(275)- 0.9772·λ(277.5)-0.7345·λ(280)-0.4039·λ(436)- 59.0258	0.851	1 357	0.824	438
280 - 290	1.144·λ(280)-0.0226·λ(282.5)-0.5911·λ(285)+ 0.0248·λ(287.5)+1.0794·λ(290)-43.6958	0.842	1 351	0.802	469
280 - 290, 436	1.1233·λ(280)-0.0343·λ(282.5)-0.592·λ(285)+ 0.034·λ(287.5)+1.0962·λ(290)+0.0155·λ(436)- 43.3059	0.842	1 351	0.802	471
290 - 300	-0.4177·λ(290)+0.5869·λ(292.5)+0.6714·λ(295)+ 0.4242·λ(297.5)+0.5151·λ(300)-35.1796	0.844	1 343	0.795	524
290 - 300, 436	-0.4348·λ(290)+0.568·λ(292.5)+0.6669·λ(295)+ 0.4434·λ(297.5)+0.5564·λ(300)-0.0287·λ(436)- 35.5044	0.844	1 344	0.795	522
300 - 310	1.3406·λ(300)+0.6212·λ(302.5)+0.6824·λ(305)+ 0.257·λ(307.5)-1.1142·λ(310)-34.7046	0.844	1 342	0.795	530

[1)] 2 storm events, 2004-07-06: 16^{48} – 18^{23} (5 samples), 2004-07-22: 16^{42} – 17^{27} (6 samples)

Table A- 33 COD_{sol} – Support Vector Machine with Sequential Minimal Optimisation Algorithm (SMO) – Part 3

Analysed Wavelength Range	Resulting Equation	Correlation Coefficient Based on 2nd and 3rd Measurement Campaign	Sum of Residuals of 2nd and 3rd Measurement Campaign	Correlation Coefficient of Storm Events[1)]	Sum of Residuals of Storm Events[1)]
[nm]			[mg/l]		[mg/l]
300 - 310, 436	0.988·λ(300)+0.5057·λ(302.5)+0.825·λ(305)+ 0.6347·λ(307.5)-0.5685·λ(310)-0.8655·λ(436)- 43.5552	0.844	1 356	0.803	479
310 - 320	1.04·λ(310)-0.4083·λ(312.5)-0.5166·λ(315)+ 0.428·λ(317.5)+1.4741·λ(320)-18.1351	0.860	1 390	0.775	675
310 - 320, 436	0.968·λ(310)-0.3583·λ(312.5)-0.3702·λ(315)+ 0.7615·λ(317.5)+1.9064·λ(320)-1.2951·λ(436)- 30.0063	0.859	1 378	0.790	548
320 - 330	0.8511·λ(320)+0.2753·λ(322.5)+0.5651·λ(325)+ 0.9104·λ(327.5)-0.5298·λ(330)-15.318	0.861	1 400	0.769	697
320 - 330, 436	0.9965·λ(320)+0.4323·λ(322.5)+0.8013·λ(325)+ 1.3135·λ(327.5)-0.0997·λ(330)-1.9302·λ(436)- 30.4751	0.861	1 385	0.788	529
330 - 340	-0.7196·λ(330)-0.5585·λ(332.5)+1.4621·λ(335)+ 1.7248·λ(337.5)+0.3251·λ(340)-7.8215	0.861	1 406	0.753	755
330 - 340, 436	-0.4969·λ(330)-0.3351·λ(332.5)+1.7839·λ(335)+ 2.1238·λ(337.5)+0.7908·λ(340)-2.2191·λ(436)- 21.0518	0.861	1 381	0.774	584
340 - 350	-1.2339·λ(340)+0.0139·λ(342.5)+0.4005·λ(345)+ 1.0085·λ(347.5)+2.1656·λ(350)-3.3036	0.861	1 408	0.745	797
340 - 350, 436	-0.8052·λ(340)+0.4815·λ(342.5)+0.8578·λ(345)+ 1.6462·λ(347.5)+2.7961·λ(350)-3.428·λ(436)- 19.871	0.860	1 372	0.772	570
350 - 360	1.489·λ(350)+1.3907·λ(352.5)+0.4003·λ(355)- 0.0749·λ(357.5)-0.8937·λ(360)-4.2094	0.861	1 405	0.747	784
350 - 360, 436	2.0541·λ(350)+1.954·λ(352.5)+1.048·λ(355)+ 0.6302·λ(357.5)-0.1886·λ(360)-4.0116·λ(436)- 20.1562	0.859	1 370	0.770	556
360 - 370	0.1658·λ(360)-0.0955·λ(362.5)+0.5027·λ(365)+ 1.6656·λ(367.5)+0.2272·λ(370)-1.1929	0.860	1 419	0.737	823
360 - 370; 436	0.8349·λ(360)+0.5688·λ(362.5)+1.1611·λ(365)+ 2.3165·λ(367.5)+0.8731·λ(370)-4.0144·λ(436)- 14.1147	0.859	1 386	0.759	626
370 - 380	1.4485·λ(370)+0.1167·λ(372.5)+0.5077·λ(375)- 0.0387·λ(377.5)+0.4792·λ(380)-0.855	0.860	1 423	0.735	832
370 - 380, 436	1.98·λ(370)+0.6444·λ(372.5)+1.0315·λ(375)+ 0.4805·λ(377.5)+0.9948·λ(380)-3.0909·λ(436)- 10.0583	0.859	1 401	0.749	698

[1)] 2 storm events, 2004-07-06: 16^{48} – 18^{23} (5 samples), 2004-07-22: 16^{42} – 17^{27} (6 samples)

Table A- 34 TSS – Support Vector Machine with Sequential Minimal Optimisation Algorithm (SMO) – Part 1

Analysed Wavelength Range	Resulting Equation	Correlation Coefficient Based on 2^{nd} and 3^{rd} Measurement Campaign	Sum of Residuals of 2^{nd} and 3^{rd} Measurement Campaign	Correlation Coefficient of Storm Events[1)]	Sum of Residuals of Storm Events[1)]
[nm]			[mg/l]		[mg/l]
200 - 750	-3.1517·λ(200)+4.6805·λ(202.5)+3.0154·λ(205)-2.3987·λ(207.5)+1.3388·λ(210)-1.3121·λ(212.5)-3.189·λ(215)- 1.8229·λ(217.5)+0.7004·λ(220)+1.8576·λ(222.5)+0.7267·λ(225)+1.7343·λ(227.5)+1.9918·λ(230)+ 1.1213·λ(232.5)+0.0767·λ(235)-1.0533·λ(237.5)-1.3098·λ(240)-0.7962·λ(242.5)-0.1835·λ(245)+ 0.3398·λ(247.5)+0.6052·λ(250)+1.0508·λ(252.5)+1.1069·λ(255)+1.2737·λ(257.5)+1.533·λ(260)+ 1.2309·λ(262.5)+0.7811·λ(265)+0.1349·λ(267.5)-0.2889·λ(270)-0.6647·λ(272.5)-0.944·λ(275)-1.6123·λ(277.5)- 1.656·λ(280)-1.6362·λ(282.5)-1.7687·λ(285)-1.5771·λ(287.5)-1.4924·λ(290)-1.512·λ(292.5)-1.2806·λ(295)- 0.972·λ(297.5)-0.6918·λ(300)-0.1915·λ(302.5)+0.0608·λ(305)+0.3669·λ(307.5)+0.773·λ(310)+0.9765·λ(312.5)+ 1.0983·λ(315)+1.2729·λ(317.5)+1.2784·λ(320)+1.2581·λ(322.5)+1.2399·λ(325)+1.1771·λ(327.5)+ 1.2958·λ(330)+0.939·λ(332.5)+0.6959·λ(335)+0.9864·λ(337.5)+0.9923·λ(340)+0.5684·λ(342.5)+0.243·λ(345)+ 0.4445·λ(347.5)+0.6025·λ(350)+0.3139·λ(352.5)+0.2606·λ(355)+0.3277·λ(357.5)+0.3698·λ(360)+ 0.2128·λ(362.5)+0.0051·λ(365)+0.1531·λ(367.5)+0.1569·λ(370)-0.1656·λ(372.5)- 0.039·λ(375)+0.0524·λ(377.5)- -0.119·λ(380)-0.5378·λ(382.5)-0.5483·λ(385)-0.1261·λ(387.5)-0.2042·λ(390)-0.3923·λ(392.5)-0.5333·λ(395)- 0.489·λ(397.5)-0.4351·λ(400)-0.5998·λ(402.5)-0.4642·λ(405)-0.531·λ(407.5)-0.8203·λ(410)-0.6201·λ(412.5)- 0.5083·λ(415)-0.7593·λ(417.5)-0.6603·λ(420)-0.6936·λ(422.5)-0.7817·λ(425)-0.7435·λ(427.5)-0.9521·λ(430)- 0.7891·λ(432.5)-0.8318·λ(435)-0.6019·λ(437.5)-0.4292·λ(440)-0.7145·λ(442.5)-0.7046·λ(445)-0.612·λ(447.5)- 0.5985·λ(450)-0.7427·λ(452.5)-0.7232·λ(455)-0.7032·λ(457.5)-0.5994·λ(460)-0.5837·λ(462.5)-0.5454·λ(465)- 0.5679·λ(467.5)-0.3863·λ(470)-0.5886·λ(472.5)-0.5206·λ(475)-0.363·λ(477.5)-0.4128·λ(480)-0.5083·λ(482.5)- 0.2703·λ(485)-0.3073·λ(487.5)-0.2505·λ(490)-0.451·λ(492.5)-0.5756·λ(495)-0.4537·λ(497.5)-0.2979·λ(500)- 0.2674·λ(502.5)-0.3473·λ(505)-0.3781·λ(507.5)-0.1701·λ(510)-0.0185·λ(512.5)-0.2153·λ(515)-0.3019·λ(517.5)- 0.1694·λ(520)-0.0024·λ(522.5)+0.0434·λ(525)-0.2882·λ(527.5)-0.3628·λ(530)-0.1202·λ(532.5)-0.0321·λ(535)- 0.2462·λ(537.5)-0.0852·λ(540)+0.2106·λ(542.5)+0.0227·λ(545)-0.0854·λ(547.5)+0.0692·λ(550)+ 0.0589·λ(552.5)+0.0366·λ(555)+0.2595·λ(557.5)+0.2945·λ(560)+0.2752·λ(562.5)+0.3633·λ(565)+ 0.276·λ(567.5)+0.0497·λ(570)+0.1163·λ(572.5)+0.3366·λ(575)+0.3244·λ(577.5)+0.1379·λ(580)+ 0.0318·λ(582.5)+0.2852·λ(585)+0.1377·λ(587.5)+0.2056·λ(590)+0.2482·λ(592.5)+0.3567·λ(595)+ 0.2912·λ(597.5)+0.066·λ(600)+0.4596·λ(602.5)+0.4271·λ(605)+0.1291·λ(607.5)+0.1359·λ(610)+ 0.4356·λ(612.5)+0.3716·λ(615)-0.1073·λ(617.5)+0.1357·λ(620)+0.437·λ(622.5)+0.759·λ(625)+0.4154·λ(627.5)- 0.039·λ(630)+0.3034·λ(632.5)+0.432·λ(635)-0.2893·λ(637.5)-0.3016·λ(640)+0.7351·λ(642.5)+0.2002·λ(645)- 0.3725·λ(647.5)-0.2197·λ(650)+0.287·λ(652.5)+0.7434·λ(655)+0.9103·λ(657.5)+0.4198·λ(660)+ 0.4081·λ(662.5)+0.9003·λ(665)+0.9254·λ(667.5)+0.538·λ(670)+0.6087·λ(672.5)+0.8222·λ(675)+ 0.4221·λ(677.5)-0.0039·λ(680)+0.0425·λ(682.5)+0.7727·λ(685)+0.2922·λ(687.5)-0.0913·λ(690)- 0.3236·λ(692.5)+0.3088·λ(695)+0.3665·λ(697.5)-0.1954·λ(700)-0.5565·λ(702.5)-0.4843·λ(705)- 0.1387·λ(707.5)- 0.1241·λ(710)-0.0423·λ(712.5)-0.1387·λ(715)+0.7445·λ(717.5)+0.0601·λ(720)+0.4328·λ(722.5)+0.647·λ(725)- 0.0756·λ(727.5)+0.2123·λ(730)+0.173·λ(732.5)-0.3909·λ(735)+0.2399·λ(737.5)+0.833·λ(740)-0.4593·λ(742.5)- 0.4624·λ(745)+0.0354·λ(747.5)+0.7467·λ(750)-325.2837	0.834	1 908	0.379	3 203

1) 2 storm events, 2004-07-06: 16^{48} – 18^{23} (5 samples), 2004-07-22: 16^{42} – 17^{27} (6 samples)

Table A- 35 TSS – Support Vector Machine with Sequential Minimal Optimisation Algorithm (SMO) – Part 2

Analysed Wavelength Range	Resulting Equation	Correlation Coefficient Based on 2nd and 3rd Measurement Campaign	Sum of Residuals of 2nd and 3rd Measurement Campaign	Correlation Coefficient of Storm Events[1)]	Sum of Residuals of Storm Events[1)]
[nm]			[mg/l]		[mg/l]
380 - 750	0.1527·λ(380)-0.079·λ(382.5)+0.0672·λ(385)+0.262·λ(387.5)+0.1197·λ(390)+0.0002·λ(392.5)+0.03·λ(395)-0.0133·λ(397.5)-0.1494·λ(400)-0.1292·λ(402.5)-0.1792·λ(405)-0.5137·λ(407.5)-0.7172·λ(410)-0.2464·λ(412.5)-0.0576·λ(415)-0.4974·λ(417.5)-0.4797·λ(420)-0.2291·λ(422.5)-0.4236·λ(425)-0.4566·λ(427.5)-0.4074·λ(430)-0.1786·λ(432.5)-0.4506·λ(435)-0.2265·λ(437.5)+0.0427·λ(440)-0.2562·λ(442.5)-0.3108·λ(445)-0.2696·λ(447.5)-0.1214·λ(450)-0.0725·λ(452.5)-0.1296·λ(455)-0.0904·λ(457.5)-0.1296·λ(460)-0.1962·λ(462.5)-0.2468·λ(465)-0.3378·λ(467.5)-0.2124·λ(470)-0.0853·λ(472.5)-0.1272·λ(475)-0.0563·λ(477.5)-0.2353·λ(480)-0.2851·λ(282.5)-0.0659·λ(485)-0.1643·λ(487.5)-0.1222·λ(490)-0.171·λ(492.5)-0.3605·λ(495)-0.2293·λ(497.5)-0.1183·λ(500)-0.1019·λ(502.5)-0.1462·λ(505)-0.1683·λ(507.5)+0.0669·λ(510)+0.3767·λ(512.5)-0.2614·λ(515)-0.3416·λ(517.5)-0.0781·λ(520)+0.1019·λ(522.5)+0.1411·λ(525)+0.0013·λ(527.5)+0.0044·λ(530)-0.1281·λ(532.5)-0.0534·λ(535)+0.0351·λ(537.5)+0.248·λ(540)+0.2662·λ(542.5)+0.115·λ(545)+0.0239·λ(547.5)+0.4218·λ(550)+0.6919·λ(552.5)+0.4911·λ(555)+0.6253·λ(557.5)+0.498·λ(560)+0.8026·λ(562.5)+0.3833·λ(565)+0.2805·λ(567.5)+0.7171·λ(570)+0.3486·λ(572.5)+0.6412·λ(575)+0.9686·λ(577.5)+0.7699·λ(580)+0.3279·λ(582.5)+0.3128·λ(585)+0.834·λ(587.5)+1.0688·λ(590)+1.0082·λ(592.5)+0.7275·λ(595)+0.9104·λ(597.5)+0.9374·λ(600)+0.8945·λ(602.5)+0.7702·λ(605)+0.9053·λ(607.5)+0.8775·λ(610)+1.0413·λ(612.5)+0.756·λ(615)+0.3957·λ(617.5)+0.6384·λ(620)+1.0984·λ(622.5)+1.1565·λ(625)+0.8372·λ(627.5)+1.0548·λ(630)+0.9381·λ(632.5)+0.3002·λ(635)+0.3045·λ(637.5)+0.4732·λ(640)+1.073·λ(642.5)+0.177·λ(645)-0.0673·λ(647.5)+0.2311·λ(650)+0.536·λ(652.5)+0.4963·λ(655)+0.6047·λ(657.5)+0.7002·λ(660)+0.9547·λ(662.5)+0.8982·λ(665)+0.9167·λ(667.5)+0.8915·λ(670)+0.6329·λ(672.5)+0.3656·λ(675)+0.0886·λ(677.5)-0.1909·λ(680)-0.1903·λ(682.5)-0.4069·λ(685)-0.9016·λ(687.5)-0.9583·λ(690)-1.0855·λ(692.5)-0.8465·λ(695)-1.4766·λ(697.5)-1.0031·λ(700)-0.2996·λ(702.5)-1.2314·λ(705)-1.4925·λ(707.5)-1.0506·λ(710)-0.2926·λ(712.5)-0.5774·λ(715)-0.8906·λ(717.5)-1.5432·λ(720)-0.0105·λ(722.5)+0.727·λ(725)-0.9615·λ(727.5)-0.5266·λ(730)-0.0726·λ(732.5)-0.6775·λ(735)-0.4213·λ(737.5)-0.568·λ(740)-1.155·λ(742.5)-0.8936·λ(745)-1.4077·λ(747.5)-1.3611·λ(750)+67.9708	0.777	1 908	0.856	835
600-647.5	-0.1848·λ(600)+1.0551·λ(602.5)+0.2991·λ(605)+0.2385·λ(607.5)+0.317·λ(610)+0.6895·λ(612.5)-0.1557·λ(615)--0.2212·λ(617.5)+1.616·λ(620)+2.2051·λ(622.5)+2.423·λ(625)+1.0946·λ(627.5)-0.8704·λ(630)+0.4434·λ(632.5)+0.8142·λ(635)-1.2056·λ(637.5)-2.2341·λ(640)+0.2856·λ(642.5)-0.9762·λ(645)-2.4284·λ(647.5)+68.4348	0.801	1 842	0.873	870
380 - 390	-0.0609·λ(380)-1.0062·λ(382.5)+0.6274·λ(385)+1.3871·λ(387.5)+1.2226·λ(390)+55.3986	0.818	1 866	0.888	993
390 - 400	0.2602·λ(390)+0.2461·λ(392.5)+0.4304·λ(395)+0.4911·λ(397.5)+0.7707·λ(400)+57.1025	0.817	1 868	0.888	982
400 - 410	-0.5293·λ(400)+0.2391·λ(402.5)+1.4128·λ(405)+0.7136·λ(407.5)+0.4206·λ(410)+58.2095	0.815	1 875	0.888	972
410 - 420	0.5372·λ(410)+0.7374·λ(412.5)+0.014·λ(415)-0.5343·λ(417.5)+1.5508·λ(420)+59.709	0.814	1 874	0.888	960
420 - 430	1.0159·λ(420)+1.3746·λ(422.5)+0.1642·λ(425)+0.1809·λ(427.5)-0.3299·λ(430)+60.627	0.813	1 873	0.888	951
430 - 440	-0.7106·λ(430)+0.7058·λ(432.5)+0.5576·λ(435)+0.6323·λ(437.5)+1.2577·λ(440)+62.9936	0.812	1 866	0.887	931
440 - 450	0.5148·λ(440)+0.6337·λ(442.5)+0.2734·λ(445)+0.2834·λ(447.5)+0.7733·λ(450)+63.3128	0.812	1 864	0.887	921
450 - 460	1.2362·λ(450)-0.35228·λ(452.5)+0.3743·λ(455)+0.7339·λ(457.5)+0.5414·λ(460)+64.7728	0.812	1 862	0.886	912

[1)] 2 storm events, 2004-07-06: 16^{48} – 18^{23} (5 samples), 2004-07-22: 16^{42} – 17^{27} (6 samples)

Table A- 36 TSS – Support Vector Machine with Sequential Minimal Optimisation Algorithm (SMO) – Part 3

Analysed Wavelength Range	Resulting Equation	Correlation Coefficient Based on 2nd and 3rd Measurement Campaign	Sum of Residuals of 2nd and 3rd Measurement Campaign	Correlation Coefficient of Storm Events 1)	Sum of Residuals of Storm Events 1)
[nm]			[mg/l]		[mg/l]
460 - 470	-0.0746·λ(460)+0.4963·λ(462.5)+1.4031·λ(465)+ 0.3703·λ(467.5)+0.4014·λ(470)+65.6279	0.811	1 860	0.885	908
470 - 480	0.4793·λ(470)+0.6454·λ(472.5)+0.7713·λ(475)+ 0.3234·λ(477.5)+0.4295·λ(480)+66.698	0.811	1 857	0.884	904
480 - 490	0.5739·λ(480)+0.2089·λ(482.5)+0.4684·λ(485)+ 0.2221·λ(487.5)+1.2416·λ(490)+67.1144	0.810	1 854	0.883	898
490 - 500	1.0766·λ(490)+1.0025·λ(492.5)-0.2553·λ(495)+ 0.1259·λ(497.5)+0.8031·λ(500)+67.839	0.809	1 854	0.882	896
500 - 510	0.6635·λ(500)+0.7114·λ(502.5)-0.2479·λ(505)+ 0.1175·λ(507.5)+1.5798·λ(510)+68.5809	0.809	1 851	0.880	893
510 - 520	1.0109·λ(510)+1.1705·λ(512.5)+0.2079·λ(515)- 0.3415·λ(517.5)+0.8113·λ(520)+68.5816	0.808	1 851	0.879	892
520 - 530	1.4377·λ(520)+2.031·λ(522.5)+0.455·λ(525)- 0.1738·λ(527.5)-0.8651·λ(530)+69.015	0.807	1 853	0.879	890
530 - 540	-0.1701·λ(530)+0.9442·λ(532.5)+1.7109·λ(535)+ 0.1674·λ(537.5)+0.326·λ(540)+70.1231	0.808	1 844	0.877	881
540 - 550	-0.3257·λ(540)+1.0069·λ(542.5)+1.2364·λ(545)+ 0.9659·λ(547.5)+0.1427·λ(550)+71.2954	0.807	1 846	0.875	879
550 - 560	0.0099·λ(550)+0.3407·λ(552.5)+0.5941·λ(555)+ 1.3113·λ(557.5)+0.8256·λ(560)+72.6149	0.808	1 841	0.873	877
560 - 570	1.0944·λ(560)-0.5681·λ(562.6)+0.0089·λ(565)+ 1.0158·λ(567.5)+1.5808·λ(570)+72.6491	0.807	1 840	0.872	874
570 - 580	0.9215·λ(570)+1.1959·λ(572.5)+0.5802·λ(575)- 0.1963·λ(577.5)+0.6587·λ(580)+72.5769	0.807	1 837	0.872	871
580 - 590	0.6398·λ(580)+1.1915·λ(582.5)+1.527·λ(585)+ 0.0761·λ(587.5)-0.2285·λ(590)+73.1291	0.806	1 838	0.870	869
590 - 600	0.9498·λ(590)+1.6222·λ(592.5)+0.5303·λ(595)- 0.1257·λ(597.5)+0.2809·λ(600)+74.7193	0.807	1 832	0.869	865
600 - 610	0.1332·λ(600)+1.3714·λ((602.5)+0.6153·λ(605)+ 0.555·λ(607.5)+0.6324·λ(610)+75.4102	0.807	1 832	0.868	862
610 - 620	0.5419·λ(610)+0.9126·λ(612.5)+0.0663·λ(615)+ 0.0002·λ(617.5)+1.8367·λ(620)+75.6177	0.806	1 832	0.867	859
620 - 630	0.9961·λ(620)+1.5862·λ(622.5)+1.8055·λ(625)+ 0.4785·λ(627.5)-1.4857·λ(630)+74.4904	0.804	1 832	0.866	860
630 - 640	0.4411·λ(630)+1.7425·λ(632.5)+2.1073·λ(635)+ 0.0896·λ(637.5)-0.945·λ(640)+75.9581	0.805	1 824	0.865	856
640 - 650	-0.3021·λ(640)+2.205·λ(642.5)+0.9433·λ(645)- 0.5055·λ(647.5)+1.1502·λ(650)+78.0281	0.805	1 825	0.862	853
650 - 660	-0.1143·λ(650)+2.6283·λ(652.5)+0.5168·λ(655)- 1.0167·λ(657.5)+1.4994·λ(660)+77.4567	0.801	1 838	0.862	852
660 - 670	2.6396·λ(660)+1.7236·λ(662.5)-0.7574·λ(665)- 0.5838·λ(667.5)+0.5041·λ(670)+78.5627	0.801	1 842	0.862	850
670 - 680	1.6641·λ(670)+2.614·λ(672.5)+1.3873·λ(675)- 0.7898·λ(677.5)-1.3329·λ(680)+80.108	0.802	1 832	0.861	848
680 - 690	0.0643·λ(680)+1.0897·λ(682.5)+1.432·λ(685)+ 0.5512·λ(687.5)+0.5323·λ(690)+83.5898	0.804	1 820	0.857	841
690 - 700	1.2665·λ(690)+1.6037·λ(692.5)+1.3428·λ(695)+ 0.3945·λ(697.5)-0.9304·λ(700)+82.3016	0.801	1 828	0.856	842
700 - 710	-0.1269·λ(700)+0.8405·λ(702.5)+1.8325·λ(705)+ 0.1538·λ(707.5)+1.048·λ(710)+86.2092	0.802	1 825	0.855	840

1) 2 storm events, 2004-07-06: 16^{48} – 18^{23} (5 samples), 2004-07-22: 16^{42} – 17^{27} (6 samples)

Table A- 37 TSS – Support Vector Machine with Sequential Minimal Optimisation Algorithm (SMO) – Part 4

Analysed Wavelength Range	Resulting Equation	Correlation Coefficient Based on 2nd and 3rd Measurement Campaign	Sum of Residuals of 2nd and 3rd Measurement Campaign	Correlation Coefficient of Storm Events 1)	Cum of Residuals of Storm Events 1)
[nm]			[mg/l]		[mg/l]
710 - 720	1.9421·λ(710)+1.2867·λ(712.5)+0.1643·λ(715)+ 0.1416·λ(717.5)+0.2322·λ(720)+86.6672	0.803	1 824	0.854	839
720 - 730	1.1901·λ(720)+1.5492·λ(722.5)+1.1638·λ(725)- 0.048·λ(727.5)-0.0465·λ(730)+89.5013	0.803	1 826	0.852	841
730 - 740	0.9335·λ(730)+0.7979·λ(732.5)+0.1527·λ(735)+ 0.7589·λ(737.5)+1.2662·λ(740)+89.624	0.804	1 808	0.850	834
740 - 750	1.7005·λ(740)+0.6777·λ(742.5)+1.8537·λ(745)- 0.3026·λ(747.5)+0.0124·λ(750)+90.2121	0.802	1 817	0.850	833

1) 2 storm events, 2004-07-06: 16^{48} – 18^{23} (5 samples), 2004-07-22: 16^{42} – 17^{27} (6 samples)

Table A- 38 COD_{tot} – Partial Least Squared Regression (PLS) – Part 1

Analysed Wavelength Range	Resulting Equation	max. K	Correlation Coefficient Based on 2nd and 3rd Measurement Campaign	Sum of Residuals of 2nd and 3rd Measurement Campaign	Correlation Coefficient of Storm Events[1)]	Sum of Residuals of Storm Events[1)]
[nm]				[mg/l]		[mg/l]
230 - 380	-98.2691·λ(247.5)+8.2975·λ(250)+ 145.248·λ(252.5)+58.4005·λ(255)- 91.2883·λ(257.5)-41.6366·λ(285)- +21.8288·λ(287.5)-60.7709	10	0.979	1 370	0.775	2 322
240 - 270	-47.4116·λ(242.5)+10.1735·λ(245)+ 53.7802·λ(252.5)+57.5423·λ(255)+ 0.3272·λ(257.5)-51.8767·λ(265)- 19.5405·λ(267.5)+9.0131	10	0.980	1 361	0.804	2 335
240 - 270	-92.7026·λ(252.5)+141.7451·λ(255)+ 26.1087·λ(257.5)+9.7242·λ(265)- 82.4263·λ(267.5)-113.9748	10	0.979	1 319	0.780	2 360
240 - 270	-66.2232·λ(255)+159.7081·λ(257.5)- 91.6909·λ(267.5)-173.7592	10	0.978	1 383	0.774	2 231
240 - 270	4.2086·λ(255)-0.0917·λ(267.5)- 96.9632	10	0.957	2 282	0.905	999
240 - 270	-66.2232·λ(255)+159.7081·λ(257.5)- 91.6909·λ(267.5)-173.7592	5	0.978	1 383	0.774	2 231
240 - 500	-114.7392·λ(247.5)-4.4276·λ((250)+ 106.452·λ(252.5)+137.3398·λ(255)+ 145.2386·λ(257.5)-268.4276·λ(260)+ 44.5072·λ(285)-78.6131·λ(287.5)- 65.3348·λ(290)+103.5823·λ(292.5)+ 84.0638	6	0.983	1 263	0.763	3 584
240 - 500	-144.3975·λ(247.5)-32.2863·λ(250)+ 174.6687·λ(252.5)+155.7279·λ(255)+ 141.7768·λ(257.5)-299.5393·λ(260)+ 8.9658·λ(287.5)+112.8966	6	0.982	1 345	0.737	3 848
240 - 500	-432.7245·λ(250)+703.6230·λ(252.5)- 287.3107·λ(255)+291.7764·λ(257.5)- 271.5654·λ(260)+43.0664	6	0.983	1 291	0.734	3 418
240 - 500	-231.1681·λ(252.5)+483.7773·λ(255)- 247.4905·λ(257.5)-19.1006	6	0.91	1 752	0.822	2 266
240 - 250	-20.7523·λ(242.5)+0.7619·λ(245)+11.1373·λ(247.5)+14.0811·λ(250)+21.3366·λ(252.5)+20.5864·λ(255)+ 12.1083·λ(257.5)-12.9424·λ(260)-14.3866·λ(262.5)-7.907·λ(265)-5.0629·λ(277.5)-20.2166·λ(280)- 11.7085·λ(282.5)-2.5451·λ(285)-12.4712·λ(287.5)-10.6863·λ(290)-4.848·λ(292.5)-1.4584·λ(295)+ 20.0111·λ(297.5)+30.014·λ(300)-9.2345	6	0.981	1 345	0.841	2 239
240 - 250	-20.7523·λ(242.5)+0.7619·λ(245)+11.1373·λ(247.5)+14.0811·λ(250)+21.3366·λ(252.5)+20.5864·λ(255)+ 12.1083·λ(257.5)-12.9424·λ(260)-14.3866·λ(262.5)-7.907·λ(265)-5.0629·λ(277.5)-20.2166·λ(280)- 11.7085·λ(282.5)-2.5451·λ(285)-12.4712·λ(287.5)-10.6863·λ(290)-4.848·λ(292.5)-1.4584·λ(295)+ 20.0111·λ(297.5)+30.014·λ(300)-9.2345	8	0.981	1 345	0.841	2 239
240 - 250	-20.7523·λ(242.5)+0.7619·λ(245)+11.1373·λ(247.5)+14.0811·λ(250)+21.3366·λ(252.5)+20.5864·λ(255)+ 12.1083·λ(257.5)-12.9424·λ(260)-14.3866·λ(262.5)-7.907·λ(265)-5.0629·λ(277.5)-20.2166·λ(280)- 11.7085·λ(282.5)-2.5451·λ(285)-12.4712·λ(287.5)-10.6863·λ(290)-4.848·λ(292.5)-1.4584·λ(295)+ 20.0111·λ(297.5)+30.014·λ(300)-9.2345	10	0.981	1 345	0.841	2 239

[1)] 2 storm events, 2004-07-06: 16^{48} – 18^{23} (5 samples), 2004-07-22: 16^{42} – 17^{27} (6 samples)

Table A- 39 COD_{tot} – Partial Least Squared Regression (PLS) – Part 2

Analysed Wavelength Range	Resulting Equation	max. K	Correlation Coefficient Based on 2nd and 3rd Measurement Campaign	Sum of Residuals of 2nd and 3rd Measurement Campaign	Correlation Coefficient of Storm Events[1)]	Sum of Residuals of Storm Events[1)]
[nm]				[mg/l]		[mg/l]
240 - 500	-3.1431·λ(240)+0.7038·λ(242.5)+2.7885·λ(245)+3.9098·λ(247.5)+4.2726·λ(250)+5.4556·λ(252.5)+ 5.365·λ(255)+4.3459·λ(257.5)+3.2034·λ(260)+2.64·λ(262.5)+2.184·λ(265)+0.6299·λ(267.5)-0.8479·λ(272.5)- 1.6744·λ(275)-2.5968·λ(277.5)-3.5574·λ(280)-3.7816·λ(282.5)-3.4372·λ(285)-4.112·λ(287.5)-4.2816·λ(290)- 4.4116·λ(292.5)-4.3497·λ(295)-3.6699·λ(297.5)-1.8848·λ(300)+1.2637·λ(302.5)+2.19·λ(305)+3.6138·λ(307.5)- 5.8987·λ(392.5)-6.4132·λ(395)-6.314·λ(402.5)-7.2216·λ(405)-6.4227·λ(407.5)-5.4876·λ(410)-5.6375·λ(412.5)- 3.8095·λ(420)-3.4168·λ(422.5)+4.6362·λ(452.5)+8.8543·λ(455)+5.2249·λ(457.5)+7.1075·λ(472.5)+ 2.6527·λ(475)+2.7166·λ(477.5)+1.5416·λ(480)-0.1472·λ(482.5)+4.0976·λ(485)+5.4204·λ(487.5)+3.889·λ(490)+ 4.3677·λ(492.5)+5.2552·λ(495)+3.9664·λ(497.5)-140.461	10	0.987	976	0.840	2 515
240 - 500	-3.1431·λ(240)+0.7038·λ(242.5)+2.7885·λ(245)+3.9098·λ(247.5)+4.2726·λ(250)+5.4556·λ(252.5)+ 5.365·λ(255)+4.3459·λ(257.5)+3.2034·λ(260)+2.64·λ(262.5)+2.184·λ(265)+0.6299·λ(267.5)-0.8479·λ(272.5)- 1.6744·λ(275)-2.5968·λ(277.5)-3.5574·λ(280)-3.7816·λ(282.5)-3.4372·λ(285)-4.112·λ(287.5)-4.2816·λ(290)- 4.4116·λ(292.5)-4.3497·λ(295)-3.6699·λ(297.5)-1.8848·λ(300)+1.2637·λ(302.5)+2.19·λ(305)+3.6138·λ(307.5)- 5.8987·λ(392.5)-6.4132·λ(395)-6.314·λ(402.5)-7.2216·λ(405)-6.4227·λ(407.5)-5.4876·λ(410)-5.6375·λ(412.5)- 3.8095·λ(420)-3.4168·λ(422.5)+4.6362·λ(452.5)+8.8543·λ(455)+5.2249·λ(457.5)+7.1075·λ(472.5)+ 2.6527·λ(475)+2.7166·λ(477.5)+1.5416·λ(480)-0.1472·λ(482.5)+4.0976·λ(485)+5.4204·λ(487.5)+3.889·λ(490)+ 4.3677·λ(492.5)+5.2552·λ(495)+3.9664·λ(497.5)-140.461	6	0.987	976	0.840	2 515
240 - 500	-54.64·λ(252.5)+60.4119·λ(255)+ 31.0459	10	0.966	2 055	0.923	1 539
250-277.5[2)]	0.245·λ(250)+0.245·λ(252.5)+ 0.245·λ(255)+0.245·λ(257.5)+ 0.245·λ(260)+0.245·λ(262.5)+ 0.245·λ(265)+0.245·λ(267.5)+ 0.245·λ(270)+0.245·λ(272.5)+ 0.245·λ(275)+0.245·λ(277.5)	-	0.956	5 830	0.914	1 079
257.5-290[2)]	37.9872·λ(257.5)- 437.8432·λ(287.5)+ 407.0842·λ(290)+17.427	-	0.961	2 537	0.863	2 315
255[3)]	4.2291·λ(255)-96.9632	-	0.957	2 272	0.905	1 007
245-265[3)]	0.4699·λ(245)+0.4699·λ(247.5)+ 0.4699·λ(250)+0.4699·λ(252.5)+ 0.4699·λ(255)+0.4699·λ(257.5)+ 0.4699·λ(260)+0.4699·λ(262.5)+ 0.4699·λ(265)-96.9632	-	0.956	2 338	0.907	997
255[3)]	5.7719·λ(255)+31.0459	-	0.957	13 780	0.905	3 234
245-265[3)]	0.6413·λ(245)+0.6413·λ(247.5)+ 0.6413·λ(250)+0.6413·λ(252.5)+ 0.6413·λ(255)+0.6413·λ(257.5)+ 0.6413·λ(260)+0.6413·λ(262.5)+ 0.6413·λ(265)+31.0459	-	0.956	14 350	0.907	3 284
255[3)]	2.9946·λ(255)+9.0131	-	0.957	4 621	0.905	1 002
245-265[3)]	0.3327·λ(245)+0.3327·λ(247.5)+ 0.3327·λ(250)+0.3327·λ(252.5)+ 0.3327·λ(255)+0.3327·λ(257.5)+ 0.3327·λ(260)+0.3327·λ(262.5)+ 0.3327·λ(265)+9.0131	-	0.956	4 433	0.907	992
250[3)]	4.03·λ(250)-115.8	-	0.954	2 348	0.902	1 048

[1)] 2 storm events, 2004-07-06: 16^{48} – 18^{23} (5 samples), 2004-07-22: 16^{42} – 17^{27} (6 samples)
[2)] provided by the manufacturer based on PLS
[3)] developed by the author on the basis of SLR and PLS

Table A- 40 COD_{tot} – Partial Least Squared Regression (PLS) – Part 3

Analysed Wavelength Range	Resulting Equation	max. K	Correlation Coefficient Based on 2nd and 3rd Measurement Campaign	Sum of Residuals of 2nd and 3rd Measurement Campaign	Correlation Coefficient of Storm Events[1]	Sum of Residuals of Storm Events[1]
[nm]				[mg/l]		[mg/l]
240 – 260[3]	0.4478·λ(240)+0.4478·λ(242.5)+ 0.4478·λ(245)+0.4478·λ(247.5)+ 0.4478·λ(250)+0.4478·λ(252.5)+ 0.4478·λ(255)+0.4478·λ(257.5)+ 0.4478·λ(260)-115.8	-	0.953	2 360	0.902	1 054
257.5[3]	7.2282·λ(257.5)+17.427	-	0.958	20 803	0.909	4 623
247.5-267.5[3]	0.8031·λ(247.5)+0.8031·λ(250)+ 0.8031·λ(252.5)+0.8031·λ(255)+ 0.8031·λ(257.5)+0.8031·λ(260)+ 0.8031·λ(262.5)+0.8031·λ(265)+ 0.8031·λ(267.5)+17.427	-	0.956	21 826	0.909	4 723

[1] 2 storm events, 2004-07-06: 16^{48} – 18^{23} (5 samples), 2004-07-22: 16^{42} – 17^{27} (6 samples)
[3] developed by the author on the basis of SLR and PLS

Table A- 41 COD_{sol} – Partial Least Squared Regression (PLS) – Part 1

Analysed Wavelength Range	Resulting Equation	max. K	Correlation Coefficient Based on 2nd and 3rd Measurement Campaign	Sum of Residuals of 2nd and 3rd Measurement Campaign	Correlation Coefficient of Storm Events[1)]	Sum of Residuals of Storm Events[1)]
[nm]				[mg/l]		[mg/l]
230 - 380	2.6213·λ(230)-13.8669·λ(237.5)+ 13.6109·λ(240)-1.0309·λ(255)+ 22.4776·λ(260)+1.3725·λ(262.5)- 25.9639·λ(277.5)-54.8466	10	0.950	673	0.859	953
240 - 500	20.6355·λ(252.5)+3.7242·λ(255)- 90.9649·λ(257.5)+78.8907·λ(260)+ 13.6962·λ(262.5)-33.869·λ(282.5)+ 6.8613·λ(285)-63.6429	6	0.948	693	0.873	857
240 - 500	1.1331·λ(252.5)+47.3853·λ(255)- 124.398·λ(257.5)+97.9906·λ(260)- 23.2148·λ(285)-67.0455	6	0.948	695	0.861	851
240 - 270	-37.0537·λ(255)+73.117·λ(257.5)- 34.7002·λ(260)+72.4764	6	0.876	998	0.781	1 274
240 - 270	-143.3999·λ(252.5)+259.4353·λ(255)- 42.5726·λ(257.5)-72.033·λ(260)+ 73.6472	6	0.916	859	0.652	1 908
240 - 500	23.4112·λ(252.5)-8.3552·λ(255)- 59.1722·λ(257.5)+42.629·λ(260)+ 27.2433·λ(262.5)+2.1758·λ(280)- 5.7915·λ(282.5)-48.691·λ(285)+ 12.0205·λ(287.5)+13.7051·λ(290)- 60.4751	6	0.948	695	0.873	909
240 - 500	-3.3586·λ(250)+1.28·λ(252.5)+2.8964·λ(255)-0.0279·λ(257.5)+11.4354·λ(260)+9.869·λ(262.5)+6.3769·λ(265)- 19.0738·λ(277.5)-5.7629·λ(280)-5.6493·λ(282.5)-6.1641·λ(285)+4.0113·λ(287.5)+11.1878·λ(290)+ 8.2109·λ(292.5)-16.2243·λ(297.5)-47.4889	6	0.948	714	0.825	1 130
240 - 500	-1.579·λ(245)-1.227·λ(247.5)-1.2646·λ(250)+2.1741·λ(252.5)+4.0798·λ(255)+3.23·λ(257.5)+8.9664·λ(260)+ 8.0837·λ(262.5)+5.9206·λ(265)-9.7837·λ(275)-10.0995·λ(277.5)-4.0847·λ(280)-4.1236·λ(282.5)-4.0421·λ(285)+ 1.35·λ(287.5)+5.8075·λ(290)+5.7677·λ(292.5)+1.8951·λ(295)-4.5594·λ(297.5)-7.4227·λ(300)-41.6737	6	0.947	714	0.824	1 156
240 - 500	0.3579·λ(242.5)+0.7981·λ(245)+1.3393·λ(247.5)+1.689·λ(250)+2.6345·λ(252.5)+3.1921·λ(255)+ 2.9979·λ(257.5)+3.5141·λ(260)+2.9502·λ(262.5)+2.0160·λ(265)-2.9469·λ(272.5)-3.1887·λ(275)-3.7·λ(277.5)- 3.2893·λ(280)-3.4393·λ(282.5)-3.3568·λ(285)-2.3815·λ(287.5)-1.3506·λ(290)-0.7099·λ(292.5)-0.7096·λ(295)- 1.1146·λ(297.5)-1.0058·λ(300)-1.0058·λ(300)-0.3865·λ(302.5)+6.9472·λ(350)+6.8434·λ(352.5)-3.041·λ(405)- 1.4115·λ(407.5)-1.4984·λ(410)-1.3157·λ(420)-1.4551·λ(422.5)-29.5909	6	0.946	715	0.826	960
240 - 500	0.3559·λ(242.5)+0.7434·λ(245)+1.2174·λ(247.5)+1.569·λ(250)+2.3165·λ(252.5)+2.8058·λ(255)+ 2.7362·λ(257.5)+3.0535·λ(260)+2.6109·λ(262.5)+1.8824·λ(265)+0.6210·λ(267.5)-1.8548·λ(272.5)- 2.1801·λ(275)-2.6601·λ(277.5)-2.5885·λ(280)-2.8574·λ(282.5)-2.9351·λ(285)-2.4308·λ(287.5)-1.8485·λ(290)- 1.4423·λ(292.5)-1.4032·λ(295)-1.6026·λ(297.5)-1.3772·λ(300)-0.7809·λ(302.5)-0.1746·λ(305)+3.0712·λ(335)+ 3.4478·λ(347.5)+4.5091·λ(350)+4.4162·λ(352.5)+3.5373·λ(355)-2.4827·λ(402.5)-4.0352·λ(405)- 3.0832·λ(407.5)-3.2505·λ(410)-2.759·λ(412.5)-3.6859·λ(420)-3.9281·λ(420)-3.9281·λ(422.5)+3.3521·λ(487.5)+ 3.4224·λ(495)+2.8789·λ(497.5)-43.0027	6	0.948	705	0.837	1 011

[1)] 2 storm events, 2004-07-06: 16^{48} – 18^{23} (5 samples), 2004-07-22: 16^{42} – 17^{27} (6 samples)

Table A- 42 COD_{sol} – Partial Least Squared Regression (PLS) – Part 2

Analysed Wavelength Range	Resulting Equation	max. K	Correlation Coefficient Based on 2^{nd} and 3^{rd} Measurement Campaign	Sum of Residuals of 2^{nd} and 3^{rd} Measurement Campaign	Correlation Coefficient of Storm Events[1)]	Sum of Residuals of Storm Events[1)]
[nm]				[mg/l]		[mg/l]
240 - 500	0.6135·λ(242.5)+0.9516·λ(245)+1.3562·λ(247.5)+1.648·λ(250)+2.2663·λ(252.5)+2.6529·λ(255)+ 2.5452·λ(257.5)+2.7457·λ(260)+2.3298·λ(262.5)+1.6774·λ(265)+0.5702·λ(267.5)-1.6055·λ(272.5)- 1.9312·λ(275)-2.3979·λ(277.5)-2.4146·λ(280)-2.6833·λ(282.5)-2.7865·λ(285)-2.4131·λ(287.5)-1.9606·λ(290)- 1.6379·λ(292.5)-1.627·λ(295)-1.8048·λ(297.5)-1.6476·λ(300)-1.1957·λ(302.5)-0.7278·λ(305)+1.2842·λ(327.5)+ 1.7030·λ(335)+1.671·λ(337.5)+1.6412·λ(342.5)+1.6829·λ(345)+1.9776·λ(347.5)+2.8365·λ(350)+ 2.7791·λ(352.5)+2.058·λ(355)+1.7457·λ(357.5)+1.6884·λ(367.5)-2.4456·λ(402.5)-3.6794·λ(405)- 2.8958·λ(407.5)-3.0003·λ(410)-2.5567·λ(412.5)-3.2156·λ(420)-3.3671·λ(422.5)-2.2422·λ(432.5)-1.9565·λ(435)- 2.1516·λ(442.5)+2.839·λ(485)+3.4776·λ(487.5)+3.6602·λ(495)+3.2565·λ(497.5)-47.7503	6	0.948	702	0.844	995
240 - 500	-21.6763·λ(255)+23.572·λ(260)+ 101.1963	6	0.865	1 049	0.683	1 581
240 - 290[2)]	0.2167·λ(240)+0.2167·λ(242.5)+ 0.2167·λ(245)+0.2167·λ(247.5)+ 0.2167·λ(272.5)+0.2167·λ(275)+ 0.2167·λ(277.5)+0.2167·λ(280)+ 0.2167·λ(282.5)+0.2167·λ(285)+ 0.2167·λ(287.5)+0.2167·λ(290)	-	0.841	7 996	0.816	2 203
250-282.5[2)]	-108.2838·λ(250)+172.8537·λ(255)- 130.6672·λ(272.5)+83.0956·λ(282.5)+ 8.8446	-	0.878	51 512	0.774	13 748
260[3)]	1.8958·λ(260)+101.1963	-	0.854	7 106	0.822	2 573
250 - 270[3)]	0.2106·λ(250)+0.2106·λ(252.5)+ 0.2106·λ(255)+0.2106·λ(257.5)+ 0.2106·λ(260)+0.2106·λ(262.5)+ 0.2106·λ(265)+0.2106·λ(267.5)+ 0.2106·λ(270)+101.1963	-	0.851	7 343	0.821	2 592
255[3)]	1.4298·λ(255)+73.6472	-	0.851	3 926	0.823	1 800
245-265[3)]	0.1589·λ(245)+0.1589·λ(247.5)+ 0.1589·λ(250)+0.1589·λ(252.5)+ 0.1589·λ(255)+0.1589·λ(257.5)+ 0.1589·λ(260)+0.1589·λ(262.5)+ 0.1589·λ(265)73.6472	-	0.849	4 067	0.825	1 812

1) 2 storm events, 2004-07-06: 16^{48} – 18^{23} (5 samples), 2004-07-22: 16^{42} – 17^{27} (6 samples)
2) provided by the manufacturer based on PLS
3) developed by the author on the basis of SLR and PLS

Table A- 43 TSS – Partial Least Squared Regression (PLS) – Part 1

Analysed Wavelength Range	Resulting Equation	max. K	Correlation Coefficient Based on 2nd and 3rd Measurement Campaign	Sum of Residuals of 2nd and 3rd Measurement Campaign	Correlation Coefficient of Storm Events[1)]	Sum of Residuals of Storm Events[1)]
[nm]				[mg/l]		[mg/l]
380 - 750	$-6.1814\cdot\lambda(380)+7.1744\cdot\lambda(382.5)+9.491\cdot\lambda(597.5)+0.3132\cdot\lambda(615)+143.6995\cdot\lambda(665)-102.8912\cdot\lambda(692.5)-53.5462\cdot\lambda(695)-97.3371$	6	0.914	1 104	0.612	2 971
380 - 750	$1.3631\cdot\lambda(382.5)+7.6031\cdot\lambda(597.5)+140.805\cdot\lambda(665)-138.244\cdot\lambda(692.5)-13.2891\cdot\lambda(695)-115.3012$	6	0.915	1 101	0.642	3 072
380 - 750	$2.5089\cdot\lambda(382.5)+144.1413\cdot\lambda(665)-127.2349\cdot\lambda(692.5)-21.2183\cdot\lambda(695)-112.1395$	6	0.914	1 112	0.634	3 066
380 - 750	$156.3621\cdot\lambda(665)-116.7687\cdot\lambda(692.5)-39.9518\cdot\lambda(695)-78.5053$	6	0.910	1 127	0.836	2 540
380 - 750	$-36.9441\cdot\lambda(692.5)+41.8275\cdot\lambda(695)+13.7175$	6	0.807	1 576	0.860	935
380 - 750	$-2.6661\cdot\lambda(380)+3.6555\cdot\lambda(382.5)-4.4571\cdot\lambda(385)+41.6188\cdot\lambda(597.5)+40.2233\cdot\lambda(615)-63.24\cdot\lambda(660)+100.4095\cdot\lambda(665)-67.3133\cdot\lambda(692.5)-42.3451\cdot\lambda(695)-9.0228\cdot\lambda(702.5)-91.2954$	6	0.916	1 095	0.330	2 782
380 - 750	$0.7379\cdot\lambda(380)+3.2837\cdot\lambda(382.5)+0.5767\cdot\lambda(385)-32.344\cdot\lambda(522.5)+20.6973\cdot\lambda(595)+26.0077\cdot\lambda(597.5)+26.4858\cdot\lambda(615)+28.2215\cdot\lambda(640)-31.6118\cdot\lambda(660)+48.1805\cdot\lambda(665)+37.5239\cdot\lambda(677.5)-49.0754\cdot\lambda(692.5)-36.7601\cdot\lambda(695)-24.0595\cdot\lambda(702.5)-20.3044\cdot\lambda(705)-119.4734$	6	0.915	1 119	0.447	2 981
380 - 750	$0.7379\cdot\lambda(380)+3.2837\cdot\lambda(382.5)+0.5767\cdot\lambda(385)-32.344\cdot\lambda(522.5)+20.6973\cdot\lambda(595)+26.0077\cdot\lambda(597.5)+26.4858\cdot\lambda(615)+28.2215\cdot\lambda(640)-31.6118\cdot\lambda(660)+48.1805\cdot\lambda(665)+37.5239\cdot\lambda(677.5)-49.0754\cdot\lambda(692.5)-36.7601\cdot\lambda(695)-24.0595\cdot\lambda(702.5)-20.3044\cdot\lambda(705)-119.4734$	8	0.915	1 119	0.447	2 981
380 - 750	$0.7379\cdot\lambda(380)+3.2837\cdot\lambda(382.5)+0.5767\cdot\lambda(385)-32.344\cdot\lambda(522.5)+20.6973\cdot\lambda(595)+26.0077\cdot\lambda(597.5)+26.4858\cdot\lambda(615)+28.2215\cdot\lambda(640)-31.6118\cdot\lambda(660)+48.1805\cdot\lambda(665)+37.5239\cdot\lambda(677.5)-49.0754\cdot\lambda(692.5)-36.7601\cdot\lambda(695)-24.0595\cdot\lambda(702.5)-20.3044\cdot\lambda(705)-119.4734$	10	0.915	1 119	0.447	2 981

[1)] 2 storm events, 2004-07-06: 16^{48} – 18^{23} (5 samples), 2004-07-22: 16^{42} – 17^{27} (6 samples)

Table A- 44 TSS – Partial Least Squared Regression (PLS) – Part 2

Analysed Wavelength Range	Resulting Equation	max. K	Correlation Coefficient Based on 2nd and 3rd Measurement Campaign	Sum of Residuals of 2nd and 3rd Measurement Campaign	Correlation Coefficient of Storm Events[1)]	Sum of Residuals of Storm Events[1)]
[nm]				[mg/l]		[mg/l]
380 - 750	0.0091·λ(380)+1.8207·λ(382.5)-0.0698·λ(385)-25.6504·λ(522.5)+11.1053·λ(562.5)+14.4034·λ(595)+18.4019·λ(597.5)+13.5779·λ(600)+13.3088·λ(605)+18.6324·λ(615)+18.8343·λ(640)-26.4694·λ(660)+33.0517·λ(665)+23.5853·λ(677.5)-43.0290·λ(692.5)-34.4247·λ(695)-25.7608·λ(702.5)-21.9238·λ(705)-19.4592·λ(710)+27.3206·λ(737.5)-111.6151	6	0.912	1 132	0.370	3 007
380 - 750	1.4336·λ(380)+3.119·λ(382.5)+1.2445·λ(385)-1.6198·λ(387.5)-19.9735·λ(520)-22.1118·λ(522.5)+10.1694·λ(562.5)+12.4484·λ(595)+16.1433·λ(597.5)+12.0531·λ(600)+11.3501·λ(605)+10.3954·λ(507.5)+10.3735·λ(612.5)+16.2287·λ(615)+11.4147·λ(617.5)+17.2826·λ(640)-18.9501·λ(652.5)-22.7912·λ(660)+29.5718·λ(665)+17.8603·λ(667.5)+21.5211·λ(677.5)-35.1652·λ(692.5)-27.5442·λ(695)-13.0818·λ(700)-19.2546·λ(702.5)-16.8689·λ(705)-14.418·λ(710)+28.8067·λ(737.5)-10.8794·λ(742.5)-11.4018·λ(745)-128.0266	6	0.918	1 093	0.415	2 840
380 - 750	1.7932·λ(380)+3.2283·λ(382.5)+1.6038·λ(385)-0.8404·λ(387.5)-0.8663·λ(390)-1.5499·λ(392.5)-17.1482·λ(520)-18.9915·λ(522.5)+8.3952·λ(562.5)+10.1464·λ(595)+13.3189·λ(597.5)+9.8489·λ(600)+6.0483·λ(602.5)+9.2126·λ(605)+8.4027·λ(607.5)+8.3541·λ(612.5)+13.3116·λ(615)+9.1701·λ(617.5)+9.3497·λ(630)+14.1273·λ(640)+7.8406·λ(642.5)+9.3169·λ(647.5)-16.7718·λ(652.5)-20.1357·λ(660)+24.4124·λ(665)+14.3753·λ(667.5)-13.1252·λ(672.5)+17.3816·λ(677.5)-11.5938·λ(690)-30.8451·λ(692.5)-24.3799·λ(695)-12.0603·λ(700)-17.2793·λ(702.5)-15.4345·λ(705)-13.3353·λ(710)-9.0597·λ(722.5)+18.5141·λ(730)+23.4764·λ(737.5)-10.2148·λ(742.5)-10.6839·λ(745)-127.447	6	0.916	1 106	0.392	2 913
380 - 750	2.6023·λ(380)+3.6659·λ(382.5)+2.5403·λ(385)+0.6162·λ(387.5)+0.5756·λ(390)+0.0328·λ(392.5)-9.362·λ(490)-9.9203·λ(492.5)-10.0832·λ(510)-12.1812·λ(520)-13.6097·λ(522.5)+7.926·λ(562.5)+4.7766·λ(590)+5.1704·λ(592.5)+9.4737·λ(595)+11.861·λ(597.5)+9.087·λ(600)+6.4145·λ(602.5)+8.7612·λ(605)+8.1088·λ(607.5)+5.4652·λ(610)+8.056·λ(612.5)+11.884·λ(615)+8.6117·λ(617.5)+8.3028·λ(630)+6.1294·λ(632.5)+11.6452·λ(640)+7.1385·λ(642.5)+7.7921·λ(647.5)-12.5625·λ(652.5)-15.6368·λ(660)+19.2235·λ(665)+11.3311·λ(667.5)-10.6936·λ(672.5)+13.2804·λ(677.5)-10.5455·λ(690)-26.5183·λ(692.5)-21.5155·λ(695)-8.6566·λ(697.5)-12.1519·λ(700)-16.3613·λ(702.5)-14.3335·λ(705)-12.8691·λ(710)-10.1316·λ(722.5)+10.9581·λ(727.5)+11.5337·λ(730)+11.5791·λ(735)+14.966·λ(737.5)-12.1955·λ(742.5)-12.2386·λ(745)-130.0736	6	0.915	1 115	0.507	2 833
550 - 600	36.3291·λ(550)+40.0209·λ(552.5)+31.4741·λ(562.5)+6.2377·λ(565)-48.837·λ(580)-35.0043·λ(582.5)-31.0955·λ(585)-15.2927	6	0.848	1 486	0.611	2 005
550 - 600	32.7689·λ(550)+34.5462·λ(552.5)+27.6077·λ(562.5)-49.8328·λ(582.5)-45.4778·λ(585)-14.1186	6	0.846	1 495	0.726	1 901
550 - 600	56.8192·λ(550)+32.5764·λ(562.5)-47.5086·λ(582.5)-42.0027·λ(585)-21.8015	6	0.845	1 497	0.766	1 878
550 - 600	52.7915·λ(550)+31.3445·λ(562.5)-84.1167·λ(585)-24.5797	6	0.844	1 500	0.801	1 847
550 - 600	63.0037·λ(562.5)-61.0871·λ(585)-2.18	6	0.839	1 489	0.899	1 389

[1)] 2 storm events, 2004-07-06: 16^{48} – 18^{23} (5 samples), 2004-07-22: 16^{42} – 17^{27} (6 samples)

Table A- 45 TSS – Partial Least Squared Regression (PLS) – Part 3

Analysed Wavelength Range	Resulting Equation	max. K	Correlation Coefficient Based on 2nd and 3rd Measurement Campaign	Sum of Residuals of 2nd and 3rd Measurement Campaign	Correlation Coefficient of Storm Events[1)]	Sum of Residuals of Storm Events[1)]
[nm]				[mg/l]		[mg/l]
550 - 600	27.2756·λ(550)+28.1468·λ(552.5)+ 13.7557·λ(560)+41.9765·λ(562.5)+ 14.2804·λ(565)-18.6473·λ(570)- 26.7354·λ(580)-29.8431·λ(582.5)- 30.427·λ(585)-20.666·λ(592.5)-23.7059	6	0.848	1 494	0.620	2 077
550 - 600	27.0783·λ(550)+24.7259·λ(552.5)+ 7.8569·λ(555)+12.5802·λ(560)+ 38.6002·λ(562.5)+15.8493·λ(565)- 11.2752·λ(570)-9.7843·λ(572.5)- 11.0022·λ(575)-18.1602·λ(580)- 26.8954·λ(582.5)-29.5442·λ(585)- 11.7743·λ(587.5)-14.3322·λ(592.5)+ 5.3552·λ(597.5)-15.1248	6	0.848	1 494	0.653	1 983
550 - 600	27.3045·λ(550)+24.5495·λ(552.5)+ 8.6157·λ(555)-0.0335·λ(557.5)+ 12.5972·λ(560)+38.9123·λ(562.5)+ 16.4698·λ(565)-5.5403·λ(567.5)- 10.1889·λ(570)-10.0551·λ(572.5)- 9.9551·λ(575)+1.8497·λ(577.5)- 16.8326·λ(580)-26.4864·λ(582.5)- 29.4312·λ(585)-10.4153·λ(587.5)- 5.1562·λ(590)-12.9753·λ(592.5)- 1.2388·λ(595)+7.287·λ(597.5)- 15.2362	6	0.848	1 494	0.655	1 955
600-647.5[2)]	0.255·λ(600)+0.255·λ(602.5)+0.255·λ(605)+ 0.255·λ(607.5)+0.255·λ(610)+0.255·λ(612.5)+ 0.255·λ(615)+0.255·λ(617.5)+0.255·λ(620)+ 0.255·λ(622.5)+0.255·λ(625)+ 0.255·λ(627.5)+0.255·λ(630)+0.255·λ(632.5)+ 0.255·λ(635)+0.255·λ(637.5)+0.255·λ(640)+ 0.255·λ(642.5)+0.255·λ(645)+0.255·λ(647.5)	-	0.806	1 728	0.865	890
695[3)]	4.8834·λ(695)+13.7175	-	0.802	1 686	0.856	940
685-705[3)]	0.5426·λ(685)+0.5426·λ(687.5)+ 0.5426·λ(690)+0.5426·λ(692.5)+ 0.5426·λ(695)+0.5426·λ(697.5)+ 0.5426·λ(700)+0.5426·λ(702.5)+ 0.5426·λ(705)+13.7175	-	0.803	1 714	0.856	943
562.5[3)]	1.9166·λ(562.5)-2.18	-	0.810	3 761	0.873	1 868
552.5 - 572.5[3)]	0.213·λ(552.5)+0.213·λ(555)+0.213·λ(557.5)+ 0.213·λ(560)+0.213·λ(562.5)+0.213·λ(565)+ 0.213·λ(567.5)+0.213·λ(570)+0.213·λ(572.5)- 2.18	-	0.808	3 760	0.873	1 871
512.5[3)]	2.75·λ(512.5)+79.81	-	0.808	1 942	0.879	896
502.5 - 522.5[3)]	0.3056·λ(502.5)+0.3056·λ(505)+ 0.3506·λ(507.5)+0.3056·λ(510)+ 0.3506·λ(512.5)+0.3506·λ(515)+ 0.3506·λ(517.5)+0.3506·λ(520)+ 0.3506·λ(522.5)+79.81	-	0.809	1 934	0.879	895

[1)] 2 storm events, 2004-07-06: 16^{48} – 18^{23} (5 samples), 2004-07-22: 16^{42} – 17^{27} (6 samples)
[2)] provided by the manufacturer based on PLS
[3)] developed by the author on the basis of SLR and PLS

TABLES OF MEAN DRY AND RAIN WEATHER CONCENTRATIONS

Table A- 46 Mean Dry Weather Concentrations of COD_{tot} Based on Simple Linear Regression (SLR) Methods

Year	Month	250 - 260			270 - 280			280 - 290		
		2-CM [mg/l]	av. [mg/l]	s.d. [mg/l]	2-CM [mg/l]	av. [mg/l]	s.d. [mg/l]	2-CM [mg/l]	av. [mg/l]	s.d. [mg/l]
2002	October	898	854	396	895	855	401	898	857	403
	November	941	857	310	938	855	312	932	849	313
	December	811	727	297	807	724	297	804	721	297
2003	January	-	-	-	-	-	-	-	-	-
	February	871	794	294	861	784	295	847	772	298
	March	759	820	335	753	813	337	746	804	340
	April	982	867	311	978	978	310	974	862	308
	May	961	880	286	956	875	286	951	871	286
	June	919	851	302	916	848	305	912	844	306
	July	971	909	307	962	901	309	952	891	310
	August	944	861	287	935	852	288	923	841	287
	September	929	848	278	920	839	279	911	830	279
	October	1 095	1 033	323	1 090	1 028	327	1 085	1 023	330
	November	1 093	1 010	361	1 082	999	362	1 075	992	364
	December	1 097	1 023	418	1 095	1 021	419	1 103	1 027	420
2004	January	1 060	986	331	1 051	977	334	1 045	972	335
	February	1 007	931	276	1 001	924	276	998	921	276
	March	865	786	289	859	781	289	858	781	289
	April	811	722	338	808	720	339	807	721	341
	May	874	766	303	873	764	305	874	765	306
	June	670	616	289	667	613	287	667	613	286
	July	564	552	302	563	550	301	562	549	299
	August	971	887	458	966	883	461	960	878	463
	2002	883	813	-	880	811	-	878	809	-
	2003	966	900	-	959	903	-	953	887	-
	2004	853	781	-	849	777	-	846	775	-
	Total	913	845	-	908	845	-	904	836	-

2-CM: two components method
av.: arithmetic mean (average value)
s.d.: standard deviation

Table A- 47 Mean Dry Weather Concentrations of COD_{tot} Based on Least Median Squares Regression (LMS) Methods

Year	Month	230 - 500			254, 436			250 -260, 436		
		2-CM [mg/l]	av. [mg/l]	s.d. [mg/l]	2-CM [mg/l]	av. [mg/l]	s.d. [mg/l]	2-CM [mg/l]	av. [mg/l]	s.d. [mg/l]
2002	October	1 043	995	447	1 102	1 063	483	1 026	978	428
	November	1 035	933	368	1 036	931	388	1 041	941	367
	December	868	766	351	853	750	349	881	780	351
2003	January	-	-	-	-	-	-	-	-	-
	February	920	833	352	872	795	376	941	852	353
	March	811	871	394	800	851	417	826	889	390
	April	1 079	949	358	1 083	968	352	1 092	959	363
	May	1 050	953	335	1 049	957	335	1 064	968	336
	June	1 018	936	380	1 037	958	429	1 023	942	372
	July	1 060	987	381	1 050	980	425	1 072	999	370
	August	1 030	929	348	1 011	909	363	1 041	941	345
	September	1 006	907	336	984	883	351	1 022	923	336
	October	1 232	1 157	398	1 252	1 175	431	1 233	1 158	388
	November	1 181	1 082	396	1 154	1 053	418	1 195	1 097	394
	December	1 118	1 033	456	1 160	1 060	455	1 194	1 106	449
2004	January	1 144	1 054	366	1 117	1 023	383	1 160	1 071	364
	February	1 109	1 015	331	1 106	1 008	347	1 120	1 026	330
	March	947	851	340	947	850	348	953	858	342
	April	880	772	406	890	780	423	891	783	403
	May	951	821	361	963	826	384	961	832	358
	June	709	643	332	714	647	330	720	654	337
	July	589	569	349	596	575	348	597	581	355
	August	1 045	954	529	1 060	979	553	1 065	972	527
	2002	982	898	-	997	915	-	983	900	-
	2003	1 046	967	-	1 041	963	-	1 064	985	-
	2004	922	835	-	924	836	-	933	847	-
	Total	992	910	-	993	910	-	1 005	923	-

2-CM: two components method
av.: arithmetic mean (average value)
s.d.: standard deviation

Table A- 48 Mean Dry Weather Concentrations of COD_{tot} Based on M5 Model Tree Regression (M5) Methods

Year	Month	254, 436			250 – 277.5, 436			310 – 320,436		
		2-CM [mg/l]	av. [mg/l]	s.d. [mg/l]	2-CM [mg/l]	av. [mg/l]	s.d. [mg/l]	2-CM [mg/l]	av. [mg/l]	s.d. [mg/l]
2002	October	984	956	388	986	957	390	952	923	388
	November	904	832	265	902	828	270	899	824	274
	December	774	699	261	771	696	263	775	698	259
2003	January	-	-	-	-	-	-	-	-	-
	February	804	754	252	803	752	255	779	725	267
	March	730	785	308	727	782	312	715	765	314
	April	921	837	272	920	833	279	921	838	259
	May	905	841	233	903	837	238	903	838	232
	June	906	847	296	904	844	299	903	842	301
	July	911	863	284	910	861	287	909	858	291
	August	882	814	232	881	811	236	881	811	237
	September	868	798	230	868	797	231	866	793	236
	October	1 028	985	285	1 028	984	287	1 028	983	287
	November	993	934	318	992	932	320	986	923	326
	December	992	940	382	1 000	946	385	1 005	948	392
2004	January	967	912	296	966	910	298	962	902	306
	February	935	876	211	934	874	215	932	869	220
	March	846	774	257	845	773	259	845	771	258
	April	809	721	341	808	721	342	806	718	341
	May	869	765	295	869	764	297	869	762	299
	June	667	609	298	665	607	301	679	620	286
	July	551	538	312	547	534	314	572	555	302
	August	913	849	445	909	843	451	923	858	431
	2002	887	829	-	886	827	-	875	815	-
	2003	904	854	-	903	853	-	900	848	-
	2004	820	756	-	818	753	-	824	757	-
	Total	871	815	-	870	813	-	869	810	-

2-CM: two components method
av.: arithmetic mean (average value)
s.d.: standard deviation

Table A- 49 Mean Dry Weather Concentrations of COD_{tot} Based on Support Vector Machines using Sequential Optimisation Algorithm (SMO)

Year	Month	240 - 250			250 - 260			290 - 300		
		2-CM [mg/l]	av. [mg/l]	s.d. [mg/l]	2-CM [mg/l]	av. [mg/l]	s.d. [mg/l]	2-CM [mg/l]	av. [mg/l]	s.d. [mg/l]
2002	October	941	886	411	947	907	422	972	924	436
	November	905	815	337	985	896	334	960	867	350
	December	806	718	305	827	737	314	820	727	323
2003	January	-	-	-	-	-	-	-	-	-
	February	821	737	319	886	808	315	842	761	336
	March	724	778	355	782	843	356	753	806	377
	April	955	841	316	1 023	903	323	1 007	891	330
	May	935	851	298	1 004	918	302	983	895	311
	June	889	816	306	966	893	337	952	876	352
	July	939	876	314	1 005	939	330	985	918	351
	August	920	830	297	980	891	311	952	859	320
	September	922	836	293	951	864	301	937	845	311
	October	1 046	977	330	1 154	1 088	357	1 143	1 073	374
	November	1 033	945	364	1 105	1 012	346	1 081	986	354
	December	1 050	968	433	1 119	1 039	430	1 118	1 033	438
2004	January	1 000	918	346	1 089	1 008	346	1 074	991	360
	February	967	881	290	1 045	960	295	1 036	948	306
	March	837	754	300	887	801	308	887	799	316
	April	815	720	353	830	733	363	829	733	381
	May	876	762	315	900	781	326	906	783	341
	June	680	623	293	683	625	304	683	622	309
	July	579	566	312	575	561	321	572	556	325
	August	971	881	456	1 026	942	488	1 006	921	503
	2002	884	806	-	920	847	-	917	839	-
	2003	930	860	-	998	927	-	978	904	-
	2004	841	763	-	879	801	-	874	794	-
	Total	891	817	-	944	870	-	932	855	-

2-CM: two components method
av.: arithmetic mean (average value)
s.d.: standard deviation

Table A- 50 Mean Dry Weather Concentrations of COD_{tot} Based on Partial Least Squares Regression (PLS) Methods

Year	Month	240-247.5 w5		240-270 w3		245-265 w9		250-277.5 w12[1)]		257.5-290 w3[2)]	
		2-CM [mg/l]	av. [mg/l]	2-CM [mg/l]	av. [mg/l]	2-CM [mg/l]	av. [mg/l]	2-CM [mg/l]	av. [mg/l]	2-CM [mg/l]	av. [mg/l]
2002	October	969	958	831	775	956	906	719	684	1 049	1 039
	November	1 212	1 139	939	855	954	870	687	631	1 109	1 024
	December	943	859	843	759	823	739	597	542	880	793
2003	January	-	-	-	-	-	-	-	-	-	-
	February	1 145	1 075	1 036	943	890	811	637	585	916	849
	March	1 045	1 135	865	948	779	841	567	611	865	921
	April	1 312	1 189	1 053	923	998	881	714	637	1 185	1 085
	May	1 303	1 219	1 044	958	975	893	699	644	1 179	1 095
	June	1 231	1 167	970	902	930	862	671	625	1 160	1 093
	July	1 254	1 189	1 101	1 035	985	922	710	668	1 171	1 108
	August	1 233	1 156	1 105	1 022	956	873	684	629	1 124	1 039
	September	1 116	1 031	1 092	1 007	942	861	675	621	1 014	923
	October	1 498	1 443	1 179	1 118	1 110	1 049	792	750	1 419	1 353
	November	1 437	1 363	1 216	1 136	1 112	1 029	813	756	1 302	1 217
	December	1 417	1 358	1 207	1 147	1 229	1 135	932	857	1 392	1 296
2004	January	1 434	1 360	1 216	1 145	1 082	1 008	788	736	1 296	1 217
	February	1 369	1 296	1 132	1 055	1 026	950	730	679	1 257	1 173
	March	1 121	1 019	977	885	881	802	634	582	1 049	949
	April	847	753	804	711	818	731	597	540	867	775
	May	930	819	850	758	884	776	647	571	929	794
	June	714	623	688	633	676	622	504	468	683	623
	July	593	584	580	570	567	555	432	424	536	517
	August	1 250	1 201	1 004	911	978	893	723	663	1 167	1 122
	2002	1 041	985	871	796	911	838	668	619	1 013	952
	2003	1 272	1 211	1 079	1 013	991	923	718	671	1 157	1 089
	2004	1 032	957	906	834	864	792	632	583	973	896
	Total	1 153	1 088	988	918	939	864	680	632	1 137	1 000

2-CM: two components method
av.: arithmetic mean (average value)
[1)]PLS regression provided by the manufacturer
[2)]PLS regression from the manufacturer based on 3rd measurement campaign

Table A- 51 Mean Dry Weather Concentrations of COD_{sol} Based on Simple Linear Regression (SLR) Methods

Year	Month	240-247.5, 272.5-290			250 - 260			270 - 280		
		2-CM [mg/l]	av. [mg/l]	s.d. [mg/l]	2-CM [mg/l]	av. [mg/l]	s.d. [mg/l]	2-CM [mg/l]	av. [mg/l]	s.d. [mg/l]
2002	October	282	261	169	278	262	155	277	262	157
	November	281	253	106	285	257	109	284	256	110
	December	239	212	99	241	213	100	239	211	100
2003	January	-	-	-	-	-	-	-	-	-
	February	264	237	97	261	235	99	257	232	99
	March	227	245	118	228	246	120	226	243	121
	April	297	257	107	299	260	106	297	258	106
	May	288	261	97	291	264	97	289	262	97
	June	272	249	99	277	254	104	276	253	105
	July	296	275	118	298	277	119	295	274	120
	August	282	255	95	286	258	97	282	254	97
	September	280	253	93	281	253	94	277	250	94
	October	333	313	112	337	316	114	336	315	117
	November	357	330	201	359	331	209	354	328	217
	December	380	351	212	362	334	204	364	336	215
2004	January	347	321	188	344	318	187	343	317	202
	February	307	282	93	307	281	94	304	278	94
	March	259	234	97	259	233	98	257	231	97
	April	238	210	112	241	213	117	240	212	118
	May	261	224	107	265	227	109	265	227	111
	June	191	173	101	195	177	102	194	176	103
	July	154	150	100	160	156	102	159	155	102
	August	292	262	171	304	274	179	303	273	184
	2002	267	242	-	268	244	-	267	243	-
	2003	298	275	-	298	275	-	296	273	-
	2004	256	232	-	259	235	-	258	234	-
	Total	279	255	-	280	256	-	278	255	-

2-CM: two components method
av.: arithmetic mean (average value)
s.d.: standard deviation

Table A- 52 Mean Dry Weather Concentrations of COD_{sol} Based on Least Median Squares Regression (LMS) Methods

Year	Month	230 - 500			254, 436			250 - 260, 436		
		2-CM [mg/l]	av. [mg/l]	s.d. [mg/l]	2-CM [mg/l]	av. [mg/l]	s.d. [mg/l]	2-CM [mg/l]	av. [mg/l]	s.d. [mg/l]
2002	October	282	267	160	286	271	158	289	274	170
	November	289	261	112	296	268	113	292	263	114
	December	244	215	101	249	221	103	247	218	102
2003	January	-	-	-	-	-	-	-	-	-
	February	262	236	101	269	243	102	261	235	103
	March	230	247	123	236	254	124	231	249	127
	April	302	263	107	309	270	109	305	267	108
	May	294	267	99	302	274	100	297	270	100
	June	281	258	106	288	264	107	284	261	108
	July	300	279	122	307	286	123	301	280	124
	August	287	259	98	294	265	100	288	259	100
	September	282	254	96	288	260	97	283	256	98
	October	341	320	119	349	328	120	345	323	122
	November	360	333	219	368	340	215	363	336	223
	December	370	341	218	376	347	216	385	355	239
2004	January	349	322	204	357	330	200	356	329	222
	February	309	283	95	317	290	96	313	287	96
	March	261	235	99	267	241	100	265	239	100
	April	244	216	119	249	220	121	248	219	123
	May	270	231	113	275	235	114	275	235	116
	June	197	179	104	201	183	105	201	183	107
	July	162	158	103	165	161	105	165	160	104
	August	309	278	186	316	285	187	312	282	192
	2002	272	248	-	277	253	-	276	252	-
	2003	301	278	-	308	285	-	304	281	-
	2004	263	238	-	268	243	-	267	242	-
	Total	283	259	-	289	265	-	287	263	-

2-CM: two components method
av.: arithmetic mean (average value)
s.d.: standard deviation

Table A- 53 Mean Dry Weather Concentrations of COD_{sol} Based on M5 Model Tree Regression (M5) Methods

Year	Month	230 - 500			240 - 250, 436			280 - 290		
		2-CM [mg/l]	av. [mg/l]	s.d. [mg/l]	2-CM [mg/l]	av. [mg/l]	s.d. [mg/l]	2-CM [mg/l]	av. [mg/l]	s.d. [mg/l]
2002	October	263	246	145	273	255	154	280	265	166
	November	288	260	101	286	259	103	281	253	112
	December	241	213	102	241	214	100	238	210	100
2003	January	-	-	-	-	-	-	-	-	-
	February	277	251	96	272	246	97	250	225	101
	March	234	254	115	234	253	118	223	239	124
	April	304	262	111	303	263	110	295	258	105
	May	294	266	99	294	266	97	287	260	97
	June	278	254	100	277	255	100	274	251	106
	July	304	282	120	302	281	120	290	270	122
	August	290	263	97	287	260	96	276	249	97
	September	285	258	93	283	256	93	273	246	95
	October	343	323	113	342	322	113	334	312	119
	November	362	334	178	362	335	187	350	322	207
	December	348	324	165	361	336	183	373	343	236
2004	January	349	324	148	355	330	180	343	316	207
	February	315	291	94	315	291	93	303	278	94
	March	264	239	98	265	239	98	257	231	98
	April	239	211	113	238	211	112	240	212	120
	May	260	225	104	261	225	106	266	227	113
	June	188	170	99	189	172	99	194	176	104
	July	150	146	100	152	148	100	159	155	101
	August	287	257	165	291	262	168	303	273	188
	2002	264	240	-	267	243	-	266	243	-
	2003	302	279	-	302	279	-	293	270	-
	2004	257	233	-	258	235	-	258	234	-
	Total	280	257	-	281	258	-	277	253	-

2-CM: two components method
av.: arithmetic mean (average value)
s.d.: standard deviation

Table A- 54 Mean Dry Weather Concentrations of COD_{sol} Based on Support Vector Machines Using Sequential Optimisation Algorithm (SMO)

Year	Month	250 - 260			260 - 270, 436			270 - 280, 436		
		2-CM [mg/l]	av. [mg/l]	s.d. [mg/l]	2-CM [mg/l]	av. [mg/l]	s.d. [mg/l]	2-CM [mg/l]	av. [mg/l]	s.d. [mg/l]
2002	October	292	277	167	271	254	147	277	262	151
	November	293	266	107	285	259	98	291	264	107
	December	248	220	98	245	219	94	248	220	99
2003	January	-	-	-	-	-	-	-	-	-
	February	269	244	98	276	249	91	271	245	97
	March	237	255	119	235	256	110	235	254	118
	April	307	269	105	300	261	103	304	264	107
	May	300	273	95	294	268	92	297	270	97
	June	286	263	102	276	255	91	281	258	99
	July	305	285	118	304	284	106	304	283	113
	August	292	265	95	296	270	89	293	265	95
	September	287	260	93	290	265	87	288	261	93
	October	347	326	114	335	316	98	339	318	108
	November	358	328	170	356	330	162	350	322	146
	December	364	337	196	354	330	173	362	336	189
2004	January	354	329	189	353	329	195	333	307	118
	February	316	291	92	310	286	87	311	286	92
	March	267	241	96	263	238	91	263	237	97
	April	247	218	115	243	215	104	246	217	112
	May	270	233	106	263	230	97	268	232	106
	June	200	183	101	201	184	97	200	182	100
	July	165	161	101	166	163	98	165	161	102
	August	310	281	174	303	273	155	306	276	173
	2002	278	254	-	267	244	-	272	249	-
	2003	305	282	-	301	280	-	302	280	-
	2004	266	242	-	263	240	-	262	237	-
	Total	287	264	-	283	261	-	283	260	-

2-CM: two components method
av.: arithmetic mean (average value)
s.d.: standard deviation

Table A- 55 Mean Dry Weather Concentrations of COD_{sol} Based on Partial Least Squares Regression (PLS) Methods

Year	Month	230-380 w7		240-500 w7		240-500 w5		240-290 w12[1)]		250-282.5 w4[2)]	
		2-CM [mg/l]	av. [mg/l]	2-CM [mg/l]	av. [mg/l]	2-CM [mg/l]	av. [mg/l]	2-CM [mg/l]	av. [mg/l]	2-CM [mg/l]	av. [mg/l]
2002	October	256	229	258	218	258	222	192	187	523	572
	November	296	272	206	181	241	216	231	221	745	762
	December	280	258	240	220	253	233	219	209	470	458
2003	January	-	-	-	-	-	-	-	-	-	-
	February	377	346	329	300	349	320	254	242	574	578
	March	286	320	214	244	235	267	301	261	305	261
	April	318	272	193	157	228	188	245	223	934	915
	May	316	289	193	170	233	209	243	231	915	901
	June	285	267	179	162	206	189	229	221	782	775
	July	363	342	283	266	306	288	256	247	736	725
	August	368	345	304	279	329	305	246	236	660	665
	September	362	339	333	312	340	319	247	238	468	453
	October	330	315	188	176	223	211	253	247	874	874
	November	373	353	289	272	318	301	273	265	901	898
	December	457	434	316	291	336	313	293	286	989	991
2004	January	351	332	253	233	289	269	274	268	962	961
	February	331	312	192	173	225	206	252	246	902	897
	March	294	270	192	177	212	196	221	214	638	599
	April	267	237	268	236	272	239	206	196	329	304
	May	262	244	248	233	249	233	221	211	430	388
	June	233	219	229	217	228	182	187	181	330	181
	July	199	198	206	207	202	203	160	162	249	261
	August	298	266	243	203	256	217	234	221	837	852
	2002	277	253	235	206	251	224	206	206	579	597
	2003	349	329	256	239	282	265	258	245	740	731
	2004	279	260	229	210	242	218	219	212	750	555
	Total	314	294	243	224	263	242	238	228	721	649

2-CM: two components method
av.: arithmetic mean (average value)
1)PLS regression provided by the manufacturer
2)PLS regression from the manufacturer based on 3rd measurement campaign

Table A- 56 Mean Dry Weather Concentrations of TSS Based on Simple Linear Regression (SLR) Methods

Year	Month	600 – 647.5			630 – 640			680 – 690		
		2-CM [mg/l]	av. [mg/l]	s.d. [mg/l]	2-CM [mg/l]	av. [mg/l]	s.d. [mg/l]	2-CM [mg/l]	av. [mg/l]	s.d. [mg/l]
2002	October	379	371	270	380	372	270	389	382	277
	November	295	271	123	296	272	124	300	275	128
	December	244	221	83	245	221	83	247	223	84
2003	January	-	-	-	-	-	-	-	-	-
	February	240	229	102	240	230	103	242	232	106
	March	243	256	163	244	257	164	247	260	170
	April	303	286	96	304	287	97	308	291	100
	May	295	277	86	294	277	87	299	281	88
	June	313	296	153	313	296	154	321	303	162
	July	311	297	177	311	298	179	318	305	186
	August	284	262	93	284	262	94	289	267	96
	September	277	254	91	277	254	91	281	258	93
	October	372	356	172	372	356	174	380	363	181
	November	363	337	266	361	336	261	366	340	264
	December	450	404	381	450	404	382	452	406	384
2004	January	345	321	249	344	320	248	348	323	252
	February	308	285	95	308	285	96	311	288	99
	March	273	252	92	273	252	93	275	254	95
	April	272	251	157	274	252	159	279	257	165
	May	304	260	147	306	261	147	312	266	151
	June	227	140	126	228	213	103	232	212	66
	July	200	195	91	200	194	91	203	197	93
	August	359	337	257	359	337	258	369	347	266
	2002	306	288	-	307	288	-	312	293	-
	2003	314	296	-	314	296	-	318	301	-
	2004	286	255	-	287	264	-	291	268	-
	Total	288	280	-	303	283	-	308	283	-

2-CM: two components method
av.: arithmetic mean (average value)
s.d.: standard deviation

Table A- 57 Mean Dry Weather Concentrations of TSS Based on Least Median Squares Regression (LMS) Methods

Year	Month	520 - 530			590 - 600			690 - 700		
		2-CM [mg/l]	av. [mg/l]	s.d. [mg/l]	2-CM [mg/l]	av. [mg/l]	s.d. [mg/l]	2-CM [mg/l]	av. [mg/l]	s.d. [mg/l]
2002	October	470	456	306	396	385	285	400	392	391
	November	375	339	164	305	277	137	304	277	138
	December	306	271	121	248	221	94	247	221	91
2003	January	-	-	-	-	-	-	-	-	-
	February	298	279	142	242	229	115	240	231	116
	March	298	314	204	246	259	178	248	261	182
	April	385	356	134	313	293	108	312	295	109
	May	373	345	123	303	283	98	302	284	96
	June	390	364	197	323	303	169	328	309	178
	July	386	365	210	320	305	191	323	309	196
	August	357	323	131	291	266	105	293	269	104
	September	346	313	127	282	257	102	284	260	101
	October	470	445	219	388	367	189	393	376	197
	November	445	407	280	373	344	271	376	347	276
	December	529	471	379	462	412	387	458	410	387
2004	January	423	389	261	354	327	256	354	328	257
	February	392	358	132	318	292	107	318	293	108
	March	343	311	130	279	255	104	279	256	104
	April	340	306	200	280	255	173	282	258	177
	May	377	318	182	315	265	160	316	267	162
	June	274	253	129	229	212	111	231	215	110
	July	237	229	126	197	191	102	200	194	100
	August	441	409	306	372	347	277	379	357	283
	2002	384	355	-	316	294	-	317	297	-
	2003	389	362	-	322	302	-	323	277	-
	2004	353	322	-	293	268	-	295	271	-
	Total	375	346	-	311	288	-	312	291	-

2-CM: two components method
av.: arithmetic mean (average value)
s.d.: standard deviation

Table A- 58 Mean Dry Weather Concentrations of TSS Based on M5 Model Tree Regression (M5) Methods

Year	Month	420 -430			660 - 670			710 - 720		
		2-CM [mg/l]	av. [mg/l]	s.d. [mg/l]	2-CM [mg/l]	av. [mg/l]	s.d. [mg/l]	2-CM [mg/l]	av. [mg/l]	s.d. [mg/l]
2002	October	229	221	114	384	376	273	248	245	57
	November	236	204	112	296	272	126	255	240	57
	December	190	156	124	245	221	83	234	217	61
2003	January	-	-	-	-	-	-	-	-	-
	February	181	156	127	240	230	104	222	211	68
	March	166	173	125	244	257	167	210	224	68
	April	255	221	101	304	288	99	268	257	39
	May	247	218	103	296	279	88	264	253	44
	June	234	206	112	317	300	158	257	244	53
	July	238	209	111	315	302	183	258	244	53
	August	236	201	114	287	265	94	258	241	53
	September	233	196	117	280	257	92	256	238	55
	October	257	241	84	376	360	177	268	261	37
	November	241	215	104	367	340	268	259	247	49
	December	252	223	97	453	406	383	263	250	46
2004	January	244	214	104	347	323	251	261	247	47
	February	247	218	101	311	287	97	263	259	45
	March	230	195	115	275	254	94	255	238	55
	April	207	170	127	274	253	162	241	222	66
	May	224	185	121	307	262	149	252	232	61
	June	166	140	126	228	213	103	227	211	66
	July	117	112	122	199	194	92	197	192	69
	August	212	187	124	362	340	262	246	234	59
	2002	218	194	-	308	290	-	246	234	-
	2003	231	205	-	316	298	-	253	243	-
	2004	206	178	-	288	266	-	243	228	-
	Total	220	194	-	305	285	-	248	236	-

2-CM: two components method
av.: arithmetic mean (average value)
s.d.: standard deviation

Table A- 59 Mean Dry Weather Concentrations of TSS Based on Support Vector Machines using Sequential Optimisation Algorithm (SMO)

Year	Month	620 - 630			670 - 680			720 - 730		
		2-CM [mg/l]	av. [mg/l]	s.d. [mg/l]	2-CM [mg/l]	av. [mg/l]	s.d. [mg/l]	2-CM [mg/l]	av. [mg/l]	s.d. [mg/l]
2002	October	376	367	274	383	374	279	397	389	286
	November	290	265	127	291	266	128	301	276	133
	December	237	213	85	239	214	85	246	221	87
2003	January	-	-	-	-	-	-	-	-	-
	February	232	221	105	232	222	106	238	230	111
	March	236	249	167	238	251	171	247	260	177
	April	298	280	99	297	280	101	307	292	105
	May	290	271	89	288	270	89	298	281	92
	June	308	290	157	310	293	162	324	306	173
	July	306	292	182	308	295	187	319	306	193
	August	279	256	96	279	257	96	289	266	100
	September	272	248	94	273	250	94	281	258	97
	October	369	352	177	371	354	181	386	370	191
	November	357	330	262	355	329	255	369	341	265
	December	447	399	385	444	398	385	449	403	384
2004	January	340	315	252	339	315	253	336	314	221
	February	303	279	98	303	280	99	312	288	104
	March	267	245	95	268	246	96	275	253	99
	April	266	244	161	268	246	165	278	256	173
	May	299	253	150	301	255	151	312	265	157
	June	219	204	104	221	207	104	230	215	107
	July	191	186	94	193	187	94	200	195	96
	August	355	332	262	358	336	267	374	352	277
	2002	301	282	-	304	285	-	315	295	-
	2003	309	290	-	309	291	-	319	301	-
	2004	280	257	-	281	259	-	290	267	-
	Total	297	277	-	303	278	-	308	288	-

2-CM: two components method
av.: arithmetic mean (average value)
s.d.: standard deviation

Table A- 60 Mean Dry Weather Concentrations of TSS Based on Partial Least Squares Regression (PLS) Methods

Year	Month	380-750 w3		380-750 w2		550-600 w3		550-600 w2		600-647.5 w20 1)	
		2-CM [mg/l]	av. [mg/l]	2-CM [mg/l]	av. [mg/l]	2-CM [mg/l]	av. [mg/l]	2-CM [mg/l]	av. [mg/l]	2-CM [mg/l]	av. [mg/l]
2002	October	854	823	405	397	285	262	348	332	443	430
	November	770	681	300	267	299	269	317	286	322	285
	December	617	527	229	197	265	236	270	240	245	208
2003	January	-	-	-	-	-	-	-	-	-	-
	February	569	509	228	217	263	226	259	232	236	229
	March	562	590	238	248	232	249	250	266	248	258
	April	829	732	315	295	302	256	314	277	335	308
	May	798	718	310	287	280	250	287	260	321	293
	June	749	683	342	319	248	224	280	256	349	322
	July	732	671	330	313	260	236	285	263	339	319
	August	668	581	291	262	248	218	258	229	305	270
	September	627	540	284	254	228	199	243	213	293	258
	October	900	831	422	400	267	242	326	303	437	411
	November	758	671	381	347	272	245	313	283	399	359
	December	843	746	457	403	289	258	387	342	481	421
2004	January	796	715	351	321	294	268	312	282	373	337
	February	812	725	320	289	272	244	298	269	341	306
	March	695	617	270	242	241	216	262	236	287	255
	April	720	629	278	248	258	227	283	253	287	252
	May	785	668	320	260	262	236	298	259	331	266
	June	568	512	209	190	208	189	220	201	217	201
	July	404	381	160	153	168	162	175	167	175	167
	August	740	676	374	348	243	211	310	279	402	372
	2002	747	677	311	287	283	256	312	286	337	308
	2003	730	661	327	304	263	237	291	266	340	313
	2004	690	615	285	256	243	219	270	243	302	270
	Total	718	647	310	284	258	233	286	260	326	296

2-CM: two components method
av.: arithmetic mean (average value)
1) PLS regression provided by the manufacturer

Table A- 61 Mean Rain Weather Concentrations of COD_{tot} by Means of the 2-Components Method – Part 1

Year	Month	SLR			LMS			M5		
		250-260	270-280	280-290	230-500	254,436	250-260, 436	254,436	250-277.5, 436	310-320, 436
		[mg/l]	[mg/l]	[mg/l]	[mg/l]	[mg/l]	[mg/l]	[mg/l]	[mg/l]	[mg/l]
2002	October	452	456	457	518	640	502	633	630	604
	November	284	286	286	292	362	284	287	274	353
	December	55	59	61	22	73	12	17	9	82
2003	January	-	-	-	-	-	-	-	-	-
	February	-	-	-	-	-	-	-	-	-
	March	-	-	-	-	-	-	-	-	-
	April	-	-	-	-	-	-	-	-	-
	May	640	633	628	707	802	711	710	699	704
	June	395	393	391	426	527	423	455	442	481
	July	316	313	311	327	415	325	346	333	394
	August	541	528	516	564	623	580	540	527	579
	September	303	298	296	303	363	301	297	289	349
	October	212	210	211	203	267	195	210	198	271
	November	443	438	437	489	559	479	520	507	555
	December	-	-	-	-	-	-	-	-	-
2004	January	-	-	-	-	-	-	-	-	-
	February	-	-	-	-	-	-	-	-	-
	March	448	451	455	526	650	500	558	548	583
	April	350	355	361	393	522	376	449	441	486
	May	238	241	244	243	336	236	238	229	301
	June	164	167	172	157	251	149	147	136	222
	July	114	118	123	105	188	97	104	98	163
	August	540	536	535	609	728	611	696	691	690
	2002	264	267	268	277	358	266	312	304	346
	2003	407	402	399	431	508	431	440	428	476
	2004	309	311	315	339	446	328	365	357	408
	Total	343	343	343	368	457	361	388	378	426

Table A- 62 Mean Rain Weather Concentrations of COD_{tot} by Means of the 2-Components Method – Part 2

Year	Month	SVM u. SMO			PLS				
		240-250 [mg/l]	250-260 [mg/l]	290-300 [mg/l]	240-270, w5 [mg/l]	240-270, w3 [mg/l]	245-265, w9 [mg/l]	250-277.5, w12[1] [mg/l]	257.5-290, w3[2] [mg/l]
2002	October	557	470	527	300	411	430	345	589
	November	324	305	306	424	290	277	244	535
	December	79	56	50	170	54	50	93	238
2003	January	-	-	-	-	-	-	-	-
	February	-	-	-	-	-	-	-	-
	March	-	-	-	-	-	-	-	-
	April	-	-	-	-	-	-	-	-
	May	672	699	688	1 099	797	636	481	1 158
	June	437	429	429	660	474	388	318	764
	July	360	338	341	566	420	311	264	668
	August	581	576	547	949	783	539	412	985
	September	346	310	315	474	448	299	255	567
	October	243	220	223	441	334	209	196	508
	November	471	490	490	854	610	439	342	913
	December	-	-	-	-	-	-	-	-
2004	January	-	-	-	-	-	-	-	-
	February	-	-	-	-	-	-	-	-
	March	488	490	522	603	464	439	360	822
	April	411	381	409	328	263	335	297	610
	May	295	254	268	234	202	226	213	382
	June	219	175	191	171	125	153	163	308
	July	167	119	136	98	80	105	128	196
	August	561	620	600	1 096	618	533	406	1 132
	2002	223	277	294	298	252	252	227	454
	2003	444	437	433	720	552	403	324	795
	2004	350	340	354	422	292	299	261	575
	Total	386	371	378	529	398	336	282	648

[1] PLS regression provided by the manufacturer

[2] PLS regression from the manufacturer based on 3rd measurement campaign

Table A- 63 Mean Rain Weather Concentrations of COD_{sol} by Means of the 2-Components Method – Part 1

Year	Month	SLR			LMS			M5		
		240-247.5 272.5-290 [mg/l]	250-260 [mg/l]	270-280 [mg/l]	230-500 [mg/l]	254,436 [mg/l]	250-260, 436 [mg/l]	230-500 [mg/l]	240-250, 436 [mg/l]	280-290 [mg/l]
2002	October	103	119	121	124	123	126	69	87	122
	November	52	64	65	67	68	68	28	43	66
	December	-	-	-	-	-	-	-	-	-
2003	January	-	-	-	-	-	-	-	-	-
	February	-	-	-	-	-	-	-	-	-
	March	-	-	-	-	-	-	-	-	-
	April	-	-	-	-	-	-	-	-	-
	May	169	184	181	185	190	186	150	164	180
	June	89	102	101	104	106	105	67	81	101
	July	63	75	74	76	78	77	37	54	74
	August	140	150	146	149	153	148	120	133	141
	September	62	71	69	71	72	72	41	54	69
	October	31	40	39	41	42	42	14	25	40
	November	99	111	110	112	116	114	81	95	111
	December	-	-	-	-	-	-	-	-	-
2004	January	-	-	-	-	-	-	-	-	-
	February	-	-	-	-	-	-	-	-	-
	March	105	121	122	125	127	130	79	97	127
	April	76	94	96	98	98	101	54	66	99
	May	38	50	51	52	52	55	25	32	53
	June	17	27	28	29	29	31	4	10	30
	July	10	16	17	18	18	19	2	6	19
	August	133	152	150	153	158	155	115	129	150
	2002	78	92	93	96	96	97	49	109	94
	2003	93	105	103	104	108	106	73	87	102
	2004	63	77	77	79	80	82	47	57	80
	Total	79	92	91	94	95	95	59	72	92

Table A- 64 Mean Rain Weather Concentrations of COD_{sol} by Means of the 2-Components Method – Part 2

Year	Month	SVM u. SMO			PLS						
		250-260 [mg/l]	260-270, 436 [mg/l]	270-280, 436 [mg/l]	230-380, w7 [mg/l]	240-500, w7 [mg/l]	240-500, w5 [mg/l]	250-270, w9 [mg/l]	245-265, w9 [mg/l]	240-290, w12[1)] [mg/l]	250-282.5, w4[2)] [mg/l]
2002	October	120	114	117	125	193	165	327	248	65	100
	November	71	69	67	87	41	52	262	200	71	282
	December	-	-	-	29	-	-	163	123	44	207
2003	January	-	-	-	-	-	-	-	-	-	-
	February	-	-	-	-	-	-	-	-	-	-
	March	-	-	-	-	-	-	-	-	-	-
	April	-	-	-	-	-	-	-	-	-	-
	May	192	191	182	218	84	117	419	322	140	905
	June	110	107	100	134	61	76	311	238	98	564
	July	83	84	75	123	55	70	276	211	97	529
	August	159	169	152	270	191	212	374	289	153	735
	September	78	84	72	146	111	111	270	207	94	233
	October	49	51	41	92	32	38	231	177	77	431
	November	123	123	114	152	24	48	327	248	108	855
	December	-	-	-	-	-	-	-	-	-	-
2004	January	-	-	-	-	-	-	-	-	-	-
	February	-	-	-	-	-	-	-	-	-	-
	March	127	115	116	93	14	20	338	260	63	281
	April	97	86	88	64	63	57	296	225	56	83
	May	55	53	49	69	73	68	241	183	63	100
	June	32	30	26	41	40	36	209	158	50	142
	July	19	18	16	30	38	30	185	139	40	87
	August	162	157	148	142	110	114	369	281	127	861
	2002	96	92	92	79	117	109	251	190	60	196
	2003	113	116	105	162	80	96	315	242	110	607
	2004	82	77	74	73	56	54	273	208	67	259
	Total	98	97	91	113	75	81	287	219	84	400

1)PLS regression provided by the manufacturer

2)PLS regression from the manufacturer based on 3rd measurement campaign

Table A- 65 Mean TSS Rain Weather Concentrations by Means of 2-Components Method – Part 1

Year	Month	SLR			LMS			M5		
		600-647.5 [mg/l]	630-640 [mg/l]	680-690 [mg/l]	520-530 [mg/l]	590-600 [mg/l]	690-700 [mg/l]	420-430 [mg/l]	660-670 [mg/l]	710-720 [mg/l]
2002	October	240	243	249	291	242	251	176	246	240
	November	162	163	166	179	152	160	39	164	167
	December	97	98	100	83	78	89	83	78	89
2003	January	-	-	-	-	-	-	-	-	-
	February	-	-	-	-	-	-	-	-	-
	March	-	-	-	-	-	-	-	-	-
	April	-	-	-	-	-	-	-	-	-
	May	283	284	293	341	288	298	341	288	298
	June	223	223	232	251	219	233	251	219	233
	July	194	195	204	210	187	203	210	187	203
	August	231	232	241	265	229	242	265	229	242
	September	168	169	174	179	158	170	179	158	170
	October	145	145	150	147	132	144	147	132	144
	November	201	202	207	235	198	207	235	198	207
	December	-	-	-	-	-	-	-	-	-
2004	January	-	-	-	-	-	-	-	-	-
	February	-	-	-	-	-	-	-	-	-
	March	262	263	269	309	263	273	309	263	273
	April	251	254	263	286	251	265	286	251	265
	May	174	176	183	188	167	179	188	167	179
	June	156	158	164	161	147	159	161	147	159
	July	141	141	146	140	128	140	140	128	140
	August	272	272	283	319	275	290	319	275	290
	2002	166	168	172	184	157	167	99	163	165
	2003	206	207	214	233	202	214	233	202	214
	2004	209	211	218	234	205	218	234	205	218
	Total	200	201	208	224	195	206	208	196	206

Table A- 66 Mean TSS Rain Weather Concentrations by Means of 2-Components Method – Part 2

Year	Month	SVM u. SMO			PLS				
		620-630 [mg/l]	670-680 [mg/l]	720-730 [mg/l]	380-750, w3 [mg/l]	380-750, w2 [mg/l]	550-600, w3 [mg/l]	550-600, w2 [mg/l]	600-647.5, w20[1)] [mg/l]
2002	October	233	239	250	584	221	182	223	241
	November	152	155	164	307	110	128	152	117
	December	85	89	97	37	28	47	65	18
2003	January	-	-	-	-	-	-	-	-
	February	-	-	-	-	-	-	-	-
	March	-	-	-	-	-	-	-	-
	April	-	-	-	-	-	-	-	-
	May	277	281	296	646	309	159	209	304
	June	215	221	234	362	223	82	134	210
	July	186	193	206	246	187	45	96	167
	August	224	230	243	377	232	94	144	223
	September	159	164	173	193	141	47	77	125
	October	135	140	148	119	104	33	62	90
	November	194	198	207	397	189	108	138	184
	December	-	-	-	-	-	-	-	-
2004	January	-	-	-	-	-	-	-	-
	February	-	-	-	-	-	-	-	-
	March	255	260	270	529	261	138	198	264
	April	244	251	264	512	251	131	205	244
	May	164	171	182	325	151	87	126	137
	June	146	152	163	234	122	49	85	109
	July	130	135	144	126	89	24	57	83
	August	266	270	289	552	278	107	181	288
	2002	157	161	170	309	120	119	147	125
	2003	199	204	215	334	198	81	123	186
	2004	201	207	219	380	192	89	142	188
	Total	192	197	208	347	181	91	135	175

1)PLS regression provided by the manufacturer

TABLES OF OVERFLOW LOADS

Table A- 67 Overflow Loads of COD_{tot} by Means of the 2-Components Method – Part 1

Year	Month	SLR			LMS			M5		
		250-260 [kg]	270-280 [kg]	280-290 [kg]	230-500 [kg]	254,436 [kg]	250-260, 436 [kg]	254,436 [kg]	250-277.5, 436 [kg]	310-320, 436 [kg]
2002	October	2 405	2 428	2 437	2 771	3 450	2 667	3 488	3 477	3 158
	November	244	247	252	403	509	390	341	314	469
	December	63	65	66	42	81	36	31	24	78
2003	January	-	-	-	-	-	-	-	-	-
	February	-	-	-	-	-	-	-	-	-
	March	-	-	-	-	-	-	-	-	-
	April	-	-	-	-	-	-	-	-	-
	May	155	154	153	174	204	172	219	218	196
	June	5 771	5 796	5 821	6 391	8 183	6 243	6 831	6 640	7 292
	July	8 242	8 197	8 178	8 751	11 048	8 642	9 101	8 795	10 221
	August	293	291	290	318	389	315	317	304	355
	September	223	222	224	216	293	206	174	164	266
	October	2 206	2 194	2 218	2 087	2 979	1 986	1 892	1 755	2 726
	November	1 132	1 126	1 127	1 257	1 462	1 224	1 316	1 280	1 395
	December	-	-	-	-	-	-	-	-	-
2004	January	-	-	-	-	-	-	-	-	-
	February	-	-	-	-	-	-	-	-	-
	March	247	251	256	289	385	268	297	287	325
	April	432	437	443	527	666	509	666	666	656
	May	2 488	2 548	2 624	2 462	3 764	2 318	2 328	2 199	3 306
	June	6 557	6 755	7 004	6 415	10 719	6 071	6 233	5 824	9 166
	July	3 111	3 253	3 415	3 157	5 654	2 926	3 449	3 333	4 645
	August	2 579	2 608	2 638	3 139	4 023	3 058	3 848	3 844	3 736
	2002	2 712	2 740	2 755	3 216	4 040	3 093	3 860	3 815	3 705
	2003	18 022	17 980	18 011	19 194	24 558	18 788	19 850	19 156	22 451
	2004	15 414	15 852	16 380	15 989	25 211	15 150	16 821	16 153	21 834
	Total	36 148	36 572	37 146	38 399	53 809	37 031	40 531	39 124	47 990

Table A- 68 Overflow Loads of COD_{tot} by Means of the 2-Components Method – Part 2

Year	Month	SVM u. SMO			PLS				
		240-250 [kg]	250-260 [kg]	290-300 [kg]	240-270, w5 [kg]	240-270, w3 [kg]	245-265, w9 [kg]	250-277.5, w12[1)] [kg]	257.5-290, w3[2)] [kg]
2002	October	3 013	2 481	2 827	1 452	2 154	2 334	1 906	3 186
	November	445	436	423	699	411	393	357	761
	December	81	65	61	133	62	59	78	175
2003	January	-	-	-	-	-	-	-	-
	February	-	-	-	-	-	-	-	-
	March	-	-	-	-	-	-	-	-
	April	-	-	-	-	-	-	-	-
	May	162	171	170	276	186	154	119	294
	June	6 397	6 308	6 485	9 212	6 135	5 664	4 707	11 183
	July	9 261	8 822	9 012	13 869	10 258	8 128	6 814	16 605
	August	320	318	319	512	367	290	236	577
	September	262	225	236	320	303	218	208	432
	October	2 573	2 280	2 363	4 443	3 244	2 162	2 120	5 396
	November	1 173	1 237	1 237	2 065	1 414	1 122	893	2 196
	December	-	-	-	-	-	-	-	-
2004	January	-	-	-	-	-	-	-	-
	February	-	-	-	-	-	-	-	-
	March	272	270	294	329	238	239	208	485
	April	490	475	518	393	345	418	325	669
	May	3 205	2 631	2 882	2 158	1 635	2 336	2 411	4 144
	June	8 900	7 041	7 901	6 086	4 166	6 078	6 646	12 151
	July	4 607	3 285	3 955	2 066	1 620	2 841	3 379	5 045
	August	2 600	3 102	3 087	5 600	2 251	2 531	1 952	6 157
	2002	3 539	2 982	3 311	2 284	2 627	2 786	2 341	4 122
	2003	20 148	19 361	19 822	30 697	21 907	17 738	15 097	36 683
	2004	20 074	16 804	18 637	16 632	10 255	14 443	14 921	28 651
	Total	43 761	39 147	41 770	49 613	34 789	34 967	32 359	69 456

1)PLS regression provided by the manufacturer

2)PLS regression from the manufacturer based on 3rd measurement campaign

Table A- 69 Overflow Loads of COD_{sol} by Means of the 2-Components Method – Part 1

Year	Month	SLR			LMS			M5		
		240-247.5 272.5-290 [kg]	250-260 [kg]	270-280 [kg]	230-500 [kg]	254,436 [kg]	250-260, 436 [kg]	230-500 [kg]	240-250, 436 [kg]	280-290 [kg]
2002	October	554	630	638	652	647	667	347	458	650
	November	67	86	87	90	92	93	36	55	89
	December	-	2	3	3	3	4	-	-	3
2003	January	-	-	-	-	-	-	-	-	-
	February	-	-	-	-	-	-	-	-	-
	March	-	-	-	-	-	-	-	-	-
	April	-	-	-	-	-	-	-	-	-
	May	39	43	43	43	45	44	33	37	43
	June	1 255	1 461	1 467	1 503	1 526	1 539	927	1 137	1 487
	July	1 735	2 021	2 005	2 058	2 096	2 090	1 125	1 532	2 011
	August	67	76	75	77	79	78	50	61	75
	September	31	42	42	43	43	45	8	22	43
	October	271	381	378	395	400	413	101	202	393
	November	269	302	300	306	313	312	221	257	302
	December	-	-	-	-	-	-	-	-	-
2004	January	-	-	-	-	-	-	-	-	-
	February	-	-	-	-	-	-	-	-	-
	March	47	59	60	62	62	65	26	40	63
	April	107	123	125	127	127	131	87	98	128
	May	302	424	441	460	455	495	205	248	480
	June	739	1 089	1 136	1 181	1 163	1 272	333	522	1 242
	July	377	543	571	591	577	637	201	285	628
	August	629	741	750	765	788	788	537	616	771
	2002	621	718	728	745	742	764	383	513	742
	2003	3 667	4 326	4 310	4 425	4 502	4 521	2 465	3 248	4 354
	2004	2 201	2 979	3 083	3 186	3 172	3 388	1 389	1 809	3 312
	Total	6 489	8 023	8 121	8 356	8 416	8 673	4 237	5 570	8 408

Table A- 70 Overflow Loads of COD_{sol} by Means of the 2-Components Method – Part 2

Year	Month	SVM u. SMO			PLS						
		250-260 [kg]	260-270, 436 [kg]	270-280, 436 [kg]	230-380, w7 [kg]	240-500, w7 [kg]	240-500, w5 [kg]	250-270, w9 [kg]	245-265, w9 [kg]	240-290, w12[1)] [kg]	250-282.5, w4[2)] [kg]
2002	October	641	602	615	677	1 119	937	1 825	1 396	1 448	2 873
	November	99	94	89	118	20	42	396	302	289	592
	December	7	5	3	25	-	1	116	88	23	23
2003	January	-	-	-	-	-	-	-	-	-	-
	February	-	-	-	-	-	-	-	-	-	-
	March	-	-	-	-	-	-	-	-	-	-
	April	-	-	-	-	-	-	-	-	-	-
	May	46	44	42	47	6	16	108	83	79	79
	June	1 578	1 459	1 422	1 462	435	614	4 674	3 570	2 980	8 054
	July	2 216	2 169	1 995	2 869	1 249	1 582	6 946	5 319	2 400	12 581
	August	50	61	75	99	35	50	230	176	81	483
	September	49	50	42	92	55	54	246	188	77	115
	October	482	483	379	852	226	296	2 592	1 980	826	3 997
	November	324	313	298	331	39	89	844	648	262	2 019
	December	-	-	-	-	-	-	-	-	-	-
2004	January	-	-	-	-	-	-	-	-	-	-
	February	-	-	-	-	-	-	-	-	-	-
	March	64	53	56	37	-	-	216	164	159	159
	April	124	112	116	66	57	52	283	216	60	105
	May	496	449	410	538	564	497	2 968	2 247	753	1 068
	June	1 257	1 106	1 024	1 227	1 276	1 126	8 595	6 485	4 946	4 957
	July	600	494	495	457	677	509	4 837	3 637	922	2 282
	August	794	681	697	149	70	74	1 831	1 384	561	3 980
	2002	747	701	707	820	1 139	980	2 337	1 786	1 760	3 488
	2003	4 745	4 579	4 253	5 752	2 045	2 701	15 640	11 964	6 705	27 328
	2004	3 385	2 895	2 798	2 474	2 644	2 258	18 730	14 133	7 401	12 551
	Total	8 827	8 175	7 758	9 046	5 828	5 939	36 707	27 883	15 866	43 367

1)PLS regression provided by the manufacturer

2)PLS regression from the manufacturer based on 3rd measurement campaign

Table A- 71 Overflow Loads of TSS by Means of the 2-Components Method – Part 1

Year	Month	SLR			LMS			M5		
		600-647.5 [kg]	630-640 [kg]	680-690 [kg]	520-530 [kg]	590-600 [kg]	690-700 [kg]	420-430 [kg]	660-670 [kg]	710-720 [kg]
2002	October	1 363	1 376	1 411	1 628	1 367	1 421	997	1 395	1 433
	November	244	247	252	262	226	242	25	248	257
	December	71	71	73	65	60	67	-	72	72
2003	January	-	-	-	-	-	-	-	-	-
	February	-	-	-	-	-	-	-	-	-
	March	-	-	-	-	-	-	-	-	-
	April	-	-	-	-	-	-	-	-	-
	May	76	76	79	90	77	80	70	78	80
	June	3 561	3 572	3 729	4 009	3 511	3 757	1 595	3 668	3 363
	July	5 060	5 079	5 324	5 548	4 919	5 326	1 661	5 232	4 819
	August	167	168	176	187	164	177	54	173	169
	September	166	167	173	169	153	168	5	171	170
	October	1 787	1 791	1 860	1 793	1 629	1 810	194	1 841	1 840
	November	567	569	584	654	559	589	321	578	612
	December	-	-	-	-	-	-	-	-	-
2004	January	-	-	-	-	-	-	-	-	-
	February	-	-	-	-	-	-	-	-	-
	March	171	172	177	195	167	179	76	176	172
	April	253	256	266	309	264	277	193	260	193
	May	2 229	2 259	2 358	2 334	2 113	2 288	437	2 287	2 114
	June	6 789	6 854	7 167	7 034	6 402	6 986	1 209	6 942	6 814
	July	4 020	4 031	4 213	4 085	3 730	4 107	836	4 088	4 043
	August	1 649	1 653	1 727	1 908	1 676	1 793	1 058	1 675	1 213
	2002	1 678	1 694	1 736	1 955	1 653	1 730	1 022	1 715	1 762
	2003	11 384	11 422	11 925	12 450	11 012	11 907	3 900	11 741	11 053
	2004	15 111	15 225	15 908	15 865	14 352	15 630	3 809	15 428	14 549
	Total	28 173	28 341	29 569	30 270	27 017	29 267	8 731	28 884	27 364

Table A- 72 Overflow Loads of TSS by Means of the 2-Components Method – Part 2

Year	Month	SVM u. SMO 620-630 [mg/l]	SVM u. SMO 670-680 [mg/l]	SVM u. SMO 720-730 [mg/l]	PLS 380-750, w3 [mg/l]	PLS 380-750, w2 [mg/l]	PLS 550-600, w3 [mg/l]	PLS 550-600, w2 [mg/l]	PLS 600-647.5, w20[1)] [mg/l]
2002	October	1 319	1 357	1 421	3 125	1 212	961	1 231	1 352
	November	228	233	249	431	162	169	216	165
	December	63	66	71	44	31	37	49	23
2003	January	-	-	-	-	-	-	-	-
	February	-	-	-	-	-	-	-	-
	March	-	-	-	-	-	-	-	-
	April	-	-	-	-	-	-	-	-
	May	74	76	80	168	82	38	52	79
	June	3 450	3 550	3 777	5 746	3 633	1 089	2 039	3 420
	July	4 871	5 052	5 392	6 883	5 050	1 115	2 555	4 586
	August	162	168	178	253	172	41	91	160
	September	156	162	173	143	132	18	58	112
	October	1 674	1 744	1 856	1 226	1 403	158	623	1 178
	November	549	558	588	1 015	547	257	370	537
	December	-	-	-	-	-	-	-	-
2004	January	-	-	-	-	-	-	-	-
	February	-	-	-	-	-	-	-	-
	March	165	169	178	296	163	67	116	159
	April	250	258	273	625	296	110	194	299
	May	2 093	2 186	2 339	3 770	1 875	917	1 468	1 640
	June	5 373	6 649	7 131	9 932	5 491	1 675	3 461	4 946
	July	3 758	3 911	4 196	4 110	2 915	487	1 591	2 748
	August	1 619	1 654	1 783	3 299	1 793	434	1 002	1 819
	2002	1 610	1 656	1 741	3 600	1 405	1 167	1 496	1 540
	2003	10 936	11 310	12 044	15 434	11 019	2 716	5 788	8 894
	2004	14 258	14 827	15 900	22 032	12 533	3 690	7 832	11 611
	Total	26 804	27 793	29 685	41 066	24 957	7 573	15 116	22 045

[1)]PLS regression provided by the manufacturer

TABLES OF LONG TERM SIMULATION RESULTS

Table A- 73 COD_{tot} Overflow Loads Results of Long Term Simulation – Part 1

	SLR	SLR	SLR	LMS	LMS	LMS	M5	M5
	250-260	270-280	280-290	230-500	254,436	250-260,436	254,436	250-277.5,436
	[kg]	[kg]	[kg]	[kg]	[kg]	[kg]	[kg]	[kg]
1996	25 657	25 648	25 641	27 548	33 801	27 078	28 746	28 041
1997	26 255	26 248	26 243	28 185	34 678	27 693	29 480	28 749
1998	40 031	40 019	40 010	42 977	52 828	42 231	44 915	43 806
1999	34 814	34 804	34 797	37 375	45 956	36 726	39 071	38 105
2000	27 206	27 197	27 190	29 211	35 854	28 711	30 490	29 742
2001	21 079	21 072	21 066	22 634	27 758	22 250	23 608	23 031
2002	27 484	27 474	27 467	29 512	36 181	29 013	30 773	30 022
2003	27 066	27 058	27 051	29 059	35 693	28 559	30 350	29 603
2004	38 003	37 990	37 980	40 806	50 046	40 114	42 563	41 523
Total [10³·kg]	267.6	267.5	267.4	287.3	353.0	282.4	300.0	292.6
DW COD_{tot}*) [mg/l]	913	908	904	992	993	1 005	871	870
RW COD_{tot}**) [mg/l]	343	343	343	368	457	361	388	378

*) COD_{tot} mean dry weather value
**) COD_{tot} mean rain weather value

Table A- 74 COD_{tot} Overflow Loads Results of Long Term Simulation – Part 2

	M5	SVM-SMO	SVM-SMO	SVM-SMO	PLS	PLS
	310-320,436	240-250	250-260	290-300	240-270,w5	240-270,w3
	[kg]	[kg]	[kg]	[kg]	[kg]	[kg]
1996	31 411	28 639	27 762	28 148	39 133	29 648
1997	32 248	29 361	28 407	28 833	40 146	30 368
1998	49 116	44 739	43 313	43 947	61 159	46 288
1999	42 730	38 917	37 668	38 224	53 203	40 259
2000	33 322	30 376	29 438	29 851	41 509	31 442
2001	25 792	23 522	22 810	23 122	32 137	24 355
2002	33 615	30 662	29 741	30 143	41 888	31 751
2003	33 178	30 234	29 286	29 705	41 322	31 288
2004	46 502	42 408	41 123	41 686	57 940	43 909
Total [10³·kg]	327.9	298.9	289.5	293.7	408.4	309.3
DW COD_{tot}*) [mg/l]	869	891	994	932	1 153	988
RW COD_{tot}**) [mg/l]	426	386	371	378	529	398

*) COD_{tot} mean dry weather value
**) COD_{tot} mean rain weather value

Table A- 75 COD_{tot} Overflow Loads Results of Long Term Simulation – Part 3

	PLS	PLS[1)]	PLS[2)]	ATV A 128
	245-265,w9	250-277.5,w12	257.5-290,w3	
	[kg]	[kg]	[kg]	[kg]
1996	25 209	20 973	47 464	8 543
1997	25 780	21 490	48 803	8 618
1998	39 315	32 751	74 293	12 203
1999	34 189	28 487	64 643	11 465
2000	26 729	22 243	50 362	9 042
2001	20 715	17 227	38 963	7 037
2002	27 011	22 458	50 771	9 192
2003	26 587	22 136	50 163	8 963
2004	37 345	31 059	70 248	12 685
Total [10³·kg]	262.9	218.8	495.7	87.7
DW COD_{tot}*) [mg/l]	939	680	1 137	600
RW COD_{tot}**) [mg/l]	336	282	648	107

*) COD_{tot} mean dry weather value
**) COD_{tot} mean rain weather value
1) provided by the manufacturer
2) provided by the manufacturer on the basis of the 3rd measurement campaign

Table A- 76 TSS Overflow Loads Results of Long Term Simulation – Part 1

	SLR	SLR	SLR	LMS	LMS	LMS	M5	M5
	600-647.5	630-640	680-690	520-530	590-600	690-700	420-430	660-670
	[kg]	[kg]	[kg]	[kg]	[kg]	[kg]	[kg]	[kg]
1996	14 552	14 649	15 149	16 390	14 241	15 016	14 995	14 301
1997	14 998	15 093	15 610	16 873	14 666	15 470	15 484	14 731
1998	22 838	22 986	23 773	25 707	22 341	23 561	23 557	22 437
1999	19 850	19 977	20 661	22 337	19 414	20 476	20 486	19 499
2000	15 418	15 518	16 049	17 357	15 084	15 906	15 899	15 148
2001	11 905	11 983	12 393	13 405	11 649	12 283	12 273	11 698
2002	15 490	15 591	16 124	17 441	15 156	15 981	15 969	15 220
2003	15 332	15 429	15 958	17 250	14 994	15 815	15 827	15 059
2004	21 524	21 668	22 408	24 247	21 066	22 211	22 173	21 154
Total [10³·kg]	151.9	152.9	158.1	171.0	148.6	156.7	156.7	149.2
DW TSS*) [mg/l]	288	303	308	375	311	312	220	305
RW TSS**) [mg/l]	200	201	208	224	195	206	208	196

*) TSS mean dry weather value
**) TSS mean rain weather value

Table A- 77 TSS Overflow Loads Results of Long Term Simulation – Part 2

	M5	SVM-SMO	SVM-SMO	SVM-SMO	PLS	PLS	PLS	PLS	PLS[1)]
	710-720	620-630	670-680	720-730	380-750	380-750	550-600	550-600	600-647.5
					w3	w2	w3	w2	w20
	[kg]	[kg]	[kg]	[kg]	[kg]	[kg]	[kg]	[kg]	[kg]
1996	14 904	14 006	14 368	15 149	25 630	13 256	6 843	9 983	12 863
1997	15 379	14 428	14 801	15 610	26 334	13 644	7 006	10 255	13 229
1998	23 405	21 975	22 543	23 733	40 159	20 790	10 702	15 640	20 165
1999	20 349	19 097	19 591	20 661	34 874	18 063	9 284	13 581	17 516
2000	15 797	14 836	15 219	16 049	27 123	14 037	7 232	10 563	13 617
2001	12 196	11 457	11 753	12 393	20 953	10 842	5 590	8 161	10 518
2002	15 869	14 906	15 291	16 124	27 260	14 105	7 272	10 617	13 684
2003	15 720	14 749	15 131	15 958	26 926	13 949	7 165	10 485	13 526
2004	22 040	20 718	21 253	22 408	37 925	19 611	10 131	14 773	19 031
Total [10^3·kg]	155.7	146.2	150.0	158.1	267.2	138.3	71.2	104.1	134.1
DW TSS*) [mg/l]	248	297	303	308	718	310	258	286	326
RW TSS**) [mg/l]	206	192	197	208	347	181	91	136	175

*) TSS mean dry weather value

**) TSS mean rain weather value

1) provided by the manufacturer

Mitteilungen des Institutes für Wasserwirtschaft und Konstruktiven Wasserbau der Technischen Universität Graz

Bisher erschienene Hefte:

Heft	1	(1959)	VEDER, Ch.: Neue Verfahren zur Herstellung von untertägigen Wänden und Injektionsschirmen in Lockergesteinen und durchlässigem Fels (vergriffen)
Heft	2	(1959)	BEER, O.: Hochwasserentlastungsanlagen österreichischer Talsperren
Heft	3	(1960)	WEHRSCHÜTZ, F.: Wasserentnahme aus alpinen Abflüssen
Heft	4	(1961)	TSCHADA, H.: Die Spiralenauslässe des Kraftwerkes St.Pantaleon
Heft	5	(1962)	GRENGG, H.: Funktion, Ordnung und Gestalt im konstruktiven Wasserbau
Heft	6	(1962)	PIRCHER, W.: Wehreichungen an der Enns
Heft	7	(1962)	WEHRSCHÜTZ, F.: Füll- und Entleerungssysteme von Schiffsschleusen mit großen Fallhöhen
Heft	8	(1962)	REITZ, A.: Das Stauwerk im Bogen
Heft	9	(1963)	PIRCHER, W.: Die Bautypen der Wasserkraft
Heft	10	(1964)	WEHRSCHÜTZ, F.: Kritische Betrachtung der Modellgesetze
Heft	11	(1965)	SIMMLER, H.: Das neue Institut für Wasserbau
Heft	12	(1964)	RADLER, S.: Die Berechnung der Abflüsse im natürlichen Gerinne
Heft	13	(1965)	ALTENBURGER, H.: Der Spiralauslaß als Hochwasserentlastung bei Donaukraftwerken
Heft	14	(1965)	KRESNIK, E.: Kunststoffe im wasserbaulichen Versuchswesen und deren rauhigkeitsmäßige Erfassung
Heft	15	(1970)	SVEE, R.: Untersuchungen über die Stabilität bei Wasserkraftanlagen mit idealer Regelung
Heft	16	(1971)	DROBIR, H.: Die Registrierung eines zeitlich rasch veränderlichen Wasserspiegels mit kapazitiven Meßsonden
			ROTH, G.: Meßanlage zum Studium instationärer Vorgänge mit Hilfe eines Digitalcomputers
Heft	17	(1971)	DROBIR, H.: Der Ausfluß aus einem Speicher beim Bruch einer Talsperre
Heft	18	(1972)	GRENGG, H.: Wörterbuch der Wasserkraftnutzung; Französisch – Deutsch, Deutsch – Französisch
Heft	19	(1973)	DRAXLER, A.: Mathematisches Modell für die Zuflußprognose als Hilfsmittel zur Optimierung des KW-Betriebes
Heft	20	(1974)	GRENGG, H.: Die Technisierung großer Ströme in Verbindung mit der Wasserkraft
Heft	21	(1975)	GRENGG, H.: Die großen Wasserkraftanlagen des Weltbestandes
Heft	22	(1977)	GRENGG, H.: Die großen Wasserkraftanlagen des Weltbestandes, 2. Teil
			KRAUSS, H.: Lufteinzug durch den Wasserabfluß in Vertikalrohren

Heft	23	(1979)	LIEBL, A.: Die Lehre aus der Katastrophe beim Aufstau des Tarbela-Dammes in Pakistan aus der Sicht der Stahlwasserbauer
		(1980)	KRÖLL, A.: Die Stabilität von Steinschüttungen bei Sohlen- und Uferbefestigungen in Wasserströmungen
Heft	24	(1981)	TSCHERNUTTER, P.: Grundsatzüberlegungen zur Rentabilität und zum Ausbau von Kleinwasserkraftwerken
Heft	25	(1984)	Helmut Simmler – Zur Vollendung seines 65.Lebensjahres gewidmet von seinen ehemaligen und derzeitigen Mitarbeitern an der TU Graz

Publikation des Institutes für Hydromechanik, Hydraulik und Hydrologie der Technischen Universität Graz

Bisher erschienene Bände:

SACKL, B.	(1987)	Ermittlung von Hochwasser - Bemessungsganglinien in beobachteten und unbeobachteten Einzugsgebieten

Veröffentlichungen des Institutes für Siedlungs- und Industriewasserwirtschaft, Grundwasserhydraulik, Schutz- und Landwirtschaftlichen Wasserbau der Technischen Universität Graz

Bisher erschienene Bände:

Band	1	(1977)	RENNER, H.: Die Berücksichtigung nichtbindiger überdeckender Schichten bei der Bemessung von Wasserschutzgebieten
Band	2	(1977)	KAUCH, E.P.: Untersuchung des Bewegungsgesetzes für die Filterströmung, im besonderen bei höheren Geschwindigkeiten einschließlich der teilturbulenten Strömung
Band	3	(1977)	PONN, J.: Geschwindigkeitsverteilungen in radial durchströmten Nachklärbecken – Verwendung einer neu entwickelten Thermosonde
Band	4	(1978)	Festschrift zum 60. Geburtstag von E.P. Nemecek
Band	5	(1979)	RENNER, H.: Die Entwicklung einer biologischen Kläranlage für kleinste Verhältnisse
Band	6	(1980)	Forschungsberichte 1979/80
Band	7	(1980)	KAUCH, E.P.: Der Pumpversuch im ungespannten Grundwasserleiter
Band	8	(1982)	DITSIOS, M.: Untersuchungen über die erforderliche Tiefe von horizontal durchströmten rechteckigen Nachklärbecken von Belebungsanlagen
Band	9	(1982)	GEIGER, D.: Einfluß der Schlammräumung im Nachklärbecken auf die erreichbare Feststoffkonzentration im Belebungsbecken
Band	10	(1984)	Forschungsbericht 1983/84 (vergriffen)
Band	11	(1984)	Beeinträchtigung der Grundwasservorkommen in qualitativer und quantitativer Hinsicht
Band	12	(1986)	KOTOULAS, K.: Natürliche Entwicklung der Längen- und Querprofilform der Flüsse - ein Beitrag zum naturnahen Flußbau

Schriftenreihe zur Wasserwirtschaft Technische Universität Graz

Bisher erschienene Bände:

Band	17	(1995)	KNOBLAUCH, H.: Dissipationsvorgänge in Rohrleitungssystemen [1)]
Band	18	(1995)	Fremdwasser in Abwasseranlagen [2)]
Band	19/1	(1996)	XVIII. Konferenz der Donauländer über hydrologische
Band	19/2		Vorhersagen und hydrologisch-wasserwirtschaftliche Grundlagen [1), 2)]
Band	20	(1996)	STRANNER, H.: Schwallwellen im Unterwasser von Spitzenkraftwerken und deren Reduktion durch flußbauliche Maßnahmen [1)]
Band	21	(1996)	DUM, T.: Verifikation eines numerischen Strömungsmodells anhand physikalischer Modelle [1)]
Band	22	(1996)	VASVÁRI, V.: Ein numerisches Modell zur Bewirtschaftung gespannter Grundwasservorkommen am Beispiel des Mittleren Safentales [1), 2)]
Band	23	(1996)	HYDROLOGISCHE MONOGRAPHIE des Einzugsgebietes der Oberen Raab [1), 2)]
Band	24	(1997)	Niederwasser [1), 2)]
Band	25	(1997)	KRALL, E.: Untersuchung der Gesamtwahrscheinlichkeit von Hochwasserereignissen in kleinen, unbeobachteten Einzugsgebieten Österreichs auf der Grundlage von Gebietskennwerten [1), 2)]
Band	26	(1997)	Abwasserentsorgung bei fehlenden Vorflutern [2)]
Band	27	(1997)	Festschrift anläßlich des 60. Geburtstages von Herrn O.Univ.-Prof. Dipl.-Ing. Dr. techn. Günther Heigerth [1)]
Band	28	(1997)	MEDVED, N.: Simulation und systematische Erfassung von Spülvorgängen in verlandeten Flussstauräumen [1)]
Band	29	(1998)	Festschrift anläßlich des 65. Geburtstages von Herrn O.Univ.-Prof. Dipl.-Ing. Dr. techn. Dr.h.c. Heinz Bergmann [1), 2)]
Band	30	(1998)	Festschrift anläßlich des 80. Geburtstages von Herrn em.O.Univ.-Prof. Dipl.-Ing. Dr.h.c. Dr. techn. Ernst P. Nemecek [2)]
Band	31	(1999)	BEUTLE, K.: Untersuchungen zur Schlammstabilisierung bei diskontinuierlich belüfteten Belebungsanlagen [2)]
Band	32	(1999)	REINHOFER, M.: Klärschlammvererdung mit Schilf [2)]
Band	33	(1999)	GRUBER, G.: Der biologisch abbaubare Kohlenstoffgehalt in der Abwassertechnik, BTOC und BDOC als Alternative zum BSB [2)]
Band	34	(2000)	Betrieb und Überwachung wasserbaulicher Anlagen - Symposium [1)]
Band	35	(2001)	FUCHS, D.: Decision Support Systeme für die Rehabilitationsplanung von Wasserrohrnetzen [2)]
Band	36	(2001)	Untersuchungen im Einzugsgebiet der Oberen Raab über hydrologische Folgen einer möglichen Klimaänderung [1), 2)]
Band	37	(2001)	HABLE, O.: Multidimensional probabilistic design concept for the estimation of the overtopping probability of dams [1), 2)]
Band	38	(2001)	VASVÁRI, V.: Geohydraulische und bohrlochgeophysikalische Untersuchungen in geklüfteten Grundwasserleitern [1), 2)]
Band	39	(2002)	SCHATZL, R.: Skalenabhängiger Vergleich zwischen Wetterradar-daten und Niederschlagsmessungen [2)]

Band	40	(2002)	GUNDACKER, F.: Untersuchungen zur Schlammstabilisierung bei diskontinuierlich belüfteten Belebungsanlagen bei tiefen Temperaturen [2)]
Band	41	(2003)	Wasserbau neu – Die Wasserbauschule an der Technischen Universität Graz [2)]
Band	42	(2004)	Innovative Messtechnik in der Wasserwirtschaft – Konzeption und Praxiserfahrungen mit einem modularen Monitoringnetzwerk zur universellen Anwendung in der Wasserwirtschaft [2)]
Band	43	(2005)	7. Treffen junger Wissenschaftlerinnen und Wissenschaftler deutschsprachiger Wasserbauinstitute [1)]
Band	44	(2005)	HOCHEDLINGER, M.: Assessment of Combined Sewer Overflow Emissions [2)]

Die Bände sind zu beziehen bei:

[1)] Institut für Wasserbau und Wasserwirtschaft
Technische Universität Graz, Stremayrgasse 10/II, A-8010 Graz
Tel. +43(0)316/873-8361, Fax +43(0)316/873-8357
E-Mail: wasserbau@tugraz.at

[2)] Institut für Siedlungswasserwirtschaft und Landschaftswasserbau
Technische Universität Graz, Stremayrgasse 10/I, A-8010 Graz
Tel. +43(0)316/873-8371, Fax +43(0)316/873-8376
E-Mail: office@sww.tugraz.at